

Origin of the Heaviest Elements: the Rapid Neutron-Capture Process

John J. Cowan^{*}

*HLD Department of Physics & Astronomy,
University of Oklahoma,
440 W. Brooks St.,
Norman, OK 73019,
USA*

Christopher Sneden[†]

*Department of Astronomy,
University of Texas, 2515 Speedway,
Austin, TX 78712-1205,
USA*

James E. Lawler[‡]

*Physics Department,
University of Wisconsin-Madison,
1150 University Avenue,
Madison, WI 53706-1390,
USA*

Ani Aprahamian[§] and Michael Wiescher[¶]

*Department of Physics and Joint Institute for Nuclear Astrophysics,
University of Notre Dame,
225 Nieuwland Science Hall,
Notre Dame, IN 46556,
USA*

Karlheinz Langanke^{**} and Gabriel Martínez-Pinedo^{††}

*GSI Helmholtzzentrum für Schwerionenforschung,
Planckstraße 1, 64291 Darmstadt,
Germany
Institut für Kernphysik (Theoriezentrum),
Department of Physics,
Technische Universität Darmstadt,
Schlossgartenstraße 2,
64298 Darmstadt,
Germany*

Friedrich-Karl Thielemann^{‡‡}

*Department of Physics,
University of Basel,
Klingelbergstrasse 82, 4056 Basel,
Switzerland
GSI Helmholtzzentrum für Schwerionenforschung,
Planckstraße 1, 64291 Darmstadt,
Germany*

(Dated: June 11, 2022)

The production of about half these heavy elements found in nature is assigned to a specific astrophysical nucleosynthesis process: the rapid neutron capture process (r-process). Although this idea has been postulated more than six decades ago, the full understanding faces two types of uncertainties/open questions: (a) The nucleosynthesis path in the nuclear chart runs close to the neutron-drip line, where presently only limited experimental information is available, and one has to rely strongly on theoretical predictions for nuclear properties. (b) While for many years the occurrence of the r-process has been associated with supernovae, where the innermost ejecta close to the central neutron star were supposed to be neutron-rich, more recent studies have cast substantial doubts on this environment. Possibly only a weak r-process, with no or negligible production of the third r-process peak, can be accounted for, while much more neutron-rich conditions,

including an r-process path with fission-cycling, are likely responsible for the majority of the heavy r-process elements. Such conditions could result during the ejection of initially highly neutron-rich matter, as found in neutron stars, or during the fast ejection of matter which has prior experienced strong electron-captures at high densities. Possible scenarios are the mergers of neutron stars, neutron-star black hole mergers, but include also rare classes of supernovae as well as hypernovae/collapsars with polar jet ejecta and possibly also accretion disk outflows related to the collapse of fast rotating massive stars. The composition of the ejecta from each event determines the temporal evolution of the r-process abundances during the “chemical” evolution of the Galaxy. Stellar r-process abundance observations, have provided insights into, and constraints on the frequency of and conditions in the responsible stellar production sites. One of them, neutron star mergers, was just identified thanks to the observation of the r-process kilonova electromagnetic transient following the Gravitational Wave event GW170817. These observations, increasingly more precise due to improved experimental atomic data and high resolution observations, have been particularly important in defining the heavy element abundance patterns of the old halo stars, and thus determining the extent, and nature, of the earliest nucleosynthesis in our Galaxy. Combining new results and important breakthroughs in the related nuclear, atomic and astronomical fields of science, this review attempts to provide an answer to the question “How Were the Elements from Iron to Uranium Made?”

CONTENTS

I. Introduction and historical reviews	3	1. Neutron Capture on neutron-rich nuclei: β -Oslo method	29
II. Observations	5	2. Neutron capture by (d, p) surrogate reactions	29
A. Stellar Abundances of Neutron-Capture Elements in Metal-Poor Stars	5	3. Neutron-capture in ring experiments	30
B. Atomic Data for the Analysis of neutron-capture Elements in Metal-Poor Stars	7	V. Nuclear modeling of r-process input	30
C. Abundance Trends in Galactic and Extragalactic Stars	9	A. Nuclear masses	30
D. The role of long-lived radioactive species	11	B. Beta-decay half-lives	32
E. Kilonovae observations	12	C. Neutron captures	34
III. Basic Working of the r-process and necessary environment conditions	14	D. Fission	35
A. Modeling Composition Changes in Astrophysical Plasmas	14	VI. Astrophysical Sites and their ejecta composition	36
B. Special features of the r-process and the role of neutron densities and temperatures	16	A. Possible r-process sites related to massive stars	38
C. How to obtain the required neutron-to-seed ratios	21	1. Neutrino winds from core-collapse supernovae	38
IV. Experimental developments for r-process studies	22	2. Electron-capture supernovae	39
A. Production of neutron-rich isotopes	23	3. Neutrino-induced r-process in the He-shell	39
1. Nuclear reactors and fission product sources	24	4. Quark deconfinement supernovae	39
2. Spallation sources and ISOL techniques	24	5. Magneto-rotational supernovae with jets	40
3. Fragmentation sources	24	6. Collapsars, Hypernovae, long-duration Gamma-Ray Bursts	41
B. Experimental Achievements in Measuring Nuclear Properties	25	B. Neutron-star and neutron-star / black hole mergers	43
1. The experimental study of nuclear masses	26	1. Dynamic ejecta	46
Mass measurements in storage rings	26	2. Neutrino Winds and the Effect of Neutrinos	48
Mass measurements in traps	26	3. Accretion Disks outflows	49
2. Beta-Decay Studies	27	VII. Electromagnetic signatures of r-process nucleosynthesis	50
3. Beta-delayed neutron emission probability measurements	27	VIII. Abundance evolution in the Galaxy and Origin of the r-process	54
C. Experiments towards Neutron Capture Rates	28	A. Supernova vs. r-process imprints in early galactic evolution	54
		B. Galactic Chemical Evolution Modelling	57
		1. Homogeneous evolution models	57
		2. Inhomogeneous galactic chemical evolution	58
		C. Connecting observational constraints on r-process abundances with different astrophysical sites	59
		D. Long-lived Radioactivities: r-process cosmochronometers and actinide boost stars	61
		IX. Final remarks and conclusions	64
		Acknowledgments	68
		References	68

* jjcowan1@ou.edu

† chris@astro.as.utexas.edu

‡ jelawler@wisc.edu

§ aapraham@nd.edu

¶ Michael.C.Wiescher.1@nd.edu

** k.langanke@gsi.de

†† g.martinez@gsi.de

‡‡ f-k.thielemann@unibas.ch

I. INTRODUCTION AND HISTORICAL REVIEWS

At present we know of 118 elements from charge number $Z = 1$ (H) to $Z = 118$ (Og). Eighty of them have at least one stable isotope (up to $Z = 82$, Pb) with $Z = 43$ (Tc) and $Z = 61$ (Pm) being unstable. Another 11 elements up to $Z = 94$ (Pu) [with the exception of $Z = 93$, Np] are naturally occurring on earth with sufficiently long half-lives, while the remaining ones with short half-lives have only been either produced in laboratory or possibly also astrophysical environments. The question of how this took place in the Universe is a long-standing one. Presently we know that of the natural elements/isotopes only ^1H , $^3,4\text{He}$ and ^7Li originate in the Big Bang, with problems remaining in understanding the abundance of ^7Li (Cyburt *et al.*, 2016; Pitrou *et al.*, 2018). All other elements were synthesized in stars, the first ones forming a few hundred million years after the Big Bang. The majority of stars, which have long evolutionary phases, are powered by fusion reactions. Major concepts for stellar burning were laid out in the 1950s (Burbidge *et al.*, 1957; Cameron, 1957), including the then called x-process which today is understood via spallation of nuclei by cosmic rays (e.g. Prantzos, 2012). During their evolution, and in explosive end phases, massive stars can synthesize elements from C through Ti, the iron-peak elements (e.g., $21 \leq Z \leq 30$ from Sc to Zn) and beyond, (as outlined over many years, e.g. Howard *et al.*, 1972; Woosley and Heger, 2007; Wanajo *et al.*, 2018; Curtis *et al.*, 2019). The major result is, however, that the production of heavier nuclei up to Pb, Bi, and the actinides requires free neutrons, as charged-particle reactions in stellar evolution and explosions lead typically to full chemical or quasi equilibria which favor the abundance of nuclei with the highest nuclear binding energies, occurring in the Fe-peak (Hix *et al.*, 2007).

A (very) small number of these heavy isotopes can be produced as a result of charged-particle and photon-induced reactions in explosive nucleosynthesis, the so called (proton-rich) p-process (e.g. Arnould and Goriely, 2003; Travaglio *et al.*, 2018; Nishimura *et al.*, 2018, and references therein), and possibly a further contribution resulting from interactions with neutrinos in such environments, including the ν process (Woosley *et al.*, 1990; Suzuki and Kajino, 2013; Sieverding *et al.*, 2019) and νp process (Fröhlich *et al.*, 2006b; Pruet *et al.*, 2006; Wanajo, 2006).

The two main processes involving the capture of free neutrons are the slow (s)-process and the rapid (r)-process (due to low or high densities of neutrons available and the resulting reaction timescales of neutron captures). In the s-process, taking place during stellar evolution and passing through nuclei near stability, there is sufficient time for beta-decay between two neutron captures. The process timescale ranges from hundreds to thousands of years. For many of these nuclei experi-

mental data are available (see e.g. Käppeler *et al.*, 2011; Karakas and Lattanzio, 2014; Reifarth *et al.*, 2014). In order to allow for the production of the heaviest nuclei over a timescale of seconds, the r-process operates far from stability, which requires high neutron densities. This involves highly unstable nuclei, for which still little experimental data are available. In addition, the quest for the stellar origin of the required conditions involved a large number of speculations for many decades (e.g. Cowan *et al.*, 1991; Arnould *et al.*, 2007). [There are also observational indications of intermediate neutron capture processes between the s and the r-process, e.g., the i-process (Cowan and Rose, 1977), possibly occurring in super-AGB stars (Jones *et al.*, 2016a).] Fig. 1 gives an overview of the major contributions to the solar system abundances. It includes the Big Bang (light elements H, He, Li and their isotopes $^1,2\text{H}$, $^3,4\text{He}$ and ^7Li , given in yellow), plus stellar sources, contributing via winds and explosions to the interstellar medium until the formation of the solar system. These stellar burning abundances result from charged-particle reactions up to the Fe-group in stellar evolution and explosions (green), and neutron capture processes. The latter are a superposition of (understood) slow neutron captures (s-process) in helium burning of stars (with abundance maxima at closed neutron shells for stable nuclei, turquoise), and a rapid neutron capture process (r-process, pink) leading to abundance maxima shifted to lighter nuclei in comparison to the s-process. We note, however, that the contributions of the i, p, ν , and νp -processes are minor and thus are not readily apparent in this figure. The focus of this review will be on the r-process and the understanding of how the corresponding isotopes were synthesized in nature.

Over the years there have been a number of comprehensive reviews on this topic (for a selected list see e.g. Hillebrandt, 1978; Cowan *et al.*, 1991; Qian and Wasserburg, 2007; Arnould *et al.*, 2007; Sneden *et al.*, 2008; Thielemann *et al.*, 2011; Thielemann *et al.*, 2017a,b; Horowitz *et al.*, 2019, and references therein). In order to get clues on the r-process origin, a wide range of subtopics need to be addressed: (1) nuclear physics input to understand the nucleosynthesis path far from stability, (2) nucleosynthesis modeling to find out conditions for neutron densities and temperatures which can reproduce the r-process abundances found in nature, (3) determining whether proposed astrophysical sites can match such conditions, (4) observations of stellar abundances throughout galactic history in order to find out which of these sites can contribute during which period of galactic evolution, (5) in order to do so with good precision a detailed study of the atomic physics is required for identifying the strengths of absorption lines needed to determine abundances, and (6) detections of long-lived radioactive species that can hint towards understanding the frequencies of r-process events in the Galaxy. Thus, a number of connected fields, including atomic physics,

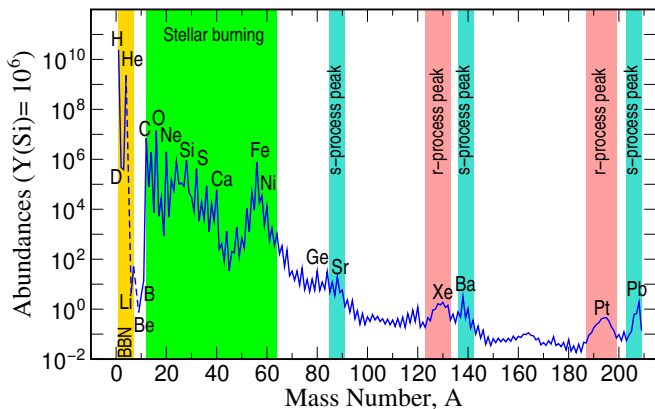


FIG. 1 Abundances, Y_i , of elements and their isotopes in the solar system as a function of mass number $A_i = Z_i + N_i$. $A_i Y_i$ is equal to the mass fraction of isotope i , the sum of mass fractions amounts to 1, $\sum_i A_i Y_i = 1$. The present figure utilizes a scaling, leading (for historical reasons) to an abundance of 10^6 for the element Si. Element ratios are obtained from solar spectra, the isotopic ratios from primitive meteorites and terrestrial values (Asplund *et al.*, 2009; Lodders *et al.*, 2009). These values represent a snapshot in time of the abundances within the gas that formed the solar system.

nuclear physics, stellar spectroscopy, stellar (explosion) modeling, and galactic chemical evolution are involved in attempting to answer the long-standing problem of “How Were the Elements from Iron to Uranium Made?”, one of the *Eleven Science Questions for the New Century* addressed by the National Academy of Sciences in 2003 (National Research Council, 2003). Detailed discussions will follow in later sections, here we list a number of considered scenarios.

While there have been many parametric studies in the early days, assuming a set of neutron densities and temperatures (e.g. Seeger *et al.*, 1965; Kodama and Takahashi, 1975; Kratz *et al.*, 1986; Kratz *et al.*, 1988, 1993; Freiburghaus *et al.*, 1999a; Pfeiffer *et al.*, 2001), the long-standing question is, where an r-process with neutron densities of 10^{26} cm^{-3} and higher, producing highly unstable neutron-rich isotopes of all heavy elements and permitting a fast build-up of the heaviest elements up to the actinides, can take place.

As will be discussed later with respect to observations, there are indications that a “weak” and a “strong” r-process seems to occur in nature, and the “strong” component is probably the dominant one, accounting essentially for solar-system r-process abundances. But some old stars, although displaying abundances of r-process elements, including Eu, show a strongly declining trend towards heavy elements, and it is not clear whether the third r-process peak with $A = 195$ or even the actinides are present. In our review we will focus mostly on the strong r-process, but discuss observations and possible sites of the weak r-process as well. There have been many suggestions relating the site of the strong r-process to

1. the innermost ejecta of regular core-collapse supernovae CCSNe (e.g. Schramm, 1973; Sato, 1974; Hillebrandt *et al.*, 1976; Hillebrandt, 1978; Woosley *et al.*, 1994; Takahashi *et al.*, 1994; Wittl *et al.*, 1994; Qian and Woosley, 1996; Hoffman *et al.*, 1997; Thompson *et al.*, 2001; Wanajo *et al.*, 2001; Terasawa *et al.*, 2001; Qian and Wasserburg, 2007; Farouqi *et al.*, 2010; Roberts *et al.*, 2010, 2012; Martínez-Pinedo *et al.*, 2012; Arcones and Thielemann, 2013; Mirizzi, 2015). However, despite all remaining uncertainties in the explosion mechanism, recent conclusions are that at most a weak r-process can occur under these conditions (Wanajo *et al.*, 2011; Martínez-Pinedo *et al.*, 2012; Roberts *et al.*, 2012; Curtis *et al.*, 2019), because weak interactions with electron neutrinos and anti-neutrinos from the newly formed hot proto-neutron star will either make initially neutron-rich matter less neutron-rich or even proton-rich or, in case of slightly neutron-rich matter, sufficiently high entropies are not attained. Another option for a weak r-process exists in so-called quark deconfinement supernovae, where after the collapse of a massive star, leading to a proto-neutron star, a quark-hadron phase transition sets in which causes the subsequent supernova explosion (Fischer *et al.*, 2018, 2020b).
2. Outer layers of supernova explosions, e.g. the helium layer where neutrons are created by (α, n) -reactions, were also suggested (Turan *et al.*, 1978; Thielemann *et al.*, 1979; Cowan *et al.*, 1980; Hillebrandt *et al.*, 1981; Klapdor *et al.*, 1981; Cameron *et al.*, 1983; Cowan *et al.*, 1983; Thielemann *et al.*, 1983; Cowan *et al.*, 1985), later also the collapsing ONeMg core of massive stars (Wheeler *et al.*, 1998). The emergence of realistic pre-explosion stellar models made this site less likely. Further options include — for low abundances of heavy elements in the early Galaxy — sufficient amounts of neutrons in the He-shell, provided via neutrino interactions (Epstein *et al.*, 1988; Nadyozhin and Panov, 2007). But this scenario, with low neutron number densities, would not be able to produce the solar r-process pattern with its correct peak locations (Banerjee *et al.*, 2011; Qian, 2014; Banerjee *et al.*, 2016).
3. Special classes of core-collapse events of massive stars with fast rotation and high magnetic fields. They can either lead to highly magnetized neutron stars (magnetars) and neutron-rich jet ejecta (MHD-jet supernovae) along the polar axis (Symbalisty *et al.*, 1985; Cameron, 2003; Nishimura *et al.*, 2006; Winteler *et al.*, 2012; Mösta *et al.*, 2014; Nishimura *et al.*, 2015; Mösta *et al.*, 2015; Nishimura *et al.*, 2017; Mösta *et al.*, 2018; Halevi and Mösta, 2018; Obergaulinger *et al.*, 2018) or to

black holes, polar jets, and black hole accretion disk outflows (hypernovae/collapsars). The latter have been attributed to neutron-rich jet ejecta (e.g. Fujimoto *et al.*, 2008; Ono *et al.*, 2012) and/or the creation of r-process elements in black hole accretion disks (e.g. Pruet *et al.*, 2003, 2004; Siegel *et al.*, 2019). The first type of events showed quite some promise for producing r-process ejecta, but the necessity that very high pre-collapse magnetic fields exist puts constraints on this scenario. The second option (collapsars) stands for a high-angular momentum subset of rotating stars which form black holes in combination with long-duration gamma-ray bursts (GRB). A variant of this, based on the spiraling in of a neutron star via merging with a giant in a binary system (leading eventually to accretion, black hole formation, and a black hole accretion disk) has been suggested by Grichener and Soker (2019).

4. Ejecta from binary neutron star (or BH-neutron star) mergers have been studied for many years before the first detection of such an event (e.g. Lattimer and Schramm, 1974; Symbalisty and Schramm, 1982; Eichler *et al.*, 1989; Freiburghaus *et al.*, 1999b; Rosswog *et al.*, 2000, 2014; Wanajo *et al.*, 2014; Goriely *et al.*, 2011; Just *et al.*, 2015a; Eichler *et al.*, 2015; Goriely *et al.*, 2015; Ramirez-Ruiz *et al.*, 2015; Mendoza-Temis *et al.*, 2015; Shibagaki *et al.*, 2016; Wu *et al.*, 2016; Lippuner *et al.*, 2017; Thielemann *et al.*, 2017b). After the gravitational wave detection GW170817 of a neutron star merger with a combined total mass of about $2.74 M_{\odot}$, (Abbott *et al.*, 2017c, 2019), accompanied by a kilonova observation supporting the production of heavy elements (see e.g. Metzger, 2017b; Tanaka *et al.*, 2017; Villar *et al.*, 2017), this type of event has attracted special attention (see reviews e.g. by Rosswog *et al.*, 2018; Horowitz *et al.*, 2019; Shibata and Hotokezaka, 2019, and references therein). More recent gravitational wave observations point to further neutron star mergers (e.g. GW190425 with a combined total mass of $\sim 3.4 M_{\odot}$, Abbott *et al.*, 2020), or even neutron star-black hole merger candidates (e.g. S190426c with a combined total mass in excess of $7 M_{\odot}$, Lattimer, 2019). The latter two events had no observed electromagnetic counterpart, due to either non-existence or non-detection, related to a larger distance and/or missing precise directions. (Foley *et al.*, 2020; Kyutoku *et al.*, 2020; Barbieri *et al.*, 2020; Ackley *et al.*, 2020)

Most of the astrophysical sites mentioned above involve ejection of material from high densities and involve a neutron star or black hole produced during core-collapse or a compact binary merger. Hence the high density equation

of state that ultimately determines the transition from a neutron star to a black hole plays an important role in the modeling of these objects. We will not discuss this topic further but refer the interested reader to recent reviews on the nuclear equation of state (Lattimer, 2012; Hebeler *et al.*, 2015; Özel and Freire, 2016; Oertel *et al.*, 2017; Tews *et al.*, 2019; Bauswein and Stergioulas, 2019).

Before discussing the r-process astrophysical sources in detail, a lot of groundwork has to be laid out. Section II provides an overview of observations (including the atomic physics for their correct interpretation), section III the basic working of an r-process and which conditions are needed for its successful operation, sections IV and V discuss the impact played by nuclear physics (with experimental and theoretical investigations), and section VI passes through the astrophysical sites which can fulfill the required conditions. Section VIII combines these astrophysical sites and how their role in galactic evolution connects to section II. Finally in the summary (section IX), after having presented all possible connections, we discuss remaining issues and open questions, i.e. whether a single r-process site has been identified by now, or whether we still might need several sources to explain observations throughout galactic evolution.

II. OBSERVATIONS

A. Stellar Abundances of Neutron-Capture Elements in Metal-Poor Stars

Stellar abundance observations over decades have provided fresh evidence about the nature and extent of heavy element nucleosynthesis. In the case of the s-process there is direct observational evidence of in situ stellar nucleosynthesis with the observation of the radioactive element Tc, discovered first by Merrill (1952). Additional stellar abundance studies have strongly linked this type of nucleosynthesis to very evolved He shell-burning asymptotic giant branch stars (e.g. Busso *et al.*, 1999; Käppeler *et al.*, 2011; Karakas and Lattanzio, 2014). There is no similar example for the r-process, related to nucleosynthesis during stellar evolution, as it requires rather extensive neutron fluxes only obtainable in explosive events. Some elements are only formed exclusively or almost so in the r-process, such as Eu, Os, Ir, Pt, Th and U. Their presence in old galactic very metal-poor (VMP) halo stars is a clear indication that this process occurred in violent astrophysical sites early in the history of the Galaxy (see e.g. Sneden *et al.*, 2008; Thielemann *et al.*, 2017b, and references therein).

Identification of r-process-rich stars began with the discovery of overabundances of neutron-capture elements in the field red giant HD 115444 (Griffin *et al.*, 1982). This was followed by the identification of an r-process pattern in the well known bright giant HD 122563, even though

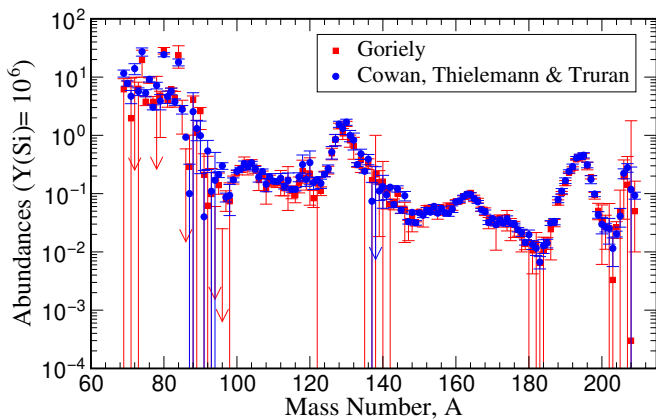


FIG. 2 Solar r-process abundances as determined by Cowan *et al.* (1991) and Goriely (1999). The largest uncertainties are clearly visible for $A \lesssim 100$ (weak s process region) and around lead.

its overall neutron-capture element level is depressed relative to Fe (Snedden and Parthasarathy 1983, see also the more extensive analysis of Honda *et al.* 2006). An initial abundance survey in metal-poor (MP) stars (Gilroy *et al.*, 1988) considered 20 red giants, finding a common and easily spotted pattern of increasing overabundances from Ba ($Z = 56$) to Eu ($Z = 63$) among the rare-earth elements. With better echelle spectrographic data came discoveries of many more r-process-rich stars, leading Beers and Christlieb (2005) to sub-classify them as “r-I” with $0.3 \leq [\text{Eu}/\text{Fe}] \leq +1.0$ and $[\text{Ba}/\text{Eu}] < 0$, and as “r-II” with $[\text{Eu}/\text{Fe}] > +1.0$ and $[\text{Ba}/\text{Eu}] < 0$.

The most detailed deconvolution of abundances into nucleosynthetic contributions exists for the solar system, as we have accurate abundances down to the isotopic level as a result of meteoritic and solar atmospheric measurements (e.g. Cameron, 1959; Asplund *et al.*, 2009; Lodders *et al.*, 2009, see Fig. 1). Identifying the r-process contributions to the solar system neutron-capture abundances is usually accomplished by first determining the s-process fractions, (e.g. Käppeler, 1999; Arlandini *et al.*, 1999; Burris *et al.*, 2000; Käppeler *et al.*, 2011). The remaining (residual) amount of the total elemental abundance is assumed to be the solar r-process contribution (see Figures 1 and 2). Aside from the so-called p-process (Arnould and Goriely, 2003; Rauscher *et al.*, 2013; Nishimura *et al.*, 2018) that accounts for the minor heavy element isotopes on the proton-rich side of the valley of instability, as well as the ν -process (Woodsley *et al.*, 1990) and the νp -process (Fröhlich *et al.*, 2006b), only the s and r-processes are needed to explain nearly all of the solar heavy element abundances.

Early observations of CS 22892-052 (Snedden *et al.*, 1994, 2003) and later CS 31082-001 (Hill *et al.*, 2002; Siqueira Mello *et al.*, 2013) and references therein), indicated a “purely” or “complete” solar system r-process abundance pattern (see Figure 3). The total abundances

of these, mostly rare-earth, elements in the stars were smaller than in the Sun but with the same relative proportions, i.e., scaled. This indicated that these stars, that likely formed early in the history of the Galaxy, experienced already a pollution by a robust r-process.

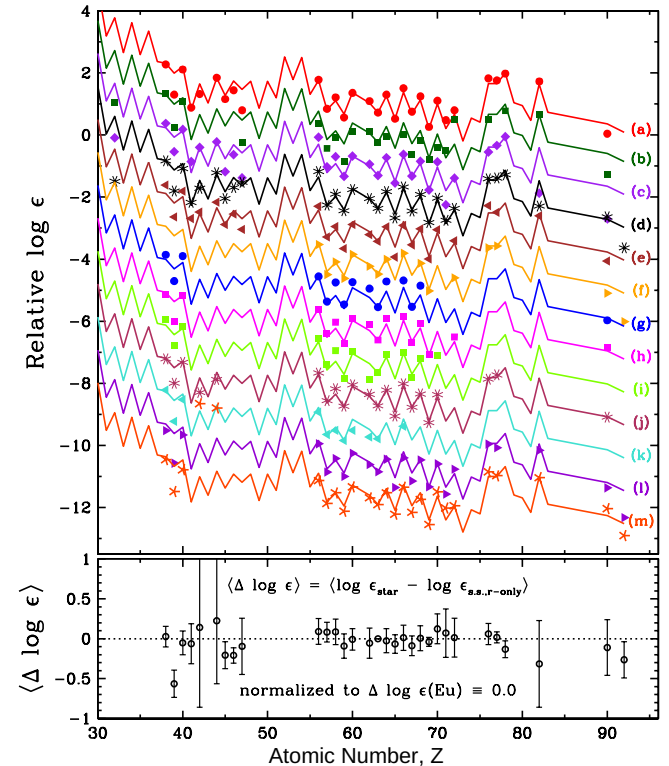


FIG. 3 Top panel: neutron-capture abundances in 13 r-II stars (points) and the scaled solar-system r-process-only abundances of (Siqueira Mello *et al.*, 2013), mostly adopted from (Simmerer *et al.*, 2004). The stellar and solar system distributions have been normalized to agree for element Eu ($Z = 63$), and then vertical shifts have been applied in each case for plotting clarity. The stellar abundance sets are: (a) CS 22892-052, (Snedden and Cowan, 2003); (b) HD 115444, (Westin *et al.*, 2000); (c) BD+17 3248, (Cowan *et al.*, 2002); (d) CS 31082-001, (Siqueira Mello *et al.*, 2013); (e) HD 221170, (Ivans *et al.*, 2006); (f) HD 1523+0157, (Frebel *et al.*, 2007); (g) CS 29491-069, (Hayek *et al.*, 2009); (h) HD 1219-0312, (Hayek *et al.*, 2009); (i) CS 22953-003, (François *et al.*, 2007); (j) HD 2252-4225, (Mashonkina *et al.*, 2014); (k) LAMOST J110901.22+075441.8, (Li *et al.*, 2015); (l) RAVE J203843.2-002333, (Placco *et al.*, 2017); (m) 2MASS J09544277+5246414, (Holmbeck *et al.*, 2018). Bottom panel: mean abundance differences for the 13 stars with respect to the solar system r-process values.

However, the growing literature on abundance analyses of VMP stars has added to our knowledge of the average r-process pattern, and has served to highlight departures from that pattern. Additions to the observational results since the review of Snedden *et al.* (2008) include Roederer *et al.* (2010b, 2014a); Li *et al.* (2015); Roederer *et al.* (2016); Roederer (2017); Aoki *et al.* (2017);

Yong *et al.* (2017); Hansen *et al.* (2018); Sakari *et al.* (2018); Roederer *et al.* (2018). These additional observations have shown that there is a complex relationship between light and heavy neutron-capture elements: Travaglio *et al.* (2004); Cowan *et al.* (2005); Hansen and Primas (2011); Hansen *et al.* (2012); Aoki *et al.* (2013); Ural *et al.* (2015); Wu *et al.* (2016). In particular it has been found in some stars that there is significant observed star-to-star abundance scatter of lighter neutron-capture elements ($Z \leq 50$), opposite to the heavier ones ($Z \geq 56$), as shown in Fig. 3. For heavy neutron-capture elements, particularly among the well-studied rare earths, an r-process origin does not always mean perfect agreement with the solar r-process pattern. So-called “truncated” (or incomplete or limited) r-process stars have been identified with sharp abundance falloffs toward the heavy end of the rare earths (Honda *et al.*, 2006, 2007; Roederer *et al.*, 2010a; Boyd *et al.*, 2012). These observed abundance patterns can be described as having a range of r-process “completeness” with some stars showing only a partial agreement. The differences in these abundance patterns have led to a flurry of stellar models and calculations to identify a site or sites for the r-process, and to determine why stars show differences in these heavy element patterns. In addition to the suggestion to the operation of a “weak” r-process, two additional processes have gained currency: the so-called Lighter Element Primary Process (LEPP of still unknown origin; Travaglio *et al.*, 2004), and the i process (Cowan and Rose 1977; see also Denissenkov *et al.* 2017 and references therein). (While the LEPP and the i process may explain certain individual stellar abundances, their contributions to the total solar system (SS) abundances appear to be very small.)

An r-process pattern (defined here as $[\text{Eu}/\text{Ba}] > +0.3$) can be seen even in MP stars with bulk deficiencies in neutron-capture elements: In Fig. 4 we show differences in abundances between stellar observations and those of the solar system attributed only to the r-process. Fig. 4 is similar in structure to those of Honda *et al.* (2007) and Roederer *et al.* (2010a). As defined in the figure, if $\Delta \log \epsilon = 0$, then the stellar neutron-capture abundance set is identical to the solar-system r-process-only distribution. This is clearly the case for elements in the atomic numbers range $Z = 57\text{--}78$, e.g. La–Pt in CS31082-001 (Siqueira Mello *et al.*, 2013). All extremely r-process-rich stars (classified as “r-II”: $[\text{Eu}/\text{Fe}] > +1$) have similar abundance runs in the heavy neutron-capture elements, as discussed above. However, many MP stars with a clear dominance of the r-process, as defined by $[\text{Eu}/\text{Ba}] > +0.3$, have abrupt drop-offs in abundances through the rare-earth domain. The most dramatic examples are the truncated r-process stars shown in Fig. 4: HD 122563 (Honda *et al.*, 2006) and HD 88609 (Honda *et al.*, 2007). Intermediate cases are abundant, as shown in

Roederer *et al.* (2010b).

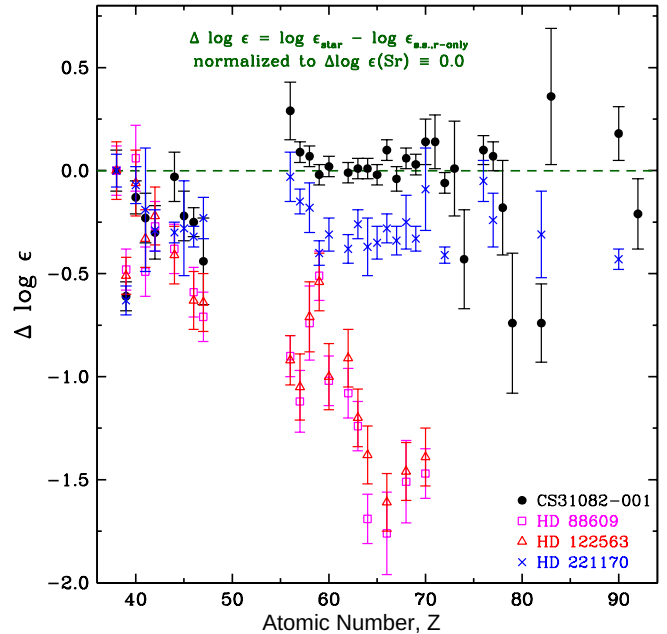


FIG. 4 Differences between stellar and r-process-only solar system (s.s.) abundances for four very MP stars with r-process abundance mixes, after Figure 5 of Honda *et al.* (2007) and Fig. 11 of Roederer *et al.* (2010b). The “s.s.,r-only” abundances are those of Siqueira Mello *et al.* (2013), mostly from Simmerer *et al.* (2004). The stellar abundance sets are: CS31082-001, (Siqueira Mello *et al.*, 2013); HD 88609, (Honda *et al.*, 2007); HD 122563, (Honda *et al.*, 2006); and HD 221170, (Ivans *et al.*, 2006).

To understand the types and nature of the nucleosynthesis, along with identifying the stellar sites and the identities of the first stars in our Galaxy, demands highly precise stellar abundance observations. Those require both high-resolution spectrographic measurements and accurate atomic data. Thus, the discovery of MP stars renewed efforts to improve atomic data for many heavy (beyond the Fe-group) neutron-capture elements (see e.g., Sneden *et al.*, 2009), as discussed below in section II.B.

B. Atomic Data for the Analysis of neutron-capture Elements in Metal-Poor Stars

Despite a great need for improved transition probabilities, the identification of lines from neutron-capture elements in stellar spectra has been possible for most elements using readily available laboratory data from about the middle of the 20th Century. Wavelengths of spectral lines of such elements were measured during the first half of the 20th Century using large grating spectrographs such as 10 m Rowland circle instruments. These early wavelength measurements often achieved 1 part per million (ppm) accuracy and were compiled in the well known

Atomic Energy Level series by Moore (1971) and for the Rare-Earth Elements by Martin *et al.* (1971). The latter of these two works includes more data from Fourier transform spectrometers (FTSs) and thus achieved $\simeq 0.01$ ppm or 10 ppb accuracy in many cases. All of these spectroscopic data are now available online¹. Although modern optical frequency comb lasers could add many additional digits to energy levels, this technology has not yet been widely applied because of the difficulty in simultaneously using it on large numbers of spectral lines.

The situation with respect to transition probabilities changed with the development of tunable dye lasers originally by Sorokin and Lankard (1966) in the US and Schäfer *et al.* (1966) in Germany. Although it took some time to thoroughly control dye laser performance, many research groups had organic dye lasers with broad tunability, narrow bandwidths (comparable to or less than Doppler widths), short (few nsec) pulse durations, and repetition rates in the 10s of Hz. Non-linear techniques, using crystals and/or gas cells, are needed to access IR and UV wavelengths, and those were also increasingly available. The remaining challenge is to make free atoms and ions of various elements in the periodic table in an optically thin sample with a low collision rate. There are several methods, including sputtering metal cathodes, in a low pressure gas cell (Hannaford and Lowe, 1981), laser driven plasma sources (e.g. Svanberg *et al.*, 1994), and the hollow cathode atom/ion beam source (Duquette *et al.*, 1981; Salih and Lawler, 1983). The broadly tunable organic dye lasers, in combination with a technique to make low pressure samples of metal atoms and ions, opened the possibility of using time-resolved laser-induced-fluorescence (TRLIF) to measure accurate and precise (about a few %) radiative lifetimes of upper levels on interest in atoms and ions. These lifetimes provide an accurate and precise total decay rate for transition probabilities from the selected upper level.

Emission branching fractions (BFs) in rich spectra still represented a challenge. The same visible and UV capable FTS instruments (e.g. Brault, 1976), used to improve energy levels, became the “work horse” of efforts on BFs in complex spectra. Reference Ar I and II lines became internal standards for many laboratory spectra from hollow cathode lamps recorded using FTS instruments (Whaling *et al.*, 1993, and references therein). The advantages of interferometric instruments such as the 1 m FTS of the National Solar Observatory on Kitt Peak, AZ, were critical for BF measurements in complex spectra. This instrument has a large etendue common to all interferometric spectrometers, wavenumber accuracy to 1 part in 10^8 , a limit of resolution as small as 0.01 cm^{-1} , broad spectral coverage from the UV to IR, and the capability

of recording a million point spectrum in minutes (Brault, 1976). Hollow cathode lamps which yield emission spectra for neutral and singly ionized atoms are available for essentially the entire periodic table.

Interest in rare-earth elements is a natural part of studies of neutron-capture elements in MP stars. Atoms and ions with open f-shells have a great many transitions in the optical. Rare-earths have important applications in general lighting and in optoelectronics because of their rich visible spectra. Rare-earth elements in MP stars are convenient for spectroscopic studies in the optical region accessible to ground based telescopes. Europium is a nearly pure r-process element and lanthanum is a nearly pure s-process element in solar system material. Although none of the r-process peaks are in the rare-earth row, the accessibility from the ground is a major advantage for rare earths.

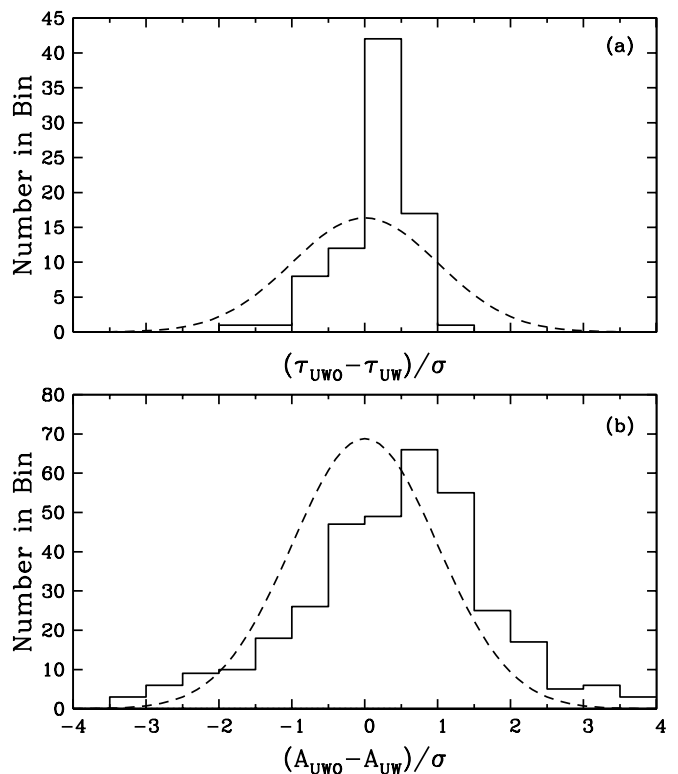


FIG. 5 Comparisons of laboratory data on Sm II from University of Western Ontario (UWO) and University of Wisconsin (UW) groups, adapted from Figs. 4 and 5 of Lawler *et al.* (2008). In panel (a) a histogram of differences in lifetimes (τ divided by their uncertainties added in quadrature) is shown, along with a dashed line representing a one standard deviation Gaussian. In panel (b) we show a similar histogram and Gaussian representation for transition probabilities (A -values).

Rare-earth elements tend to be singly ionized in the photospheres of F, G, and K stars of interest for many elemental abundance studies. The spectrum of singly ionized samarium (Sm II) received special attention (Lawler

¹ <http://physics.nist.gov/asd>

et al., 2006; Rehse *et al.*, 2006), Lawler *et al.* (2008) completed comparisons from the two sets of measurements. Fig. 5 shows a histogram of lifetime measurement differences between the two studies with a one standard deviation Gaussian superposed, and a similar histogram comparison for Einstein A coefficients which include BFs. It is clear from these histograms that radiative lifetime uncertainties are overly conservative and BFs uncertainties are satisfactory but perhaps slightly too optimistic in at least one of two sets of measurements.

Uncertainties in radiative lifetimes from TRLIF experiments have proven to be easier to minimize than uncertainties in emission BFs. Various techniques can conveniently be used to check for optical depth (vary the atom/ion beam intensity), to check for collisional effects (throttle a vacuum pump), and to eliminate errors from Zeeman quantum beats (zero the magnetic field in the experimental region for short lifetimes and introduce a high, 30 Gauss, magnetic field for long lifetimes). Most importantly benchmark lifetimes in simple spectra such as He I, Be I, Be II, Mg II, etc., which are well known from accurate theory, can be periodically re-measured as an end-to-end test of the TRLIF experiment (Den Hartog *et al.*, 2002). There are multiple challenges in BF measurements. It is essential to have a reliable relative radiometric calibration, and a source that is optically thin for strong lines of interest. One must resolve lines of interest from nearby blending partners and line identifications must be correct. These latter two constraints are most easily achieved using FTS instruments due to their exceptional resolving power and absolute wave number accuracy and precision. Weak lines from an upper level of interest are clearly most vulnerable to blending, poor signal-to-noise ratios (S/N), and other problems. Uncertainty migrates to weak lines because BFs from an upper level of interest sum to unity by definition.

Elements with wide hyperfine structure and/or a wide range of isotopes require some additional effort, but in most cases the needed hyperfine splitting (hfs) data can be extracted from FTS spectra. The existence of even a few hfs data from single frequency laser measurements is helpful since such data can serve to constrain nonlinear least square fitting of partially resolved hfs patterns in FTS data. Laboratory transition probability measurements on rare-earth ions were summarized during a study of Ce II by Lawler *et al.* (2009) and were applied to five r-process rich very MP stars in a companion paper by Sneden *et al.* (2009). The most striking conclusion from the decade long rare-earth study is that the relative r-process abundance pattern is stable over time and space. Third r-process peak elements, including Os, Ir, and Pt were observed in MP stars by Cowan *et al.* (2005). Some useful lines of Os I and Ir I are accessible to ground based studies. Unfortunately lines suitable for abundance studies of many lighter neutron-capture elements are not accessible to ground based observations. Elements near the

first r-process peak such as a As and Se have their valence electrons in nearly closed p-shells. The huge gap between the ground and first resonance levels exists in both the neutral and ion energy level structure, although the neutral atom population is dominant in most stars of interest for both of these elements. A similar problem arises for Te at the second r-process peak with only deep UV lines. Fortunately HST time was allocated for a study of Te I lines in multiple MP stars (Roederer *et al.*, 2012). The success of the Te study inspired a careful search through the HST archives for one or more stars with sufficiently deep UV spectral coverage for observations on all three r-process peaks (Roederer and Lawler, 2012). Unfortunately the star HD 160617 is likely the only such star with sufficient deep UV spectral coverage. Laboratory data sets for many of the lighter r-process elements are included. Laboratory data sets for many of the lighter r-process elements could be improved, but a successor telescope to HST with a high resolution spectrograph and UV capability will be needed to exploit improvements in the laboratory data.

The discovery of a single line of U II in an MP star (complicated by being located on the shoulder of a much stronger Fe I line) by (Cayrel *et al.*, 2001) was a milestone in stellar spectroscopy. Despite this complication, there is some confidence in its identification. Thorium is also an element of choice for stellar chronometry (e.g. Sneden *et al.*, 2003).

C. Abundance Trends in Galactic and Extragalactic Stars

As already discussed in section II.A, the galactic MP stars show indications of neutron-capture abundances, in fact, it appears as if ALL such stars (to an observational limit) exhibit some level of neutron-capture abundances. In addition, observations have indicated the presence of elements such as Ba in nearby dwarf spheroidal galaxies (e.g. Shetrone *et al.*, 1998, 2003; Venn *et al.*, 2003; Skúladóttir *et al.*, 2019). Recently there has been evidence of these elements in ultra-faint dwarf (UFD) galaxies, structures of only about $10^4 M_{\odot}$ and possibly being also the building blocks and substructures of the early Galaxy (Brauer *et al.*, 2019). By now more than 10 UFDs are discovered around our Galaxy, being very metal-poor with metallicities of $[Fe/H] \approx -3$ (Kirby *et al.*, 2013; Frebel and Norris, 2015; Ji *et al.*, 2019b; Simon, 2019), and most of them show very low r-process enhancements. However, one of them (Reticulum II) shows highly r-process enhanced stars comparable to galactic r-process rich stars such as CS 22892-052 (Roederer, 2013; Ji *et al.*, 2016; Roederer, 2017; Ji and Frebel, 2018) which seems to go back to one very early r-process event. In addition to Reticulum II, a further dwarf galaxy, Tucana III, has recently been observed and also shows r-process features (Hansen *et al.*, 2017; Marshall *et al.*, 2019a,b).

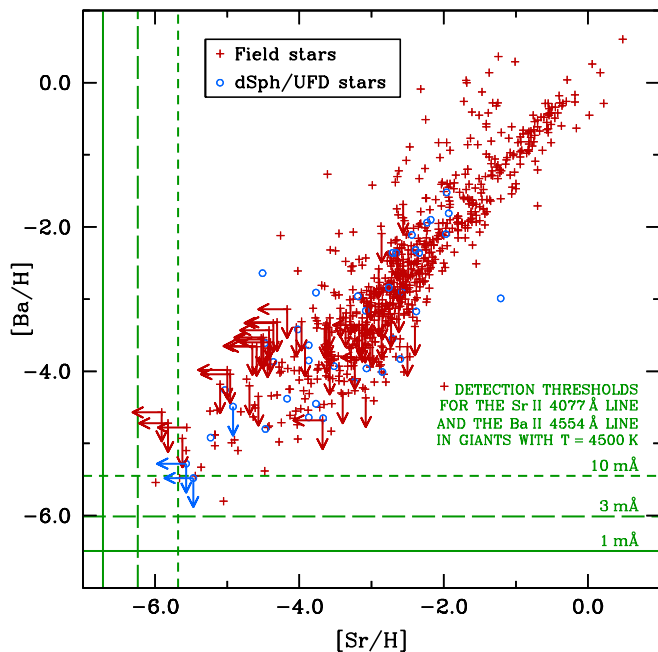


FIG. 6 Abundances of $[\text{Sr}/\text{Fe}]$ vs. $[\text{Ba}/\text{Fe}]$ in a large number of galactic and extragalactic stars from Roederer (2013) and references therein.

We show in Fig. 6, (taken from Roederer, 2013, and references therein), a compilation of abundances in both galactic and extragalactic stars. In these observations the Sr abundance acts as a surrogate for the overall metallicity of these stars and Ba indicates the enrichment of neutron-capture elements. The figure illustrates that stars down to the lowest metallicities contain Sr and/or Ba. In a solar mix these are predominantly s-process elements, i.e. their s-process isotopes dominate in present solar abundances. If massive stars with fast rotation rates contributed already some s-process in early galactic evolution (Frischknecht *et al.*, 2016), this could be due to such s-process sources. However, global trends, where observed elemental or isotopic ratios can be deconvolved into s- and r-process contributions, show an s-process appearance only in later periods of galactic evolution. Thus, this compilation strongly suggests that all of these stars have been enriched in r-process material, which also has implications for early nucleosynthesis in galaxies.

Clues about early galactic nucleosynthesis are also found in comparison of elements with different nucleosynthetic origin. We show one such comparison in Figure 7, observed in halo stars, i.e. containing elements synthesized prior to the formation of these stars. It is evident that alpha elements (such as Mg) appear early in galactic evolution at low metallicities, originating from fast evolving massive stars and core-collapse supernovae as their final endpoints. Such events occur with a high frequency during galactic evolution and show little scatter. Common r-process elements, like Eu, display, however, an ex-

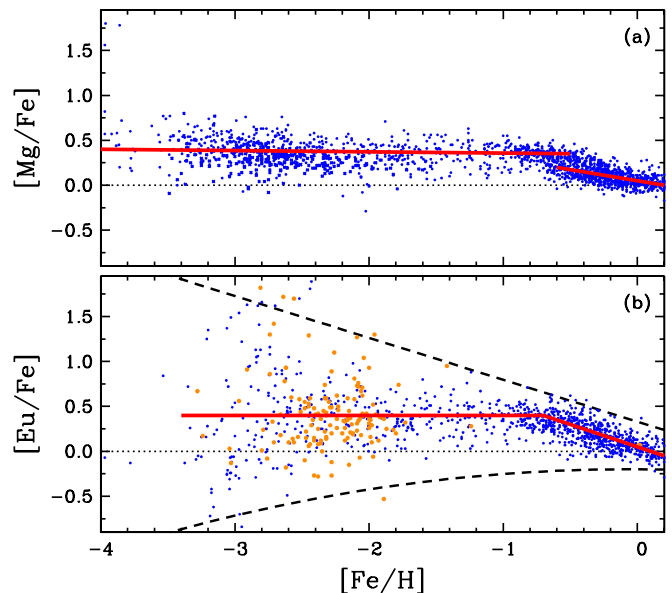


FIG. 7 Abundances as a function of metallicity for $[\text{Mg}/\text{Fe}]$ (panel a) and $[\text{Eu}/\text{Fe}]$ (panel b). This is an update of Fig. 14 in (Snedden *et al.*, 2008). Red straight lines are approximate fits to the averages of halo, thick disk, and thin disk stars. Black dashed lines in panel (b) highlight the growing star-to-star scatter in $[\text{Eu}/\text{Fe}]$ with decreasing metallicity. Individual data points are taken from Fulbright (2000); Hill *et al.* (2002); Reddy *et al.* (2003); Cayrel *et al.* (2004); Simmerer *et al.* (2004); Cohen *et al.* (2004); Barklem *et al.* (2005); Reddy *et al.* (2006); François *et al.* (2007); Bensby *et al.* (2014); Roederer *et al.* (2014a); Battistini and Bensby (2016).

tensive scatter. These observations, combined with those from ultrafaint dwarf galaxies, indicate that the heavy r-process elements are made in rare events which contribute significant amounts of material, when they occur (see Fig. 7). Such abundance comparisons can be used to put constraints on the site (or sites) for the r-process in terms of (a) ejecta compositions, (b) amounts of r-process ejecta, and (c) their mixing with the extended interstellar medium in order to understand the history of element formation in the Galaxy (i.e., Galactic Chemical Evolution, GCE). With respect to (a) Ji *et al.* (2019a) have analyzed extended sets of low metallicity observations with $[\text{Fe}/\text{H}] < -2.5$ (attempting to select stars being polluted only by single events) and $[\text{Eu}/\text{Ba}] > 0.4$ (to ensure a pure r-process origin, avoiding s-process contributions) with the aim to find the typical lanthanide (plus actinide) fraction X_{La} among the global r-process element distribution. This permits on the one hand to look for variations among old stars, indicating apparently a different result for the bulk of low metallicity stars with $\log X_{\text{La}} \approx -1.8$, while the most r-process enriched stars with $[\text{Eu}/\text{Fe}] > 0.7$ have $\log X_{\text{La}} > -1.5$. This measure will also permit comparisons to future kilonova events, if observations allow to determine this quantity (see section VII). With respect to (b) and (c) of the list

above we will return to galactic evolution issues later in section VIII, after having presented the nucleosynthesis yields of different astrophysical sites.

The eventual demise of the Hubble Space Telescope, able to obtain high-quality UV observations, will hamper future progress in the observation of heavy elements in low-metallicity stars. The James Webb Space Telescope (JWST), the scientific “successor” of HST, will have no UV capability but an IR capability. Identification of neutron-capture element lines in the IR region could provide new avenues for understanding the operation and nature of the r-process (see subsection II.B).

D. The role of long-lived radioactive species

Identification and detailed spectroscopic analysis of a handful of r-II stars, e.g., CS 22892-052 (Snedden *et al.*, 1994, 2003) CS 31082-001 (Hill *et al.*, 2002; Siqueira Mello *et al.*, 2013, and references therein), and HE 1523-0901 (Frebel *et al.*, 2007) brought forth detections of the long-lived very heavy neutron-capture radioactive elements Th ($t_{1/2} = 13.0$ Gyr) and U ($t_{1/2} = 4.6$ Gyr), which can only be made in the r-process, and in addition a neutron-capture element abundances ranging from $Z \approx 30$ to 92, indicating also an r-process pattern. This makes detailed comparisons possible between observations and r-process theory. More Th detections have been made since then, and more recently U has also been detected in some halo stars. Due to its shorter half-life, its abundance is inherently smaller and detections are difficult. Shown in Fig. 8 from (Holmbeck *et al.*, 2018) is a uranium detection in 2MASS J09544277+5246414, the most actinide-enhanced r-II star known.

These Th and U discoveries led to cosmochemistry estimates, independent of a cosmological model, based solely on decay half-lives of involved isotopes. This method requires, however, Th/U ratios from theoretical r-process predictions (geared to fit a solar r-process pattern) plus the observed abundance ratios. This enabled estimates on the decay-time since the birth of a star (when the addition of new material from nucleosynthesis sites stopped) and promising results were obtained (Cowan *et al.*, 1991; Cowan *et al.*, 1999; Kratz *et al.*, 2000; Schatz *et al.*, 2002; Hill *et al.*, 2017). The same can in principle also be done utilizing the Th/Eu ratio for some stars, yielding values in concordance with cosmological age estimates (see above). The fact that some stars seem to have experienced an “actinide boost”, i.e. an enhanced amount of Th and U in comparison to lighter r-process elements, could point back to a non-universal r-process production pattern and possibly varying r-process compositions from different production sites. This made the [Th/Eu] chronology uncertain or non-reliable for such stars (e.g. Cayrel *et al.*, 2001; Honda *et al.*, 2004), having experienced a non-solar

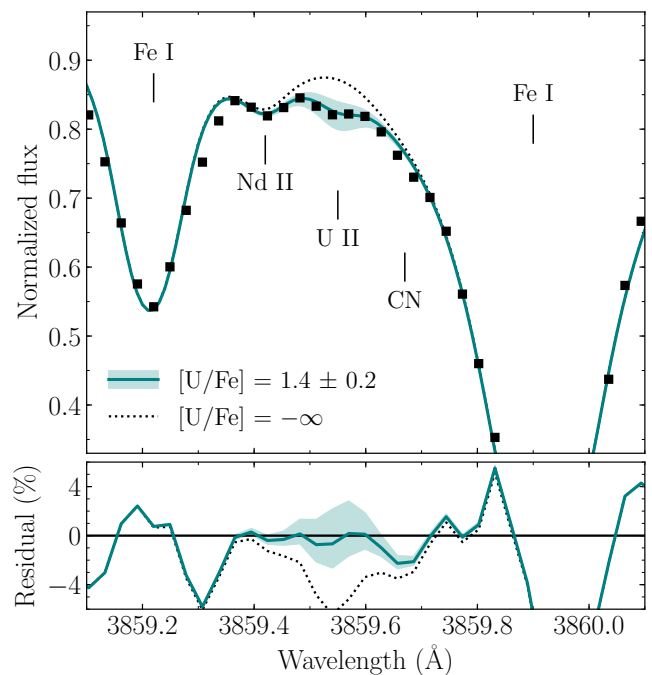


FIG. 8 Synthesis and derived abundance for U in the star 2MASS J09544277+5246414 from Figure 2 of (Holmbeck *et al.*, 2018).

r-process contribution, while the [U/Th] did not show these anomalies (Mashonkina *et al.*, 2014). Such an actinide boost is found in a few stars with metallicities $[Fe/H] \approx -3$. This indicates that (a) an r-process was already contributing in very early galactic evolution, but also (b) with possibly varying conditions for producing the heaviest elements, dependent on the r-process site. Unfortunately it has proved difficult to obtain U detections in many stars, but it is surprising that an actinide boost has not been seen at higher metallicities (see Fig. 9 from Holmbeck *et al.*, 2018).

In addition to observations of long-lived radioactive species seen via the spectra of stars throughout galactic evolution, there have also been detections in deep-sea sediments, indicating more recent additions of these elements to the earth. While the discussion in II.C points to rare strong r-process events in the early Galaxy, the latter detections, suggest the same in recent history. Long-lived radioactive species can act as witness of recent additions to the solar system, dependent on their half-lives. For a review on the signature of radioactive isotopes alive in the early solar system see e.g. Davis and McKeegan (2014). Two specific isotopes have been utilized in recent years to measure such activities in deep sea sediments. One of them, ^{60}Fe , has a half-life of 2.6×10^6 yr and can indicate recent additions from events occurring up to several million years ago. ^{60}Fe is produced during the evolution and explosion of massive stars, leading to supernovae (Thielemann *et al.*, 2011; Wanajo *et al.*, 2013; Limongi and Chi-

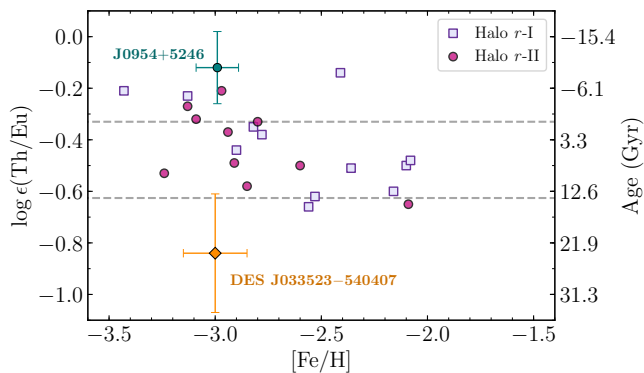


FIG. 9 Th/Eu ratios for stars with detected thorium abundances from [Holmbeck et al. \(2018\)](#). One can see that at low metallicities around $[Fe/H] \approx -3$ quite a number of so-called actinide boost stars can be found. If utilizing initial r-process production ratios which fit solar r-abundances ([Schatz et al., 2002](#)), unreasonable, and even negative, ages of these stars are obtained, not at all consistent with their metallicity, which points to the formation of these stars in the very early Galaxy.

[effi, 2018](#); [Thielemann et al., 2018](#)). It is found in deep-sea sediments which incorporated stellar debris from a nearby explosion about two million years ago ([Knie et al., 2004](#); [Ludwig et al., 2016](#); [Wallner et al., 2016](#); [Sørensen et al., 2017](#)). Such a contribution is consistent with a supernova origin and related occurrence frequencies, witnessing the last nearby event. Another isotope utilized, ^{244}Pu , has a half-life of 8.1×10^7 yr and would contain a collection from quite a number of contributing events. If the strong r-process would take place in every core-collapse supernova from massive stars, about 10^{-4} – $10^{-5} M_{\odot}$ of r-process matter would need to be ejected per event in order to explain the present day solar abundances (see Fig. 39). The recent ^{244}Pu detection ([Wallner et al., 2015](#)) is lower than expected from such predictions by two orders of magnitude, suggesting that considerable actinide nucleosynthesis is very rare (permitting substantial decay since the last nearby event). This indicates that (regular) core-collapse supernovae did not contribute significantly to the strong r-process in the solar neighborhood for the past few hundred million years, but does not exclude a weak r-process contribution with very minor Eu production ([Fields et al., 2019](#); [Wallner et al., 2019](#)). Thus, in addition to the inherent problems of (regular) core-collapse supernova models (to be discussed in later sections) to provide conditions required for a strong r-process — also producing the actinides in solar r-process proportions — these observational constraints from nearby events also challenge them as source of main r-process contributions. A recent careful study of the origin of the strong r-process with continuous accretion of interstellar dust grains into the inner solar system ([Hotokezaka et al., 2015](#)) concluded that the experimen-

tal findings ([Wallner et al., 2015](#)) are in agreement with an r-process origin from a rare event. This can explain the ^{244}Pu existing initially in the very early solar system as well as the low level of more recent additions witnessed in deep-sea sediments over the past few hundred million years.

E. Kilonovae observations

For many years a connection between observations of short-duration gamma-ray bursts (sGRBs), supernova-like electromagnetic transients (macronovae/kilonovae), and compact binary mergers has been postulated (see e.g. [Piran, 2004](#)). The first observational evidence of an excess of near infrared emission over the standard GRB afterglow came in 2013 with the observation of GRB 130603B by [Tanvir et al. \(2013\)](#)² and suggested a thermal component consistent with kilonova emissions. Further, evidence has been obtained from a reanalysis of the GRB 060614 ([Yang et al., 2015](#)), GRB 050709 ([Jin et al., 2016](#)), and GRB 070809 ([Jin et al., 2020](#)) afterglow data including a first estimate of the kilonova emission temperature ([Jin et al., 2015](#)). See [Gompertz et al. \(2018\)](#) for a review of kilonova candidates associated to short GRB observations.

Following the seminal work of [Li and Paczyński \(1998\)](#), first predictions of light curves powered by radioactive decay were done by [Metzger et al. \(2010b\)](#); [Roberts et al. \(2011\)](#); [Goriely et al. \(2011\)](#). These initial studies used grey opacities appropriate to the Fe-rich ejecta in type Ia SNe and predicted peak luminosities at timescales of a day in the blue. However, the opacity of heavy r-process elements is substantially higher due to the high density of line transitions associated with the complex atomic structure of lanthanides and actinides. This led to a light curve peak at timescales of a week in the red/near-infrared ([Kasen et al., 2013](#); [Barnes and Kasen, 2013](#); [Tanaka and Hotokezaka, 2013](#)). [Metzger et al. \(2015\)](#) speculated on the possibility that in fast expanding ejecta unburned neutrons are left and lead via their decay to a ultraviolet/blue precursor event. Early blue emission has also been suggested to originate from the hot cocoon that surrounds the GRB jet as it crosses the ejecta ([Gottlieb et al., 2018](#)).

On August 17, 2017 the gravitational wave event GW170817 was observed ([Abbott et al., 2017c](#)) and identified as merger of two neutron stars. With the combination of gravitational wave signals and electromagnetic observations, its location was identified ([Abbott et al., 2017d](#)), a (weak) sGRB detected ([Abbott et al., 2017b](#)) (weak probably due to an off-axis observation, [Wu](#)

² see <https://kilonova.space> for an up to date catalog of kilonova observations

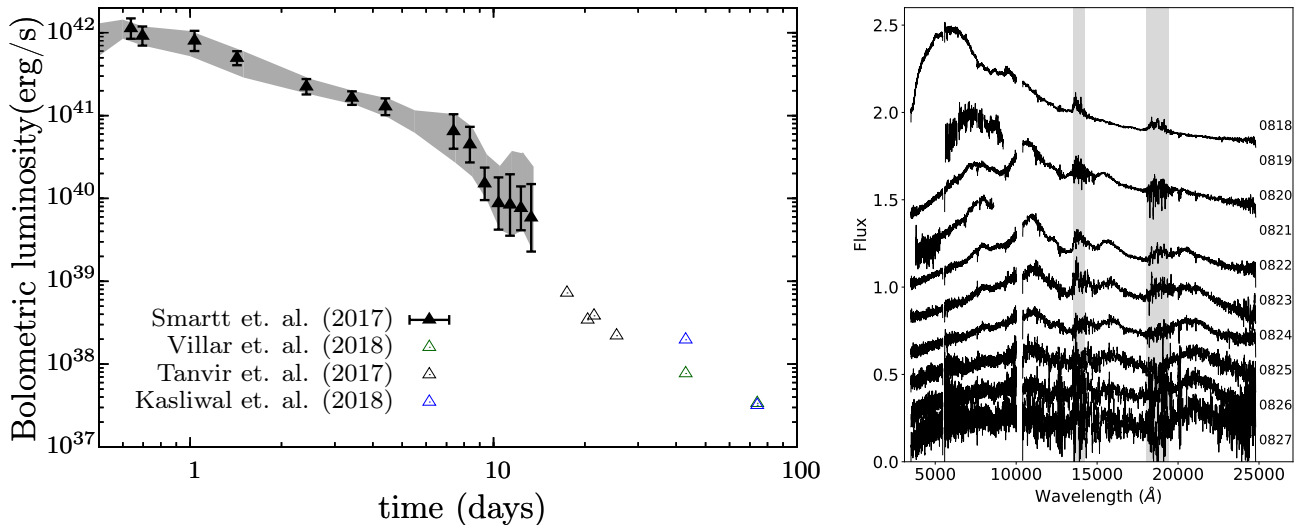


FIG. 10 (left panel) Bolometric light curve of AT 2017gfo, the kilonova associated with GW170817. The filled black triangles are from Smartt *et al.* (2017). Uncertainties derived from the range of values given in the literature (Waxman *et al.*, 2018; Cowperthwaite *et al.*, 2017; Smartt *et al.*, 2017) are shown as a grey band. Also shown are lower limits (empty triangles) on the late-time luminosity as inferred from the Ks band with VLT/HAWK-I (Tanvir *et al.*, 2017) (black) and the $4.5 \mu\text{m}$ detections by the *Spitzer Space Telescope* from Villar *et al.* (2018) (green) and Kasliwal *et al.* (2019) (blue) (adapted from Wu *et al.*, 2019). (right panel) Evolution of the kilonova flux spectrum during the first 10 days. Each spectrum is labelled by the observation epoch. The shaded areas mark the wavelength ranges with very low atmospheric transmission (Reprinted by permission from Springer Nature, Pian *et al.*, 2017).

and MacFadyen, 2018; Mooley *et al.*, 2018), accompanied by secondary X-ray and radio signals.

Within eleven hours of the merger the electromagnetic transient, named AT 2017gfo, was observed in the ultraviolet, optical and near infrared wavelength bands in the galaxy NGC 4993 (Arcavi *et al.*, 2017; Chornock *et al.*, 2017; Coulter *et al.*, 2017; Cowperthwaite *et al.*, 2017; Drout *et al.*, 2017; Evans *et al.*, 2017; Kasliwal *et al.*, 2017; Nicholl *et al.*, 2017b; Pian *et al.*, 2017; Smartt *et al.*, 2017; Soares-Santos *et al.*, 2017; Tanvir *et al.*, 2017). The left panel of Fig 10 shows the bolometric light curve for the two-week-long epoch of detailed observations adapted from Wu *et al.* (2019). The figure also includes late-time observations from the Ks band with the VLT/HAWK-I (Tanvir *et al.*, 2017) and the $4.5 \mu\text{m}$ detections by the *Spitzer Space Telescope* (Villar *et al.*, 2018; Kasliwal *et al.*, 2019). The right panel shows the evolution of the kilonova flux spectra from the X-shooter VLT spectrograph during the first 10 days from Pian *et al.* (2017). Further analysis of these spectra even led to the first identification of an element, Sr (Watson *et al.*, 2019).

The luminosity and its evolution agreed with predictions for the light powered by the radioactive decay of heavy nuclei synthesized via the r-process in the neutron-rich merger ejecta (Li and Paczyński, 1998; Metzger *et al.*, 2010b; Roberts *et al.*, 2011; Barnes and Kasen, 2013; Rosswog *et al.*, 2018) (see section VII). Additional evidence is provided by the spectral/color evolution. The

presence of luminous visual wavelength (“blue”) emission at early times was interpreted by most groups as arising from the fastest outer layers of the ejecta, which contained exclusively light *r*-process nuclei with a relatively low visual wavelength opacity (Metzger and Fernández, 2014; Nicholl *et al.*, 2017b; Drout *et al.*, 2017), see however (Waxman *et al.*, 2018; Kawaguchi *et al.*, 2018). The observed transition of the emission colors to the near-infrared confirmed predictions for the inner ejecta layers containing lanthanide elements, with atomic mass number $A \gtrsim 140$ (Kasen *et al.*, 2013; Barnes and Kasen, 2013; Tanaka and Hotokezaka, 2013).

In order to explain the color evolution of the emission, models with at least two-components are necessary. Simulations suggest that at least three components are necessary to account for the ejecta of neutron star mergers: dynamic, winds, and secular outflows from the disk (Perego *et al.*, 2017a). Combining all observations Villar *et al.* (2017) find a best-fit kilonova model consisting of three-components: a “blue” lanthanide-poor component (opacity $\kappa = 0.5 \text{ cm}^2 \text{ g}^{-1}$) with $M_{\text{ej}} \approx 0.020 M_{\odot}$, moving with a velocity of approximately $0.27 c$, an intermediate opacity “purple” component ($\kappa = 3 \text{ cm}^2 \text{ g}^{-1}$) with $M_{\text{ej}} \approx 0.047 M_{\odot}$ at $0.15 c$, and a “red” lanthanide-rich component ($\kappa = 10 \text{ cm}^2 \text{ g}^{-1}$) with $M_{\text{ej}} \approx 0.011 M_{\odot}$ at $0.14 c$. The three-component model is compatible with a two-component model containing only blue and red components. The blue component is expected to con-

tain light r-process elements with a negligible mass fraction of lanthanides/actinides $X_{\text{lan}} \lesssim 10^{-4}$ (Kasen *et al.*, 2017). The mass fraction of lanthanides/actinides necessary to account for the reddening of the spectra has been inferred to be $X_{\text{lan}} \sim 10^{-3}$ – 10^{-2} (Kasen *et al.*, 2017; Tanaka *et al.*, 2017; Waxman *et al.*, 2018) and hence contains both light and heavy r-process material assuming solar proportions. The purple component corresponds to ejecta with a small, but non-negligible, lanthanide fraction. The early blue emission has been interpreted to originate from the fastest outer layers of the ejecta originating from material ejected in the polar direction and containing exclusively light r-process nuclei (Metzger and Fernández, 2014; Nicholl *et al.*, 2017b; Drout *et al.*, 2017) (see however, Waxman *et al.*, 2018; Kawaguchi *et al.*, 2018, for alternative explanations). The later transition of the emission colors to the near infrared suggest ejecta containing high r-process elements originating from the post-merger accretion disk ejecta given their smaller velocities and larger masses (Siegel and Metzger, 2017; Siegel and Metzger, 2018; Kasen *et al.*, 2017; Perego *et al.*, 2017a; Fernández *et al.*, 2019; Siegel, 2019) (see section VI.B). The total amount of ejecta has been estimated to be $M_{\text{ej}} \approx 0.03$ – $0.08 M_{\odot}$ (Kasen *et al.*, 2017; Kasliwal *et al.*, 2017; Cowperthwaite *et al.*, 2017; Perego *et al.*, 2017a; Villar *et al.*, 2017; Waxman *et al.*, 2018; Kawaguchi *et al.*, 2018). This milestone observation provided the first direct indication that r-process elements are produced in neutron-star mergers including estimates of the amount of ejecta, composition and morphology. Additional information about kilonova modeling and the connection of these observations with models of compact binary mergers can be found in section VII.

III. BASIC WORKING OF THE R-PROCESS AND NECESSARY ENVIRONMENT CONDITIONS

A. Modeling Composition Changes in Astrophysical Plasmas

Before discussing the working of the r-process in detail, a short introduction into the methods should be given, how the build-up of elements in astrophysical plasmas can be described and determined. The mechanism to model composition changes is based on nuclear reactions, occurring in environments with a given temperature and density. Integrating the reaction cross section $\sigma(E)$ over the energy distribution of reacting partners at a given T , abbreviated as $\langle\sigma v\rangle(T)$, determines the probability for reactions to happen. For most conditions in stellar evolution and explosions a Maxwell-Boltzmann distribution is attained (e.g. Clayton, 1968; Rolfs and Rodney, 1988; Iliadis, 2007; Lippuner and Roberts, 2017). Nuclear decays can be expressed via the decay constant λ , related to the half-life of a nucleus $t_{1/2}$ via $\lambda = \ln 2/t_{1/2}$. Interac-

tions with photons (photodisintegrations) are described by the integration of the relevant cross section over the energies of the photon Planck distribution for the local temperature. This results in an effective (temperature-dependent) “decay constant” $\lambda(T)$. Reactions with electrons (electron captures on nuclei) (e.g. Fuller *et al.*, 1980; Langanke and Martínez-Pinedo, 2001; Langanke and Martínez-Pinedo, 2003; Juodagalvis *et al.*, 2010) or neutrinos (e.g. Langanke and Kolbe, 2001, 2002; Kolbe *et al.*, 2003) can be treated in a similar way, also resulting in effective decay constants λ , which can depend on temperature T and density ρ (determining for electrons whether degenerate or non-degenerate Fermi distributions are in place). The λ 's for neutrinos require their energy distributions (Tamborra *et al.*, 2012) from detailed radiation transport, not necessarily reflecting the local conditions (see e.g. Liebendörfer *et al.*, 2005, 2009; Richers *et al.*, 2017; Janka, 2017b; Burrows *et al.*, 2018; Pan *et al.*, 2019).

All these reactions contribute to changes of the abundances Y_i , related to number densities $n_i = \rho Y_i/m_u$ and mass fractions of the corresponding nuclei via $X_i = A_i Y_i$, where A_i is the mass number of nucleus i , $\sum_i X_i = 1$, ρ denotes the density of the medium, and m_u the atomic mass unit. The reaction network equations for the time derivatives of the abundances Y_i include three types of terms (e.g., Hix and Thielemann, 1999)

$$\frac{dY_i}{dt} = \sum_j P_j^i \lambda_j Y_j + \sum_{j,k} P_{j,k}^i \frac{\rho}{m_u} \langle j, k \rangle Y_j Y_k \quad (1)$$

$$+ \sum_{j,k,l} P_{j,k,l}^i \frac{\rho^2}{m_u^2} \langle j, k, l \rangle Y_j Y_k Y_l,$$

summing over all reaction partners related to the different summation indices. The P 's include an integer (positive or negative) factor N^i (appearing with one, two or three lower indices for one-body, two-body, or three-body reactions), describing whether (and how often) nucleus i is created or destroyed in this reaction. Additional correction factors $1/m!$ are applied for two-body and three-body reactions in case two or even three identical partners are involved. This leads to $P_j^i = N_j^i$, $P_{j,k}^i = N_{j,k}^i/m(i,j)!$, or $P_{j,k,l}^i = N_{j,k,l}^i/m(i,j,k)!$. $m(i,j)$ is equal to 1 for $i \neq j$ and 2 for $i = j$, $m(i,j,k)$ can have the values 1 (for non-identical reaction partners), 2 for two identical partners, and 3 for the identical partners. Thus, this (additional) correction factor is 1 for non-identical reaction partners, $1/2=1/2!$ for two identical partners or even $1/6=1/3!$ for three identical partners. The λ 's stand for decay rates (including decays, photodisintegrations, electron captures and neutrino-induced reactions), $\langle j, k \rangle$ for $\langle\sigma v\rangle$ of reactions between nuclei j and k . Although in astrophysical environments true three-body reactions are negligible, a sequence of two two-body reactions — with an intermediate extremely short-lived

nucleus — is typically written as a three-body reaction term, resulting in the expression $\langle j, k, l \rangle$ (Nomoto *et al.*, 1985; Görres *et al.*, 1995). The nuclei involved in the first reaction, including the highly unstable intermediate nucleus, are typically in chemical equilibrium (see below). A survey of computational methods to solve nuclear networks is given in Hix and Thielemann (1999); Timmes (1999); Hix and Meyer (2006); Lippuner and Roberts (2017). The solution of the above set of differential equations provides the changes of individual nuclear abundances for any burning process in astrophysical environments, requiring the inclusion of all possible reactions and the relevant nuclear physics input³. In astrophysical applications the composition changes determined by Eq. (1) cause related energy generation which couples to the thermodynamics and hydrodynamics of the event (Mueller, 1986). For large reaction networks that can be computationally rather expensive due to two effects: (a) nuclear reaction time scales vary by orders of magnitude and the resulting reaction networks represent so-called stiff systems of differential equations which can only be solved with implicit computational methods, requiring huge systems of non-linear equations with several Newton-Raphson iterations. (b) the size of time steps needed to follow nuclear composition changes can be much smaller than those relevant for hydrodynamic changes. For these reasons in most cases the problem is split in a hydrodynamics/thermodynamics part with a limited reaction network, sufficient for the correct energy generation, and postprocessing of the obtained thermodynamic conditions with a detailed nucleosynthesis network (see e.g. Ebinger *et al.*, 2019; Curtis *et al.*, 2019, and references therein).

If matter experiences explosive burning at high temperatures and densities, the reaction rates for fusion reactions and the photodisintegration rates (due to a Planck photon distribution extending to high energies) are large. This will lead to chemical equilibria, i.e. balancing of forward and backward flows in reactions, in particular also for proton or neutron capture reactions $p + (Z, A) \rightleftharpoons (Z + 1, A + 1) + \gamma$ and $n + (Z, A) \rightleftharpoons (Z, A + 1) + \gamma$, corresponding to a relation between the chemical potentials $\mu_p + \mu(Z, A) = \mu(Z + 1, A + 1)$ and $\mu_n + \mu(Z, A) = \mu(Z, A + 1)$, as the chemical potential of photons vanishes. If this is not only the case for a particular reaction, but across the whole nuclear chart, the complete reaction sequence is in chemical equilibrium, i.e. $Z\mu_p + N\mu_n = \mu(Z, A)$, termed complete chemical or also nuclear statistical equilibrium (NSE) (e.g. Clayton, 1968; Hix and Thielemann, 1999). For Boltzmann distri-

butions (which apply in general in astrophysical plasmas, with the exception of highly degenerate conditions, where Fermi distributions have to be utilized for the chemical potentials) (see e.g. Thielemann and Truran, 1986; Bravo and García-Senz, 1999; Yakovlev *et al.*, 2006; Haensel *et al.*, 2007), the abundances of nuclei can be expressed by nuclear properties like the binding energies $B(Z, A)$, the abundances of free neutrons and protons, and environment conditions like temperatures T and densities ρ , leading to the abundance of nucleus i (with Z_i protons and N_i neutrons or $A_i = Z_i + N_i$ nucleons, Clayton, 1968)

$$Y_i = Y_n^{N_i} Y_p^{Z_i} \frac{G_i(T) A_i^{3/2}}{2^{A_i}} \left(\frac{\rho}{m_u} \right)^{A_i - 1} \times \left(\frac{2\pi\hbar^2}{m_u kT} \right)^{3(A_i - 1)/2} \exp\left(\frac{B_i}{kT} \right), \quad (2)$$

where B_i is the nuclear binding energy of the nucleus. G_i corresponds to the partition function of nucleus i , as the ground and excited state population is in thermal equilibrium. Reactions moderated by the weak interaction, i.e. β -decays, electron captures, and charged-current neutrino interactions, change the overall proton to nucleon ratio $Y_e = \sum Z_i Y_i$ and occur on longer time scales than particle captures and photodisintegrations. They are not necessarily in equilibrium and have to be followed explicitly. Thus, as a function of time the NSE will follow the corresponding densities $\rho(t)$, temperatures $T(t)$, and $Y_e(t)$, leading to two equations based on total mass conservation and the existing Y_e

$$\begin{aligned} \sum_i A_i Y_i &= Y_n + Y_p + \\ &\sum_{i, (A_i > 1)} (Z_i + N_i) Y_i(\rho, T, Y_n, Y_p) = 1 \quad (3) \\ \sum_i Z_i Y_i &= Y_p + \sum_{i, (Z_i > 1)} Z_i Y_i(\rho, T, Y_n, Y_p) = Y_e. \end{aligned}$$

In general, very high densities favor heavy nuclei, due to the high power of $\rho^{A_i - 1}$, and very high temperatures favor light nuclei, due to $(kT)^{-3(A_i - 1)/2}$ in Eq. (2). In the intermediate regime $\exp(B_i/kT)$ favors tightly bound nuclei with the highest binding energies in the mass range $A = 50$ – 60 of the Fe-group, but depending on the given Y_e . The width of the composition distribution is determined by the temperature (already derived in Clayton, 1968).

Under certain conditions, i.e. not sufficiently high temperatures when not all reactions are fast enough, especially due to small reaction rates caused by too small Q -values, i.e. proton or neutron binding energies across magic proton or neutron numbers (closed shells), not a full NSE emerges but only certain areas of the nuclear chart are in equilibrium, called quasi-equilibrium groups

³ for data repositories see e.g. <https://jinaweb.org/reaclib/db>, <https://nucastro.org/reaclib.html>, <http://www.kadonis.org>, and <http://www.astro.ulb.ac.be/pmwiki/Brusslib/HomePage>.

(or QSE). This happens e.g. during early or late phases of explosive burning, before or after conditions for a full NSE have been fulfilled (In the latter case this is referred to as “freeze-out”). A typical situation is a break-up in three groups, the Fe-group above Ca ($N = Z = 20$), the Si-group between Ne ($N = Z = 10$) and Ca, the light group from neutrons and protons up to He, and nuclei not in equilibrium from there up to Ne, as discussed in great detail in (Hix and Thielemann, 1999).

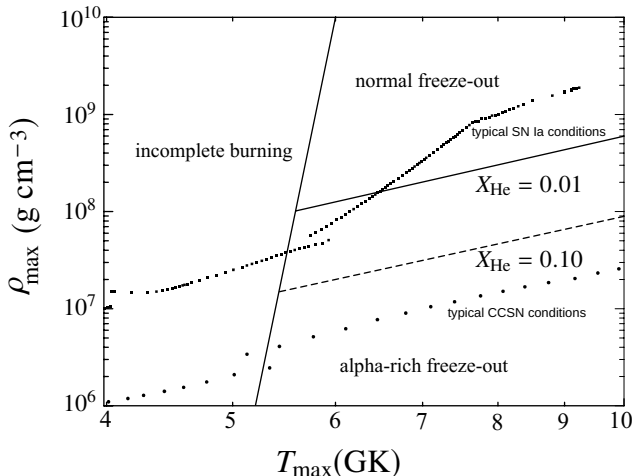


FIG. 11 Plane of maximum temperatures and densities, indicating for explosive Si-burning the boundaries of conditions after freeze-out of charged-particle reactions with an adiabatic expansion for an electron fraction $Y_e = 0.498$. High densities, permitting “three-body” reactions to build-up C (and heavier nuclei), lead a normal freeze-out NSE composition. For lower densities unburned α -particles remain, i.e. the final outcome is a so-called α -rich freeze-out (see the lines of remaining He mass fractions X_{He}). The figure also displays typical conditions experienced in Si-burning mass zones of type Ia and core-collapse supernovae (CCSN), determining the nucleosynthesis outcome of such explosions.

A so-called α -rich freeze-out is a special case of such QSE conditions, when the build-up of nuclei beyond ${}^4\text{He}$ is hampered by the need of “three-body” reaction sequences, involving highly unstable ${}^8\text{Be}$ (e.g. $\alpha + \alpha + \alpha \rightarrow {}^{12}\text{C} + \gamma$ or $\alpha + \alpha + n \rightleftharpoons {}^9\text{Be}$) which are strongly dependent on the density of matter (see Fig. 11). The first part of these reaction sequences involves a chemical equilibrium for $\alpha + \alpha \rightleftharpoons {}^8\text{Be}$ which is strongly shifted to the left side of the reaction equation, due to the half-life of ${}^8\text{Be}$ ($t_{1/2} = 6.7 \times 10^{-17}\text{s}$). Reasonable amounts of ${}^8\text{Be}$, which permit the second stage of these reaction sequences via an alpha or neutron-capture, can only be built-up for high densities. The reaction rates for the combined (three-body) reactions have a quadratic dependence on density in comparison to a linear density dependence in two-body fusion reactions. Therefore, for low densities the NSE cannot be kept and an overabundance of alpha particles (${}^4\text{He}$) remains, permitting only a (much) smaller

fraction of heavier elements to be formed than in an NSE (determined by binding energies of nuclei). This α -rich freeze-out leads to two features: (a) the abundance of nuclei heavier than ${}^4\text{He}$ is (strongly) reduced in comparison to their NSE abundances, and (b) the abundance maximum of the (fewer) heavy nuclei is shifted (via final alpha captures) to heavier nuclei in comparison to an NSE. While this maximum would normally be around Fe and Ni (the highest binding energies) with $A = 50\text{--}60$, it can be shifted up to A about 90.

Other quasi-equilibrium conditions are encountered in proton or neutron-rich environments. The first case permits proton captures and reverse photodisintegrations, causing QSE-clusters along isotonic lines in the nuclear chart, connected via β^+ -decays and/or (α, n) -reactions on longer timescales (see e.g. Rembges *et al.*, 1997). For the second case Burbidge *et al.* (1957) (followed up later by Seeger *et al.*, 1965) postulated already in their 1957 review that isotopic lines in the nuclear chart are in quasi-equilibrium for neutron-rich r-process conditions (i.e. via neutron captures and their reverse photodisintegrations), connected via β^- -decays on longer timescales. The latter will be discussed in more detail with respect to the r-process. Both latter applications act close to the proton or neutron drip-lines. Thus, small reaction Q -values are involved for proton or neutron captures, and also only small photon energies for the inverse reactions are needed to establish such an equilibrium. This changes temperature requirements somewhat. While a full NSE, close to stability with Q -values of the order 8–10 MeV, is only established for temperatures around 4–5 GK (as a rule of thumb temperatures kT need to exceed $Q/30$, Thielemann *et al.*, 2018), for Q -values of the order 1–2 MeV close to the drip-lines such equilibria can still be established at temperatures exceeding about 1–1.5 GK.

B. Special features of the r-process and the role of neutron densities and temperatures

The previous subsection explained how a complete NSE or QSE-subgroups can be established. Here we want to discuss the special case of QSE-subgroups along isotopic chains, before entering a description of the possible sites which permit such quasi-equilibria. When charged-particle reactions are frozen, the only connection between isotopic chains is given by weak processes, i.e. β -decay, or for large mass numbers fission and alpha decay (producing lighter nuclei). High neutron densities make the timescales for neutron capture much faster than those for β -decay and can produce nuclei with neutron separation energies $S_n \sim 2$ MeV and less (close to the neutron-drip line, where S_n goes down to 0). This is the energy gained (Q -value) when capturing a neutron on nucleus $A - 1$ or the photon energy required to release a neutron from nucleus A via photo-disintegration. For tem-

peratures around 1 GK, (γ, n) photodisintegrations in a thermal plasma can still be very active for such small reaction S_n -values (see above). With both reaction directions being faster than astrophysical (and β -decay) timescales a chemical equilibrium between neutron captures and photodisintegrations is attained. This establishes (quasi-)equilibrium clusters along isotopic chains of heavy nuclei. The abundance distribution in each isotopic chain follows the ratio of two neighboring isotopes

$$\frac{Y(Z, A + 1)}{Y(Z, A)} = n_n \frac{G(Z, A + 1)}{2G(Z, A)} \left[\frac{A + 1}{A} \right]^{3/2} \times \left[\frac{2\pi\hbar^2}{m_u kT} \right]^{3/2} \exp\left(\frac{S_n(A + 1)}{kT}\right), \quad (4)$$

with partition functions G , the nuclear-mass unit m_u , and the neutron-separation (or binding) energy of nucleus $(Z, A + 1)$, $S_n(A + 1)$. This relation for a chemical equilibrium of neutron captures and photodisintegrations in an isotopic chain follows from utilizing the appropriate chemical potentials (see the previous subsection) or equivalently due to the fact that the cross sections for these reactions and their reverses are linked via detailed balance between individual states in the initial and the final nucleus of each capture reaction. The abundance ratios are dependent only on $n_n = \rho Y_n / m_u$, T , and S_n . S_n introduces the dependence on nuclear masses, i.e. a nuclear-mass model for these very neutron-rich unstable nuclei. Under the assumption of an $(n, \gamma) \rightleftharpoons (\gamma, n)$ equilibrium, no detailed knowledge of neutron-capture cross sections is needed.

Given that $Y(A + 1)/Y(A)$ first rises with increasing neutron excess before it decreases further out [caused by the last two factors in Eq.(4)], leads to abundance maxima in each isotopic chain which are only determined by the neutron number density n_n and the temperature T . Approximating $Y(Z, A + 1)/Y(Z, A) \simeq 1$ at the maximum, as well as $G(Z, A + 1) \approx G(Z, A)$, the neutron-separation energy S_n has to be the same for the abundance maxima in all isotopic chains, defining the so-called r-process path.

Fig. 12 shows such an r-process path for $S_n \simeq 2$ MeV, when utilizing masses based on the Finite Range Droplet Model FRDM (Möller *et al.*, 1995, for a detailed discussion of nuclear properties far from stability see the following sections IV and V). In environments with sufficiently high neutron densities, the r-process continues to extremely heavy nuclei and finally encounters the neutron shell closure $N = 184$, where fission plays a dominant role. Fig. 12 displays also the line of stability. As the speed along the r-process path is determined by β -decays, being longest closer to stability, abundance maxima will occur at the top end of the kinks in the r-process path at neutron shell closures $N = 50, 82, 126$. After decay to stability at the end of the process, these maxima

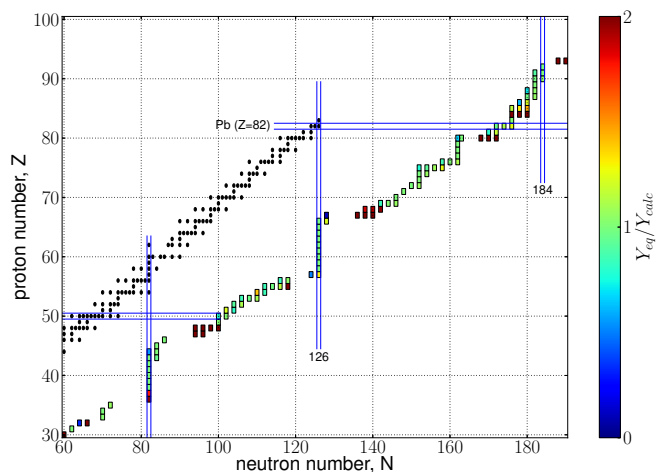


FIG. 12 Shown is (a) the line of stability (black squares) and (b) an r-process path. The special conditions here are taken from a neutron star merger environment which will be discussed further below (Eichler *et al.*, 2015). The position of the path follows from a chemical equilibrium between neutron captures and photo-disintegrations in each isotopic chain ($(n, \gamma) \rightleftharpoons (\gamma, n)$ equilibrium). However, the calculation was performed with a complete nuclear network, containing more than 3000 nuclei. The colors along the path indicate how well the full network calculation follows such an $(n, \gamma) \rightleftharpoons (\gamma, n)$ equilibrium. It can be seen that such full calculations agree with this equilibrium approach within a factor of 2 along the r-process path, which continues to the heaviest nuclei.

appear at the corresponding mass numbers A . These A 's are smaller than those of stable nuclei for the same neutron shell closures. [The latter experience the smallest neutron capture cross sections and cause the s-process maxima].

Fig. 13 shows the regions of the nuclear chart where fission dominates and the location of fission fragments for various mass models and fission barriers. Nuclear properties like mass models, fission, and weak interactions will be discussed in extended detail in the following two sections. Early r-process calculations always made use of an $(n, \gamma) \rightleftharpoons (\gamma, n)$ equilibrium, but had to assume neutron densities, temperatures, and a specific duration time (before the final decay to stability, via β -decay and β -delayed neutron emission) (Burbidge *et al.*, 1957; Seeger *et al.*, 1965; Kodama and Takahashi, 1975). They realized that with such calculations not a unique set of conditions could reproduce solar r-process abundances. Within this approach, and with increasing knowledge of nuclear properties, Kratz and collaborators provided a large series of parameter studies (see e.g. Kratz *et al.*, 1993; Pfeiffer *et al.*, 2001). An optimal fit for the three r-process peaks and the amount of matter in the actinides required a superposition of four components.

Dynamical calculations with varying $n_n(t)$, and $T(t)$, and discarding the $(n, \gamma) \rightleftharpoons (\gamma, n)$ equilibrium, follow the abundance changes in detail (e.g. Blake and Schramm,

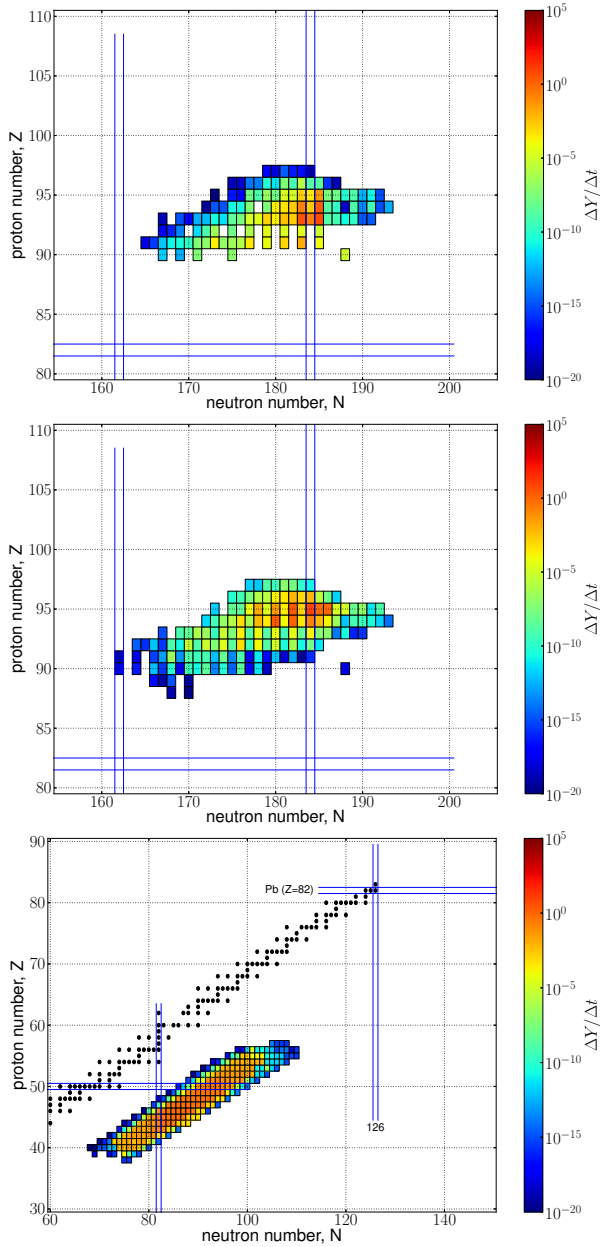


FIG. 13 Color-coded time derivatives of nuclear abundances Y during an r-process simulation (Eichler *et al.*, 2015), describing the destruction via neutron-induced fission (top) and β -delayed fission (center) (Panov *et al.*, 2010) and (bottom) the production of fission fragments (Kelic *et al.*, 2008). The largest destruction rates occur at and close to the neutron closure $N = 184$, due to the smallest fission barriers encountered at these locations. Fission fragments are produced in a broad distribution, ranging in mass numbers A from 115 to 155.

1976; Truran *et al.*, 1978; Cowan *et al.*, 1980; Cameron *et al.*, 1983; Cowan *et al.*, 1985). These calculations showed that the r-process can operate under two different regimes with very different nuclear physics demands (Wanajo, 2007; Arcones and Martínez-Pinedo, 2011): a “hot” r-process in which the temperatures are

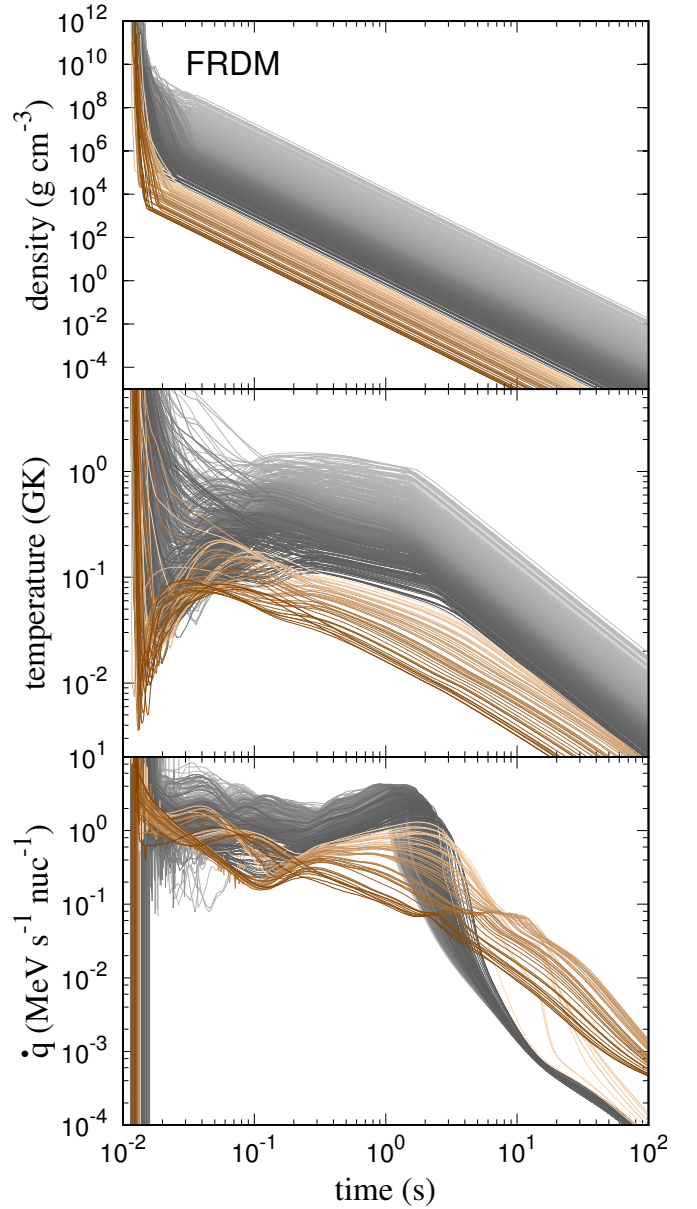


FIG. 14 Evolution of temperature, density, and nuclear energy generation for different trajectories corresponding to material ejected dynamically in neutron star mergers. Gray (brown) lines correspond to the “slow (fast) ejecta” discussed in section VI.B.1. For both gray and brown lines, light (dark) colors correspond to hotter (colder) conditions (adapted from Mendoza-Temis *et al.*, 2015)

large enough to reach $(n, \gamma) \rightleftharpoons (\gamma, n)$ equilibrium and a “cold” r-process in which the temperatures are so low that photodissociation reactions are irrelevant (Blake and Schramm, 1976). Notice that the differentiation between “hot” and “cold” refers to the temperature conditions during the neutron capture phase and not during the earlier phase when the seeds are formed (see next section). Material could be initially very cold and later reheated by nuclear-processes, resulting in a hot r-process or initially

very hot and during the expansion cool to low temperatures producing a cold r-process. In general, astrophysical environments produce a broad range of conditions in which both high and low temperatures are reached, this is illustrated in Fig. 14. In some cases the material can reach such low densities that free neutrons remain after the r-process (brown lines in the figure) with potentially important observational consequences (Metzger *et al.*, 2015). The figure also shows the nuclear energy generation during the r-process (lower panel) that is particularly relevant for very neutron-rich conditions, as expected in dynamic ejecta from neutron star mergers (see section VI.B.1), and for simulations of kilonova r-process electromagnetic transients (see section VII).

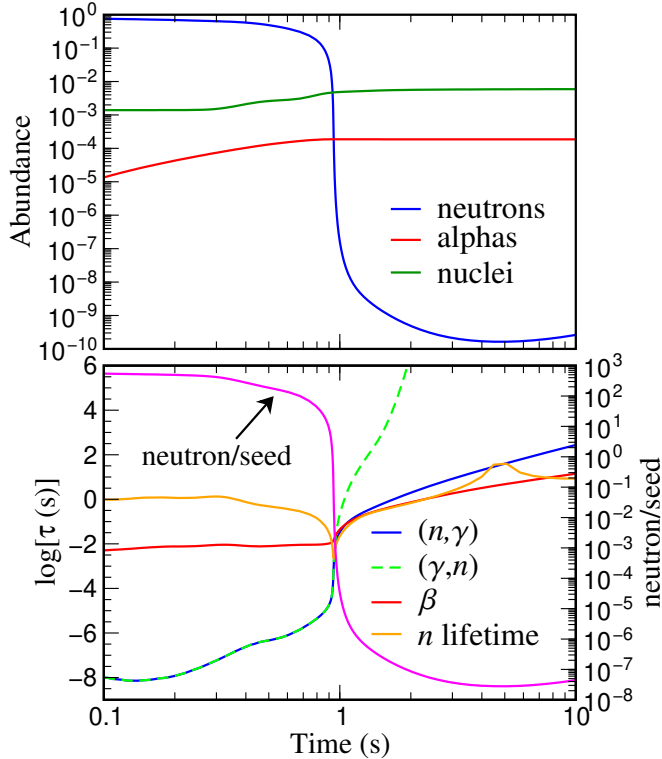


FIG. 15 (Upper panel) Evolution of the abundances of neutrons, alphas and heavy nuclei during the r-process. (Bottom panel) Evolution of the neutron-to-seed ratio and average timescales for neutron captures, photodissociation and β -decays. The absolute value of the neutron lifetime, defined in the text, is also shown. Notice that for $t \lesssim 1$ s neutron capture and photodissociation timescales coincide (courtesy of M.-R. Wu).

Following the freeze-out of charged-particle reactions, the r-process consists typically of two phases: an initial phase dominated by neutron captures and, depending on temperature, photodissociations and a later phase in which neutron captures and β -decays operate on very similar time scales during the decay to stability in what is typically known as r-process freeze-out. The transition between both phases occurs when the neutron-to-seed ra-

tio (i.e. the ratio of free neutrons to heavy nuclei) reaches values close to one. This is illustrated in Fig. 15. The upper panel shows the evolution of the abundances of neutrons, alphas and heavy nuclei for a typical trajectory from those shown in Fig. 14. The lower panel shows the effective neutron lifetime, τ_n , the average radiative neutron capture timescale per nucleus, $\tau_{(n,\gamma)}$, the average photodissociation timescale per nucleus, $\tau_{(\gamma,n)}$, and the average β -decay timescale per nucleus, τ_β , defined as the inverse of their average destruction rates per nucleus for the respective processes:

$$\frac{1}{\tau_n} = \left| \frac{1}{Y_n} \frac{dY_n}{dt} \right| \quad (5a)$$

$$\frac{1}{\tau_{(n,\gamma)}} = \frac{\sum_{Z,A} Y(Z,A) n_n \langle \sigma v \rangle_{A,Z}}{\sum_{Z,A} Y(Z,A)} \quad (5b)$$

$$\frac{1}{\tau_{(\gamma,n)}} = \frac{\sum_{Z,A} Y(Z,A) \lambda_\gamma(Z,A)}{\sum_{Z,A} Y(Z,A)} \quad (5c)$$

$$\frac{1}{\tau_\beta} = \frac{\sum_{Z,A} Y(Z,A) \lambda_\beta(Z,A)}{\sum_{Z,A} Y(Z,A)} \quad (5d)$$

Thus, the latter three equations provide the neutron capture rate on an average seed nucleus (averaged over all nuclei with their abundances $Y(Z,A)$), the photodisintegration (γ, n) rate and the β -decay rate, respectively, being the inverse to the corresponding average reaction time scales.

Fig. 15 shows results of calculations with an initial neutron-to-seed (nucleus) ratio $n_s \sim 600$, allowing for several fission cycles before the end of the r-process, i.e. subsequent sequences of fission, leading to (lighter) fission fragments which can again capture neutrons until heavier nuclei are produced, encountering fission again and the production of fission fragments. The impact of fission cycling, doubling the number of heavy nuclei with each cycle can be seen in the upper panel of the figure by the increase in the abundance of heavy nuclei. A similar increase is also seen in the abundances of alpha particles mainly due to the α -decay of translead nuclei. At early times (< 1 s) the neutron abundance is large and changes slowly with time. This is a consequence of the almost identical (n, γ) and (γ, n) timescales as the temperatures are large enough to maintain $(n, \gamma) \rightleftharpoons (\gamma, n)$ equilibrium. Neglecting the production of neutrons by β -decay and fission one finds the following relation for $1/\tau_n$, corresponding to Eq.(5a), which is equal to the difference between average neutron destructions via neutron capture and productions via photodisintegrations per nucleus, divided by the neutron-to-seed (nucleus) ratio n_s

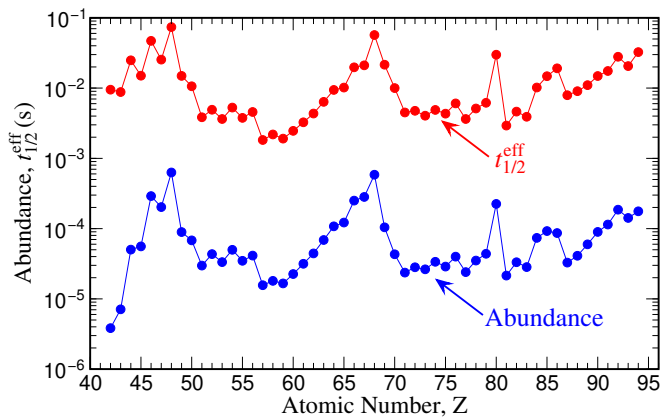


FIG. 16 r-process elemental abundances at freeze-out compared with the effective β -decay half-life of an isotopic chain.

$$\frac{1}{\tau_n} = \frac{1}{n_s} \left(\frac{1}{\tau_{(n,\gamma)}} - \frac{1}{\tau_{(\gamma,n)}} \right) \quad (6)$$

illustrating the important role played by the neutron-to-seed ratio. Whenever $n_s > 1$, the effective neutron lifetime is large and there is enough time for the r-process to pass via successive β -decays through many isotopic chains and to reach a β -flow equilibrium (Kratz *et al.*, 1993; Freiburghaus *et al.*, 1999a). The time derivative $\dot{Y}(Z)$ of the abundance in a whole isotopic chain $Y(Z) = \sum_N Y(Z, N)$, due to β -decays, is given by

$$\begin{aligned} \sum_N \lambda_\beta(Z, N) Y(Z, N) &= Y(Z) \sum_N \lambda_\beta(Z, N) \frac{Y(Z, N)}{Y(Z)} \\ &= Y(Z) \lambda_\beta^{\text{eff}}(Z) = \text{const}, \end{aligned} \quad (7)$$

with $\lambda_\beta^{\text{eff}}(Z)$ being the effective decay rate of the whole chain. In a β -flow equilibrium this flux is constant through all affected Z 's. As decay rates are related to half-lives via $\lambda = \ln 2/t_{1/2}$, the abundance of a complete isotopic chain is proportional to its effective β -decay half-life $Y(Z) \propto t_{1/2}^{\text{eff}}(Z)$ (see Fig. 16).

During this early phase, the r-process path is mainly determined by the two-neutron separation energies, S_{2n} as only even neutron number nuclei are present, due to the pairing effect on binding energies (see Fig. 12). Typically, S_{2n} values decrease smoothly with neutron excess with a sudden decrease at magic neutron numbers. However, for several mass models the S_{2n} are either constant or show a saddle point behavior in regions where there is a transition from deformed to spherical nuclei (or vice-versa) just before or after magic shell closures. This leads also to saddle points in contour lines of constant S_n in the nuclear chart and translates to the appearance of gaps in the r-process path (see Fig. 12) producing troughs in the abundance distribution (Thielemann *et al.*, 1994;

Arcones and Martínez-Pinedo, 2011) before the onset of the freeze-out of neutron captures. These troughs have been extensively discussed in the literature (see e.g. Chen *et al.*, 1995; Pfeiffer *et al.*, 1997, and references therein) as a signature of quenching of the $N = 82$ shell gap. However, whether the related behavior of neutron separation energies is due to quenching of shell effects far from stability or insufficiencies in the challenging treatment of nuclei around the transition from well deformed to spherical is still debated (see e.g. Grawe *et al.*, 2007).

Before freeze-out the nuclei with the strongest impact in the r-process dynamics are those with the longest β -decay half-lives. These are the nuclei closest to the stability at or just after the magic shell closures. Uncertainties in the nuclear physics properties of those nuclei may have a strong impact on the final abundances. This is particularly the case for nuclei located after the $N = 82$ shell closure. This is confirmed by sensitivity studies (see e.g. Mumpower *et al.*, 2016) that explore the impact on r-process abundances due to variations of nuclear properties.

Once the r-process reaches $n_s \approx 1$, there is an important change in the dynamics. Nuclei start to compete for the few available neutrons and the effective neutron lifetime decreases dramatically, see Eq. (6) and Fig. (15). The neutron lifetime increases again once the β -decay timescale becomes shorter than the (n, γ) timescale, resulting in a more gradual decline of n_s at later times. The evolution after $n_s \lesssim 1$ is known as r-process freeze-out. During this phase, the timescales of neutron captures and β -decays become similar. It is precisely the competition between neutron captures and β -decays (often followed by neutron emission) during the decay to stability that is responsible of smoothing the r-process abundances. Just before the freeze-out the abundances exhibit strong oscillations versus mass number. However, after freeze-out they are rather smooth in agreement with the solar system r-process abundances. This is a characteristic feature of the r-process when compared to the s-process. In the latter case, there is (almost) never a competition between β -decays and neutron captures and hence the abundances show a strong sensitivity on A .

Any process that produces neutrons during freeze-out can affect the final abundances. This includes β -delayed neutron emission and fission with the first one dominating for $n_s \lesssim 150$. One should keep in mind that the impact of neutron production is non-local, in the sense that neutrons can be produced in one region of the nuclear chart and captured in another. The freeze-out is responsible of shaping the final abundances. The rare-earth peak is known to be formed during the r-process freeze-out. At low n_s , this is due to a competition between neutron captures and β -decays (Surman *et al.*, 1997), at high n_s , when fission is important, the fission yields play also an important role (Steinberg and Wilkins, 1978; Panov *et al.*, 2008; Gorieli *et al.*, 2013; Eichler *et al.*, 2015).

The freeze-out has also a strong impact on the abundances at the r-process peaks at $A \sim 130$ and 195 (see e.g. [Mendoza-Temis et al., 2015](#)). Due to the large n_s , material accumulates at the $N = 184$ shell closure with $A \sim 280$. During the decay to β -stability the material fissions, producing nuclei with $A \lesssim 140$ and neutrons. Depending on the fission rates and yields used it may result in very different final abundances ([Eichler et al., 2015](#); [Goriely and Martínez-Pinedo, 2015](#); [Vassh et al., 2019b](#); [Giuliani et al., 2019](#)). Neutrons emitted by fission have a strong impact on the abundances of the 3rd r-process peak. Depending on the masses of nuclei around $N = 130$ ([Mendoza-Temis et al., 2015](#)) and the β -decay rates of nuclei with $Z \gtrsim 80$ ([Eichler et al., 2015](#)) the peak could be shifted to higher mass numbers when compared with solar system abundances.

After having discussed here the general working of and the nuclear physics input for an r-process, the following subsection discusses how to obtain the required neutron-to-seed ratios, before discussing the astrophysical sites in section VI. However, independently, the influence of nuclear uncertainties should be analyzed, which will be done in sections IV and V. They can also affect the validity of suitable astrophysical environments. Recent studies of the impact of mass models, β -decay half-lives, and fission rates and fragment distributions have been (among others) performed by [Arcones and Martínez-Pinedo \(2011\)](#); [Eichler et al. \(2015\)](#); [Goriely \(2015\)](#); [Mendoza-Temis et al. \(2015\)](#); [Mumpower et al. \(2016\)](#); [Marketin et al. \(2016b\)](#); [Panov et al. \(2016\)](#); [Mumpower et al. \(2018\)](#); [Vassh et al. \(2019a\)](#); [Giuliani et al. \(2019\)](#); [Vassh et al. \(2019b\)](#).

C. How to obtain the required neutron-to-seed ratios

Explosive environments with high temperatures exceeding about 5 GK, lead to a nuclear statistical equilibrium NSE, consisting of neutrons, protons, and α -particles, as discussed subsection III.A. The Y_e , which affects the NSE composition, is given by the initial abundances and the weak interactions, which determine the overall neutron to proton (free and in nuclei) ratio. Essentially all sites of interest for the r-process, whether starting out with hot conditions or emerging from cold neutron star material, which heats up during the build-up of heavier nuclei, pass through such a phase. Thus, both cases will lead to similar compositions of light particles and nuclei before the subsequent cooling and expansion of matter, still being governed initially by the trend of keeping matter in NSE before the charged-particle freeze-out and the onset of neutron captures in the r-process.

In hot environments the total entropy is dominated by the black-body photon gas (radiation). In such radiation-dominated plasmas the entropy is proportional to T^3/ρ ([Hartmann et al., 1985](#); [Woosley and Hoffman,](#)

[1992](#); [Meyer, 1993](#); [Witti et al., 1994](#)), i.e. the combination of high temperatures and low densities leads to high entropies. Thus, high entropies lead to an α -rich freeze-out (see Fig. 11), and — dependent on the entropy — only small amounts of Fe-group (and heavier) elements are produced, essentially the matter which passed the three-body bottle neck reactions (triple-alpha or $\alpha\alpha n$) transforming He to Be and/or C. This can also be realized when examining Fig. 17, obtained from detailed nucleosynthesis calculations, not assuming any equilibrium conditions. Initially NSE has been obtained. However, dependent on the entropy, different types of charged-particle freeze-out occur, paving the way to the subsequent evolution.

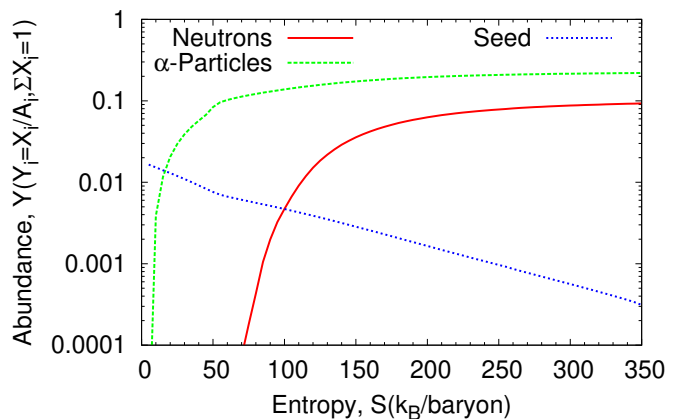


FIG. 17 Abundances of neutrons Y_n , ${}^4\text{He}$ (α -particles) Y_α , and so-called seed nuclei Y_{seed} (in the mass range $50 \leq A \leq 100$), resulting after the charged-particle freeze-out of explosive burning (for a $Y_e = 0.45$), as a function of entropy in the explosively expanding plasma (based on results by [Farouqi et al., 2010](#)). It can be realized that the ratio of neutrons to seed nuclei ($n_s = Y_n/Y_{seed}$) increases with entropy. The number of neutrons per seed nucleus determines whether the heaviest elements (actinides) can be produced in a strong r-process, requiring $A_{seed} + n_s \gtrsim 230$.

The calculation for Fig. 17, starts out with matter in an NSE composition for $Y_e = 0.45$, at $T_0 = 8$ GK and a density ρ_0 corresponding to the given entropy. The expansion from those conditions follows on a so-called free-fall timescale $t_{ff} = (3\pi/(32G\rho_0))^{1/2}$ (the timescale on which a homogeneous gas cloud of initial density ρ_0 would contract). This timescale is comparable to the expansion caused by an explosion. Fig. 17 shows how — with increasing entropies — the alpha mass-fraction ($X_\alpha = 4Y_\alpha$) is approaching a constant value and the amount of heavier elements (which would provide the seed nuclei for a later r-process) is going to zero. This is similar to the big bang, where extremely high entropies permit essentially only the production of elements up to He, and tiny amounts of Li. Opposite to the Big Bang, experiencing very proton-rich conditions, the $Y_e = 0.45$ chosen here is slightly neutron-rich, leading at high entropies predom-

inantly to He and free neutrons. The small amount of heavier nuclei after this charged-particle freeze-out (in the mass range of $A = 50$ – 100), depending on the entropy or α -richness of the freeze-out, can then act as seed nuclei for capture of the free neutrons. Once the charged-particle freeze-out has occurred, resulting in a high neutron-to-seed ratio n_s , the actual r-process — powered by the rapid capture of neutrons — can start, at temperatures below 3 GK. Whether this r-process is a “hot” or “cold” one, as discussed in subsection III.B, depends on the resulting neutron densities and temperatures.

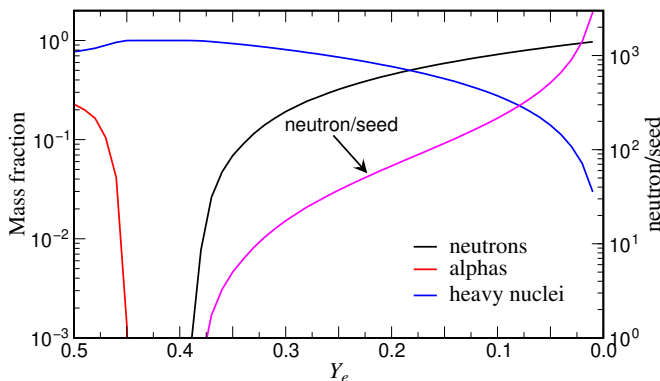


FIG. 18 Evolution of the mass fractions of neutrons, alphas and heavy nuclei versus Y_e (left y-axis scale) and neutron-to-seed (right y-axis scale) at a temperature of 3 GK for an adiabatic expansion with an entropy per nucleon $s = 20 k_B$.

For both cases, the neutron-to-seed ratio n_s determines the mass range of nuclei to be produced. Starting with $A = 50$ – 100 nuclei, the production of lanthanides requires $n_s \sim 50$ while for actinides an $n_s \sim 150$ is needed.

When considering the result of these investigations, there remain two options for a strong r-process in matter which was heated sufficiently to pass through NSE: (a) for moderately neutron-rich conditions with Y_e not much smaller than 0.5, only very high entropies can provide the necessary environment (see Fig.17 and [Freiburghaus et al., 1999a](#)). (b) For very low entropies, when after charged-particle freeze-out only (NSE-)seed nuclei and free neutrons remain ($Y_n + A_{\text{seed}}Y_{\text{seed}} = 1$ with $Y_e = Z_{\text{seed}}Y_{\text{seed}}$) the n_s ratio Y_n/Y_{seed} becomes essentially entropy-independent, $n_s \approx A_{\text{seed}}[Z_{\text{seed}}/(A_{\text{seed}}Y_e) - 1]$, such that only very neutron-rich matter ($Y_e \lesssim 0.15$) can support a strong r-process. Fig. 18 shows such a case of low entropies per nucleon using $s = 20 k_B$, typical for matter ejected in neutron star mergers. It shows several quantities as a function of Y_e . Comparing with Fig. 17 at $S = 20$ ($s = 20 k_B$) and for $Y = 0.45$ one finds consistent results, i.e. essentially only alphas and heavy nuclei (no free neutrons) with typical charges $Z_{\text{seed}} \approx 28$ and $A_{\text{seed}} \approx 63$. Only for $Y_e \lesssim 0.38$ free neutrons start to appear and lanthanides are produced for $Y_e \lesssim 0.25$ (see [Lippuner and Roberts, 2015](#), for a systematic study of

the astrophysical conditions necessary to produce lanthanides).

IV. EXPERIMENTAL DEVELOPMENTS FOR R-PROCESS STUDIES

The r-process path runs through nuclei with extreme neutron excess. Most of these nuclei have yet not been produced in the laboratory and their properties are experimentally unknown. Hence the major nuclear physics input required for r-process simulation must largely be modelled, although recent measurements have led to a significant decrease in uncertainties. Intermediate-mass r-process nuclei could be produced at existing radioactive ion-beam facilities like CERN/Isolde, GSI and, and more recently in particular, RIKEN. Significant advance, however, is expected in the future when key r-process nuclei, including those around the third r-process peak, become accessible at the next-generation RIB facilities like FAIR and FRIB. This will be discussed in more detail in the following sections. Data taken at these facilities will not only directly substitute theory predictions, but will also serve as stringent and valuable constraints to advance model predictions for even then not accessible nuclei.

The next two sections deal with the nuclear ingredients needed for r-process simulations. At first we will discuss the various experimental approaches to produce and study neutron-rich nuclei and summarize the experimental data relevant for r-process nucleosynthesis which have been achieved recently. In the next section we present the nuclear models applied to interpret the experimental results and derive the vast nuclear data sets needed for large scale simulations. We will focus on theoretical advances achieved by improved models and experimental constraints and guidance, and finally discuss the impact on the improved nuclear data on our understanding of r-process nucleosynthesis.

There has been considerable experimental effort over the last forty years to explore the nuclear physics of the r-process and the structure and properties of r-process nuclei along the projected reaction path; a goal that is nearly equivalent with exploring the evolution of nuclear structure towards the limits of stability. This was one of the strong motivations towards the development of facilities capable of producing radioactive ion beams. The experiments have concentrated on measurement of masses, β decay and β -delayed neutron emission probabilities of neutron-rich nuclei towards and even at the anticipated r-process path. More recently new methods are developed for the study of neutron capture reactions on nuclei near or at the r-process path. A multitude of experimental probes have been used to facilitate the production and separation of very neutron-rich short-lived nuclei and to measure their specific properties. The traditional tools in the past ranged from extracting fission

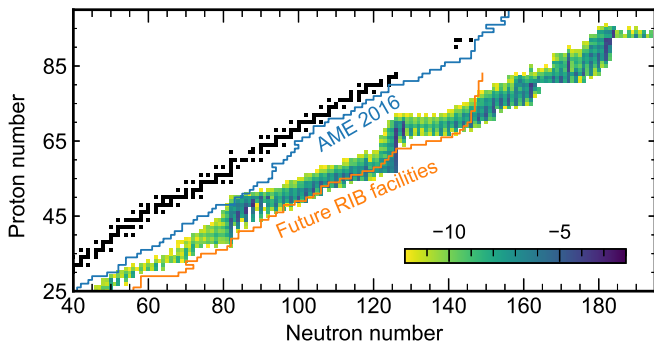


FIG. 19 The nuclear chart with stable nuclei indicated by black squares, the limit of known masses from the Atomic Mass Evaluation 2016 (blue line), the future reach of Radioactive Ion Beam (RIB) facilities (like FRIB or FAIR), and abundance results (color coded) at neutron freeze-out from an r-process calculation taken from (Giuliani *et al.*, 2019), utilizing the FRDM mass model, combined with Thomas-Fermi fission barriers. (courtesy Samuel A. Giuliani)

products from reactors to the use of spontaneous fission sources, to the analysis of short-lived reaction products at spallation and fragmentation facilities. The enormous progress in producing neutron-rich isotopes with increasing intensity and resolution was enabled by the simultaneous progress in the development of new experimental techniques and detectors. The traditional approach of tape-collection and decay analysis leading to half-life and β -endpoint determination for single separation products was replaced by large scale ring experiments for measuring hundreds of masses at once, or complementary to that by sophisticated trapping experiments for determining the masses and decay properties of individual neutron-rich nuclei with unprecedented accuracy. The utilization of these facilities and techniques produced and will produce a wealth of data, which primarily address the needs for knowledge about the properties of neutron-rich nuclei near or at the r-process path (see Fig.19).

These studies provided important information and input for r-process simulations based on the $(n, \gamma) \rightleftharpoons (\gamma, n)$ equilibrium assumptions. Specific challenges remained, such as the (n, γ) nuclear cross section reaction data for simulating the r-process nucleosynthesis after freeze-out. The associated reaction cross sections and reaction rates that are now used in dynamic r-process simulations rely entirely on statistical model calculations, utilizing Hauser-Feshbach codes like SMOKER, NON-SMOKER⁴, and TALYS⁵. It is not clear how reliable these predictions for the (n, γ) reaction rates are and how valid they are for reactions on neutron-rich closed-shell nuclei that are characterized by low Q -values (neutron binding ener-

gies) (Rauscher *et al.*, 1997). In fact, it is expected that far from stability the direct capture component dominates, permitting possibly an $(n, \gamma) \rightleftharpoons (\gamma, n)$ equilibrium down to low temperatures (Mathews *et al.*, 1983), but how reliable are the predictions for the strength of such direct capture components (Goriely, 1998; Arnould *et al.*, 2007)? A direct measurement of neutron capture reactions on short-lived neutron-rich nuclei is challenging and certainly not feasible within the near future. The experimental developments have focused on two approaches that combine theory and experiment in order to get at the neutron capture cross-sections, the β -Oslo method (Spyrou *et al.*, 2014, 2017; Tornyi *et al.*, 2014; Guttormsen *et al.*, 1987) and surrogate reactions (Escher *et al.*, 2012; Kozub *et al.*, 2012; Manning *et al.*, 2019; Tang *et al.*, 2020), mostly (d, p) to get access to (n, γ) rates. New initiatives have also recently been proposed for direct neutron capture studies at ring experiments (Reifarth *et al.*, 2017). This proposal is particularly challenging since the idea is to combine, for the first time, a method that couples radioactive beam with radioactive target experiments.

Below, we discuss in detail the facilities and approaches presently used for the production of neutron-rich nuclei on or near the r-process path, along with some of the noteworthy experimental developments in tools and techniques that allow measurements of nuclear masses, β -decay rates, β -delayed neutron emission probabilities, and neutron capture rates of nuclei required as inputs for reliable simulations of the r-process.

A. Production of neutron-rich isotopes

The biggest challenge in experimentally studying isotopes near or at the r-process path is the production of these isotopes in sufficient abundances to explore their properties. This is closely correlated with the selectivity of the separators necessary to select the isotopes in question and the sensitivity of the detectors for measuring the respective properties. The overall production of rare isotopes has not significantly improved over the last decades due to the cross section limitations in the production reactions, or the energetics of the facilities to produce beams. However, substantial improvements have been made in the selection process due to innovative techniques in the isotope separation through electro-magnetic systems and the increasing utilization of laser based separation techniques. Also, enormous progress has been made on the detection side, and the development of ion trapping techniques has overcome many of the statistical limitations in the more traditional measurements of lifetimes, masses, and direct measurements of β -delayed neutron emission probabilities of the very neutron-rich nuclei. This section addresses the production of neutron-rich nuclei in reactors, in spontaneous fission sources, in

⁴ <https://nucastro.org/reactlib.html>

⁵ <http://www.talys.eu/more-about-talys>

fission products in accelerators, at spallation sources or ISOL facilities, and at fragmentation facilities.

1. Nuclear reactors and fission product sources

One of the traditional methods for the production of neutron-rich nuclei is the extraction and separation of neutron-rich fission products from high flux nuclear reactors. Pioneering work has been done at the TRIS-TAN separator (McConnell and Talbert, 1975; Talbert *et al.*, 1979) at the Ames Laboratory Research Reactor in Iowa which was moved in the mid 1970's to the 60 MW High Flux Beam Reactor (HFBR) at Brookhaven National Laboratory (Crease and Seidel, 2000). The fission products were ionized, extracted from a ^{235}U target placed in an ion source located in a beam line close to the reactor core, and separated. A similar separator was installed at the High Flux Reactor of the Institute Laue Langevin (ILL) in Grenoble, where the LOHENGRIN fission fragment separator is used to extract and analyze fission products in order to study their decay properties (Armbruster *et al.*, 1976). This facility was complemented by the installation of thermoionization separators, OSTIS I & II. The OSTIS separator concept (Wünsch, 1978; Münzel *et al.*, 1981) was based on the use of an external neutron guide line bombarding an external ^{235}U source. This approach allowed the measurement of shorter-lived fission products since it reduced the transport times to the ion-source. Studies of neutron-rich nuclei were also performed at smaller reactors, even at the Californium fission source (CARIBU) (Pardo *et al.*, 2016) at Argonne National Laboratory, as long as separators were available to select the desired fission product. Measurements of masses, decay half-lives, β -delayed neutron emission probabilities, and γ -ray decay properties were performed with the best techniques available, utilizing moving tape systems. The measurement of neutron-rich isotopes reached close to some of the r-process trajectories, in particular for the alkali isotopes. The measurements on the neutron-rich Rubidium isotopes made at that time (Kratz, 1984) are only rivaled now some thirty years later (Lorusso *et al.*, 2015). The main handicaps, for reaching the r-process path and mapping the very neutron-rich nuclei, were the fission product distribution and long extraction times for the fission products. All of these measurements had limitations that were overcome with the new advances and technical developments in detectors, including new neutron detection technologies based on ^6Li -glass, ^3He tubes, and ^3He spectrometer systems (Kratz *et al.*, 1979; Yeh *et al.*, 1983).

2. Spallation sources and ISOL techniques

The on-line separators for fission products were complemented by ISOLDE (Isotope Separator On-Line Detector), designed in the mid-sixties for separating spallation products produced by impinging 600 MeV protons from the synchro-cyclotron at CERN on a stationary target. The spallation of the heavy target nuclei produced a distribution of target fragments, which were extracted and filtered to separate the desired isotope. The time required for extraction placed a lower limit on the half-life of isotopes which could be produced by this method. Once extracted, the isotopes were directed to one of several detector stations for measuring the decay properties. The ISOLDE separator was moved in 1990 to the CERN PS booster to increase the yield of the spallation products (Kugler *et al.*, 1992). In a two-step process, the 1 GeV proton beam from the PS-Booster, impinging on a Ta or W rod positioned in close proximity to the uranium-carbide target, produced the fast spallation neutrons to induce fission. This method was essential for suppressing the proton-rich isobaric spallation products that dominated the spallation yield. The new ISOLDE system was one of the most successful sources for neutron-rich isotopes and dominated the production of neutron-rich isotopes for nearly two decades. The implementation of laser ion-source techniques for improving the Z -selectivity was a significant improvement to studies of neutron-rich nuclei. The laser ionization of the fission products led to a significant reduction in isobar background. This was further improved by using the hyperfine splitting to select or separate specific isomers in neutron-rich isotopes. These gradual improvements of ion source and separator techniques finally led to the detailed measurement of the r-process waiting point nucleus ^{130}Cd , the first milestone in reaching and mapping the r-process path (Kratz *et al.*, 2000; Dillmann *et al.*, 2003), as well as the recent mass measurements of $^{129-131}\text{Cd}$ nuclei (Atanasov *et al.*, 2015) near the doubly closed magic shell nucleus of ^{132}Sn , a capability that is unmatched to date.

3. Fragmentation sources

Another successful technique for the production of neutron-rich isotopes is the use of fragmentation for the production of neutron-rich, or fusion-evaporation for the production of neutron-deficient, isotopes in heavy ion reactions. The GSI Online Mass Separator was one of the first instruments to utilize fusion-evaporation for studying isotopes far from stability using heavy-ion beams from the UNILAC accelerator. The reaction products were stopped in a catcher inside an ion source, from where they were extracted as singly charged (atomic or molecular) ions and re-accelerated to 60 keV. These

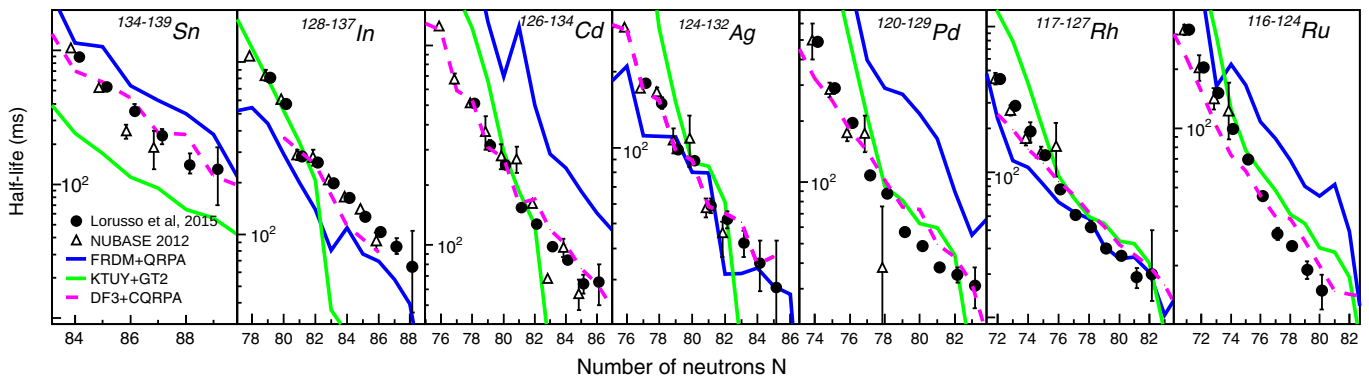


FIG. 20 β -decay half-lives measured by Lorusso *et al.* (2015) (solid circles) for a number of isotopic chains as a function of neutron number, compared with the 2012 NUBASE evaluation (Audi *et al.*, 2012) (open triangles) and the predictions of the models: Finite Range Droplet Model with Quasi Random Phase Approximation FRDM-QRPA (blue) (Möller *et al.*, 2003), Gross Theory KTUY-GT2 (green) (Tachibana *et al.*, 1990; Koura *et al.*, 2005), Fayans Density Functional with Continuum Quasi Random Phase Approximation DF3-CQRPA (magenta) (Borzov *et al.*, 2008) when available. (figure from Lorusso *et al.*, 2015)

beams were implanted, yielding sources for β or particle decay spectroscopy (Bruske *et al.*, 1981). This method, however, was more suitable for the study of neutron-deficient isotopes and remained not competitive with fission product or spallation based production of neutron-rich isotopes. This instrument was gradually replaced by the Projectile Fragment Separator FRS to focus on the neutron-rich side of the line of stability (Geissel *et al.*, 1992). Fragmentation was based on smashing a high energy heavy ion beam on light target material and collecting the fragments through electromagnetic separator systems for subsequent on-line analysis. The great advantage of this technique over the traditional ISOL approach was that even short-lived isotopes could be studied if properly separated. Fragmentation played an increasingly important role for β -decay studies of r-process isotopes both at the fragment separators at GSI (Kurcewicz *et al.*, 2012), at NSCL/MSU in the US (Quinn *et al.*, 2012), and RIKEN in Japan (Lorusso *et al.*, 2015). The measurement of a very neutron-rich, doubly closed shell nucleus, ^{78}Ni , at the on-set of the r-process, presented a particularly impressive example on the new relevance of fragment separators for the study of r-process nuclei (Hosmer *et al.*, 2005). The simultaneous measurement of the half-lives of 110 neutron-rich nuclei near the $N = 82$ closed shell at RIKEN (Lorusso *et al.*, 2015) proved a substantial step forward for studies of r-process nuclei (see Fig. 20). Another example is the systematic study of β -decay half-lives and β -delayed neutron emission processes using the BELEN ^3He detector array for 20 heavier isotopes of Au, Hg, Tl, Pb, and Bi in the neutron-rich mass region above the neutron shell closure $N = 126$ (Caballero-Folch *et al.*, 2016) to probe the feeding pattern of the third r-process peak at $A \approx 195$ in astrophysical studies (Caballero *et al.*, 2014; Eichler *et al.*, 2015).

B. Experimental Achievements in Measuring Nuclear Properties

In the following section, we want to discuss in more detail the experimental progress in measuring the different nuclear parameters that have been achieved over the four decades of studying nuclei far off the neutron-rich side of stability.

The production of neutron-rich isotopes at ISOL-based systems, both at reactors as well as at spallation facilities, was mainly limited by the chemistry and extraction time from the ion source. Large effort went in the development of suitable target materials and ion source techniques (Ravn *et al.*, 1975). The choice of isotopes for the study of masses, half-lives and other decay properties was often dictated by the availability of isotope products rather than by physics priorities (Kratz, 2001).

However, during the last decade fragmentation techniques improved enormously. They allowed the measurement of much shorter lived neutron-rich radioisotopes, since they were not handicapped by chemical delay processes that were typical for ISOL target systems. With the right target and projectile combination they were able to reach far beyond the range accessible by ISOL facilities. Yet in other cases, such as noble gas and alkali elements, the chemistry conditions are advantageous for ISOL production techniques yielding superior beam intensities. Recent measurements of neutron-rich Rb isotopes (Lorusso *et al.*, 2015) are still at the limits reached at ISOLDE twenty years earlier (Kratz, 1984; Lhersonneau *et al.*, 1995a,b).

Based on the availability of these complementary isotope production modes, during the last decades several new technical developments led to an enormous improvement in the study of r-process masses and decay properties. These were partly driven by the development of

larger high efficiency detection devices, but also by new techniques using storage ring technology to determine masses of multiple isotopes at once, instead of painstakingly extracting and probing one isotope after the other. Other advances were based on the development of laser traps designed to trap only a few of the selected and collected neutron-rich isotopes and determine their masses and decay characteristics with unprecedented accuracy. The most significant developments will be discussed in the following sections.

1. The experimental study of nuclear masses

Mass measurements of selected isotopes near stability were traditionally performed using mass spectrometers based on magnetic and electric sector fields for separating single isotopes. Modern experimental methods of mass measurement of rare isotopes are generally based on three experimental techniques. Time-of-flight mass spectrometry (TOF-MS) (Meisel and George, 2013) is based on the velocity measurement of short-lived isotopes produced in fragment processes that are analyzed in single-pass spectrometers. The other techniques are frequency-based spectrometry of isotopes in storage rings using Schottky pick-up signals of rapidly circulating particles (Litvinov *et al.*, 2004) and Penning traps capable of making measurements with even single trapped particles (Blaum, 2006; Blaum *et al.*, 2013). The TOF and frequency-based methods are often mentioned as direct mass measurement methods because unknown masses (in fact, mass-to-charge ratios) are directly determined by calibration with well-known masses.

Indirect methods usually rely on the measurement of the energy balance in reaction or decay processes of the isotopes in question. The unknown mass is calculated from known ones in the reaction or decays, plus the determined Q values. This classical approach requires a substantial production of the radioactive isotopes in question to ensure sufficient statistical reliability of the data.

Mass measurements in storage rings

Spectrometry of masses at storage rings allows the simultaneous measurements of many nuclei. The ions produced at fragmentation facilities are then stored in storage rings where the relative frequencies of ion revolutions or relative revolution times of the stored ions are related to their relative mass to charge ratios and velocities (Yan *et al.*, 2016). In order to measure the masses of the ions in storage rings, the ions are cooled in order to minimize the velocity spread. The cooling process requires time, and therefore limits the half-lives that can be measured. This was the principle of the Schottky Mass Measurement Method (Radon *et al.*, 2000; Litvinov

et al., 2004). Another approach, named the Isochronous Mass Spectrometry (Hausmann *et al.*, 2000, 2001; Sun *et al.*, 2008) removed the limitation on half-lives since it does not depend on cooling. This ISM approach resulted in a reduction of the velocity spread by injection of the ions into the isochronous ion optical mode of the ring. That is, the fast and slow ions of the same species are deliberately placed in the longer and shorter orbital paths, respectively, of the ring in order to yield essentially the same revolution frequency and therefore a reduced velocity spread. Two facilities use these methods for mass measurements at storage rings, the GSI Helmholtz Center in Germany and the Institute of Modern Physics in Lanzhou, China. While these two methods have been used mainly for neutron-deficient nuclei, the masses of $^{129,130,131}\text{Cd}$ have been recently measured at GSI (Knöbel *et al.*, 2016). There are ongoing plans to implement the same approaches at the Radioactive Ion Beam Factory in RIKEN and the future FAIR facility at GSI.

Mass measurements in traps

Measurements of masses in traps have yielded the most precise and accurate mass measurements to date, and present a significant advance over any other methods, including the storage rings and the traditional β -endpoint measurements. There are basically two types of traps. Paul traps are based on radio-frequency confinement of ions and Penning traps use electromagnetic fields to trap ions (magnetic fields for radial confinement and electrostatic ones for axial trapping). Coupling of traps to fragmentation or spallation facilities or coupling to spontaneous fissioning sources has tremendously extended the reach of high precision and high accuracy measurements, setting new worldwide standards for studies of this very fundamental property of the nucleus and its impact on simulations of the r -process (Blaum, 2006; Blaum *et al.*, 2013). There are now numerous facilities worldwide, including the Canadian Penning Trap at Argonne National Laboratory; LEBIT at the National Superconducting Cyclotron Laboratory at MSU in the USA; TITAN at TRIUMF in Canada; JYFLTRAP in Jyväskylä, Finland; SHIPTRAP at GSI Darmstadt and MAFFTRAP in Munich, Germany; ISOLTRAP at CERN; and RIKEN trap at the SLOWRI facility in Japan. Many of the facilities have implemented or intend to implement MRTOF devices (multi-reflection time-of-flight spectrographs) to increase the purity of the ions as well as the range of short-lived exotic nuclei that can be measured. ISOLTRAP at CERN was a pioneer in the field of traps, reaching an uncertainty of a few parts in 10^8 with a resolving power of up to 10^6 with nuclear half-lives in the order of seconds (Eliseev *et al.*, 2013). Exotic neutron-rich nuclei with shorter half-lives required much greater re-

solving power and led to the introduction of the phase-imaging ion-cyclotron resonance technique (Eliseev *et al.*, 2013). This new technique is based on determining the frequency of the ion by the projection of the ion motion in the trap onto a high resolution position sensitive micro-channel plate detector. The method has been shown to increase the resolving power forty-fold, and at the same time, to tremendously increase the speed with which measurements can be made. The higher precision of the measurements has a strong impact on attempts to distinguish sites of the r-process (Mumpower *et al.*, 2015, 2016, 2017b). Recent highlights include precision mass measurement of neutron-rich Neodymium and Samarium Isotopes at the CARIBU facility (Orford *et al.*, 2018), of neutron-rich rare-earth isotopes at JYFLTRAP (Vilen *et al.*, 2018), and neutron-rich Gallium isotopes at TITAN (Reiter *et al.*, 2020).

2. Beta-Decay Studies

Beta-decay measurements are critical for the determination of the half-lives of nuclei along the r-process path and for investigating the decay patterns that form the final r-process abundance distribution along the line of stability. Beta-decay measurements are typically challenged by the detection efficiency of electrons and neutron-rich ions. This not only requires high production rates at radioactive beam facilities but also sophisticated detector arrangements. New pioneering results for half-lives along the r-process path have been measured at RIKEN using stacking of eight silicon double-sided strip detectors such as WAS3ABi (Wide-range Active Silicon-Strip Stopper Array for Beta and ion detection) (Lorusso *et al.*, 2015; Wu *et al.*, 2017) surrounded by an array of 84 High Purity Germanium detectors (HPGe) of the EURICA array (Söderström *et al.*, 2013). The results are shown in Fig. 20, with a substantially lower experimental uncertainty than previous results, but also indicating substantial disagreements with the theoretical half-life predictions (see also section V). While silicon has been an excellent choice as detector material, other materials such as Ge with higher Z have recently been commissioned at the NSCL fragmentation facility for use with β -decay experiments. The GeDSSD array (Germanium Double-Sided Silicon Detector) shows 50% electron efficiency and greater mechanical stability in allowing the manufacture of thicker detectors (Larson *et al.*, 2013). TRIUMF in Canada has also developed the Scintillating Electron-Positron Tagging Array (SCEPTAR) comprised of 20 thin plastic scintillator beta detectors that surround the implantation point of radioactive ion beams inside a central vacuum chamber surrounded by 16 Clover type, large volume Germanium detectors. SCEPTAR has been shown to have an efficiency of $\sim 80\%$ for electrons emitted from radioactive decays, and also provides information

on their directions of emission in order to veto background in the surrounding GRIFFIN HPGe detectors from the bremsstrahlung radiation produced by the stopping of the energetic beta particles. Neutron-rich nuclei are transported to the center of GRIFFIN by a moving tape collector (MTC) system. The efficiency of this approach has been beautifully demonstrated with the measurements of the β -decay half-lives of ground state and two isomeric states in ^{131}In and the subsequent γ -decay patterns of ^{131}Sn (Dunlop *et al.*, 2019). The sensitivity of this experiment allowed the first detection of γ -rays following β -delayed neutron decay for $^{131}\text{In} \rightarrow ^{130}\text{Sn}$, an important decay branch for many r-process nuclei.

3. Beta-delayed neutron emission probability measurements

Beta-delayed neutron emission changes the availability of neutrons and is particularly important since the delayed neutrons can significantly change the abundances of neutron-rich nuclei during freeze-out. While the probabilities of β -delayed neutron emission (P_n) are of great impact for r-process simulations, as well as nuclear power reactor designs (for early work see e.g. Kratz and Herrmann, 1973; Kratz *et al.*, 1982), the experimental situation is quite poor since very few of the P_n -values have been measured. Facilities capable of producing neutron-rich nuclei by fragmentation, spallation, or fission sources have invested in a variety of approaches to measure these P_n -values.

A number of neutron detection techniques were applied, but multiple counter systems, consisting of a number of ^3He counters embedded in a paraffin matrix to thermalize the neutrons for better efficiency, emerged as a standard approach for these kind of studies. One more recent example was the neutron counter NERO (Pereira *et al.*, 2010), developed at the NSCL/MSU to measure the P_n -values of neutron-rich isotopes in the lower mass range that was accessible using fragment production and separation at the A1900 separator. NERO consists of sixty ^3He counters embedded in a polyethylene matrix surrounding the collection station to maximize counting efficiency. The efficiency was tested using a ^{252}Cf spontaneous fissioning source and the energy detection range of the detectors was expanded using (α, n) reactions on various target materials. NERO was utilized primarily for the study of medium mass nuclei in the Co to Cu region (Hosmer *et al.*, 2010) and in the range of very neutron-rich Y, Mo, and Zr isotopes (Pereira *et al.*, 2009), pushing the experiments to nuclei in the $N=82$ closed neutron shell region (Montes *et al.*, 2006).

The BELEN (BEta-deLayEd Neutron) detector array is another development of a neutron counter that follows the same concept as NERO. BELEN was conceived as a modular detector that has been developed in preparation for experiments at FAIR. Specifically, the DEcay SPEC-

troscopy (DESPEC) experiment at FAIR is planned for the measurement of β -decays in an array of Double Sided Silicon Detectors (DSSD) called AIDA, in coincidence with the ^3He neutron detectors of BELEN, in order to measure P_n -values of exotic nuclei. BELEN-20 consists of two concentric rings of ^3He counters (8 and 12 counters, respectively), arranged inside a polyethylene neutron moderator. Early measurements included testing the system by transporting a beam of ions to the center of the neutron detector in front of a Si detector to measure the β -decay (Gómez-Hornillos *et al.*, 2011). The most current version of BELEN includes 48 ^3He tubes (Calvino *et al.*, 2014; Agramunt *et al.*, 2016) and was recently tested, similarly to BELEN-20, at Jyvaskyla, with fission products produced from the proton-induced fission of Thorium. Fission products were swept away by a Helium gas jet system into a double Penning trap system that acts as a mass separator, resulting in a relatively pure beam of β -decaying products. The transport system takes on the order of a few hundred milliseconds and imposes a limitation on the lifetimes that can be studied. The BELEN detector is soon to become a part of the largest ever neutron detector of its kind as a part of a 160 ^3He counter arrangement being built by the BRIKEN collaboration for measurements of exotic nuclei at RIKEN. The challenges that remain are the trade-offs between the highest efficiencies and the best energy resolutions for the detection of neutrons. First measurements at the GSI fragment separator focused on the study of nuclei around the $N = 126$ closed shell in the Au to Rn range, in order to determine the half-lives of these isotopes and the P_n -values, to compare with theoretical model predictions (Caballero-Folch *et al.*, 2016). This work demonstrated that the FRDM+QRPA (Finite-Range Droplet Model coupled with the Quasiparticle Random Phase Approximation) predictions differ sometimes by up to an order of magnitude from the experimental values. These discrepancies between theoretical predictions and experimental result underline the importance of such studies for exploring the evolution of nuclear structure towards the r-process path and beyond.

Recently, a new technique was demonstrated in which the challenges of neutron detection are circumvented by measuring the nuclear recoil (Yee *et al.*, 2013), instead of the neutron energy, using traps. The traps can confine a radioactive ion and basically β -decay at rest. The emitted radiation emerges with minimal scattering, allowing the measurement of the ion recoil. The β is measured in coincidence with the ion, recoiling due to neutron emission, resulting in a time of flight spectrum. The proof of principle was demonstrated with a ^{252}Cf fission source, where fission fragments are thermalized in a large volume gas catcher, extracted, bunched, trapped and mass separated in a Penning trap, then delivered into a β -decay Paul Trap (BPT). The β -particles are detected in a ΔE -E plastic scintillator while the recoil ions are detected in

a microchannel plate detector. The technique allows the measurements of exotic isotopes with half-lives as short as 50 ms while avoiding some of the complications of neutron measurements (Munson *et al.*, 2018; Siegl *et al.*, 2018).

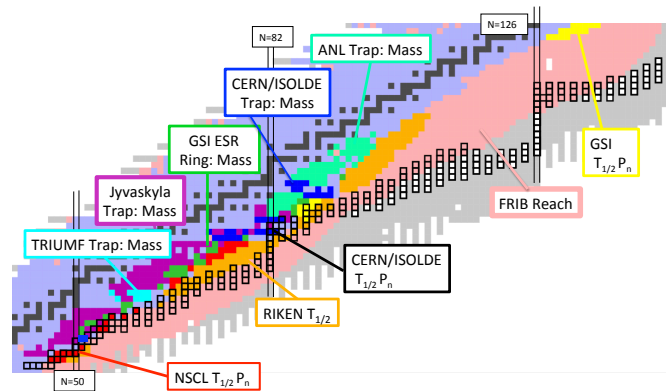


FIG. 21 A summary of recent efforts undertaken at experimental facilities world-wide (see Horowitz *et al.*, 2019) in order to attain precise (a) nuclear masses and (b) β -decay properties like half-lives $T_{1/2}$ and delayed neutron probabilities P_n . The individual results at TRIUMF, Jyvaskyla, GSI, CERN, ANL, NSCL, and RIKEN (discussed earlier in this section) are indicated via color-coding. Shown is also the region in the nuclear chart in reach of the RIB facilities.

Fig. 21 provides a summary of the recent experimental efforts and achievements discussed in this and the previous subsection

C. Experiments towards Neutron Capture Rates

For a long time, the determination of neutron capture rates on neutron-rich nuclei has been considered of secondary relevance for the simulation of r-process nucleosynthesis and scenarios. This is due to the fact that the r-process is governed by an $(n, \gamma) \rightleftharpoons (\gamma, n)$ equilibrium, where the actual reaction rates cancel out as described earlier. However, after freeze-out the equilibrium is no longer maintained and neutron capture reactions on the neutron-rich reaction products may well shift the abundance distribution towards heavier nuclei. Sensitivity studies with variations of the neutron capture rates by factors of ten can result in significant variations in the resulting abundances of the heavy elements (Mumpower *et al.*, 2015). However, the experimental measurements of neutron capture on exotic beams pose significant challenges, both in the production of the exotic nuclei as well as the neutrons and in turn in the measurements of the reaction rates.

While the direct measurement of neutron capture reactions on stable and even long-lived radioactive for the s-process has been very successful (Guerrero *et al.*, 2017), a similar approach to study neutron capture on short-lived

neutron-rich isotopes provides considerable challenges. Most of the r-process neutron capture rates rely on theoretical predictions based on the Hauser-Feshbach statistical model formalism (Rauscher *et al.*, 1997; Goriely, 1998). To test and verify these predictions a number of indirect methods have been developed over the last decade. This includes the so-called Oslo method (Guttormsen *et al.*, 1987) as well as the surrogate reaction technique (Escher *et al.*, 2012; Kozub *et al.*, 2012; Manning *et al.*, 2019; Tang *et al.*, 2020), while new methods are being envisioned towards a direct experimental approach.

1. Neutron Capture on neutron-rich nuclei: β -Oslo method

The Oslo method involves the extraction of level densities and γ -ray strength functions by the measurements of the total de-excitation of a nucleus as a function of energy. The different excitation ranges to be studied are populated by different nuclear reaction modes that can range from light ion transfer reactions to inelastic scattering techniques. This approach requires high intensity beams and the direct measurements of cross sections (Guttormsen *et al.*, 1987) to obtain the level density and strength function data with sufficient statistics for extracting neutron capture cross sections. The recent adaptation of the Oslo method has been demonstrated in the β -Oslo method in which the β -decay of a neutron-rich nucleus populates the levels at high excitation range and the subsequent γ -decay is measured using total absorption spectroscopy (Spyrou *et al.*, 2017). A first version of this approach was developed on the basis of β -decay data obtained at the ILL Grenoble and at ISOLDE at CERN (Kratz *et al.*, 1983; Leist *et al.*, 1985). A benchmark test for quantifying the method was the successful comparison between the level density analysis from the study of $^{87}\text{Br}(\beta^-n)^{86}\text{Kr}$ through neutron unbound states in ^{87}Kr and the direct $^{86}\text{Kr}(n,\gamma)^{87}\text{Kr}$ resonant neutron capture data (Raman *et al.*, 1983). An important aspect in this work is the fact that the extracted level density is based on the analysis of the neutron decay data, selecting configurations prone to neutron capture (and not solely on the γ -decay analysis), which contain all possible excitation modes.

The present β -Oslo method, however, rests mostly on the analysis of γ -decay of highly excited states. Neutron unbound states, populated by the β -decay are less likely to be observed because they primarily decay into the particle rather than the γ channel as observed in the early studies (Raman *et al.*, 1983). Nevertheless, the study of the β -delayed γ -decay is a useful tool for determining level densities up to the threshold. The new approach relies on the use of a 4π summing detector device instead of a single Ge detector to analyze the γ -decay pattern. The spectra are then unfolded as a function

of excitation energy in order to determine the nuclear level density and the γ -strength function. The neutron capture cross section is derived by folding the level density and γ -ray strength function with a nucleon-nucleus optical model potential, adopting statistical assumptions for the neutron transmission channels. The analysis depends critically on a number of assumptions with respect to level density normalization and the optical potential, which possibly introduces systematic uncertainties. However, the largest uncertainty is in the assumption of the density of neutron unbound states above the threshold and the associated neutron strength distribution. This is typically determined from systematics and statistical model simulations. It works well near the stability where the level density above the neutron threshold is high. It becomes more questionable when the method is applied to nuclei at the r-process path, where the neutron thresholds and therefore the level density are much lower. A number of measurements have been performed and the extracted results agree well with the predictions of Hauser-Feshbach simulations (Spyrou *et al.*, 2014) and the uncertainty range in the prediction is claimed to be significantly reduced (Liddick *et al.*, 2016).

The approach suggests a certain redundancy since the experimental data do not consider the neutron strength function above the threshold, but adopt the one predicted by the same statistical model against which the predicted reaction rates are being tested. A study of the systematic uncertainties by Spyrou *et al.* (2017) suggests that the overall uncertainty in the rates obtained by the β -Oslo method is within a factor of ~ 3 which is comparable to the uncertainty range of case-optimized Hauser Feshbach calculations (Beard *et al.*, 2014).

2. Neutron capture by (d,p) surrogate reactions

Single particle transfer reactions such as (d,p) have emerged as a powerful tool for probing the single particle structure of neutron-rich nuclei near the r-process path. First (d,p) transfer measurements, using radioactive $^{130,132}\text{Sn}$ beams on CD2 (deuterated polyethylene) targets at the Holifield Radioactive Ion Beam Facility (HRIBF) of the Oak Ridge National Laboratory, led to a better understanding of the single particle structure of bound states in $^{131,133}\text{Sn}$ (Kozub *et al.*, 2012; Jones *et al.*, 2010). The extracted single particle spectroscopic factors allowed calculating the direct reaction components for neutron capture reactions. Higher energy unbound states were not observed. The observation of such states is critical for extracting reliably the single resonant or statistical resonant contributions expected for high level density compound nuclei in (n,γ) reactions. More recently, a similar study has been performed at ISOLDE aiming at the determination of the neutron shell structure below lead and beyond $N = 126$ by probing the neu-

tron excitations in ^{207}Hg in the reaction $^{206}\text{Hg}(d,p)^{207}\text{Hg}$ in inverse kinematics (Tang *et al.*, 2020).

The study of the unbound regions of neutron-rich compound nuclei in (n, γ) reactions near the r-process path is the primary goal of the surrogate reaction approach where single particle transfer reactions are utilized to bypass the challenges of measuring neutron capture cross sections on short lived nuclei. Neutron transfer reactions such as (d, p) or $(d, p\gamma)$ are frequently highlighted as surrogates for direct neutron capture studies (Escher *et al.*, 2012). In surrogate reactions the neutron is carried within a ‘‘Trojan’’ projectile and brought to react with the target. The neutron-capture cross sections on the target nucleus can be extracted by measuring the proton in the final stage (Escher and Dietrich, 2006; Forssén *et al.*, 2007). First benchmark experiments have been performed at the 88-inch cyclotron at Lawrence Berkeley National Laboratory probing the $^{171,173}\text{Yb}(n, \gamma)$ cross section via the surrogate reaction $^{171,173}\text{Yb}(d, p\gamma)$, using a high intensity deuterium beam (Hatarik *et al.*, 2010). The extracted neutron capture cross sections agreed within 15% with direct measurements (Wisshak *et al.*, 2000) at energies above 90 keV, while at lower energies considerably larger discrepancies are observed.

In the case of neutron capture on short-lived nuclei, inverse kinematics techniques will be necessary with short-lived radioactive beams interacting with a deuterium target. Neutron-transfer measurement on a radioactive r-process nucleus needs large area silicon detector arrays at backward angles in coincidence with an ionization counter at forward angles to detect the beam-like recoils to reduce the beam induced background. Such a system was developed as the Oak Ridge-Rutgers University Barrel Array (ORRUBA) (Pain *et al.*, 2007). The ORRUBA detector has been used in the center of the Gammasphere Ge-array in a combination called Gammasphere Orruba Dual DETectors for $(d, p\gamma)$ studies using stable ^{95}Mo beams (Cizewski *et al.*, 2018) but no conclusive results have been presented. Extracting the neutron capture cross section out of the surrogate reaction measurements offers its own challenges since it requires proper treatment of nuclear model parameters. Deviations between the results of direct measurements and surrogate reaction studies may reflect insufficient treatment and separation between different reaction mechanisms, such as direct transfer and break-up components (Avrigneanu and Avrigneanu, 2016). While promising as a method, a deeper understanding of the reaction mechanism seems necessary (Potel *et al.*, 2015). This is also indicated in a recent paper on neutron capture reactions on neutron-rich Sn nuclei using the surrogate method (Manning *et al.*, 2019). The goal was not to determine the resonant contributions, but the direct capture components to low excited states. The spectroscopy method indicated a few single states rather than a broad level distribution. The results deviate with theoretical predictions at a fixed

neutron energy of 30 keV, but a broader analysis, including resonances over a wider range of methods, would be necessary for a detailed evaluation.

3. Neutron-capture in ring experiments

Recently a new method has been proposed for the direct study of neutron capture on short-lived nuclei, using high intensity radioactive beams in a storage ring on a thermalized neutron target gas produced on-line by proton-induced spallation reactions. (Reifarth *et al.*, 2017). The cross section of the neutron capture reactions would be measured in inverse kinematics, detecting the heavy ion recoils in the ring, using for example the Schottky method developed at the GSI storage ring facilities (Nolden *et al.*, 2011). This concept is an expansion of earlier work that proposed the use of the high neutron flux in a reactor core as possible target environment with the radioactive beam passing through the reactor core in a storage ring (Reifarth and Litvinov, 2014). A number of simulations demonstrate that both methods seems feasible albeit technically challenging, since it requires the combination of a storage ring facility with either a spallation or fission neutron source. There is a half-life limit that is mostly determined by the production rate at the radioactive ion facility or the beam intensity and the beam losses due to interactions with the rest gas in the ring. Yet, such a facility would allow for the first time to address the challenges of neutron capture reaction measurements on neutron rich radioactive isotopes with half-lives less than a minute in the decay products of r-process neutron-rich nuclei.

V. NUCLEAR MODELING OF R-PROCESS INPUT

A. Nuclear masses

The most basic nuclear property for any r-process calculation is the mass of the nuclei involved. It determines the threshold energy for the main reactions during the r-process: β decay, neutron capture and photodissociation. Neutron separation energies, S_n , are particularly important if the r-process proceeds in $(n, \gamma) \rightleftharpoons (\gamma, n)$ equilibrium, as the reaction path is then fixed at a constant value of S_n , for given values of neutron density and temperature of the astrophysical environment. The most commonly used mass tabulations can be grouped in three different approaches: a) microscopic-macroscopic models like the finite-range droplet model (FRDM) approach (Möller *et al.*, 1995, 2012a,b, 2015, 2016), the Extended Thomas-Fermi model with Strutinski Integral (ETFSI) approach (Aboussir *et al.*, 1995), the extended Bethe-Weizsäcker formula (Kirson, 2008) and the Weizsäcker-Skyrme mass models (Wang *et al.*, 2010; Liu *et al.*, 2011); b) a microscopically inspired

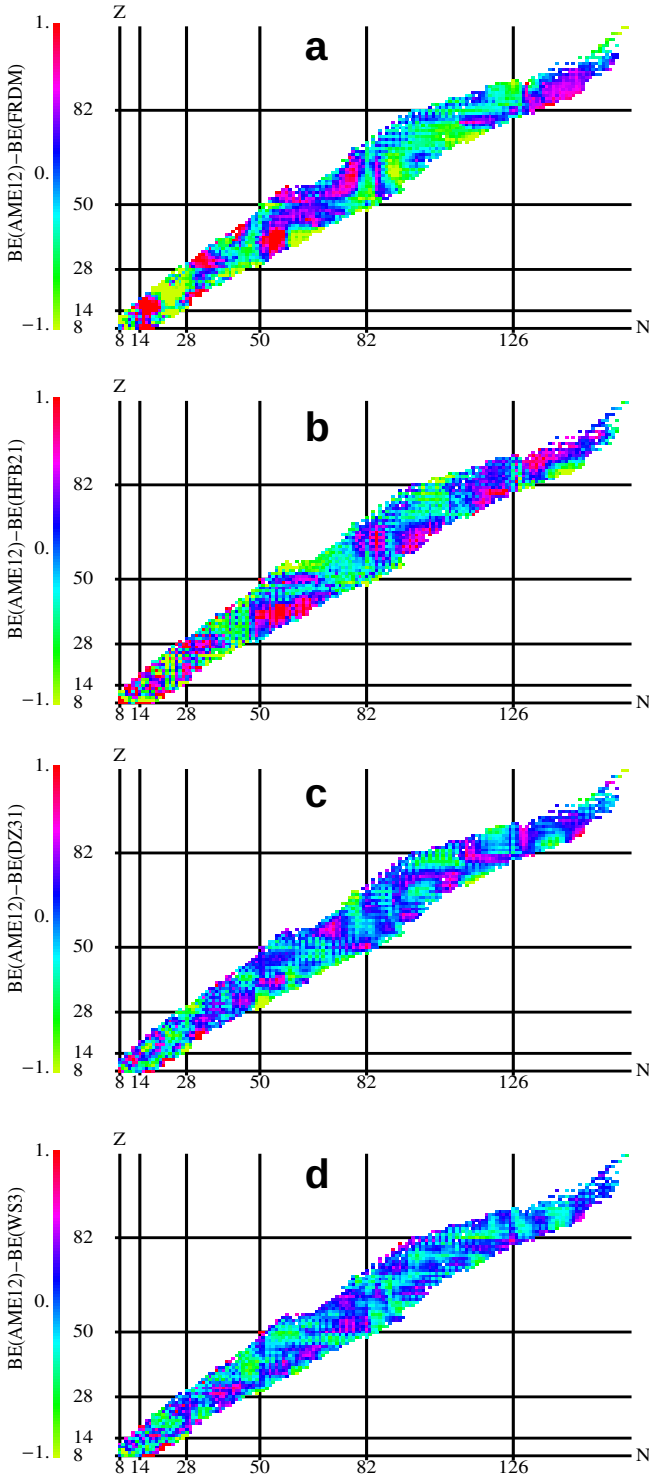


FIG. 22 Differences, in MeV, between experimental, taken from the 2012 version of the atomic mass evaluation AME12 (Wang *et al.*, 2012), and theoretical binding energies. The following mass models are shown: (FRDM-1992 Möller *et al.*, 1995, a), (HFB-21 Goriely *et al.*, 2010, b), (DZ31 Duflo and Zuker, 1995, c), (WS3 Liu *et al.*, 2011, d). (Figure from Mendoza-Temis, 2017).

parametrization based on the averaged mean field extracted from the shell model and extended by Coulomb, pairing and symmetry energies (Duflo and Zuker, 1995); and c) microscopic models based on the non-relativistic (Goriely *et al.*, 2016) or relativistic (Sun and Meng, 2008) mean-field models.

TABLE I Comparison of the root mean square deviation, in keV, between mass models and experiment; mass models: FRDM-1992 (Möller *et al.*, 1995), HFB-21 (Goriely *et al.*, 2010), DZ10, DZ31 (Duflo and Zuker, 1995), and WS3 (Liu *et al.*, 2011), experimental values taken from the 2003 (Audi *et al.*, 2003) and 2012 evaluations (Wang *et al.*, 2012). The columns labeled “full” consider all masses present in each evaluation while the column labeled “new” includes only masses found in AME-2012 but not in AME-2003.

Model	AME-2003 (full)	AME-2012 (new)	AME-2012 (full)
FRDM-1992	655	765	666
HFB-21	576	646	584
WS3	336	424	345
DZ10	551	880	588
DZ31	363	665	400

All mass models have in common that, by fitting a certain set of parameters to known experimental data, they are then being used to predict the properties of all nuclei in the nuclear landscape. The models reproduce the experimentally known masses quite well, with mean deviations between 350 keV and 600 keV (see Table I). It is quite satisfying to see that, when in 2012 a new atomic mass evaluation (AME) (Wang *et al.*, 2012), including 219 new experimental masses, became available the agreement with data worsened only slightly compared to the comparison with the previous AME. However, when considering only the new experimental masses found in AME-2012 the agreement deteriorates. As the new masses typically involve more exotic nuclei than those found in a previous evaluation, they provide a measure of the capabilities of each model to extrapolate to regions far from stability. This is in general one of the most challenging aspects to determine when using a given mass model in r-process calculations. Neufcourt *et al.* (2018) has recently applied Bayesian machine-learning techniques to assess the predictive power of global mass models towards more unstable neutron-rich nuclei and provide uncertainty quantification of predictions. Nevertheless, deviations between model and data for neutron-rich nuclei are typically related to bulk properties that may not dramatically affect the abundance predictions, e.g. the symmetry energy whose value is known with an uncertainty 3.8 MeV to be the range 29.7–33.5 MeV (Hebel *et al.*, 2013).

Fig. 22 provides a closer comparison between models and data. One notices systematic deviations, e.g. for

neutron numbers around $N \sim 90$ and 130 just above the neutron shell closures at $N = 82$ and 126 (Fig. 22). These mass regions are known as ‘transitional regions’ where nuclear shapes change from spherical to deformed configurations, accompanied by a sudden drop in neutron separation energies. The description of these shape changes is very sensitive to correlations which are not fully accounted for in the current mass models. Noticeable differences among the various mass models, and the data, are also observed in the differences of neutron separation energies for odd- A and odd-odd nuclei (Arzhanov, 2017), likely pointing to the need for an improved description of neutron-proton correlations. A better description, in particular of the transitional region, requires beyond-mean-field techniques. A first attempt has been presented in Rodríguez *et al.* (2015), based on the Generator Coordinator Method which considers superpositions of different shapes and restores the breaking of particle number and angular momentum as inherent in the Hartree-Fock-Bogoliubov (HFB) approach. However, first calculations of nuclear masses show only rather slight effects for nuclei in the $N \sim 90$ range.

Although the differences between the various mass models might be rather minute in the transitional regions at $N \sim 90$ and 130, they can have noticeable impact in r-process simulations. The FRDM (Möller *et al.*, 1995) and version 21 of the Brussels Hartree-Fock-Bogoliubov mass model (HFB21 Goriely *et al.*, 2010) predict noticeably smaller neutron separation energies than the Duflo-Zuker (Duflo and Zuker, 1995) or the Weizsäcker-Skyrme (WS3 Wang *et al.*, 2010; Liu *et al.*, 2011) models in the $N \sim 130$ mass range. As a consequence, for the former two mass tabulations, these nuclei act as obstacles in the r-process mass flow and produce a third r-process abundance peak which is narrower in width, overestimated in height, slightly shifted to larger mass numbers and followed by an abundance trough just above the peak if compared to simulations using the Duflo-Zuker and WS3 masses and to observational data (see Fig. 23). At $N \sim 90$ the FRDM predicts very low neutron separation energies, in contrast to the other mass models (Arcones and Martínez-Pinedo, 2011). As is discussed in Mendoza-Temis *et al.* (2015) these low S_n values have consequences for the matter flow between the second and third r-process peaks and result in a narrow peak around $A \sim 136$ in the r-process abundances at freeze-out, which is, however, washed out at later times due to continuous productions of material in this region by fission. Similar effects have also been observed in Martin *et al.* (2016) using masses derived from Skyrme energy density functionals based on different optimization protocols. This allows for systematic studies of uncertainty bands under the same underlying physical model for the description of nuclear masses.

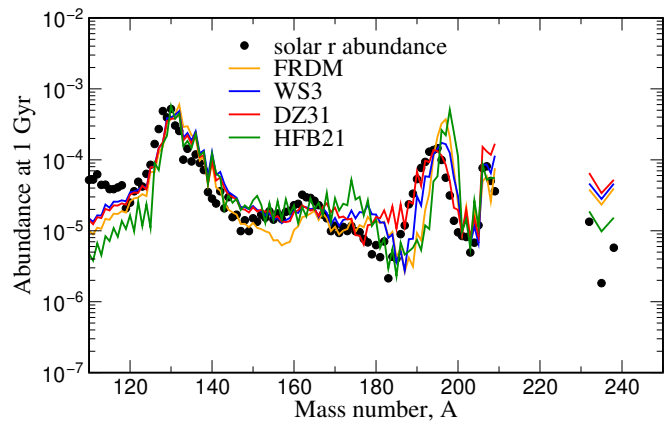


FIG. 23 Final mass-integrated r-process abundances obtained in a neutron-star merger simulation using four different mass models (adopted from Mendoza-Temis *et al.*, 2015)

B. Beta-decay half-lives

Nuclear beta-decays, which change a neutron into a proton, are responsible for the mass flow to elements with increasingly heavier Z -number. As the r-process occurs in a dynamical environment, the time, needed for the succession of beta-decays to produce thorium and uranium from the seed nuclei available after freeze-out of charged-particle fusion reactions, is competing with the dynamical timescale of the explosion, during which matter is transported to larger radii and lower densities. The latter suppresses the neutron number density required for the mass flow to heavier nuclei by neutron captures. Particularly important are beta-decays of nuclei with magic neutron numbers N_{mag} , as the matter flow is hindered by the reduced neutron separation energies of the nuclei with $N_{\text{mag}} + 1$. Furthermore, due to the extra binding of the magic nuclei, the Q -value of their beta-decays is relatively reduced, resulting in longer lifetimes.

Calculations of beta-decays require two ingredients: the relative energy scale between parent and daughter nuclei (Q value) and the transition strength distribution in the daughter nucleus. We note that the Q values are large for r-process nuclei due to the extreme neutron excess. As a consequence uncertainties in this quantity (usually of order 0.5–1 MeV) have a mild effect on the half lives, despite the strong energy dependence of the involved phase space (E^5 for allowed Gamow-Teller transition, and even higher powers for forbidden transitions). However, this strong energy dependence makes the half-life sensitive to the detailed low-lying strength distribution, which is also crucial to determine whether the beta-decay is accompanied by the emission of neutrons, i.e. whether the transition proceeds to states in the daughter nucleus above or below the neutron threshold (which is only 2–3 MeV in r-process nuclei). This so-called β -delayed neutron emission is a source of free neutrons and plays an impor-

tant role in determining the final r-process abundances during the freeze-out of neutron captures (Arcones and Martínez-Pinedo, 2011).

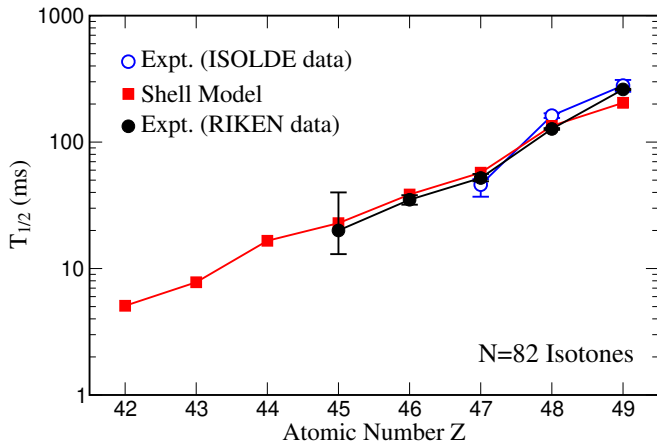


FIG. 24 Comparison of experimental (Pfeiffer *et al.*, 2001; Dillmann *et al.*, 2003; Fogelberg *et al.*, 2004; Lorusso *et al.*, 2015) and shell-model half-lives (Zhi *et al.*, 2013) for $N = 82$ r-process nuclei

Nucleon-nucleon correlations are responsible for the strong fragmentation of the transition strengths and for its suppression compared to the Independent Particle Model. These correlations are accounted for in the interacting shell model (Caurier *et al.*, 2005), and in fact large-scale shell model calculations have been proven as the appropriate tool to describe nuclear Gamow-Teller distributions (Caurier *et al.*, 1999; Cole *et al.*, 2012) for stellar weak interaction processes (Langanke and Martínez-Pinedo, 2000, 2003). Shell-model calculations proved also very valuable for the calculation of the half-lives of r-process key-nuclei with magic neutron numbers. For ^{78}Ni the shell model predicted a half-life of 127 ms (Langanke and Martínez-Pinedo, 2003), which was significantly shorter than the value estimated by global models at the time, and was subsequently experimentally verified (110 ± 40 ms, Hosmer *et al.*, 2005). As is shown in Fig. 24, the half-lives for the $N = 82$ r-process nuclei recently measured at RIKEN (Lorusso *et al.*, 2015) agree very well with the earlier shell model values (Zhi *et al.*, 2013), once the quenching of GT transitions is adjusted to the new ^{130}Cd half-life. The shell model calculations imply that the half-lives for the $N = 50$ and 82 r-process nuclei are dominated by Gamow-Teller transitions and forbidden strengths contribute only on the few-percent level. This is different for the $N = 126$ r-process waiting points. Here two independent large-scale shell model calculations (Suzuki *et al.*, 2012; Zhi *et al.*, 2013) give evidence that, due to the presence of intruder states with different parity, forbidden transitions contribute significantly and make the half lives about a factor of 2 shorter than estimated for pure allowed transitions. In turn, the shorter half-lives allow for a faster mass flow through the

$N = 126$ waiting points. We note that the relevant forbidden transitions are at low excitation energies, where due to their enhanced phase space energy dependence they can compete with allowed transitions, and hence they have a strong impact on the β -delayed neutron emission probability.

The shell model is the method-of-choice for β -decay calculations. However, due to the model spaces involved, calculations are only possible for r-process nuclei near closed neutron shells. Thus, the global beta-decay rates for r-process simulations have to be modelled by less sophisticated many-body models. Traditionally these studies were performed by calculation of the Gamow-Teller strength distributions within the Quasiparticle Random Phase Approximation on the basis of the Finite Range Droplet Model (Möller *et al.*, 1997) or the ETFSI approach (Extended Thomas Fermi Model with Strutinsky Integral, Borzov and Goriely, 2000). Experimental data for half-lives of r-process nuclei around $N = 50$ and 82 (Pfeiffer *et al.*, 2001; Lorusso *et al.*, 2015) showed that these estimates were systematically too long. The FRDM+QRPA model was subsequently extended to include forbidden transitions within the phenomenological “gross theory” (Möller *et al.*, 2003). A new promising road towards globally calculating half-lives for r-process nuclei has recently been developed by performing QRPA studies on top of the self-consistent Hartree-Fock-Bogoliubov (HFB+QRPA, Engel *et al.*, 1999) method or density functionals, either non-relativistic (Borzov, 2003) or relativistic (Marketin *et al.*, 2007). Recent covariant density functional theory (D3C*+QRPA, Marketin *et al.*, 2016a) and Skyrme finite-amplitude (Mustonen and Engel, 2016; Shafer *et al.*, 2016) studies, which accounted for allowed and forbidden transitions, yielded noticeably shorter half-lives for medium and heavy nuclei than obtained by the FRDM+QRPA approach.

Shorter half-lives for r-process nuclei with $Z > 80$ have a strong impact on the position of the third r-process peak (Eichler *et al.*, 2015) and enhance the mass flow through the $N = 126$ waiting points (Mendoza-Temis *et al.*, 2015). The latter implies more material available for fission, thus affecting the abundances of the second r-process peak, and the late-time α decays from the decaying r-process matter in a neutron star merger event (Wu *et al.*, 2019). Studies of the influence on beta-decays on the r-process abundances for different astrophysical sites have been reported in (Mumpower *et al.*, 2016; Shafer *et al.*, 2016; Kajino and Mathews, 2017).

In principle, the transformation of neutrons into protons can also be achieved by charged-current (ν_e, e^-) reactions. In fact, there have been various suggestions how neutrino-induced reactions on nuclei might affect r-process nucleosynthesis (e.g. Qian *et al.*, 1997; Haxton *et al.*, 1997; Meyer *et al.*, 1998; Otsuki *et al.*, 2000; Terasawa *et al.*, 2004). All these studies were based on the assumption that the r-process operates in the neutrino-

driven wind scenario in the presence of strong neutrino fluxes. These assumptions are not supported by modern supernova simulations. In the neutron star merger scenario neutrino fluxes once the r-process operates are too low to substantially influence the abundances by charged-current reactions (Roberts *et al.*, 2017). However, the initial proton-to-neutron ratio of the matter ejected in neutron star mergers and its spatial and time dependence is set by weak reactions on free nucleons (see section VI)

C. Neutron captures

During the r-process phase, in which the temperature is large enough ($T \gtrsim 1$ GK), neutron captures and their inverse reactions, photo-dissociations, are in equilibrium. The rates become, however, relevant once the nucleosynthesis process drops out of this equilibrium. During this period of decreasing temperatures, it is mainly neutron capture that matters.

The neutron capture and photo-dissociation rates for r-process nuclei (the latter can be derived by detailed balance from the former) are traditionally determined within the statistical model. This assumes a sufficiently high density of states in the daughter nucleus at the relevant capture energies just above the neutron threshold, which is not given for the most neutron-rich nuclei close to the neutron dripline. A systematic estimate about the range of nuclei for which the statistical model is applicable to calculate neutron capture rates is given in (Rauscher *et al.*, 1997). It has been proposed that for the most neutron-rich nuclei the capture rates should be calculated within a direct-capture approach based on a potential (Mathews *et al.*, 1983; Rauscher *et al.*, 1998; Otsuki *et al.*, 2010; Xu and Goriely, 2012; Xu *et al.*, 2014). In such an approach the rate is often determined by a single resonance in the Gamow window (Loens *et al.*, 2012). This makes rate predictions quite uncertain, as nuclear models are not capable to predict the resonance energies with sufficient accuracy. It has therefore been suggested to describe the final states by a level density rather than by discrete levels (Goriely, 1997; Ejnisman *et al.*, 1998). Calculations of neutron capture rates, which include a statistical component and a direct contribution, are reported in Mocelj *et al.* (2007).

The main ingredients of statistical model calculations within the Hauser-Feshbach approach are the nuclear level density, the γ -strength function for the decay of the compound state, and various light-particle potentials. The γ transition can occur with different multipolarities, requiring either different ($E1$) or equal parities ($M1$, $E2$) between the involved states. To also fulfil angular momentum selection rules, requires the knowledge of parity- and angular-momentum-dependent level densities.

There has been significant progress in modelling nuclear level densities in recent years. With the Shell Model

Monte Carlo approach (SMMC) (Johnson *et al.*, 1992; Koonin *et al.*, 1997) a tool became available which allowed to determine level densities in unprecedentedly large model spaces. The method to derive level densities within the SMMC was presented in Ormand (1997), Nakada and Alhassid (1997), and Langanke (1998) and then systematically extended to explore the parity-dependence (Alhassid *et al.*, 1999) and angular-momentum-dependence (Alhassid *et al.*, 2007). In Özen *et al.* (2015) the collective vibrational and rotational enhancement factors have been explored, finding that the decay of these enhancement factors is correlated with the pairing and shape phase transitions. The vanishing of pairing and its effect on the level density has been studied in Langanke (2006). In the Bethe Fermi Gas (BFG) level density formula this vanishing has been described by a temperature-dependent pairing parameter (Grossjean and Feldmeier, 1985; Mustafa *et al.*, 1992; Junghans *et al.*, 1998) for which Langanke (2006) gives a parametrization on the basis of the SMMC calculations. SMMC calculations have been performed for many mid-mass and heavy nuclei. These include even-even, odd-A and odd-odd nuclei, allowing to microscopically test the standard prescription in the BFG level density to describe the systematic differences in these nuclei due to the pairing effect by a pairing shift parameter (e.g. Cowan *et al.*, 1991; Rauscher and Thielemann, 2000).

These calculations have initiated and guided attempts to extend a microscopically derived parity dependence into phenomenological level density formulae like the BFG approach. This is achieved by deriving the excitation-energy dependent parity ratio in the level density by the assumption of Poisson distributed independent quasi-particles combined occupation numbers obtained from the BCS (Bardeen-Cooper-Schrieffer) model, in this way including pairing (Alhassid *et al.*, 2000). In Mocelj *et al.* (2007) this approach has been applied to the large set of r-process nuclei (incorporating also a temperature-dependent pairing parameter suggested from SMMC studies) and its effects on astrophysically relevant reaction rates was studied in Loens *et al.* (2008). This improved level density description is part of the statistical model packages NON-SMOKER and SMARAGD developed by Rauscher (Rauscher and Thielemann, 2001; Rauscher, 2011).

A different path to derive parity- and angular-momentum-dependent level densities has been followed by Goriely and co-workers, based on a combinatorial approach within HFB calculations. Also this approach has been incorporated into a statistical model package and applied to the calculation of neutron capture rates for r-process nuclei within the Brussels Nuclear Library for Astrophysics Applications (BRUSLIB)⁶ data compi-

⁶ <http://www.astro.ulb.ac.be/bruslib>

lation (Koning *et al.*, 2008; Goriely *et al.*, 2008; Hilaire *et al.*, 2010; Goriely *et al.*, 2012).

Traditionally the different γ -strength functions have been described by global parametrizations (Cowan *et al.*, 1991) which were adjusted to photo-dissociation for $E1$ transitions or electron scattering data for $M1$ transitions (e.g. Cowan *et al.*, 1991). Recently $E1$ strength functions became available which were microscopically calculated for individual nuclei within the framework of the HFB model (Goriely and Khan, 2002; Goriely *et al.*, 2004) or based on the relativistic mean field model (Litvinova *et al.*, 2009). These calculations support the presence of enhanced dipole strength at energies just above the neutron threshold (see also Rauscher, 2008). Experimentally such enhanced strength is observed as ‘pygmy dipole strength’ in nuclei with large neutron excess, like those involved in r-process nucleosynthesis (Adrich *et al.*, 2005). As shown in Goriely (1998) this enhanced dipole strength can have significant impact on neutron capture cross sections.

Dipole γ -strength functions determined from particle- γ coincidence data in neutron pick-up and inelastic scattering data for several mid-mass nuclei exhibit a remarkable upbend of the strength towards $E_\gamma = 0$ (e.g. Guttormsen *et al.*, 2005; Larsen *et al.*, 2006, 2007). The data also allow for the derivation of the nuclear level density, making a few assumptions (the Oslo method, Schiller *et al.*, 2000) (see section IV.C.1). The impact of this upbend on neutron capture rates for r-process nuclei has been studied (Larsen and Goriely, 2010; Larsen *et al.*, 2015, 2019) and a potential increase of the capture rate by up to two orders of magnitude has been calculated. The origin of the low-energy upbend has yet not been completely identified. Coherent adding of magnetic moments of high- j orbitals has been suggested as a possible mechanism for low-energy $M1$ enhancement (Schwengner *et al.*, 2013; Brown and Larsen, 2014; Schwengner *et al.*, 2017), while a low-energy upbend in the $E1$ strength was obtained within finite-temperature relativistic QRPA calculations (Litvinova and Belov, 2013). An upbend in the $M1$ strength function has also been found in large-scale shell model calculations for selected pf -shell nuclei (Sieja, 2017) and $A \gtrsim 100$ (Sieja, 2018). Goriely *et al.* (2018) have performed large scale calculations of $E1$ and $M1$ strength functions by a combination of shell-model and Gogny-HFB+QRPA calculations.

Several general questions regarding basic assumptions made in statistical model evaluations of capture rates have been addressed in large-scale shell model calculations of the $M1$ strength functions for several mid-mass nuclei (similar studies for $E1$ transitions are yet prohibited by computing limitations as they require the inclusion of two major shells, Loens *et al.*, 2012). The results are briefly summarized as: a) The shell-model $M1$ strength functions turned out to give smaller cross sections than the usually adopted parametrizations; b) the

scissors mode, a fundamental orbital $M1$ excitation observed in deformed nuclei at low energies (Bohle *et al.*, 1984), might lead to a noticeable enhancement of the capture rates; c) the assumption of the Brink hypothesis, i.e. the strength function is the same for all nuclear states (Brink, 1955; Brink, 1957) is only valid with moderate accuracy d) the cross section calculated microscopically by a state-by-state approach had the largest contribution from a single state with $M1$ excitations just in the Gamow window. Such a nuclear structure effect cannot be caught by any global parametrization. The potential impact of the $M1$ scissors mode on r-process neutron capture cross sections has subsequently been revisited by Mumpower *et al.* (2017a).

The transmission coefficients required in statistical model calculations of astrophysical rates (Cowan *et al.*, 1991; Rauscher and Thielemann, 2000) are calculated on the basis of global optical potentials. For the proton and neutron potentials several rather reliable potentials exist (e.g., Jeukenne *et al.*, 1977; Bauge *et al.*, 2001; Koning and Delaroche, 2003; Goriely and Delaroche, 2007). The situation is different for the α -optical potential. Although several global potentials exist (e.g., McFadden and Satchler, 1966; Demetriou *et al.*, 2002, 2003; Kiss *et al.*, 2009; Mohr *et al.*, 2013), none of them is able to consistently describe the existing data at low energies in statistical model approaches. Using ^{64}Zn as an example, Mohr *et al.* (2017) explored the sensitivity of the α -induced reaction cross section to the variation of different alpha optical potential (and other parameters in the statistical model). Attempts have been made to cure the problem. Rauscher suggested that the consideration of Coulomb excitation leads to a better agreement with data (Rauscher, 2013). In Demetriou *et al.* (2002) and Szücs *et al.* (2020) it was shown that a modified imaginary part of the optical potential, in particular at large radii, can improve the reproduction of experimental reaction data at low energies. Based on a large set of α -induced reaction data at sub-Coulomb energies, Avrigeanu *et al.* (2014); Avrigeanu and Avrigeanu (2015) have presented a global α -optical potential for nuclei in the mass range $45 \leq A \leq 209$.

D. Fission

Fission plays an important role in the r-process, in particular within the NS-NS merger scenario. Fission determines the region of the nuclear chart at which the flow of neutron captures and beta-decays stops (Thielemann *et al.*, 1983; Petermann *et al.*, 2012; Giuliani *et al.*, 2018; Mumpower *et al.*, 2018; Vassh *et al.*, 2019a; Giuliani *et al.*, 2019). In the particular case of dynamic cold ejecta from mergers, several fission cycles are expected to operate before all neutrons are used (Korobkin *et al.*, 2012; Goriely, 2015; Goriely and Martínez-Pinedo, 2015).

Fission has been suggested to be responsible for producing a robust r-process pattern (Korobkin *et al.*, 2012; Rosswog *et al.*, 2014; Goriely, 2015), in which the abundances of nuclei with $A \lesssim 140$ are determined during the r-process freeze-out from the fission yields of nuclei with $A \lesssim 280$ (see Mendoza-Temis *et al.*, 2015).

The description of fission for r-process nuclei is very challenging as it sensitively depends on the knowledge of the fission barriers for a broad range of very neutron-rich nuclei. In addition, the evolution of the shell structure as function of neutron excess is very uncertain. Several competing reaction channels need to be modelled, including neutron capture, neutron-induced fission, beta-decay, β -delayed fission, spontaneous fission, alpha decay and gamma-induced fission. Hence, parallel to the calculation of fission barriers one has to develop models for all these different reaction channels. Several studies have computed barriers for r-process nuclei (Howard and Möller, 1980; Myers and Świątecki, 1999; Mamdouh *et al.*, 2001; Goriely *et al.*, 2009; Erler *et al.*, 2012; Möller *et al.*, 2015; Giuliani *et al.*, 2018). It has been shown that the dominating fission channel during r-process nucleosynthesis is neutron-induced fission (Panov *et al.*, 2005; Martínez-Pinedo *et al.*, 2007; Petermann *et al.*, 2012). However, the necessary reaction rates have been computed for a rather limited set of barriers (Thielemann *et al.*, 1989; Panov *et al.*, 2005; Goriely *et al.*, 2009; Panov *et al.*, 2010; Giuliani *et al.*, 2018, 2019). This hinders studies of the sensitivity of the r-process abundances to the fission barriers. Due to the dominance of neutron-induced fission, the fission barrier itself is the most important quantity for the determination of reliable fission rates, as the fission process occurs at energies just above the fission barrier. In this case, the inertial mass parameter plays a minor role as tunneling through the barrier has only a negligible contribution. This fact, however, simplifies calculations considerably as the calculation of the inertial mass parameter is rather challenging (Sadhukhan *et al.*, 2013; Giuliani *et al.*, 2014; Giuliani *et al.*, 2018).

In addition to the description of the different fission reaction channels, also the corresponding fission yields, which depend on the excitation energies of the compound nucleus (Kelic *et al.*, 2008, 2009; Schmidt *et al.*, 2016; Sadhukhan *et al.*, 2016; Zhang *et al.*, 2016; Schmitt *et al.*, 2018; Schmidt and Jurado, 2018; Mumpower *et al.*, 2019; Vassh *et al.*, 2019b; Sadhukhan *et al.*, 2020), have to be known for r-process simulations. As discussed above, the fission yields determine the abundance of r-process elements in the second r-process peak and above and can play an important role for abundance distribution of rare-earth elements (Bengtsson and Howard, 1975; Steinberg and Wilkins, 1978; Panov *et al.*, 2008; Goriely *et al.*, 2013; Eichler *et al.*, 2015; Vassh *et al.*, 2019a).

It should be emphasized that during the last phase of the r-process alpha decays compete with fission. This competition determines the final abundances of Pb, U

and Th and of long-lived actinides. Consequently, an improved description of transuranic nuclides is necessary for the determination of the r-process abundances produced in neutron star mergers, with important consequences for the kilonova lightcurves (Hotokezaka *et al.*, 2016; Barnes *et al.*, 2016; Rosswog *et al.*, 2017; Zhu *et al.*, 2018; Wanajo, 2018; Wu *et al.*, 2019).

VI. ASTROPHYSICAL SITES AND THEIR EJECTA COMPOSITION

Section III has discussed conditions that any astrophysical site should attain in order to produce r-process nuclei. They reduce to particular combinations of entropy, expansion time scale, and Y_e in the ejecta. As a minimum requirement the ejecta should be characterized by a high neutron-to-seed nuclei ratio. This is certainly the case for neutron-rich matter, pointing naturally to neutron stars as an important reservoir of neutrons. However, ejecting material from the deep gravitational field of a neutron star requires a cataclysmic event. This could be either associated to the birth of a neutron star in a supernova explosion or to ejecta from a compact binary merger involving a neutron star, leading logically to the most promising sites for a strong r-process: (i) the innermost ejecta of regular core-collapse supernovae, (ii) a special class of core collapse supernovae (magnetorotational MHD-jet supernovae or collapsars), with fast rotation and high magnetic fields responsible for their explosion mechanism, which can produce neutron-rich jet ejecta along the poles or from accretion disk outflows, and (iii) ejecta from binary neutron star mergers or neutron star black hole systems which are naturally neutron-rich and have been considered already extensively before the observation of GW170817.

A common feature of these scenarios, which will be discussed in detail below, is that matter reaches such high temperatures that nuclei are dissociated into free nucleons, and neutrinos become the main cooling mechanism. Those neutrinos and in particular electron flavor (anti)neutrinos can interact with the ejecta and reset the composition that is commonly determined by a balance between the following reactions:



In the case of neutrino-driven winds and potentially also for neutron star merger ejecta, the material is subject long enough to these processes to reach an equilibrium between neutrino and antineutrino captures (Qian and Woosley, 1996; Thompson *et al.*, 2001; Martínez-Pinedo *et al.*, 2017), resulting in

$$Y_e = Y_{e,\text{eq}} = \left[1 + \frac{L_{\bar{\nu}_e} W_{\bar{\nu}_e} \varepsilon_{\bar{\nu}_e} - 2\Delta + \Delta^2 / \langle E_{\bar{\nu}_e} \rangle}{L_{\nu_e} W_{\nu_e} \varepsilon_{\nu_e} + 2\Delta + \Delta^2 / \langle E_{\nu_e} \rangle} \right]^{-1}, \quad (10)$$

with L_{ν_e} and $L_{\bar{\nu}_e}$ being the neutrino and antineutrino luminosities, $\varepsilon_{\nu} = \langle E_{\nu}^2 \rangle / \langle E_{\nu} \rangle$ the ratio between the second moment of the neutrino spectrum and the average neutrino energy (similarly for antineutrinos), $\Delta = 1.2933$ MeV the neutron-proton mass difference, and $W_{\nu} \approx 1 + 1.01 \langle E_{\nu} \rangle / (m_u c^2)$, $W_{\bar{\nu}} \approx 1 - 7.22 \langle E_{\bar{\nu}} \rangle / (m_u c^2)$ the weak-magnetism correction to the cross sections for neutrino and antineutrino absorption (Horowitz, 2002) with m_u being the nucleon mass.

If matter is exposed long enough to neutrinos to reach an equilibrium, these reactions turn matter neutron-rich, provided the following condition is fulfilled:

$$\varepsilon_{\bar{\nu}_e} - \varepsilon_{\nu_e} > 4\Delta - \left[\frac{L_{\bar{\nu}_e} W_{\bar{\nu}_e}}{L_{\nu_e} W_{\nu_e}} - 1 \right] (\varepsilon_{\bar{\nu}_e} - 2\Delta). \quad (11)$$

One should keep in mind an important difference between neutrino emission from protoneutron stars formed in core-collapse supernovae and the emission from a neutron-star merger remnant (see Fig. 25). In the supernova case, we deal with the deleptonization of a hot neutron star and consequently we expect slightly higher fluxes for ν_e 's than $\bar{\nu}_e$'s. However, due to the fact that the $\bar{\nu}_e$ spectrum is slightly hotter than the ν_e spectrum, the luminosities of both flavors are rather similar. According to Eq. (11) this implies that the average energies between $\bar{\nu}_e$ and ν_e should differ by at least $4\Delta \approx 5.2$ MeV to produce neutron rich ejecta. Such large differences are not reached in any modern neutrino-wind simulation (Hüdepohl *et al.*, 2010; Fischer *et al.*, 2010; Martínez-Pinedo *et al.*, 2012; Roberts *et al.*, 2012; Martínez-Pinedo *et al.*, 2014; Mirizzi *et al.*, 2015; Fischer *et al.*, 2020a).

In the case of a neutron star merger the initial configuration corresponds to a cold very neutron-rich neutron star. Due to the merger dynamics the final merger remnant and accretion disk is heated to large temperatures. The large temperatures favor the production of electron-positron pairs and the material tends to protonize towards the new equilibrium Y_e on timescales of hundreds of ms as determined by the weak interaction timescale in matter affected by neutrino interactions (Beloborodov, 2003; Arcones *et al.*, 2010). During this phase the luminosities and average energies of $\bar{\nu}_e$ are much larger than those of ν_e (see right panels of Fig. 25), reducing the required energy difference of Eq. (11). Hence, even if the impact of neutrino reactions in mergers is expected to be substantial (Wanajo *et al.*, 2014; Perego *et al.*, 2014; Sekiguchi *et al.*, 2015; Martin *et al.*, 2015; Sekiguchi *et al.*, 2016; Foucart *et al.*, 2016; Martin *et al.*, 2018) the (late) ejecta affected by neutrino interactions are expected to be

still neutron-rich enough to produce a (weak) r-process, while early dynamic ejecta, emerging from spiral arms after the collision, stay in any case very neutron-rich and lead to a strong r-process.

There is also an important difference between the nucleosynthesis operating in neutrino heated ejecta for supernova and mergers. In the supernova case, due to the high entropies and moderate electron fractions, the material suffers an α -rich freeze-out (see Fig. 17). Under these conditions, if the material is subject to strong neutrino fluxes during the phase of alpha formation, the so-called α -effect (Meyer *et al.*, 1998) will drive the composition to $Y_e \approx 0.5$, hindering the occurrence of an r-process. In the case of merger ejecta, due to the more moderate entropies, no alpha formation takes place for $Y_e \lesssim 0.45$ (see Fig. 18) and hence the α -effect plays no role.

The discussion above neglects neutrino flavor transformations and their impact on the Y_e of the ejected material. In the supernova case, the existence of very similar spectra for all neutrino flavors hinders the impact of neutrino active-active flavor transformations (see e.g. Wu *et al.*, 2015). Active-sterile transformations, involving sterile neutrinos on the eV mass scale, as suggested by the reactor (Mention *et al.*, 2011) and Gallium (Giunti *et al.*, 2012) anomalies, tend to drive the composition more neutron-rich (Nunokawa *et al.*, 1997; McLaughlin *et al.*, 1999; Wu *et al.*, 2014; Plumbi *et al.*, 2015). As discussed above, in the case of mergers the $\bar{\nu}_e$ fluxes dominate over those of ν_e . Hence, the neutrino self-interaction potential has a different sign than the neutrino matter potential in the Hamiltonian that describes flavor transformations. This induces conversions via matter-neutrino resonances (Malkus *et al.*, 2012; Foucart *et al.*, 2015; Malkus *et al.*, 2016; Zhu *et al.*, 2016; Frensel *et al.*, 2017) and fast pairwise conversions (Wu and Tamborra, 2017; Wu *et al.*, 2017). The existing investigations clearly point to a potential impact on Y_e and thus on the resulting nucleosynthesis.

After this general outline, discussing in detail how weak interactions are setting the stage for the resulting Y_e (and entropy), being the dominant criteria for the operation of an r-process, we will discuss in the following potential environments/sites related either to massive stars or compact objects in binary systems. This leaves out sites of neutron-rich ejecta from core-collapse supernovae (see e.g. Hillebrandt, 1978), ruled out since the neutrino-powered explosion mechanism has been established (Bethe, 1990), as well as an r-process in He-layers due to the $^{13}\text{C}(\alpha, n)^{16}\text{O}$ reaction, ruled out since realistic models of massive stars are existent (Woosley *et al.*, 2002).

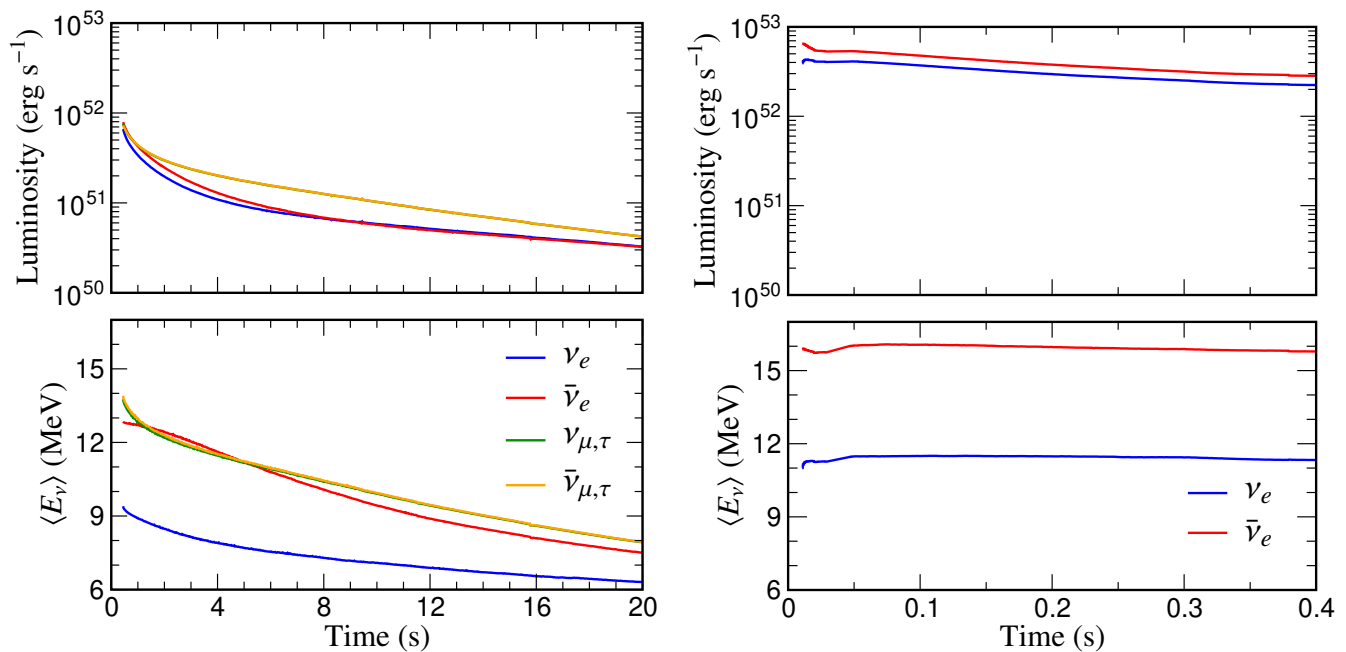


FIG. 25 (left panel) Evolution of the luminosities and average energies of neutrinos emitted during the protoneutron star cooling phase following a core-collapse supernova explosion (adapted from [Martínez-Pinedo *et al.*, 2014](#), courtesy of Tobias Fischer). (right panel) Luminosities and average energies of neutrinos emitted after a NS-NS merger that forms a hypermassive neutron star surrounded by an accretion disk. (based on the simulations from [Perego *et al.*, 2017b](#), courtesy of Albino Perego).

A. Possible r-process sites related to massive stars

1. Neutrino winds from core-collapse supernovae

Supernovae have been thought to be the origin of the strong r-process for many years (see e.g. the reviews by [Cowan *et al.*, 1991](#); [Sumiyoshi *et al.*, 2001](#); [Arnould *et al.*, 2007](#)). While the prompt explosion mechanism has been shown to fail ([Bethe, 1990](#)), the development of multidimensional neutrino radiation transport simulations has shown that the neutrino delayed explosion mechanism remains the most promising scenario to explain the observations (see [Kotake *et al.*, 2012](#); [Burrows, 2013](#); [Foglizzo *et al.*, 2015](#); [Janka *et al.*, 2016](#); [Müller, 2016](#); [Hix *et al.*, 2016](#); [Janka, 2017a](#); [Burrows *et al.*, 2018](#); [Cabezón *et al.*, 2018](#); [Burrows *et al.*, 2020](#), for reviews). These simulations predict that after the onset of the supernova explosion the hot proto-neutron star enters the so-called Kelvin-Helmholtz cooling phase. During this phase that lasts around 10 s, the proto-neutron star deleptonizes, emitting neutrinos of all flavors. Those neutrinos are responsible of producing an outflow of matter known as neutrino-driven wind ([Duncan *et al.*, 1986](#)) that is expected to operate in each supernova explosion that produces a neutron star. The basic properties of the wind are well understood, based on semianalytical models ([Duncan *et al.*, 1986](#); [Qian and Woosley, 1996](#); [Hoffman *et al.*, 1997](#); [Thompson *et al.*, 2001](#); [Otsuki *et al.*, 2000](#); [Arcones and Thielemann, 2013](#)). These

models relate the nucleosynthesis relevant conditions (see sect. III.C) to fundamental properties including neutrino luminosities, average energy, and mass and radius of the proto-neutron star. Early simulations and parametric models ([Woosley and Hoffman, 1992](#); [Meyer *et al.*, 1992](#); [Woosley *et al.*, 1994](#); [Witti *et al.*, 1994](#); [Takahashi *et al.*, 1994](#); [Freiburghaus *et al.*, 1999a](#); [Farouqi *et al.*, 2010](#); [Arcones and Martínez-Pinedo, 2011](#); [Kratz *et al.*, 2014](#)) led to impressive results. However, large uncertainties remained, particularly in the determination of entropy and Y_e . Fig. 26, taken from [Kratz *et al.* \(2014\)](#), shows that the solar r-process abundances can be reproduced, especially when utilizing modern input from nuclear mass models, but requiring a superposition of entropies of up to $280 k_B$ per baryon (and a $Y_e < 0.5$).

The development of hydrodynamic simulations ([Arcones *et al.*, 2007](#); [Arcones and Janka, 2011](#)) showed that such high entropies were out of reach. Nevertheless, they still allowed for the occurrence of a weak r-process ([Roberts *et al.*, 2010](#); [Arcones and Montes, 2011](#); [Akram *et al.*, 2020](#)). Further progress, including the development of neutrino radiation hydrodynamics simulations that follow the whole cooling phase ([Hüdepohl *et al.*, 2010](#); [Fischer *et al.*, 2010](#); [Roberts, 2012](#)), improvements in the treatment of neutrino opacities in the decoupling region ([Martínez-Pinedo *et al.*, 2012](#); [Roberts *et al.*, 2012](#); [Horowitz *et al.*, 2012](#); [Rrapaj *et al.*, 2015](#); [Janka, 2017b](#); [Roberts and Reddy, 2017](#); [Martínez-Pinedo *et al.*, 2014](#); [Bollig *et al.*, 2017](#); [Fischer *et al.*,](#)

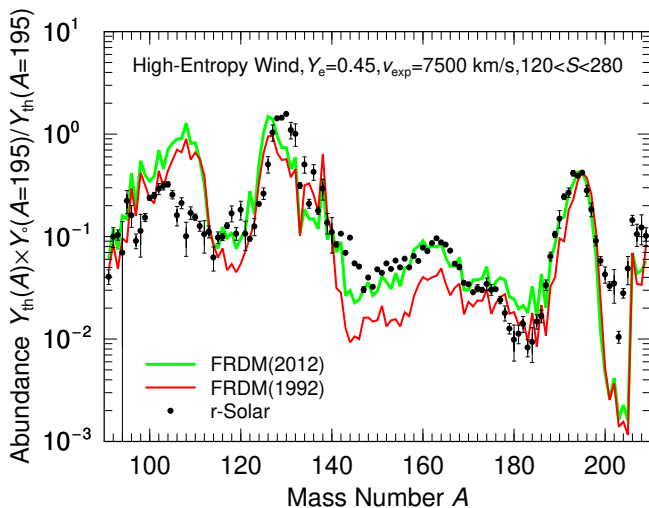


FIG. 26 Results of an r-process calculation (Kratz *et al.*, 2014), assuming an initial $Y_e=0.45$, adiabatic expansion of matter in a so-called neutrino wind with a given expansion speed v_{exp} of ejected mass shells, and a superposition of entropies S between 120 and 280 k_B /baryon with equal amounts of matter ejected per entropy interval. The plot indicates the changes due to utilizing an improved nuclear mass model (Möller *et al.*, 2012a, 2016).

2020a), and the treatment of convection in the proto-neutron star (Roberts *et al.*, 2012; Mirizzi *et al.*, 2016) have shown that most or all of the ejecta are proton-rich. Under these conditions the nucleosynthesis proceeds via the νp process (Fröhlich *et al.*, 2006b; Pruet *et al.*, 2006; Wanajo, 2006), producing neutron deficient isotopes (Fröhlich *et al.*, 2006a), including light p-process nuclei like ^{92}Mo (see Martínez-Pinedo *et al.*, 2014; Pllumbi *et al.*, 2015; Wanajo *et al.*, 2018; Eichler *et al.*, 2018).

The above result can be understood by considering that in neutrino-driven winds matter is ejected by neutrino energy deposition and is subject to neutrino reactions for sufficiently long time to permit Y_e to attain the equilibrium value given in Eq. (10). Modern simulations predict very similar spectra of ν_e and $\bar{\nu}_e$ leading to proton-rich ejecta (see Fig. 25). These results are robust against the inclusion of neutrino flavor transformations between active flavors (Wu *et al.*, 2015; Pllumbi *et al.*, 2015) but may be affected by the active-sterile flavor transformations (Wu *et al.*, 2014; Pllumbi *et al.*, 2015).

2. Electron-capture supernovae

A way out of the problem that neutrino irradiation is turning matter proton-rich is by considering matter that is ejected promptly with little exposure to neutrinos. This occurs in the so-called electron-capture supernovae

in the stellar mass range 8-10 M_\odot (Jones *et al.*, 2014), which could lead to a weak r process (Kitaura *et al.*, 2006; Janka *et al.*, 2008; Wanajo *et al.*, 2009; Wanajo *et al.*, 2011), possibly producing nuclei up to Eu, but not up to and beyond the third r-process peak (for more details see Mirizzi *et al.*, 2016). However, there are also strong indications, based on multidimensional hydrodynamic simulations of the oxygen deflagration (Jones *et al.*, 2016b) and nuclear physics data on the electron capture rate on ^{20}Ne (Martínez-Pinedo *et al.*, 2014; Kirsebom *et al.*, 2019a,b), that intermediate mass stars may end their lives as a thermonuclear supernova triggered by electron captures on ^{20}Ne (see Nomoto and Leung, 2017a, for a recent review).

3. Neutrino-induced r-process in the He-shell

One of the major requirements for an r-process to take place is to attain a sufficiently high neutron-to-seed ratio. As already discussed above for the high entropy wind, this can also be achieved via a (very) low seed abundance. Banerjee *et al.* (2011) and Banerjee *et al.* (2016), following on an idea by Epstein *et al.* (1988), could show that for core-collapse supernovae with metallicities as low as $[\text{Fe}/\text{H}] \leq 3$, i.e. indicating a very low seed abundance, the neutrons released in the He-shell by $^4\text{He}(\bar{\nu}_e, e^+n)^3\text{H}$ can be captured to produce nuclei with mass numbers up to $A = 200$ in the stellar mass range of 11–15 M_\odot , which are subsequently ejected during the supernova explosion. The caveat of this environment is, that while a sufficiently high neutron-to-seed ratio permits the production of heavy nuclei via neutron captures, the relatively low neutron density n_n leads to an abundance pattern between the r-process and an s-process with peaks shifted to higher masses numbers than found for the solar r-abundances. Thus, such a process cannot be an explanation for solar r-process abundances and abundance patterns observed in low-metallicity stars.

4. Quark deconfinement supernovae

This scenario considers objects which undergo core collapse and form a central compact proto-neutron star, but the neutrino emission from the hot proto-neutron star and accreted matter is not sufficient to prevent a further collapse with ongoing mass accretion. The question is whether this second collapse leads directly to black hole formation or can come to a halt (Fischer *et al.*, 2018). A specific equation of state effect was initially introduced by Sagert *et al.* (2009) and Fischer *et al.* (2011), with a quark-hadron phase transition taking place just at the appropriate density/temperature conditions. When adjusting the equation of state properties to presently observed maximum neutron star masses, Fischer *et al.*

(2020b) could show that in such supernovae explosions, expected for a certain stellar mass range, an r-process can take place in the innermost ejecta. When examining their results, they show that abundance up to the third r-process peak can be obtained, however, the relative abundances beyond the second r-process peak are strongly suppressed with respect to solar.

Summarizing the discussion in the previous subsections, there remains a possibility that core-collapse supernovae can produce r-process elements but they probably do not support a solar-type r-process up to the third r-process peak.

5. Magneto-rotational supernovae with jets

Core-collapse with fast rotation and strong magnetic fields is considered to lead to neutron stars with extremely high magnetic fields of the order 10^{15} G (magnetars, see e.g. Duncan and Thompson, 1992; Kramer, 2009; Kaspi and Beloborodov, 2017; Beniamini *et al.*, 2019), connected to a special class of supernovae (Kasen and Bildsten, 2010; Greiner *et al.*, 2015; Nicholl *et al.*, 2017a). Such supernovae, induced by strong magnetic fields and/or fast rotation of the stellar core, i.e., magneto-rotational supernovae (MHD-SNe), could provide an alternative and robust astronomical source for the r-process (Symbalisty *et al.*, 1985). Nucleosynthetic studies were carried out by Nishimura *et al.* (2006), based on MHD simulations which exhibited a successful r-process in jet-like explosions. One important question is whether these earlier results, assuming axis symmetry, also hold in full three-dimensional (3D) simulations, i.e., lead to the ejection of jets along the polar axis. Relativistic 3D MHD simulations with an improved treatment of neutrino physics were performed by Winteler *et al.* (2012) for a $15 M_{\odot}$ progenitor, utilizing an initial dipole magnetic field of 5×10^{12} G and a ratio of magnetic to gravitational binding energy, $E_{\text{mag}}/W = 2.63 \times 10^{-8}$. These calculations supported and confirmed the ejection of polar jets in 3D, attaining magnetic fields of the order 5×10^{15} G and $E_{\text{mag}}/W = 3.02 \times 10^{-4}$ at core-bounce, with a successful r-process up to and beyond the third r-process peak at $A = 195$ (see e.g. Fig. 27). Subsequent general relativistic simulations in 3D-MHD (Mösta *et al.*, 2014), involving a $25 M_{\odot}$ progenitor with an initial magnetic field of 10^{12} G, led in the early phase to jet formation, but experienced afterwards a kink instability, deforming the jet-like feature. Probably this marks a transition between jet-like explosions and deformed explosions, depending on critical limits in stellar mass, initial rotation, and magnetic fields.

Further high resolution investigations (resolving the magneto-rotational instability MRI, Mösta *et al.*, 2015) have shown that this mechanism can produce magnetar-strength magnetic fields and lead to magneto-rotationally

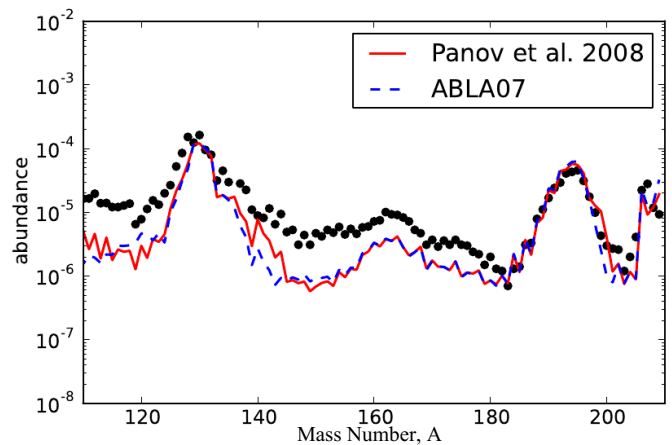


FIG. 27 In an MHD-jet supernova the winding up of magnetic field lines causes the “squeezing-out” of polar jets, along the rotation axis (Winteler *et al.*, 2012). This environment leads to quite low entropies, much lower than those discussed in Fig. 17. But opposite to the Y_e -values utilized for Fig. 17, the collapse to high densities resulted in large amounts of electron captures and Y_e -values close to 0.1-0.15 (see top part of this figure as well as Fig. 18). Such low Y_e 's, similar to neutron star merger conditions (where even values as low as 0.03-0.05 can be attained, see next subsection) lead to a strong r-process and abundance predictions displayed in the bottom part (shown for two fission fragment distributions utilized Kellec *et al.*, 2008; Panov *et al.*, 2008). As Y_e is only moderately low, the effect of late neutron-capture by fission neutrons is also moderate, avoiding a final shift of the third r-process peak as indicated in Figs. 32 and 33. (Reprinted by permission from Springer Nature, Thielemann *et al.*, 2017a)

powered explosions, even for smaller initial magnetic fields, probably causing the majority of magnetars (Beniamini *et al.*, 2019). However, these are not prompt jet-like explosions on timescales of 10th of ms, but rather deformed (dual-lobe) explosions on timescales of 100th of ms, which experienced the above-mentioned kink instability (Mösta *et al.*, 2018). This underlines that only for very high initial magnetic fields such kink instabilities and long exposures to neutrinos (increasing Y_e) can be avoided, ensuring a strong r-process. Studies by Halevi and Mösta (2018) also analyzed the dependence on the alignment between rotation axis and magnetic fields, where the most aligned cases result in the strongest r-process. Recent studies of this phenomenon have been undertaken (Obergaullinger *et al.*, 2018; Obergaullinger and Aloy, 2020; Bugli *et al.*, 2020; Reichert *et al.*, 2019). The major constraint is the prerequisite of high initial magnetic fields combined with high rotation rates in order to lead to an early (prompt) polar jet-like ejection of neutron-rich matter. In delayed ejections matter experiences interactions with neutrinos, which enhance Y_e and weaken the strength of the r-process, like in the supernova neutrino wind (see the above discussion on that topic).

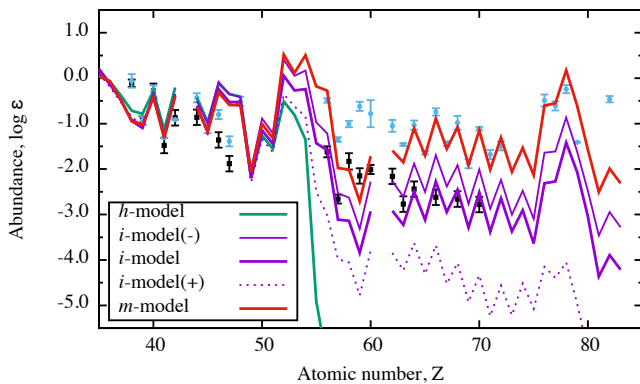


FIG. 28 Abundances from nucleosynthesis calculations with varying ratios of magnetic field strength vs. the neutrino heating of regular core-collapse SNe, increasing for the models h, i-, i, i+, and m (for details see Nishimura *et al.*, 2017). For comparison also abundances from MP stars with a weak r-process are shown, i.e. HD122563 (black dots, Honda *et al.*, 2006), and solar-type r-process observations from CS22892-052 (blue dots, Sneden *et al.*, 1996). Abundances are normalized for $Z = 40$ of HD122563. Observations of low metallicity stars with strong r-process contributions vary for abundances below $Z=50$ (Sneden *et al.*, 2008).

A number of 2D axisymmetric simulations tested nucleosynthesis features (e.g. Nishimura *et al.*, 2015; Shibagaki *et al.*, 2016; Nishimura *et al.*, 2017; Reichert *et al.*, 2019), depending on a variety of conditions in terms of rotation rates, initial magnetic fields, and ratios of neutrino luminosities vs. magnetic field strengths. Nishimura *et al.* (2017) performed a series of long-term explosion simulations, based on special relativistic MHD (Takiwaki *et al.*, 2009; Takiwaki and Kotake, 2011) with outcomes from prompt magnetic jet over delayed magnetic explosions up to dominantly neutrino-powered explosions, determined by the ratio of magnetic field strengths in comparison to neutrino heating. This causes also a variation of r-process nucleosynthesis results (see Fig. 28), from full-blown strong r-process environments, over a weak r-process, not producing nuclei of the third r-process peak, down to no r-process at all. Thus, the production for heavy neutron capture elements varies strongly, being either Fe and Zn dominated like in regular core-collapse SNe or Eu dominated, indicating a strong r-process. This is shown in Fig. 29.

The relative fraction which such MHD-jet supernovae contribute to all core-collapse supernovae depends on the distribution of pre-collapse magnetic field strength and rotation among progenitor stars, probably being metallicity dependent. Higher metallicities lead to stronger stellar wind loss, accompanied by a loss of angular momentum and thus reducing the fast rotation necessary for this type of SN explosions. These events would eject only small amounts of Fe-group nuclei in case of strong r-processing (Nishimura *et al.*, 2015, 2017). Fig. 29

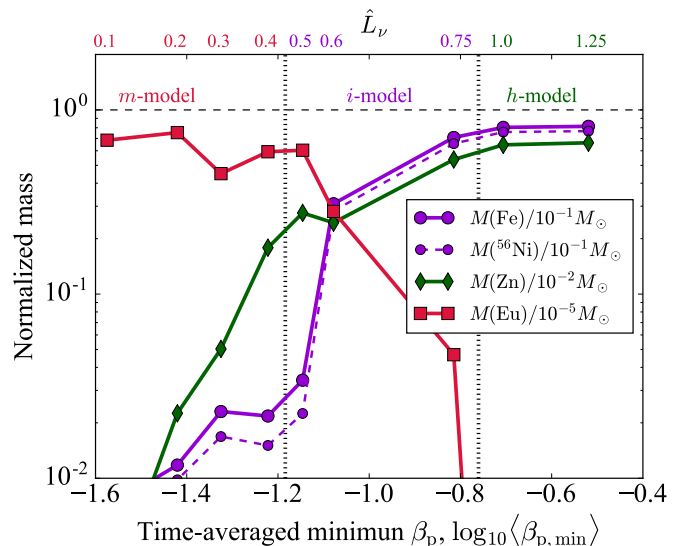


FIG. 29 Nucleosynthetic features of rotating core-collapse SN models (h, i-, i, i+, m) with varying ratios of neutrino luminosity and magnetic field strengths as in Fig. 28. Model m represents a strong MHD-jet supernova. One can see the transition from a regular core-collapse SN pattern, dominated by ^{56}Ni , total Fe (after decay), and Zn, to a strong r-process pattern with a high Eu abundance (for details see Nishimura *et al.*, 2017).

shows how the Ni/Eu-ratio (and similarly the Fe/Eu-ratio) varies strongly as a function of neutrino heating vs. magnetic field effects. Thus, these types of supernovae alone would be able to provide a large spread in Eu/Fe and might even explain the variations in actinides vs. Eu, seen in a number of cases at low metallicities (see e.g. Wehmeyer *et al.*, 2015; Thielemann *et al.*, 2017a). The influence of the explosion mechanism of this type of rare supernovae on their lightcurves and spectra is discussed in (Siegel *et al.*, 2019).

6. Collapsars, Hypernovae, long-duration Gamma-Ray Bursts

One of the most interesting developments in the study of supernovae (SNe) is the discovery of some very energetic supernovae (for a review see e.g. Nomoto *et al.*, 2006), dubbed hypernovae, whose kinetic energy (in spherically symmetric analysis, see also Piran, 2004) exceeds 10^{52} erg. The most luminous and powerful of these objects, the Type Ic supernova (SN Ic) 1998bw (Galama *et al.*, 1998; Patat *et al.*, 1998), was probably linked to the gamma-ray burst GRB 980425, thus establishing for the first time a connection between (long-duration) gamma-ray bursts (IGRBs) and the well-studied phenomenon of core-collapse SNe. However, SN 1998bw was exceptional, indicating that it synthesized $\sim 0.5 M_{\odot}$ of ^{56}Ni with an estimated explosion energy of $E \sim 3 \times 10^{52}$ erg (Iwamoto *et al.*, 1998; Woosley *et al.*, 1999).

The question is where these events should be placed in

the stellar mass range and which other features should be related. For non-rotating massive stars only the (regular) supernova “branch” (with neutron stars as final outcome) can be attained, followed towards increasing stellar mass by a faint or failed supernova branch (leading eventually to black holes, but not to gamma-ray bursts and high ejecta masses). Thus, massive stars, which fail to explode as supernovae via neutrino-powered explosions, will eventually experience the formation of a central black hole (BH, see e.g. Pan *et al.*, 2018; Kuroda *et al.*, 2018). However, rotating BHs and the formation of accretion disks with accretion rates of about $\approx 0.1 M_{\odot} \text{ s}^{-1}$ can lead — for certain conditions (strong magnetic fields) — to long duration gamma-ray bursts (lGRBs) or hypernovae, also dubbed collapsars. The collapsar model was proposed by Woosley, MacFadyen and others (see also MacFadyen and Woosley, 1999; MacFadyen *et al.*, 2001; Nagataki *et al.*, 2007; Sekiguchi and Shibata, 2011; Nagataki, 2011), including neutrino heating from the accretion disk and the winding of strong magnetic fields, causing MHD jets (e.g. Fujimoto *et al.*, 2006; Ono *et al.*, 2012; McKinney *et al.*, 2013; Janiuk *et al.*, 2018). Early hydrodynamic simulations (injecting explosion energies artificially) were performed either by introducing high explosion energies (up to 10^{52} erg) in a spherically symmetric way or aspherically in order to understand jet-like explosions (MacFadyen and Woosley, 1999; Nakamura *et al.*, 2001; Nomoto *et al.*, 2006, 2013; Nomoto, 2017).

The basic (consensus) picture has been the following: explosion energies can be found up to 5×10^{52} erg, ^{56}Ni ejecta up to $0.5 M_{\odot}$, and there exist relativistic jets responsible for lGRBs. There exists uncertainty in predicting Y_e , due to weak interactions and especially neutrino transport. The observational constraint of high ^{56}Ni ejecta argues for a dominant Y_e in matter of the order 0.5. High explosion energies also lead to high entropies and a strong α -rich freeze-out, including large amounts ^{45}Sc (that is difficult to produce in other environments), ^{64}Zn (from ^{64}Ge -decay), and also other Fe-group elements. Nakamura *et al.* (2001) and Nomoto (2017) concluded that larger abundance ratios for (Zn, Co, V, Ti)/Fe and smaller (Mn, Cr)/Fe ratios are expected than for normal SNe, a feature which seems to be consistent with observations in extremely metal-poor (EMP) stars.

Self-consistent modeling of the complete event, from collapse, black hole formation, accretion disk modeling, jet ejection, and GRB occurrence is a formidable challenge. Specific investigations, with respect to the role of weak interactions, magnetic fields, and resulting nucleosynthesis in the accretion disk and corresponding outflows, have been undertaken, related either to individual magnetic bubbles (e.g. Pruet *et al.*, 2003, 2004) or to the main wind outflows (see e.g. Beloborodov, 2003; McLaughlin and Surman, 2005; Surman *et al.*, 2006; Janiuk, 2014; Siegel and Metzger, 2017; Janiuk, 2017; Ja-

niuk and Sapountzis, 2018; Siegel *et al.*, 2019). Beloborodov (2003) found conditions for the minimum accretion rate required, leading to neutron-rich environments with low Y_e ’s at a given radius:

$$\dot{M}_n = 3.821 \times 10^{-3} \left(\frac{r}{3r_g} \right)^{1/2} \left(\frac{\alpha}{0.1} \right) \left(\frac{M_{\text{BH}}}{M_{\odot}} \right)^2 M_{\odot} \text{ s}^{-1}. \quad (12)$$

Here r_g is the gravitational Schwarzschild radius, α the disk viscosity, M_{BH} the mass of the central black hole. For typical accretion rates of $0.1 M_{\odot} \text{ s}^{-1}$ this can lead to a low Y_e at small radii in the disk. Larger accretion rates favor smaller Y_e out to larger radii.

Fig. 30 shows the Y_e distribution obtained by Janiuk (2014) as a function of the radius. While the central parts of the disk experience a low Y_e , its value reaches $Y_e \approx 0.5$ in the outermost regions and even exceeds beyond 0.5 in intermediate regions. If the disk outflow occurs from the outer regions, this is consistent with the large ^{56}Ni ejecta (observed and) found e.g. by Pruet *et al.* (2004); Surman *et al.* (2006); Janiuk (2014, 2017); Janiuk and Sapountzis (2018). However, Pruet *et al.* (2004) also speculated that in case of strong magnetic fields low Y_e matter can be flung out from more central regions of the disk along magnetic field lines, possibly causing r-process production. Additionally, MHD-driven collapsar models, involving black hole accretion disk systems (Nagataki *et al.*, 2007; Fujimoto *et al.*, 2008; Harikae *et al.*, 2009), have argued that the jets produced by the central engine of long duration gamma-ray-bursts can produce heavy r-process nuclei (Fujimoto *et al.*, 2007, 2008; Ono *et al.*, 2012; Nakamura *et al.*, 2015). However, it should be mentioned that early studies assumed a quite simplified treatment of the black hole and the required microphysics. Siegel and Metzger (2017); Siegel *et al.* (2019); Janiuk (2019a), having performed multi-D MHD simulations for accretion disk outflows, argue that large amounts ($> 0.1 M_{\odot}$) of r-process material can be ejected. If this scenario materializes, it would be sufficient to have about one such event per 1000–10000 core-collapse supernovae to explain the solar r-process abundances.

The open question is whether both, large amounts of ^{56}Ni expected for hypernovae, as well as r-process ejecta, can be produced in the same event. Siegel *et al.* (2019) argue that the ^{56}Ni would have to come from a preceding supernova explosion phase, leaving an intermittent neutron star before further accretion causes black hole formation and a black hole accretion disk. This brings up the following questions: (a) At which stellar progenitor masses do we have a transition from the formation of neutron stars to the formation of black holes after collapse? (b) In which transition region are initially neutron stars formed, causing a regular supernova explosion, but ongoing accretion leads to a black hole? (c) For which progenitor masses are black holes formed directly dur-

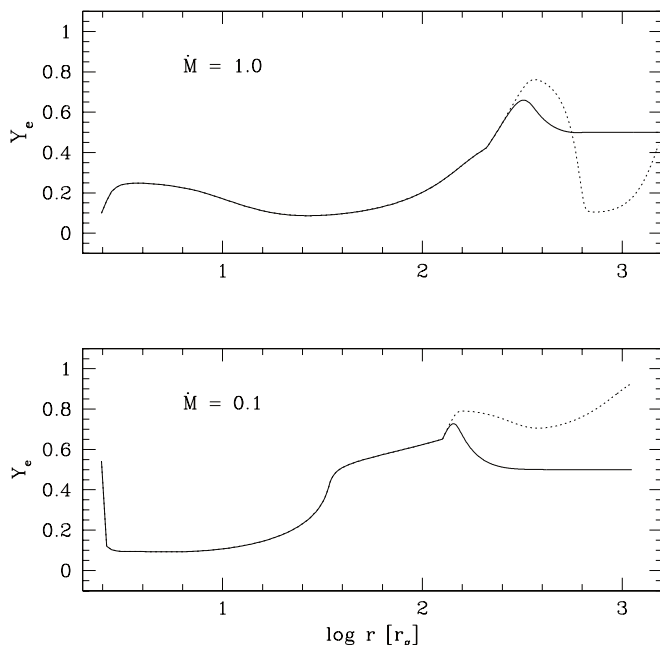


FIG. 30 Radial distribution of Y_e (thick line) and proton fraction (dashed line) in a disk, with $\alpha=0.1$ and $M_{BH}=3M_{\odot}$, for different accretion rates. r_g , the gravitational radius, stands for the Schwarzschild radius of the black hole. Y_e indicates very neutron-rich conditions deep inside the disk but develops asymptotically to values of 0.5 in the outer layers above $100 r_g$ from where the nucleosynthesis outflow will occur (from Janiuk, 2014)

ing collapse and how can this be observed? (d) What is the role of rotation and magnetic fields to cause IGRBs and can we give reliable nucleosynthesis yields for such events? (e) Is there a separation in different types of events, depending on the parameters in (d), leading either to hypernovae and strong ^{56}Ni ejecta or systems with a large outflow of r-process elements? (f) Are jets and IGRBs occurring in both types of events?

The scenario suggested by Siegel *et al.* (2019) would relate to questions (b) and case (c). The main question is whether a strong supernova/hypernova explosion with large Ni production can take place before the accretion disk outflows eject r-process material in the same event or could r-process outflows occur without causing a hypernova? Further observations will have to constrain such events.

B. Neutron-star and neutron-star / black hole mergers

Neutron stars, (for historical references see e.g. Landau, 1932; Baade and Zwicky, 1934; Hewish and Okoye, 1965), when found in a binary system (e.g. Hulse and Taylor, 1975) lose energy by emission of gravitational waves as predicted by General Relativity and are expected to merge in timescales $\sim 10^8$ years (Weisberg

and Huang, 2016). Simultaneously to the discovery of binary pulsars, it was suggested that neutron star or neutron star-black hole mergers would eject r-process nuclei (Lattimer and Schramm, 1974, 1976; Symbalisty and Schramm, 1982), followed up by a first detailed analysis of possible abundance distributions (Meyer and Schramm, 1988). Later predictions showed that such mergers would be accompanied by neutrino bursts and gamma-ray bursts (Eichler *et al.*, 1989). The first predictions of mass ejection from neutron star mergers in Newtonian approximation were given in Davies *et al.* (1994), Ruffert *et al.* (1996), and Rosswog *et al.* (1999, 2000). The first detailed nucleosynthesis prediction was provided by Freiburghaus *et al.* (1999b).

Thereafter, extensive investigations have been undertaken with respect to nucleosynthesis predictions (Panov and Thielemann, 2004; Panov *et al.*, 2008; Goriely *et al.*, 2011; Korobkin *et al.*, 2012; Panov *et al.*, 2013; Bauswein *et al.*, 2013; Goriely *et al.*, 2013; Hotokezaka *et al.*, 2013; Rosswog *et al.*, 2014; Wanajo *et al.*, 2014; Just *et al.*, 2015a; Goriely *et al.*, 2015; Perego *et al.*, 2014; Eichler *et al.*, 2015; Martin *et al.*, 2015; Mendoza-Temis *et al.*, 2015; Ramirez-Ruiz *et al.*, 2015; Hotokezaka *et al.*, 2015; Shibagaki *et al.*, 2016; Just *et al.*, 2016; Wu *et al.*, 2016; Radice *et al.*, 2016; Roberts *et al.*, 2017; Martin *et al.*, 2018; Wojczuk and Janiuk, 2018; Papenfort *et al.*, 2018; Radice *et al.*, 2018b; Holmbeck *et al.*, 2019b). Initial Newtonian approaches have been replaced with conformally flat and fully relativistic treatments (e.g. Shibata and Uryū, 2000; Ruffert and Janka, 2001; Oechslin *et al.*, 2002, 2004; Shibata and Uryū, 2006; Oechslin *et al.*, 2007; Shibata and Taniguchi, 2011; Bauswein and Janka, 2012; Bauswein *et al.*, 2013; Hotokezaka *et al.*, 2013; Wanajo *et al.*, 2014; Sekiguchi *et al.*, 2015, 2016; Radice *et al.*, 2016; Baiotti and Rezzolla, 2017; Bovard *et al.*, 2017; Papenfort *et al.*, 2018), and further followed by the inclusion of magnetic fields (Price and Rosswog, 2006; Anderson *et al.*, 2008; Liu *et al.*, 2008; Giacomazzo *et al.*, 2009; Obergaulinger *et al.*, 2010; Zrake and MacFadyen, 2013; Kiuchi *et al.*, 2015; Giacomazzo *et al.*, 2015) as well as their interplay with neutrinos (Palenzuela *et al.*, 2015; Guilet *et al.*, 2017)

In parallel to neutron star (NS-NS) mergers also neutron star-black hole (NS-BH) mergers have been investigated (e.g. Rosswog, 2005; Shibata and Uryū, 2006; Chawla *et al.*, 2010; Shibata and Taniguchi, 2011; Korobkin *et al.*, 2012; Wanajo and Janka, 2012; Kyutoku *et al.*, 2013; Foucart *et al.*, 2014; Mennekens and Vanbeveren, 2014; Rosswog *et al.*, 2017; Brege *et al.*, 2018). A common outcome of a NS-NS merger and in some NS-BH mergers is the formation of an accretion disk surrounding a central remnant (Ruffert *et al.*, 1997; Shibata and Taniguchi, 2006), (see below).

From the point of view of r-process nucleosynthesis, simulations should predict the amount of ejecta, their properties (particularly Y_e), spatial distribution and tem-

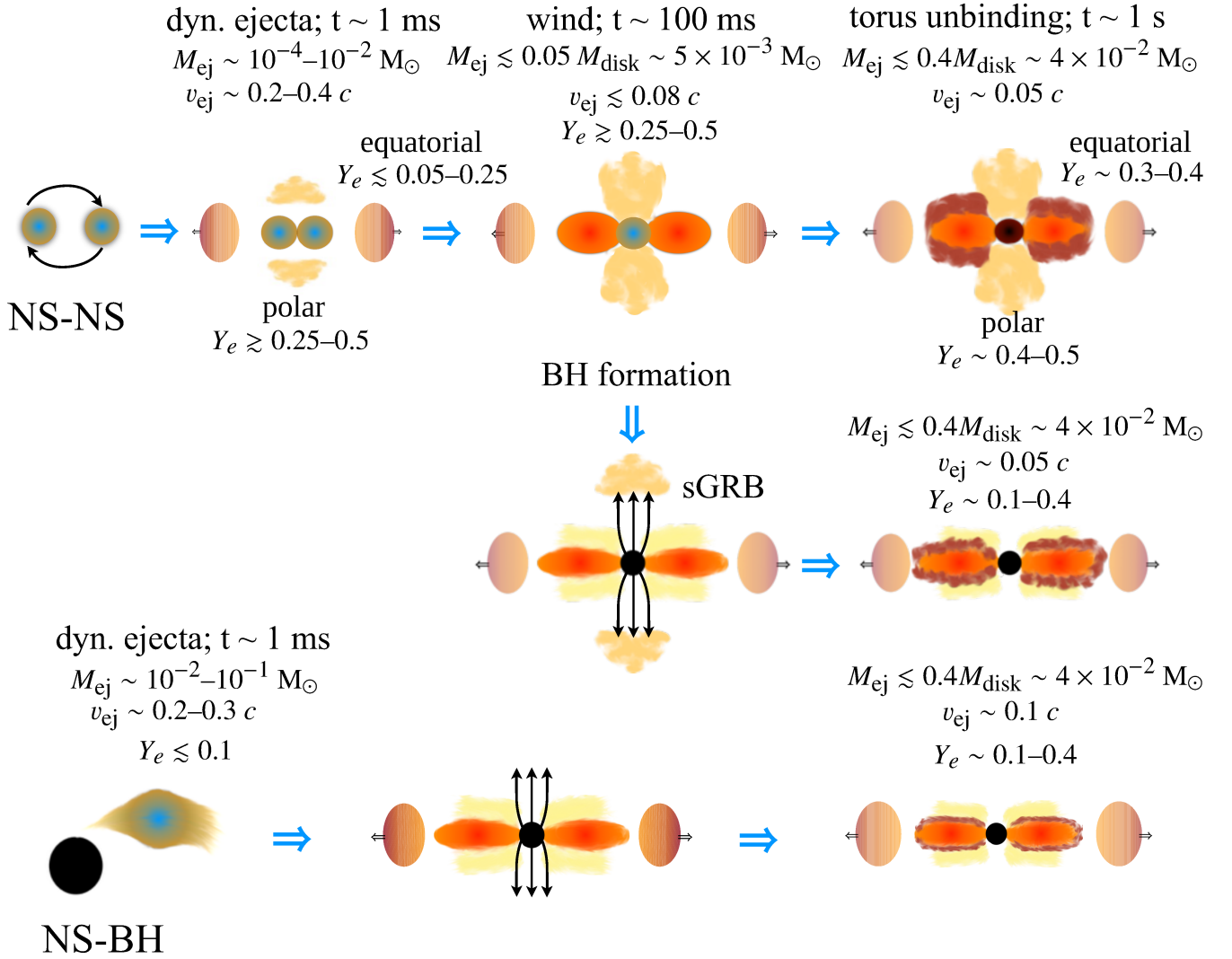


FIG. 31 Ejection channels in compact binary mergers including estimates based on simulations of the ejecta mass, Y_e , and velocity during the different ejection phases. The NS-NS merger system is shown in the upper part including the two possible outcomes: a long lived massive neutron star and a hypermassive neutron star that collapses to a black hole on a timescale shorter than the disk lifetime. The BH-NS merger is shown in the lower part. (Adapted from [Rosswog et al., 2017](#))

poral evolution. In the following, we discuss the major phases of ejection and the general dependencies on the merging system. The discussion is mostly based on a presentation of [Shibata \(2018\)](#), see also [Shibata and Hotokezaka \(2019\)](#) and [Radice et al. \(2020\)](#). Fig. 31 summarizes the main ejection channels in compact binary mergers and provides estimates of ejecta mass, Y_e , and velocity. See also Fig. 1 in [Bartos et al. \(2013\)](#) for estimated behaviors dependent on the mass of the binary components involved.

Due to the emission of gravitational waves, that reduces the eccentricity of the orbit, at times close to coalescence NS-NS systems are expected to have almost circular orbits and spins much smaller than the orbital frequency ([Rosswog, 2015](#)). During the coalescence phase matter is ejected dynamically due to angular momentum

conservation on timescales of milliseconds with mildly relativistic speed $v \sim 0.2 - 0.4 c$ ([Rosswog et al., 1999, 2000](#); [Bauswein et al., 2013](#); [Hotokezaka et al., 2013b](#); [Palenzuela et al., 2015](#); [Sekiguchi et al., 2015, 2016](#); [Radice et al., 2016](#); [Foucart et al., 2016](#)).

The amount of dynamic ejecta and their properties depend on the compactness of the neutron stars and their mass ratio ([Bauswein et al., 2013](#); [Hotokezaka et al., 2013b](#); [Radice et al., 2018b](#)). Two components can be distinguished: cold tidal ejecta in the equatorial plane and shock-heated ejecta originating from the contact interface with a more isotropic distribution. Systems with small mass ratios tend to eject larger amounts of material mainly in the equatorial region, while for similar masses the shock heated component dominates ([Bauswein et al., 2013](#); [Hotokezaka et al., 2013b](#); [Palenzuela et al., 2015](#);

Lehner *et al.*, 2016). While the cold tidal ejecta maintain the original low Y_e of the neutron star crust from which they are ejected, the shock component is heated to very large temperatures. This drives electron and positron captures which increase Y_e from a very low initial value. As the material moves away, Y_e is further increased by ν_e and $\bar{\nu}_e$ absorption (Wanajo *et al.*, 2014; Goriely *et al.*, 2015; Martin *et al.*, 2015; Sekiguchi *et al.*, 2016; Radice *et al.*, 2016; Martin *et al.*, 2018). The impact of neutrino absorptions is sensitive to the evolution of the central remnant (Sekiguchi *et al.*, 2015). The total amount of dynamic ejecta are in the range 10^{-4} – 10^{-2} M_\odot (Bauswein *et al.*, 2013; Hotokezaka *et al.*, 2013b; Sekiguchi *et al.*, 2015, 2016; Lehner *et al.*, 2016; Radice *et al.*, 2018b) with an angular mass distribution well approximated by $F(\theta) = \sin^2 \theta$ (Perego *et al.*, 2017a) and a Y_e distribution that can reach up to $Y_e \sim 0.5$ in the polar region (Shibata *et al.*, 2017; Radice *et al.*, 2018b; Shibata and Hotokezaka, 2019). Magneto-hydrodynamic instabilities, operating during the merger, can produce a third component denoted as “viscous-dynamical” ejecta (Radice *et al.*, 2018a) with asymptotic velocities extending up to $\sim 0.8 c$. Population synthesis studies (Belczynski *et al.*, 2008), formation studies (Tauris *et al.*, 2017), pulsar observations (Özel and Freire, 2016), and the gravitational wave signal from GW170817 (Abbott *et al.*, 2017c; De *et al.*, 2018; Abbott *et al.*, 2019) favor binary NS systems with nearly equal-mass stars $\sim 1.35 M_\odot$. For such systems the ejecta are mainly sensitive to the compactness of the neutron stars. The analysis of the tidal deformability from the Gravitational Wave observations of GW170817 (Most *et al.*, 2018; De *et al.*, 2018; Abbott *et al.*, 2018; Capano *et al.*, 2020), the observation of an electromagnetic transient which disfavors a prompt collapse to a black hole (Margalit and Metzger, 2017; Bauswein *et al.*, 2017; Shibata *et al.*, 2017; Coughlin *et al.*, 2019; Margalit and Metzger, 2019), together with nuclear physics constraints (Fattoyev *et al.*, 2018; Annala *et al.*, 2018; Tews *et al.*, 2018; Tews *et al.*, 2019; Capano *et al.*, 2020) favor moderately compact neutron stars with a radius in the range 8.9–13.2 km. In this case, the major source of ejecta is the contact interface between the neutron stars (Bauswein *et al.*, 2013; Sekiguchi *et al.*, 2015; Radice *et al.*, 2018b). The maximum mass of a neutron star has been constrained to $M_{\max} \lesssim 2.17 M_\odot$ (Margalit and Metzger, 2017; Shibata *et al.*, 2017; Rezzolla *et al.*, 2018; Ruiz *et al.*, 2018) following the observation of GW170817. Recently another NS-NS merger GW190425 with a combined total mass of $\sim 3.4 M_\odot$ has been observed (Abbott *et al.*, 2020). The high total mass together with the absence of an electromagnetic signal suggest a prompt collapse to a black hole (Foley *et al.*, 2020). In the case of NS-BH systems it is necessary that the NS is tidally disrupted by the BH, in order to eject material. Tidal disruption means that the BH tidal force is larger than the self-gravity of the NS. The amount of ejected

mass depends on the relative competition between the orbital separation at which tidal disruption occurs and the radius of the innermost stable circular orbit of the BH. The larger this ratio, the larger is the amount of ejecta. This requires a large NS radius, a small BH mass or small BH/NS mass ratio, or a high spin for the BH (Kyutoku *et al.*, 2015; Capano *et al.*, 2020). We notice that mass ejection may occur even if the neutron star is disrupted inside the innermost stable circular orbit (Faber *et al.*, 2006). Population synthesis studies favor a BH/NS mass ratio ~ 7 (Belczynski *et al.*, 2010). This, together with the NS radius constraints mentioned above, suggests that mass ejection will only take place for a BH with a spin parameter $\chi = cJ/(GM^2) \gtrsim 0.5$ (Foucart, 2012; Foucart *et al.*, 2013, 2014; Kyutoku *et al.*, 2015; Kawaguchi *et al.*, 2016; Brege *et al.*, 2018; Kyutoku *et al.*, 2018). For possible χ -values of the recent BH-NS candidate S190426c see Fig.4 in Lattimer (2019). The tidal dynamic ejecta are much more anisotropic than those of NS-NS mergers. They are mainly concentrated around the orbital plane and often sweep out only half of the plane. The ejected mass can reach $\sim 0.1 M_\odot$ with asymptotic velocities of 0.2–0.3 c . The material is very neutron-rich $Y_e \lesssim 0.1$ and not affected by neutrino irradiation (Foucart *et al.*, 2014; Kyutoku *et al.*, 2018).

An equally common outcome of compact binary mergers is the production of a rotating torus surrounding the newly-formed central object with a typical mass of $0.1 M_\odot$ (Ruffert *et al.*, 1997; Shibata and Taniguchi, 2006; Radice *et al.*, 2018b). In the case of BH-NS mergers the central remnant is a BH and we deal with a neutrino cooled disk that evolves on viscous timescales of seconds. The study of such systems has evolved from the use of α -viscosity prescriptions to parametrize dissipation (Fernandez and Metzger, 2013; Metzger and Fernández, 2014; Just *et al.*, 2015a; Fernández *et al.*, 2015; Fernández and Metzger, 2016; Just *et al.*, 2016; Wu *et al.*, 2016; Wojczuk and Janiuk, 2018; Fujibayashi *et al.*, 2018) to three-dimensional General-Relativistic Magneto-hydrodynamic simulations (Siegel and Metzger, 2017; Siegel and Metzger, 2018; Fernández *et al.*, 2019; Janiuk, 2019b) in which dissipation emerges naturally via the magneto-rotational instability. These works find that up to 40% of the disk mass, depending on the BH spin, is unbound in a quasi-spherical fashion. The electron fraction in the outflow is in the range $Y_e \sim 0.1$ – 0.4 with velocities $v \approx 0.1 c$ (Siegel and Metzger, 2018; Fernández *et al.*, 2019; Christie *et al.*, 2019; Fujibayashi *et al.*, 2020) depending on the efficiency of dissipation in the disk. For the case of NS-NS mergers, the possibilities for the central object are a stable NS, a long-lived massive neutron star (MNS, i.e. a NS with a mass above the maximum mass for a non-spinning NS and below the one for a uniformly rotating NS), a hypermassive neutron star (HMNS, i.e. a NS with a mass above the maximum mass for a uniformly rotating NS, Baumgarte *et al.*,

2000) or a black hole (BH) depending primarily on the total mass of the binary, M_t (Hotokezaka *et al.*, 2013a; Shibata, 2018). If M_t exceeds a critical value M_c , the central object produced by the merger collapses promptly to a BH on the dynamical time scale of a few ms (Sekiguchi *et al.*, 2011). On the other hand, if $M_t < M_c$ the resulting HMNS is at least temporarily supported against gravitational collapse by differential rotation and thermal pressure (Hotokezaka *et al.*, 2013a; Kaplan *et al.*, 2014). The value of M_c depends on the uncertain EoS of nuclear matter, particularly its stiffness, mainly related to the symmetry energy (Baldo and Burgio, 2016; Oertel *et al.*, 2017). The discovery of massive $\sim 2 M_\odot$ neutron stars (Demorest *et al.*, 2010; Antoniadis *et al.*, 2013), places a lower limit to $M_c \gtrsim 2.6 - 2.8 M_\odot$ (Hotokezaka *et al.*, 2013a). Hydrodynamical simulations of neutron star mergers for a large sample of temperature-dependent equations of state, show that the ratio between critical mass and the maximum mass of a non-rotating NS are tightly correlated with the compactness of the non-rotating NS (Bauswein *et al.*, 2013). This allows to derive semi-analytical expressions for the critical mass (Bauswein and Stergioulas, 2017; Bauswein *et al.*, 2016; Bauswein and Stergioulas, 2019) that, combined with the GW170817 constraints on the maximum mass and radius of NS, give $M_c \approx 2.8 M_\odot$. It thus appears likely that the canonical $1.35 + 1.35 M_\odot$, including GW170817, binary merger goes through a HMNS phase. The duration of this phase depends on angular momentum transport processes (gravitational wave emission, magnetic fields, ...) and the EoS as it determines the value of M_c (Shibata *et al.*, 2005; Shibata and Taniguchi, 2006; Kiuchi *et al.*, 2009; Hotokezaka *et al.*, 2011; Kastaun *et al.*, 2016): For a soft EoS that results in rather compact initial neutron stars before the merger, the HMNS collapses to a black hole on timescales of several 10s of milliseconds, while for a stiff EoS the HMNS is long-lived with a lifetime longer than the timescales relevant for matter ejection. The NS radius constraints mentioned above favor the first case. For the case of prompt collapse to a BH, the BH-torus system evolves similarly to the BH-NS merger case considered before. However, systems with large M_t are expected to eject little mass dynamically and produce a low mass accretion disk. In these cases, the total amount of ejecta, dynamical plus accretion disk, is $\sim 10^{-3} M_\odot$ of neutron-rich material, $Y_e \lesssim 0.1$ (Shibata, 2018).

The HMNS-torus is characterized by a more important role of neutrino heating that increases the amount of ejecta and raises their Y_e to values that depend on the lifetime of HMNS remnant (Metzger and Fernández, 2014; Perego *et al.*, 2014; Kaplan *et al.*, 2014; Martin *et al.*, 2015; Lippuner *et al.*, 2017; Fujibayashi *et al.*, 2018). The ejecta consist of two components being either neutrino-driven or viscous-driven (also known as secular). The neutrino-driven component is ejected mainly in the

polar direction with velocities $v \lesssim 0.08 c$ and $Y_e \gtrsim 0.25$ and containing around 5% of the disk mass (Martin *et al.*, 2015; Perego *et al.*, 2017a). The viscous-driven component occurs mainly in the equatorial direction with a velocity $v \sim 0.05 c$ and contains around 40% of the disk mass (Metzger and Fernández, 2014; Lippuner *et al.*, 2017; Fujibayashi *et al.*, 2018). The Y_e distribution depends on the lifetime of the HMNS (Fujibayashi *et al.*, 2018). If the HMNS survives at least for the timescale of neutrino cooling of the disk (~ 10 s), neutrino heating drives Y_e to values above 0.25. If the HMNS collapses to a black hole on a timescale shorter than the disk lifetime, the Y_e distribution is in the range 0.1–0.4, similar to the BH-torus case.

There exists extensive literature relating these events to short duration Gamma-Ray Bursts (sGRBs) and kilonovae as electromagnetic counterparts (see e.g., Li and Paczyński, 1998; Nakar, 2007; Metzger and Berger, 2012; Tanvir *et al.*, 2013; Piran *et al.*, 2013; Tanaka and Hotokezaka, 2013; Kasen *et al.*, 2013; Grossman *et al.*, 2014; Rosswog *et al.*, 2014; Metzger and Fernández, 2014; Wanderman and Piran, 2015; Rosswog, 2015; Fryer *et al.*, 2015; Hotokezaka *et al.*, 2016; Barnes *et al.*, 2016; Fernández and Metzger, 2016; Rosswog *et al.*, 2017; Metzger, 2017a; Ascenzi *et al.*, 2019). Although these objects are also of major importance as strong sources for gravitational wave emission (Shibata and Taniguchi, 2011; Baiotti and Rezzolla, 2017), especially after GW170817 (Abbott *et al.*, 2017d), underpinning the importance of multi-messenger observations, we will focus here on the ejected nucleosynthesis composition. In the following subsections we will concentrate on (i) the dynamic ejecta, (ii) the post-merger neutrino wind ejecta, and (iii) the late time viscous or secular outflow from the accretion disk.

1. Dynamic ejecta

The dynamic ejecta consist of two components: a cold component consisting of very neutron-rich matter originating from the neutron star crust that is “thrown out” via tidal interaction in the equatorial plane, and a hotter component originating from the contact interface. The first component is the only one present in NS-BH mergers and the second represents most of the unbound material in NS-NS mergers. The tidal component was originally found in Newtonian simulations (first investigations by Davies *et al.* 1994; Rosswog *et al.* 1999 and more detailed discussions by Korobkin *et al.* 2012), while the contact interface component was found in relativistic simulations, first within the conformal flatness approximation (Oechslin *et al.*, 2007; Goriely *et al.*, 2011; Bauswein *et al.*, 2013) and then in fully relativistic simulations (Hotokezaka *et al.*, 2013b). The latter simulations neglected the impact of weak processes in the ejecta and hence the

ejected material kept the very neutron-rich conditions corresponding to β -equilibrium in the cold neutron star crust, $Y_e \lesssim 0.01$.

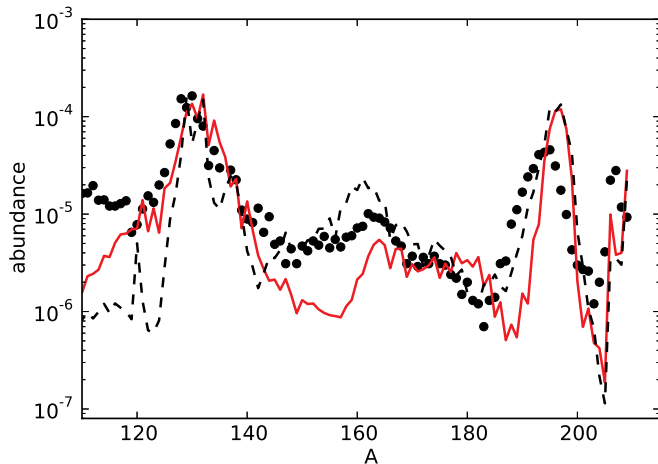


FIG. 32 Resulting r-process abundances for dynamic tidal ejecta (in comparison to solar values-black dots) from neutron star merger simulations (Eichler *et al.*, 2015), making use of β -decay half-lives from Möller *et al.* (2003) (red line) and recent β -decay half-life predictions (Marketin *et al.*, 2016a, black line) together with the fragment distributions from fissioning nuclei of Kelic *et al.* (2008).

The nucleosynthesis in low Y_e ejecta, as found in BH-NS mergers and the tidal component of NS-NS mergers, has been extensively studied (Freiburghaus *et al.*, 1999b; Korobkin *et al.*, 2012; Bauswein *et al.*, 2013; Rosswog *et al.*, 2014; Mendoza-Temis *et al.*, 2015; Eichler *et al.*, 2015; Martin *et al.*, 2016; Mumpower *et al.*, 2016; Bovard *et al.*, 2017) and found to be independent of the astrophysical conditions (Korobkin *et al.*, 2012) but rather sensitive to the nuclear physics input (Panov and Thielemann, 2004; Panov *et al.*, 2008; Bauswein *et al.*, 2013; Eichler *et al.*, 2015; Mendoza-Temis *et al.*, 2015; Goriely, 2015; Goriely and Martínez-Pinedo, 2015; Martin *et al.*, 2016; Mumpower *et al.*, 2016; Shibagaki *et al.*, 2016; Thielemann *et al.*, 2017b; Vassh *et al.*, 2019a). For very neutron-rich ejecta neutron-to-seed ratios can even reach several 1000 and the associated nucleosynthesis becomes insensitive to the initial composition. The temperature evolution is characterized by having a high temperature plateau, T_{\max} , (see Fig. 14) whose value is determined by a competition between the r-process energy generation rate, \dot{Q} , and the expansion dynamical timescale (Mendoza-Temis *et al.*, 2015):

$$T_{\max} \approx 0.8 \text{ GK} \left[\left(\frac{\rho}{10^5 \text{ g cm}^{-3}} \right) \left(\frac{\dot{Q}}{4 \text{ MeV s}^{-1}} \right) \left(\frac{\tau_{\text{dyn}}}{10 \text{ ms}} \right) \right]^{1/4} \quad (13)$$

Independent of the initial conditions, during the phase of neutron captures one can have a hot or cold r-process,

see section III and Fig. 14 where dark gray and brown lines correspond to cold r-process conditions and light gray lines to hot r-process conditions. Typically the expansion of the material is “slow” enough to allow for all neutrons to be captured. This leads to the occurrence of several fission cycles with large amounts of very heavy nuclei prone to fission, mainly around $A \sim 280$, remaining at freeze-out, see Fig. 13. During the final freeze-out phase the fission yields of the heaviest nuclei determine the final abundances of nuclei with $A \lesssim 140$ (Goriely and Martínez-Pinedo, 2015). Fission also produces large amounts of neutrons that tend to be captured on the third r-process peak material. Depending on the amount of neutrons produced and the speed at which they are released, the third r-process peak can be shifted to higher mass numbers when compared with solar abundances (see Fig. 32 from Eichler *et al.*, 2015, and for more details on the effects of fission, subsection V.D). This depends on the mass model, see Fig. 23, and β -decay half-lives (Marketin *et al.*, 2016a; Panov *et al.*, 2016). In particular, shorter β -decay half-lives for very heavy nuclei result in smaller abundances in the fissioning region and hence less and faster release of neutrons during the freeze-out (Eichler *et al.*, 2015).

Fission rates and yields for neutron-rich heavy and superheavy nuclei are then fundamental for the determination of the r-process abundances (Goriely, 2015). This requires not only the determination of the region of the nuclear chart where fission occurs (Thielemann *et al.*, 1983; Petermann *et al.*, 2012; Giuliani *et al.*, 2018; Giuliani *et al.*, 2019), but also the modeling of all relevant fission channels, including neutron-induced fission, β -delayed fission, and spontaneous fission (Thielemann *et al.*, 1983; Panov *et al.*, 2005; Panov and Thielemann, 2004; Goriely *et al.*, 2009; Panov *et al.*, 2010; Mumpower *et al.*, 2018; Vassh *et al.*, 2019a) and corresponding yields (Kelic *et al.*, 2009; Goriely *et al.*, 2013; Schmidt *et al.*, 2016; Schmitt *et al.*, 2018; Schmidt and Jurado, 2018; Vassh *et al.*, 2019a). Low Y_e ejecta produce a final abundance distribution that follows the solar r-process abundance distribution for $A > 140$ independently of the fission yields used (Goriely and Martínez-Pinedo, 2015). The production of lighter nuclei is rather sensitive to the fission rates and yields used and typically no nuclei below $A \sim 110$ are produced in substantial amounts (Panov *et al.*, 2008; Goriely *et al.*, 2013; Mendoza-Temis *et al.*, 2015; Eichler *et al.*, 2015; Vassh *et al.*, 2019a). Fission is also important for the production of actinides with important consequences for late time kilonova light curves (Barnes *et al.*, 2016; Rosswog *et al.*, 2017; Wanajo, 2018; Wu *et al.*, 2019; Zhu *et al.*, 2018; Holmbeck *et al.*, 2019b) and U/Th cosmochronometry (see section VIII.D).

Several studies (Goriely *et al.*, 2014; Metzger *et al.*, 2015; Mendoza-Temis *et al.*, 2015; Radice *et al.*, 2018a; Fernández *et al.*, 2019; Ishii *et al.*, 2018) have shown that part of the material, up to 10% in mass, is ejected very

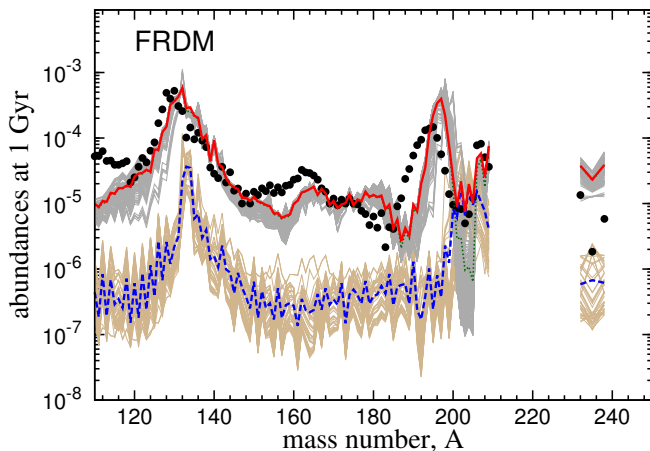


FIG. 33 R-process abundances after a decay time of 1 Gyr for all trajectories shown in Fig. 14. The grey (brown) curves correspond to the abundances of the trajectories of the slow (fast) ejecta. The mass-averaged abundances for all trajectories (red curves), the slow ejecta (green curves), and the fast ejecta (blue curves) are also shown. The abundances for the slow and fast trajectories and their averages have been scaled by the value of their fractional contribution to the total ejecta. (Figure adapted from [Mendoza-Temis et al., 2015](#)).

fast and reaches such low densities that the timescale for neutron captures becomes much longer than the expansion timescale ([Mendoza-Temis et al., 2015](#)) (see brown lines on Fig. 14). Under such conditions most of the neutrons are not captured, despite of having a large neutron-to-seed ratio. The final abundances of this “frustrated” r-process does not correspond to solar abundances (see Fig. 33) and hence it cannot constitute a major component of the total ejected mass, assuming mergers are a major r-process site. However, it can significantly contribute for nuclei around $A \sim 200$ (see difference between green and red lines in Fig. 33) and can drive an early (timescales of hours) electromagnetic emission that is powered by the radioactive decay of the free neutrons left after completion of the r-process ([Metzger et al., 2015](#)).

[Wanajo et al. \(2014\)](#) showed that weak processes operating on the shock heated ejecta of NS-NS mergers can increase the Y_e . They are particular efficient in the polar region, where the large neutrino fluxes from the HMNS increase substantially the Y_e of the ejecta, provided the HMNS does not collapse promptly to a BH. Depending on the neutrino luminosities, Y_e could be increased to values between 0.25 and 0.4. While it is currently accepted that weak processes increase the Y_e of the ejecta, an aspect confirmed by the kilonova observations discussed in section VII, there is still a relatively large spread between the predictions of different groups ([Shibata et al., 2017](#); [Sekiguchi et al., 2016, 2015](#); [Radice et al., 2016, 2018b](#); [Foucart et al., 2016](#); [Bovard et al., 2017](#); [Foucart et al., 2018](#)) related to the different approximations in the treatment of neutrino radiation transport and/or to

differences in the thermodynamical conditions of matter reached after the merger ([Perego et al., 2019](#)) as they determine the magnitude of electron and positron capture processes. Dynamic ejecta from NS-NS mergers are expected to contribute to the synthesis of a broad range of r-process nuclei, including both light and heavy, once weak processes are considered ([Wanajo et al., 2014](#); [Gorieli et al., 2015](#); [Martin et al., 2018](#)). However, it should be kept in mind that the predicted amount of high Y_e matter is typically much smaller than found in accretion disk outflows.

2. Neutrino Winds and the Effect of Neutrinos

In addition to the dynamic ejecta, related directly to the merging/collision, post merger ejecta will emerge as well. One component is a “neutrino-wind” as found in core-collapse supernovae. For the typical merging system, the hot central NS remnant, supported by high temperatures and differential rotation, will not collapse to a black hole immediately (provided that the combined total mass of the system M_t is smaller than M_c , see the introductory part of this subsection VI.B), and will be surrounded by a hot and dense torus. Hence, the structure of the wind is quite different from the isolated NSs usually found in core-collapse supernovae. The wind outflow occurs mainly in the polar direction ([Rosswog et al., 2014](#); [Perego et al., 2014](#); [Metzger and Fernández, 2014](#); [Martin et al., 2015](#)). Matter is exposed to neutrinos long enough for the material to reach an equilibrium between electron neutrino and antineutrino absorption, changing Y_e , see Eq. (10), from the initial (neutron-rich) conditions towards higher values that can even be above $Y_e = 0.5$. Due to the much larger $\bar{\nu}_e$ luminosities and energy differences between $\bar{\nu}_e$ and ν_e , found during the post-merger evolution when compared with core-collapse supernova (see Fig. 25), the peak of the Y_e distribution is expected to be neutron-rich with $Y_e \gtrsim 0.25$ ([Martin et al., 2015](#); [Lippuner et al., 2017](#); [Fujibayashi et al., 2017, 2018](#)). This leads to a weak r-process and produces mainly matter below the second r-process peak, i.e. no lanthanides are produced. Fig. 34 displays the results of [Martin et al. \(2015\)](#) for the neutrino wind component as a function of the delay time until black hole formation. It can be seen that predominantly nuclei below $A = 130$ are produced, complementing nicely the abundance features originating from dynamic low Y_e ejecta, which are also displayed and result here from Newtonian simulations ([Korobkin et al., 2012](#)).

Similar to the situation in core-collapse supernovae, the properties of neutrino-wind ejecta, and particularly Y_e , are expected to be sensitive to the spectral differences between ν_e and $\bar{\nu}_e$. This requires an accurate prediction of neutrino luminosities and spectra. Supernova neutrino-wind transport simulations are nowadays based

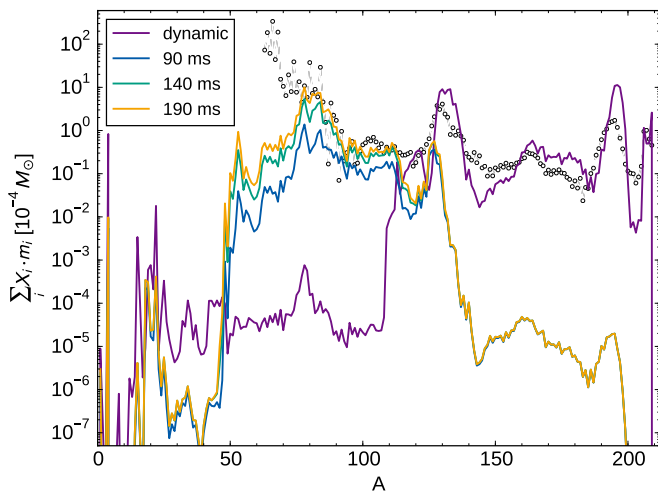


FIG. 34 Neutrino wind contribution to neutron star merger ejecta, dependent on the delay time between the merger and BH formation (Martin *et al.*, 2015). In comparison also the dynamic, tidal ejecta of (Korobkin *et al.*, 2012) are shown. The neutrino wind, ejected dominantly in polar regions, contributes nuclei with $A < 130$, due to the effect of the neutrinos on Y_e .

on accurate numerical solutions of the Boltzmann transport equation (e.g. Hüdepohl *et al.*, 2010; Fischer *et al.*, 2010; Roberts, 2012) exploiting the spherically symmetric nature of the problem. In the case of mergers, which require multidimensional treatments, simulations so far are based on neutrino leakage schemes (Perego *et al.*, 2014; Metzger and Fernández, 2014; Radice *et al.*, 2016; Ardevol-Pulpillo *et al.*, 2018) and $M1$ schemes (Just *et al.*, 2015a,b; Foucart *et al.*, 2015; Fujibayashi *et al.*, 2017, 2018). There are indications that they may not properly capture the energy densities and fluxes of neutrinos in the polar regions (Just *et al.*, 2015a), hence, affecting the Y_e estimates in the polar region (Foucart *et al.*, 2016; Foucart *et al.*, 2018). Additional opacity reactions, like neutrino-pair annihilation, are so far not considered, but may also play an important role in determining the properties of the ejecta (Just *et al.*, 2016; Fujibayashi *et al.*, 2017; Perego *et al.*, 2017b; Fujibayashi *et al.*, 2018; Foucart *et al.*, 2018).

Y_e can also be affected by modifications of neutrino and antineutrino spectra due to neutrino flavor conversion. There have been a number of tests to verify such neutrino conversions via matter-neutrino resonances (Malkus *et al.*, 2012; Foucart *et al.*, 2015; Malkus *et al.*, 2016; Zhu *et al.*, 2016; Frensel *et al.*, 2017) and fast pairwise flavor conversions (Wu and Tamborra, 2017; Wu *et al.*, 2017). Due to the more complicated geometry of a disk environment in comparison to core-collapse supernovae, most of the calculations are based on single-angle approximations. Spherically symmetric test calculations show that the matter-neutrino resonance still occurs in multi-angle models (Vlasenko and McLaughlin, 2018), but with re-

duced efficiency. Nevertheless, the existing investigations clearly point to a potential effect on Y_e , and thus the resulting nucleosynthesis can be affected.

A further wind component, not addressed here, relates to magnetically driven winds from the central remnant (Kiuchi *et al.*, 2012; Siegel *et al.*, 2014; Ciolfi *et al.*, 2017; Metzger *et al.*, 2018). However, their nucleosynthesis yields and interaction with neutrino driven winds have not been explored yet.

3. Accretion Disks outflows

The long-term evolution, $t \sim 1-10$ s, of the accretion disc produces outflows of material powered by viscous heating and nuclear recombination (Lee and Ramirez-Ruiz, 2007; Beloborodov, 2008; Metzger *et al.*, 2009; Fernandez and Metzger, 2013). Those outflows can contain up to 40% of the disk mass. The amount of ejected mass increases with the lifetime of the MNS formed in the merger, but most importantly for nucleosynthesis the Y_e distribution is dramatically affected by the lifetime of the MNS (Metzger and Fernández, 2014). For a long lived MNS, $t \gtrsim 1$ s, neutrino irradiation from the MNS results in ejecta with $Y_e > 0.3$ (Metzger and Fernández, 2014; Lippuner *et al.*, 2017; Fujibayashi *et al.*, 2018). The nucleosynthesis in these ejecta is similar to the neutrino-wind ejecta discussed in the previous subsection.

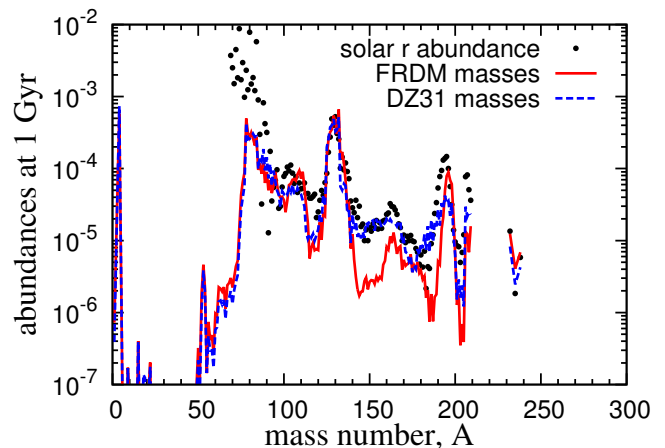


FIG. 35 Resulting r-process abundances (in comparison to solar values — black dots) from black hole accretion disk simulations (Wu *et al.*, 2016), making use of a black hole mass of $3 M_\odot$, a disk mass of $0.03 M_\odot$, an initial Y_e of 0.1, entropy per baryon of $8k_b$, an alpha parameter of the viscous disk of 0.03, and a vanishing black hole spin. The figure illustrate the impact of two different mass models, FRDM and DZ31, in the final abundances.

For a short-lived MNS, $t \lesssim 1$ s, the impact of neutrino-irradiation is small and, from the point of view of nucleosynthesis, outflows from accretion disks formed in NS-NS and BH-NS mergers give similar results. Early

nucleosynthesis studies were mainly parametric and considered mainly the “neutrino-driven” wind outflow from the surface of the disk (Pruet *et al.*, 2003; Fujimoto *et al.*, 2003, 2004; Pruet *et al.*, 2004; McLaughlin and Surman, 2005; Surman *et al.*, 2006; Metzger *et al.*, 2008; Surman *et al.*, 2008; Dessart *et al.*, 2009; Kizivat *et al.*, 2010; Wanajo and Janka, 2012; Surman *et al.*, 2014). Detailed simulations, based initially on α -viscosity prescriptions, and more recently on three-dimensional General-Relativistic magneto-hydrodynamics (for references see the introductory part of this section VI.B), show that neutrino winds from the accretion disk eject little mass and that most of the material is ejected by viscous heating (e.g. Just *et al.*, 2015a). The results for disk outflows by Wu *et al.* (2016) are displayed in Fig. 35, which shows the integrated abundance pattern of all tracer particles. This underlines that, in principle, disk outflows alone can produce the whole range of r-process nuclei, with a significant production of $A \lesssim 130$ nuclei, also reaching the third peak at $A = 195$ in most of the simulations. The detailed results depend on the disk viscosity, the initial mass or entropy of the torus, the black hole spin, and (of course) the nuclear physics input. The latter is illustrated in Fig. 35 that compares the nucleosynthesis results for two different mass models, FRDM (Möller *et al.*, 1995) and Duflo-Zuker (Duflo and Zuker, 1995). The production of heavy ($A \gtrsim 195$) nuclei is also affected by uncertainties of the disk properties discussed above (Just *et al.*, 2015a; Wu *et al.*, 2016; Fernández *et al.*, 2019; Christie *et al.*, 2019; Fujibayashi *et al.*, 2020). Recent α -viscous simulations (Fujibayashi *et al.*, 2020) using torus masses compatible with GW170817, $M \sim 0.1\text{--}0.02 M_\odot$, predict relatively large Y_e ejecta mainly due to the disk reaching dynamical beta-equilibrium (Arcones *et al.*, 2010) between electron and positron captures. The associated nucleosynthesis is strongly suppressed in $A > 130$ nuclei when compared with solar. However, such a possible deficit can be counterbalanced by the dynamic ejecta, as the total nucleosynthesis of the merger includes the components of the dynamic ejecta, the neutrino wind, and the accretion disk.

Nucleosynthesis studies in mergers are commonly based on simulation data that follow the evolution of the ejecta for timescales shorter, \sim ms, than the r-process nucleosynthesis timescale, \sim s. This makes it necessary to extrapolate the time evolution of thermodynamic properties like temperature and density in order to follow the nucleosynthesis to completion. It is commonly assumed that the expansion is homologous, $\rho \sim t^{-3}$, with the temperature evolution determined by the nuclear energy production of the r-process. It originates mainly from β -decays and is in the range $\dot{Q} \approx 1 - 4 \text{ MeV s}^{-1} \text{ nuc}^{-1}$ (see lower panel of Fig. 14). Rosswog *et al.* (2014) have performed long-term simulations and found that the r-process energy release does not qualitatively alter the properties of dynamic ejecta. Wu *et al.* (2016) found that

r-process heating can increase the amount of ejecta up to a factor 2 in viscous outflows from accretion disks and remove an anomalously high abundance of $A = 132$ nuclei (see Fig. 35 and Lippuner *et al.*, 2017; Siegel and Metzger, 2018). R-process heating can critically shape the dynamics of marginally bound ejecta responsible for fall-back accretion on timescales of seconds to minutes (Metzger *et al.*, 2010a; Desai *et al.*, 2019). Late-time fall-back accretion has been suggested as possible mechanism to explain the extended X-ray emission observed in some short GRBs (Rosswog, 2007). R-process heating on timescales of days to weeks after the merger has been found responsible for powering the “kilonova” electromagnetic emission (Li and Paczyński, 1998; Metzger *et al.*, 2010b) as will be discussed in the next section.

VII. ELECTROMAGNETIC SIGNATURES OF R-PROCESS NUCLEOSYNTHESIS

While we have evidence for the existence of some of the events listed in the previous section VI, i.e. among the sites of subsection VI.A possibly for electron-capture supernovae (e.g. Wanajo *et al.*, 2009; Moriya *et al.*, 2014), for supernovae resulting in magnetars (e.g. Vink, 2008; Greiner *et al.*, 2015; Zhou *et al.*, 2019; Beniamini *et al.*, 2019), and clearly for hypernovae and IGRB’s (e.g. Nomoto *et al.*, 2010), there exists no observational evidence, yet, for their production of heavy r-process elements. This is different for compact binary mergers (subsection VI.B) since GW170817, a neutron star merger with the combined mass M_t of about $2.74 M_\odot$ (Abbott *et al.*, 2017a,c, 2019). The observation of an electromagnetic counterpart delivered clear indications for the existence of heavy r-process elements in the ejecta (Metzger, 2017b; Tanaka *et al.*, 2017; Villar *et al.*, 2017), and even identified one element, Sr (Watson *et al.*, 2019). This will be discussed in detail below. By now, additional gravitational wave observations point to further neutron star mergers (e.g. GW190425 with $M_t \sim 3.4 M_\odot$, Abbott *et al.*, 2020), or even neutron star-black hole merger candidates (e.g. S190426c with M_t in excess of $7 M_\odot$, Lattimer, 2019). However, the latter two events had no observed accompanying electromagnetic counterpart (Hosseinzadeh *et al.*, 2019; Foley *et al.*, 2020; Ackley *et al.*, 2020), due to either non-existence or non-detection, related to a larger distance and/or missing precise directions. This will hopefully change with future GW events.

The r-process produces very neutron-rich unstable nuclei on timescales of a few seconds that decay to stability by a combination of β , α and fission decays. These decays produce large amounts of energy and can lead to an observable electromagnetic emission. The first suggestion of such an electromagnetic emission was due to Burbidge *et al.* (1956) who attributed type Ia supernova light curves to the decay of ^{254}Cf , produced by the r-

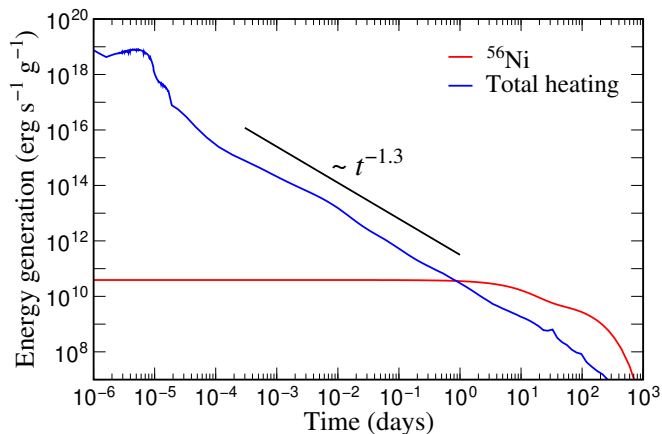


FIG. 36 Specific energy generation rate, \dot{Q} , in r-process ejecta (black line). For comparison the energy production from the decay chain $^{56}\text{Ni} \rightarrow ^{56}\text{Co} \rightarrow ^{56}\text{Fe}$ (red) and the analytical estimate $\dot{Q} \sim t^{-1.3}$ are also shown (adapted from Metzger *et al.*, 2010b).

process. Today, we know that both type Ia and type II supernova light curves are due mainly to the decay of ^{56}Ni . The study of light curves and spectra does not only constrain the nucleosynthesis yields (Diehl and Timmes, 1998; Seitenzahl *et al.*, 2014), but also provides information about the physical parameters of the progenitor system and the explosion itself (Bersten and Mazzali, 2017; Zampieri, 2017). This illustrates the physics potential of an electromagnetic transient observation associated with r-process ejecta. It can identify a site where the r-process occurs (Metzger *et al.*, 2010b), serve as electromagnetic counterpart to the gravitational wave detection following a neutron star merger (Metzger and Berger, 2012), and the nature of the merging system, NS-NS vs NS-BH, and remnant (Margalit and Metzger, 2019; Barbieri *et al.*, 2019; Kawaguchi *et al.*, 2020; Zhu *et al.*, 2020). All these aspects were confirmed by the electromagnetic transient AT 2017gfo, following the gravitational wave event GW170817 (Abbott *et al.*, 2017d).

Li and Paczyński (1998) were the first to propose that radioactive ejecta from a NS-NS merger could power a supernova-like transient. However, they did not possess a physical model to describe the origin of the radioactive heating, \dot{Q} , and considered two possible limiting cases: an exponential-law decay and a power-law $\dot{Q} \sim t^{-1}$. In both cases the normalization was left as a free parameter. Hence, even if the model predicted the right timescale for the peak luminosity, it could not determine the absolute luminosity, spectral peak frequency and time-evolution of the luminosity. Indeed, their fiducial model reached extremely high values of the luminosity $\sim 10^{44}$ erg s $^{-1}$ with a spectral peak in the ultra-violet. Kulkarni (2005) considered two possible origins for the heating: neutron and ^{56}Ni decay; and named such events “macronova”. Metzger *et al.* (2010b) were the first to relate the late

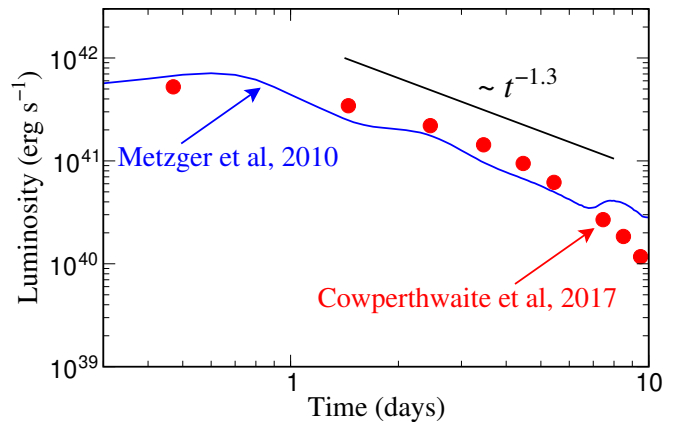


FIG. 37 Bolometric light curve of the optical/infrared counterpart, AT 2017gfo, of GW170817 (red circles) from multi-band photometry (Cowperthwaite *et al.*, 2017), compared with the fiducial model of Metzger *et al.* (2010b). For comparison a line with the approximate power-law decay $\dot{Q} \sim t^{-1.3}$ for r-process heating (see Fig. 36).

time radioactive heating to the decay of freshly produced r-process nuclei. Based on heating rates derived self-consistently from a nuclear reaction network, they showed that the heating rate follows a power law at time scales of a day with a steeper dependence than the one assumed by Li and Paczyński (1998), $\dot{Q} \sim t^{-1.3}$. As shown in Fig. 36, the heating evolves very differently for r-process material than for supernova-like ejecta dominated by ^{56}Ni . A power law dependence is expected whenever the heating is dominated by a broad distribution of nuclei all of them decaying exponentially. It can be understood from basic physics of β -decay and the properties of neutron-rich nuclei (Metzger *et al.*, 2010b; Hotokezaka *et al.*, 2017). A similar dependence is found for the decay rate of terrestrial radioactive waste (Way and Wigner, 1948).

The work of Metzger *et al.* (2010b) predicted peak luminosities $\sim 3 \times 10^{41}$ erg s $^{-1}$ for 0.01 M_{\odot} of ejecta, expanding at $v \sim 0.1 c$, and a spectral peak at visual magnitude. As such value corresponds to 1000 times the luminosity of classical novae they named these events “kilonova”. Fig. 37 compares their prediction with the observation of AT 2017gfo (Cowperthwaite *et al.*, 2017). Similar results were also found by Roberts *et al.* (2011) and Goriely *et al.* (2011).

The physical processes determining the kilonova light curve are (see Fernández and Metzger, 2016; Metzger, 2017a; Tanaka, 2016, for reviews):

a. Radioactive heating. The radioactive heating of r-process products is expected to follow a power law whenever a large statistical ensemble of nuclei is produced. This is the case for ejecta with $Y_e \lesssim 0.2$. For higher Y_e ejecta, the heating rate has ‘bumps’ as a function of time

caused by being dominated by a few nuclei (Grossman *et al.*, 2014; Martin *et al.*, 2015; Lippuner and Roberts, 2015; Rosswog *et al.*, 2018; Wanajo, 2018). However, when averaged over Y_e distributions, as predicted by simulations, the heating rate at timescales of days to a week (of greatest relevance to determine the peak luminosity) varies only slightly within a factor of a few for $Y_e \lesssim 0.4$ (Lippuner and Roberts, 2015; Wu *et al.*, 2019). R-process nuclei decay in a variety of channels including β -decay, α -decay and fission. The energy production in each individual channel is important as the absorption of the energy depends on the decay products being electrons, photons, alphas and fission products. For high Y_e ejecta, heating is dominated by β -decay and only electrons and photons are relevant with neutrinos being just an energy loss. For low Y_e ejecta, actinides are produced and alpha decay and fission can be substantial for the energy production and sensitive to the underlying mass model (Barnes *et al.*, 2016; Rosswog *et al.*, 2017; Wu *et al.*, 2019). The exact form of the heating depends also on the time after the freeze-out of neutron captures. At early times of a few hours the heating may be dominated by neutron decay, assuming the presence of free neutrons in the outermost layers of the ejecta, producing an ultraviolet/blue precursor to the kilonova emission (Metzger *et al.*, 2015; Metzger, 2017a). Early blue emission can also originate from the hot cocoon that surrounds the GRB jet as it crosses the ejecta (Gottlieb *et al.*, 2018). At intermediate times, up to ~ 10 days, β -decays dominate the energy production (Barnes *et al.*, 2016) and the effective heating rate, including thermalization effects (see below), follows a power law, $\propto t^{-2.8}$, (Waxman *et al.*, 2019; Hotokezaka and Nakar, 2020) if the electrons are confined to the plasma due to magnetic fields. At times between 10 and 100 days, the heating is dominated by a few decays (see Wu *et al.*, 2019, for a complete listing), due to the scarcity of nuclei with the appropriate half-life and hence the heating can substantially differ from a power law dependence.

b. Thermalization efficiency. At early times the ejected material is very dense and the energy produced by radioactive decay, except for neutrinos, is completely re-absorbed. However, with decreasing density an increasing fraction of the energy is lost, which is incorporated normally via a time dependent thermalization efficiency of the energy produced by radioactive processes (Barnes *et al.*, 2016). This efficiency depends on bulk properties of the ejecta like mass and velocity as they determine the evolution of the density. It also depends on the presence of magnetic fields and their geometry. Furthermore, it varies with the decay product and time evolution of the heating for each particular decay channel (Kasen and Barnes, 2019), i.e. whether we have a statistical distribution of decaying nuclei or a heating dominated by a

few isotopes, which is probably more appropriate for late times. Earlier works considered the thermalization of γ -rays (Hotokezaka *et al.*, 2016) and were later extended to consider charged particles (Barnes *et al.*, 2016). This has been recently extended to the case of a few decays dominating the heating (Kasen and Barnes, 2019; Wu *et al.*, 2019). Qualitatively one finds that the thermalization efficiency for γ -rays decreases very rapidly and becomes negligible on timescales of a few 10's of days. The thermalization efficiency for charged particles, and particularly alphas and fission products, remains substantial at late times. This makes kilonova light curves rather sensitive to the heating contribution of alpha decays and fission (Barnes *et al.*, 2016; Rosswog *et al.*, 2017; Wu *et al.*, 2019; Zhu *et al.*, 2018; Vassh *et al.*, 2019a; Giuliani *et al.*, 2019).

c. Atomic opacities. A significant electromagnetic luminosity is only possible once the density decreases sufficiently that photons can escape the ejecta on the expansion time-scale (Arnett, 1980, 1982). Assuming a homogeneous spherical distribution of ejecta with mass M , expanding homologously with velocity v and radius $R = vt$, the diffusion time scale of the ejecta can be approximated as $t_{\text{diff}} \approx \rho \kappa R^2 / (3c)$, with $\rho = 3M / (4\pi R^3)$ the density and κ the opacity of the ejecta. Once the ejecta expand enough to become transparent, they release line radiation. This occurs when the diffusion timescale, t_{diff} , becomes comparable to the dynamical timescale, $t = R/v$, and defines the time at which the maximum of the luminosity is reached (see e.g. Metzger *et al.*, 2010b; Fernández and Metzger, 2016):

$$t_{\text{peak}} \approx \left(\frac{\kappa M}{4\pi c v} \right)^{1/2} \quad (14)$$

$$\approx 1.5 \text{ days} \left(\frac{M}{0.01 M_{\odot}} \right)^{1/2} \left(\frac{v}{0.1c} \right)^{-1/2} \left(\frac{\kappa}{\text{cm}^2 \text{g}^{-1}} \right)^{1/2}$$

At timescales beyond the peak time the luminosity can be approximated using Arnett's Law (Arnett, 1980, 1982): $L(t) = M \dot{Q}_{\text{dep}}(t)$. \dot{Q}_{dep} is the energy deposition rate, corrected by the thermalization efficiency, and can be approximated as $\dot{Q}_{\text{dep}} \approx \varepsilon \times 10^{10} (t/\text{day})^{-\alpha} \text{ erg s}^{-1} \text{g}^{-1}$, with $\varepsilon < 1$ the thermalization efficiency. At peak time the kilonova luminosity is given by:

$$L_{\text{peak}} \approx 1.1 \varepsilon \times 10^{41} \text{ erg s}^{-1} \quad (15)$$

$$\left(\frac{M}{0.01 M_{\odot}} \right)^{1-\alpha/2} \left(\frac{v}{0.1c} \right)^{\alpha/2} \left(\frac{\kappa}{\text{cm}^2 \text{g}^{-1}} \right)^{-\alpha/2}$$

The effective emission temperature can be obtained from the luminosity using the Stefan-Boltzmann law that to-

gether with the Wien displacement law gives the characteristic wavelength of the emission:

$$\lambda_{\text{peak}} \approx 514 \text{ nm} \quad (16)$$

$$\left(\frac{M}{0.01M_{\odot}}\right)^{\alpha/8} \left(\frac{v}{0.1c}\right)^{(2-\alpha)/8} \left(\frac{\kappa}{\text{cm}^2\text{g}^{-1}}\right)^{(2+\alpha)/8}$$

The above formulas illustrate several characteristic features of kilonova light curves. Even if the emission mechanism is similar to supernovae the typical ejecta mass is much smaller and the velocity larger. The equations illustrate the important role played by the opacity that is dominated by Doppler-broadened atomic line bound-bound transitions (Kasen *et al.*, 2013; Fontes *et al.*, 2015; Tanaka *et al.*, 2018). Ejecta containing light r-process elements ($A \lesssim 140$) with d -shell valence electrons possess an opacity $\kappa \lesssim 1 \text{ cm}^2 \text{ g}^{-1}$. In this case the emission peaks in the blue after about a day. This was, indeed, the case for AT 2017gfo (Nicholl *et al.*, 2017b). If the ejecta contain lanthanide or actinide nuclei ($A \gtrsim 140$), then the optical opacity is very high, $\kappa \gtrsim 10\text{--}100 \text{ cm}^2 \text{ g}^{-1}$, due to the complex structure of f -shell valence electrons for these elements, resulting in a dense forest of lines, and the emission shifts to the red/infrared (Kasen *et al.*, 2013; Barnes and Kasen, 2013; Tanaka and Hotokezaka, 2013; Fontes *et al.*, 2017, 2020). Having a kilonova observation, like in the case of AT 2017gfo, it is possible to adjust the multi-wavelength evolution of the light curve using a variation of the model described above and to determine the amount of ejecta, velocity and opacity that is a proxy for the composition. As discussed in section II.E, to reproduce the AT 2017gfo observations requires at least two different ejecta components, with three-component models being slightly favored (see e.g. Villar *et al.*, 2017). This result is consistent with the existence of several ejecta components in mergers giving rise to different nucleosynthesis products (see section VI.B). The analysis of sGRB observations (Wu and MacFadyen, 2018) and the kilonova transient (Perego *et al.*, 2017a) favors an off-axis viewing angle of $\sim 30^\circ$ deg. Hence, the early blue phase of the kilonova light curve has been suggested to originate from lanthanide-poor polar ejecta (see e.g. Kasen *et al.*, 2017) (however, see Kawaguchi *et al.*, 2018, for an alternative explanation). This result is consistent with simulations that predict that weak processes, including electron (anti)neutrino absorption, drive the composition to $Y_e \gtrsim 0.25$. It provides observational evidence of the important role of neutrinos in determining the composition of the ejecta. However, there is a tension between the velocity of the ejecta, $v \approx 0.27 c$, that is consistent with simulations of dynamical ejecta, and the large ejecta mass, $M_{\text{ej}} \approx 0.020 M_{\odot}$, that is not. Additional lanthanide-poor material is expected to originate from the post-merger neutrino-wind ejecta. However, its velocity is expected to be smaller, unless the wind is mag-

netically accelerated by the strongly magnetized HMNS remnant (Metzger *et al.*, 2018). The amount of material and velocity of material involved in the “purple” and “red” components suggest that they originate from post-merger outflows from the accretion disk (see e.g. Kasen *et al.*, 2017). Simulations predict that the ejecta contain a broad distribution of Y_e and are able to produce both light and heavy r-process material including the lanthanides/actinides necessary to account for the high opacity (Just *et al.*, 2015a; Wu *et al.*, 2016).

It is, indeed, the observation of the lanthanide-rich “red” emission that provided the first observational evidence that neutron-star mergers produce r-process nuclei. The only element identified in the spectra is Sr (Watson *et al.*, 2019), providing further evidence that also weak processes (enhancing Y_e) operate in the ejecta and demonstrating that first r-process-peak elements are produced in mergers. This is consistent with the inferred lanthanide mass fraction $X_{\text{lan}} \sim 10^{-3}\text{--}10^{-2}$ (Kasen *et al.*, 2017; Tanaka *et al.*, 2017; Waxman *et al.*, 2018) that together with the assumption that the GW170817 yield follows solar proportions requires the production of all r-process nuclei with additional contributions of trans-iron nuclei (Wu *et al.*, 2019). However, if GW170817 represents a typical r-process yield from NS mergers, it suggest that an alternative r-process site may be responsible for the r-process abundances observed in r-enhanced metal poor stars (Ji *et al.*, 2019a, see also section VIII.A).

No direct spectroscopic evidence has been obtained pointing to the production of heavy r-process elements. The high density of lines for lanthanides/actinides together with the large velocities of the ejecta produces line blending and smoothens the spectra (Chornock *et al.*, 2017). This aspect has been used to determine the velocity of the ejecta from spectroscopic information (see e.g. Chornock *et al.*, 2017). Nevertheless, the spectra present peaks that may probe the abundance of further individual elements beyond Sr (see figure 4 of Kasen *et al.*, 2017). However, uncertainties in current atomic data hinder a detailed spectral analysis. The lanthanide/actinide opacities are uncertain because the atomic states and line strengths of these elements are not measured experimentally. Theoretically, such high-Z atoms represent a challenging problem in many-body quantum mechanics, and hence are based on statistical models that must be calibrated to experimental data (Kasen *et al.*, 2013; Fontes *et al.*, 2015; Tanaka *et al.*, 2018, 2019; Radziūtė *et al.*, 2020). Beyond identifying the line transitions themselves, there is considerable uncertainty in how to translate these data into an effective opacity. The commonly employed “line expansion opacity” formalism (Pinto and Eastman, 2000a,b; Li, 2019), based on the Sobolev approximation and applied to kilonovae by Barnes and Kasen (2013) and Tanaka and Hotokezaka (2013), may break down if the line density is sufficiently high that the wavelength spacing of strong lines becomes comparable

to the intrinsic thermal width of the lines (Kasen *et al.*, 2013; Fontes *et al.*, 2015; Fontes *et al.*, 2017, 2020).

Lacking a direct spectroscopic identification of the abundance of individual elements, recent work has focused in identifying fingerprints of heavy elements in kilonova light curves. Particularly promising are late-time observations as the decay heating can be dominated by a few nuclei (Wu *et al.*, 2019). Kasliwal *et al.* (2019) suggest heavy isotopes (e.g. ^{140}Ba , ^{143}Pr , ^{147}Nd , ^{156}Eu , ^{191}Os , ^{223}Ra , ^{225}Ra , ^{233}Pa , ^{234}Th) with β -decay half-lives around 14 days. Wu *et al.* (2019) have shown that at times of weeks to months, the decay energy input may be dominated by a discrete number of α -decays, ^{223}Ra (half-life $t_{1/2} = 11.43$ d), ^{225}Ac ($t_{1/2} = 10.0$ d, following the β -decay of ^{225}Ra with $t_{1/2} = 14.9$ d), and the fissioning isotope ^{254}Cf ($t_{1/2} = 60.5$ d) (see also Zhu *et al.*, 2018), which liberate more energy per decay and thermalize with greater efficiency than β -decay products. Late-time nebular observations of kilonovae, which constrain the radioactive power, provide the potential to identify signatures of these individual isotopes, thus confirming the production of heavy nuclei. In order to constrain the bolometric light to the required accuracy, multi-epoch and wide-band observations are required with sensitive instruments like the James Webb Space Telescope.

An alternative mechanism to probe the in-situ production of r-process nuclei is the identification of X-ray or γ -ray lines from their decay similar to the observations of ^{44}Ti γ -rays in Cas A (Vink *et al.*, 2001; Renaud *et al.*, 2006) and SN 1987A (Grebenev *et al.*, 2012) remnants. Qian *et al.* (1998, 1999), Wu *et al.* (2019), and Korobkin *et al.* (2020) have provided estimates of γ -ray fluxes for several r-process nuclei and Ripley *et al.* (2014) have extended those estimates to X-ray lines. The predicted fluxes are too low to be detected by current missions, however improvements in detection techniques may allow for the first detection of a merger remnant in our Galaxy (see Wu *et al.*, 2019, for a search strategy).

VIII. ABUNDANCE EVOLUTION IN THE GALAXY AND ORIGIN OF THE R-PROCESS

In section VI we presented possible astrophysical sites and the related abundance predictions. This section addresses some of the additional features like their occurrence frequency and its time evolution throughout galactic history, with the aim to provide an understanding of the impact of these individual sites on the evolution of the Galaxy.

A. Supernova vs. r-process imprints in early galactic evolution

Based on the nucleosynthesis predictions for (regular) core-collapse and for type Ia supernovae, plus their occur-

rence rates, one finds that the early phase of the evolution of galaxies is dominated by the ejecta of (fast evolving) massive stars, i.e. those leading to core-collapse supernovae. While there exist variations for the ejecta composition of different progenitor masses, average abundance ratios in the interstellar gas will be found after some time delay when many such explosions and the mixing of their ejecta with the interstellar medium have taken place. These averaged abundance ratios reflect ejecta yields integrated over the distribution of initial stellar masses (initial mass function, IMF). Type Ia supernovae originate from exploding white dwarfs in binary systems, i.e. (a) from slowly evolving stars with initially less than $8 M_{\odot}$ in order to become a white dwarf and (b) requiring time delaying mass transfer in a binary system before the type Ia supernova explosion (unless they are produced by very rare collisions of white dwarfs). Thus, such events are delayed in comparison to the explosion of massive single stars. Type Ia supernovae, which are only important at later phases in galactic evolution, dominate the overall production of Fe and Ni (typically $0.5\text{--}0.6 M_{\odot}$ per event), but are only minor contributors to intermediate mass elements $Z = 8\text{--}22$. As core-collapse supernovae produce larger amounts of O, Ne, Mg, Si, S, Ar, Ca, Ti (so-called α -elements) than Fe-group nuclei like Fe and Ni (only of the order $0.1 M_{\odot}$), their average ratio of α/Fe is larger than the corresponding solar ratio.

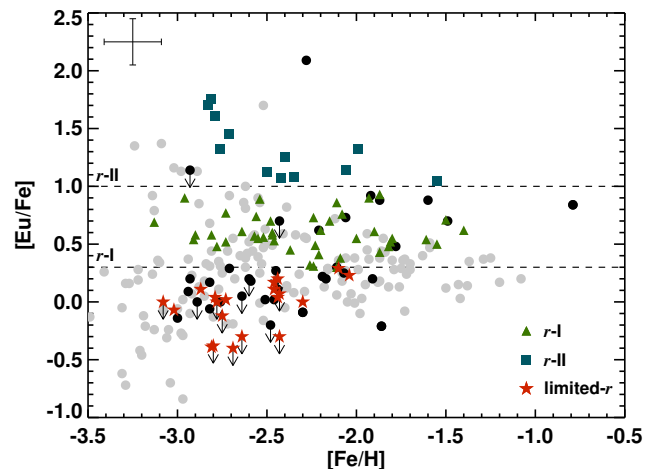


FIG. 38 Derived $[\text{Eu}/\text{Fe}]$ abundances as a function of metallicity (Hansen *et al.*, 2018): r-I stars (green triangles), r-II stars (blue squares), limited-r (red stars), and non r-process-enhanced stars (black dots), see classifications defined in section II; upper limits are shown with black arrows. Grey dots refer to an earlier overview (Roederer *et al.*, 2014b).

For most stars, with the exception of evolved stars which blew off part of their envelope by stellar winds or stars in binary systems with mass exchange, their surface abundances represent the composition of the interstellar gas out of which they formed. Thus, we can look

back into the early history of the Galaxy via the surface abundances of unevolved low-mass stars, witnessing the composition of the interstellar medium at the time of their birth. In Fig. 7 of section II.A some of these aspects were displayed, with $[\text{Mg}/\text{Fe}]$ plotted as a function of metallicity $[\text{Fe}/\text{H}]$ for stars in our Galaxy. For Mg (a typical α -element) one sees — with a relatively small scatter — a flat value of $[\text{Mg}/\text{Fe}]$ between 0.3 and 0.5 up to $[\text{Fe}/\text{H}] \leq -1$, which decreases down to solar values at $[\text{Fe}/\text{H}] = 0$. This can be explained by the early appearance of core-collapse supernovae from fast evolving massive, single stars, producing on average $[\text{Mg}/\text{Fe}] = 0.4$ (see e.g. Woosley *et al.*, 2002; Woosley and Heger, 2007; Limongi and Chieffi, 2018) before type Ia supernovae set in. The properties of the latter have been reviewed in Hillebrandt *et al.* (2013); Maoz *et al.* (2014); Goldstein and Kasen (2018); Livio and Mazzali (2018) as well as their nucleosynthesis properties (Seitenzahl and Townsley, 2017; Nomoto and Leung, 2017b; Seitenzahl *et al.*, 2019). These basic features of galactic evolution have been understood reasonably well for the majority of elements (Matteucci and Greggio, 1986; Timmes *et al.*, 1995; Nomoto *et al.*, 2013), while open questions remain in stellar evolution and supernova explosion mechanisms. This includes the question of the role of more massive stars, probably ending as black holes (Heger *et al.*, 2003; Ertl *et al.*, 2016; Sukhbold *et al.*, 2016; Thielemann *et al.*, 2018; Ebinger *et al.*, 2019, 2020; Ertl *et al.*, 2020), and for sufficiently high angular momentum related to so-called hypernovae/long-duration gamma-ray bursts (see subsection VI.A) or even more massive pair instability supernovae.

The solar abundance of Eu is more than 90% dominated by those isotopes which are produced in the r-process (Bisterzo *et al.*, 2015, 2017). Therefore it is considered as a major r-process indicator. The ratio Eu/Fe in the Galaxy, already displayed in Fig. 7 of section II.A and its recent update in Fig. 38 (above), shows a huge scatter by more than two orders of magnitude at low metallicities, corresponding to very early galactic evolution. While the evolution of the average ratio resembles that of the alpha elements (see Fig. 7), being of a core-collapse supernova origin and also experiencing a decline to solar ratios for $[\text{Fe}/\text{H}] \geq -1$ (for similar trends in Mo and Ru see recent observations by Mishenina *et al.*, 2019b), it is far more complex to understand Eu and other r-process dominated elements than α -elements like Mg. This is also true for elements whose solar abundances are not dominated by the r-process, but which show a large scatter at low metallicities as well, probably also related to r-process contributions (e.g. for Sr and Ba, see Mishenina *et al.*, 2019a; Hill *et al.*, 2019, and references therein). In this section, we will discuss the suggested origins for the r-process and the possibility of their discrimination. A large scatter seems to indicate a not yet well mixed or averaged interstellar medium,

permitting us to actually see the abundance patterns of individual events. The approach to an average $[\text{Eu}/\text{Fe}]$ value with a small scatter is only observed in the interval $-2 \leq [\text{Fe}/\text{H}] \leq -1$. For $[\text{Mg}/\text{Fe}]$ (but also other alpha elements and e.g. Zn and Ge), produced by supernovae, the approach to average values occurs already at about $[\text{Fe}/\text{H}] = -3$ (see Figs. 7 and 38). An obvious conclusion from this would be that r-process events occur at a much lower rate than supernovae. In order to be consistent with total solar abundances this would need to be compensated by larger amounts of their ejecta (see Fig. 39). If the observed abundance ratio of an r-process element over Fe ($[\text{r}/\text{Fe}]$), for example $[\text{Eu}/\text{Fe}]$, scatters at low metallicities due to individual events, this could have two origins: (a) the pollution varies dependent on the birth location of the observed star with respect to the r-process event and/or (b) the strength of individual r-process events varies. There exists also the option that a high-frequency weak r-process site, related to supernovae, is responsible for the “limited-r” sample of Fig. 38, which only shows a small scatter at low metallicities.

A further interesting aspect of this analysis is related to the question whether r-process elements are correlated or not correlated with other nucleosynthesis products, in order to determine whether they were co-produced in the same nucleosynthesis site or require a different origin. Cowan *et al.* (2005) compared the abundances of Fe, Ge, Zr, and r-process Eu in low metallicity stars. They found a strong correlation of Ge with Fe, indicating the same nucleosynthesis origin (core-collapse supernovae), a weak correlation of Zr with Fe, indicating that other sites than core-collapse supernovae (without or low Fe-ejection) contribute as well, and no correlation between Eu and Fe, pointing essentially to a pure r-process origin with negligible Fe-ejection. More recent data from the SAGA database (Suda *et al.*, 2008) permit a weak correlation for $[\text{Eu}/\text{Fe}] < 0.3$, i.e. for stars with lower than average r-process enrichment. Interpreted in a straight-forward way this would point to a negligible Fe/Eu ratio (in comparison to solar ratios) in the major r-process sources, while a noticeable co-production of Fe with Eu is possible in less strong r-process sources, e.g. possibly with a weak r-process. Such cases could again be identified with the stars labeled “limited-r” in Fig. 38. Not focusing on Eu as a single r-process indicator, Ji *et al.* (2019a) looked for low metallicity stars ($[\text{Fe}/\text{H}] < -2.5$, with compositions indicating an r-process origin, $[\text{Eu}/\text{Ba}] > 0.4$), at the typical lanthanide (plus actinide) fraction X_{La} among the global r-process element distribution. They found for the bulk of low metallicity stars $\log X_{\text{La}} \approx -1.8$ and for the most r-process enriched stars $\log X_{\text{La}} > -1.5$. This might hint at different sources.

Without pursuing this aspect further at the moment, we list here preliminary conclusions for the sites discussed in section VI (see references therein):

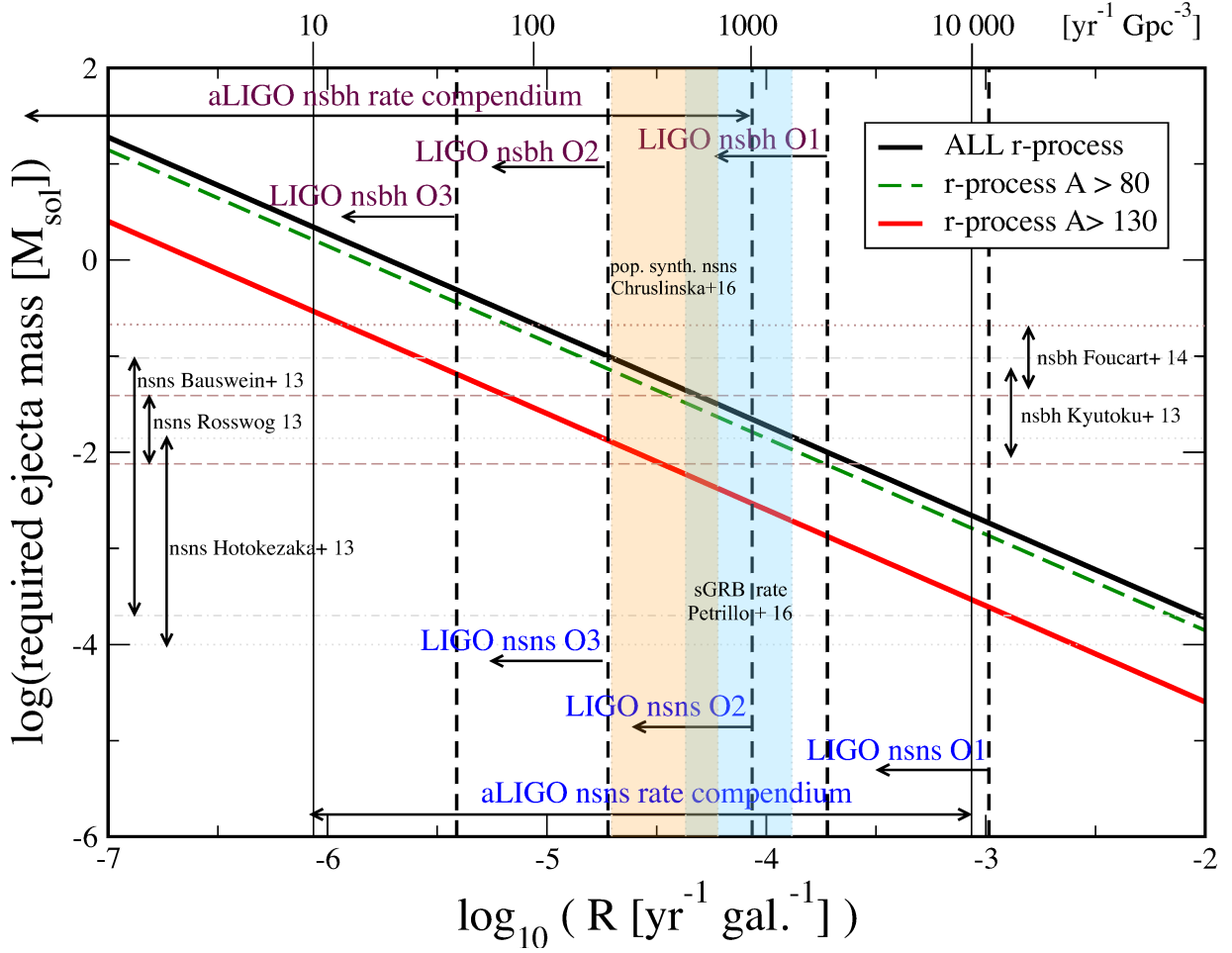


FIG. 39 Figure taken from [Rosswog et al. \(2017\)](#), indicating the required r-process ejecta masses as a function of the occurrence frequency of the production site (for references we refer to the original paper). The figure shows that on a typical SN frequency of 1/100 yrs about 10^{-4} to $10^{-5} M_{\odot}$ of r-process matter would need to be produced, for binary merger ejecta with about $10^{-2} M_{\odot}$ the frequency must be rarer by a factor of 100 to 1000, and if $1 M_{\odot}$ of r-process matter would be ejected in specific events, the frequency must be again lower by another factor of 100.

- Electron-capture supernovae can possibly produce a weak r-process, not a strong one. If their existence is not ruled out by recent investigations (see section II) and they take place for stars in the interval of 8 to $10 M_{\odot}$ of the initial mass function, they are probably not rare. This contradicts a large scatter in $[\text{Eu}/\text{Fe}]$, but they could be candidates for “limited-r” observations.
- The neutrino-induced processes in He-shells of low-metallicity massive stars would be frequent events at low metallicities, and thus could not lead to a large scatter of e.g. $[\text{Eu}/\text{Fe}]$. In addition, the related abundance peaks would not be consistent with a strong r-process.
- The regular neutrino-driven core-collapse SNe produce Fe, but at most a weak r-process (for an extended set of references see section VI.A.1). They are excluded as site of a strong r-process, because

they do not produce the correct abundance pattern and would also be too frequent, not permitting a large scatter in $[\text{Eu}/\text{Fe}]$ at low metallicities. However, they could be candidates for “limited-r” observations.

- It is not known if quark deconfinement supernovae exist. While present model predictions do not yield a full strong r-process, the production of elements up to the actinides is possible, however, with the heaviest elements strongly reduced.
- Magneto-rotational supernovae, starting from a variety of initial magnetic fields, possibly enhanced via magneto-rotational (MRI) instabilities, can produce magnetars. While more than 10% of neutron stars seem to be born as magnetars ([Beniamini et al., 2019](#)), only progenitors with pre-collapse magnetic fields of the order 10^{12} – 10^{13} G and fast rotation can lead to fast jet ejection with a strong r-

process composition. Smaller fields result in a weak or no r-process, i.e. following a transition to regular CCSNe. To be consistent with solar r-process abundances a core-collapse supernova with these extreme initial conditions should represent 1/100 to 1/1000 of regular core-collapse supernovae (see Fig. 39), and produce also a large [Eu/Fe] scatter. Such events still require observational confirmation.

- f. Collapsars, (i.e. high mass stars leading to central black holes, long-duration gamma-ray bursts, hypernovae, and accretion disk outflows) could also be consistent with the overall r-process production in the Galaxy, if they would occur rarer than core-collapse supernovae by more than a factor of 1000 (Siegel, 2019). In such a scenario they would coproduce Fe ($\sim 0.5 M_{\odot}$) and r-process matter ($> 0.1 M_{\odot}$), but with negligible ratios in comparison to solar (i.e. a ratio of < 5 in mass and about less than 2 in abundances vs. about 1000 in a solar composition), and thus not lead to a visible correlation, consistent with Cowan *et al.* (2005).
- g. Compact binary mergers lead to r-process ejecta masses of the order $10^{-2} M_{\odot}$ and small occurrence frequencies (less than 1 in 100 CCSNe), similar to the ones required for case (e). Their existence and their contribution to heavy elements is observationally proven via gravitational wave, (short) GRB, as well as macronova/kilonova observations. Whether the ejected composition is on average consistent with overall solar r-abundances will have to be seen in the future.

Summarizing the properties of the events listed above, the following sites remain as strong r-process candidates: (e) magneto-rotational jet supernovae, (f) collapsars, and (g) compact binary mergers. Of these (e) and (f) would belong to massive stars, i.e. occurring during the earliest instances of galactic evolution. (g) is related to the coalescence of compact objects resulting from the prior collapse of massive stars and would therefore experience a delay in their appearance.

Macias and Ramirez-Ruiz (2019) suggested a further test to be fulfilled by the site: the maximum pollution a star of the next generation would experience, if it is born from a remnant of such an r-process event. A Sedov-Taylor blast wave of an explosion with 10^{51} erg results in mixing with about $5 \times 10^4 M_{\odot}$ of interstellar medium and about $5 \times 10^5 M_{\odot}$ for the more energetic explosions of collapsars. Montes *et al.* (2016) come for compact binary mergers to a similar conclusion as for supernovae. If applying this to the cases e, f, and g, one would find maximum values of [Eu/Fe] > 3 for collapsars and MHD jet supernovae and [Eu/Fe] ~ 2.3 for compact binary mergers, appearing at [Fe/H] ≈ -3.4 , -3.9 , and -2.6 ,

if the explosions occurred in a pristine, previously unpolluted ISM (except for the Fe from two prior CCSNe in case of compact binary mergers). When comparing this to Fig. 38 it might argue against the first two sites. The question is, however, whether Fe-production by earlier CCSNe could have reduced [Eu/Fe]. In a similar way uncertainties in the Fe contribution of the CCSN progenitors of case g or further mixing processes could reduce [Fe/H].

The following subsection will address the question how rare and frequent events can be modeled consistently in galactic chemical evolution. Another aspect is how actually early galactic evolution takes place. There exist indications that (ultra-faint) dwarf galaxies are the earliest building blocks of galactic evolution and their merger will finally lead to the evolution of the early Galaxy as a whole. Due to different gas densities they might experience different star formation efficiencies and due to a low gravitational pull they might lose explosive ejecta more easily. This can have an effect on the point in time (and metallicity) when the first imprints of explosive ejecta can be observed. These features will be addressed as well.

B. Galactic Chemical Evolution Modelling

1. Homogeneous evolution models

In chemical evolution models of galaxies it is still common to use the instantaneous mixing approximation (IMA), i.e. assuming that ejecta compositions were instantaneously and completely mixed throughout the Galaxy. Neglecting this complete mixing can explain radial gradients, but would still assume mixing within large and extended volumes (e.g. radial shells). Further developments included infall of primordial matter into and outflow of enriched material out of the Galaxy (for a review of early investigations see e.g. Audouze and Tinsley, 1976; Tinsley, 1980). When taking into account that (explosive) stellar ejecta enter the interstellar medium (ISM) delayed with respect to the birth of a star by the duration of its stellar evolution, detailed predictions for the time evolution of element abundances can be made. Based on nucleosynthesis predictions for stellar deaths, a number of detailed analyses have been performed, from light elements up to the Fe-group (e.g. Matteucci and Greggio, 1986; Wheeler *et al.*, 1989; Timmes *et al.*, 1995; Matteucci and Chiappini, 2001; Kobayashi *et al.*, 2006; Pagel, 2009; Matteucci, 2012; Nomoto *et al.*, 2013). Such approaches have also been applied to understand the enrichment of heavy elements in the Galaxy (including r-process contributions) as a function of time or metallicity [Fe/H] (see e.g. Travaglio *et al.*, 1999; Ishimaru and Wanajo, 1999; De Donder and Vanbeveren, 2004; Wanajo and Ishimaru, 2006; Matteucci *et al.*, 2014; Ishimaru *et al.*, 2015; Vangioni *et al.*, 2016; Côté *et al.*, 2017; Ho-

tokezaka *et al.*, 2018; Côté *et al.*, 2018, 2019a; Schönrich and Weinberg, 2019; Siegel, 2019; Grisoni *et al.*, 2020).

The IMA simplifies a chemical evolution model in terms of mass movement. In detail, all event outputs are expected to cool down and mix with the surrounding ISM instantaneously. Thus, a problem of this simplification is: All stars born at a given time inherit the same averaged abundance patterns of elements and therefore it is impossible to reproduce a scatter in the galactic abundances, which is a crucial aspect, especially at low metallicities. As a consequence a unique relation between galactic evolution time and metallicity $[\text{Fe}/\text{H}]$ emerges, and for each $[\text{Fe}/\text{H}]$ only a mean value of $[\text{X}/\text{Fe}]$ (X being the element of interest to follow in chemical evolution) is obtained. The IMA approach can be used to get a quick overview of the trends in chemical evolution with a considerably lower computational effort for such a model, and is probably approximately valid, also in case of rare r-process events, for $[\text{Fe}/\text{H}] > -2$. For a detailed study of especially early chemical evolution, including the reproduction of spreads in abundance ratios due to local inhomogeneities, however, this approach is not sufficient.

2. Inhomogeneous galactic chemical evolution

Local inhomogeneities can be produced if only limited amounts of ISM are polluted by and mixed with the ejecta of an event. The latter effect is of essential importance, especially at low metallicities, where portions of the ISM are already polluted by stellar winds and supernovae, and others are not. Inhomogeneous mixing could produce large element ratios in strongly polluted areas by only one or few events. This means that the scatter in $[\text{X}/\text{Fe}]$ at low metallicities can be a helpful asset in hinting at the origin of element X. Inhomogeneous mixing can experience similar $[\text{Fe}/\text{H}]$ values in different locations of the Galaxy at different times or different $[\text{Fe}/\text{H}]$ values at the same time. In addition, different portions of the ISM are polluted by different types of events, leading to a scatter at the same metallicity, which can in fact be utilized as a constraint for these different stellar ejecta. This is especially the case in the very early galactic evolution ($[\text{Fe}/\text{H}] \leq -2.5$), when locally (out of a whole initial mass function, IMF) only a few stars with varying masses might have exploded and imprinted their stellar neighborhood with their ejecta. Thus, rare events, which produce large amounts of element X, would cause a large scatter, being helpful to identify the production site. Therefore, more advanced chemical evolution studies revoked the IMA (e.g. Chiappini *et al.*, 2001; Recchi *et al.*, 2001; Argast *et al.*, 2004; Spitoni *et al.*, 2009; Recchi *et al.*, 2009; van de Voort *et al.*, 2015; Cescutti *et al.*, 2015; Wehmeyer *et al.*, 2015; Shen *et al.*, 2015; Hirai *et al.*, 2015, 2017; Haynes and Kobayashi, 2019; Wehmeyer *et al.*, 2019; van de Voort *et al.*, 2019). For

the reasons summarized above, especially for the abundance evolution of r-process elements like Eu, such inhomogeneous chemical evolution models are well suited.

While some of the models mentioned here are of a more stochastic nature, Minchev *et al.* (2014) started with truly chemo “dynamical” galactic evolution models. These, as well as e.g. van de Voort *et al.* (2015); Hirai *et al.* (2015); Shen *et al.* (2015); Kobayashi (2016); Hirai *et al.* (2017); Haynes and Kobayashi (2019), are based on smoothed-particle hydrodynamics (SPH) simulations. They can model in a self-consistent way massive mergers of galactic subsystems (treated as infall in simpler models), energy feedback from stellar explosions causing outflows (and introduced as such in simpler models), radial migrations in disk galaxies, mixing and diffusion of matter in the ISM, and the initiation of a star formation dependence with progenitor mass. Thus, these global SPH approaches are on the one hand most suited to model such environments. However, the mass and smoothing length utilized for the SPH particles will also determine the resolution and cause an artificial mixing on such scales which are not necessarily related to the real mixing mechanisms. This happens as events within the total mass of one SPH particle are added and fully mixed in this approach. Such effects go into the direction of an IMA on related scales. In reality a Sedov blast wave mixes only with a limited amount of ISM (see subsection VIII.A), while SPH particle masses or smoothing lengths can exceed these scales. The truly chemodynamic code AREPO is probably the most advanced one with the highest resolution, including also MHD and large-scale mixing effects self-consistently (van de Voort *et al.*, 2019), however, still not resolving Sedov-Taylor blast wave scales. This is done in simpler stochastic approaches (e.g. Wehmeyer *et al.*, 2015, 2019) which, however, lack most of the advances included in chemodynamic codes like AREPO.

Within all these approaches a challenge remains: How to model substructures of only about $10^4 M_{\odot}$, observed as ultra-faint dwarf (UFD) galaxies, possibly being building blocks of the early Galaxy. In a superposition of IMA treatments Ojima *et al.* (2018), utilizing a variation of sizes of such galactic substructures, made use of related different star formation rates and different outflows according to their gravity, and added stochastically neutron star mergers in these substructures within the range of possible coalescence delay times. The merging of these substructures is expected to represent eventually the early Galaxy as a whole. Tsujimoto and Shigeyama (2014) discuss how Eu of neutron star merger ejecta is dispersed in UFDs, where — due to ejection velocities of $0.1\text{--}0.2c$ — such heavy elements can experience cosmic-ray type propagation rather than follow a hydrodynamical treatment and mix throughout the whole UFD. They applied this effect within a chemodynamical model of hierarchical galaxy formation/evolution in Komiya and

Shigeyama (2016).

The treatment of compact binary mergers needs to connect the early supernova events that produce the neutron stars and Fe ejecta with the delayed merger event that produces the r-process ejecta. Special binary evolution aspects might apply for such close binary systems and the resulting supernovae (Müller *et al.*, 2018, 2019), not necessarily accompanied by the same amount of Fe/Ni ejecta as for regular CCSNe. Since explosive events give rise to nucleosynthesis inside a supernova remnant bubble (given by a Sedov-Taylor blastwave), the abundances of metals are higher than outside such a remnant. A star which is born later *inside* such a remnant will inherit more metals than a star born *outside*. Thus, it is of high importance, *where* a star is born during galactic evolution, especially in the early phases. If the later merger, producing large amounts of r-process matter, is occurring within the supernova remnant bubble, the $[\text{Fe}/\text{H}]$ has been set already by the earlier supernova explosions and the related $[\text{Eu}/\text{Fe}]$ ratios will appear at the appropriate $[\text{Fe}/\text{H}]$. The main challenge is to have a large $[\text{Eu}/\text{Fe}]$ ratio at the lowest metallicities, which could be achieved in the following ways: (a) neutron star kicks during the supernova explosions act in such a way that the actual neutron star merger takes place outside the initial Fe pollution by the preceding supernovae, (b) neutron star-black hole mergers would have only experienced the Fe-ejecta of one supernova, (c) large-scale turbulent mixing could lead to the dilution of Fe on timescales shorter than the coalescence delay time of the mergers. Such effects are not (yet) necessarily treated correctly by present models.

C. Connecting observational constraints on r-process abundances with different astrophysical sites

In subsection VIII.A, we listed possible production sites for a strong r-process. They need to fulfill the observational constraints: (i) in order to lead to a large scatter of $[\text{r}/\text{Fe}]$ at low metallicities these events must be rare in comparison to regular core-collapse supernovae (this does not exclude the latter from being the site of a weak r-process), and (ii) if they should be the dominant site responsible for the solar r-abundances, the combination of their ejecta mass and occurrence frequency must be able to match this requirement. Three of the listed possible sites may fulfill both criteria: (e) magnetorotational jet supernovae, (f) collapsars, and (g) compact binary mergers. Site (g) is a rare, but observed event with ejecta amounts consistent with solar abundances. Sites (e) and (f) are potential r-process scenarios but still lacking observational confirmation. If the required high rotation rates and extreme magnetic fields for magnetorotational jet supernovae can exist, they would eject similar amounts of r-process matter as binary mergers. These

requirements would also make them rare events. (f) Collapsars, also known as hypernovae or observed as IGRBs, have been related to high ^{56}Ni ejecta, but recently also postulated to eject more than $0.1 M_{\odot}$ of r-process matter (Siegel and Metzger, 2017; Siegel *et al.*, 2019; Janiuk, 2019a). In such a case, these events should be very rare, even a factor of 10 or more rarer than compact binary mergers.

A further requirement, in addition to the two discussed above (rarity and reproducing the total amount of solar r-abundances), is that galactic evolution modeling should reproduce the observed metallicity (or time) evolution. As discussed in the previous subsections, homogeneous approaches with IMA are justified if applied for metallicities $[\text{Fe}/\text{H}] > -2$. This has been especially utilized for testing the distribution of delay times for neutron star mergers after the formation of a binary neutron star system. Early investigations utilized coalescence delay times with a narrow spread. Population synthesis studies, consistent with the occurrence of short-duration gamma-ray bursts (sGRBs, related to compact binary mergers) indicate that the possible delay times follow a distribution with a large spread, ranging over orders of magnitude with a t^{-1} behavior. Based on such a behavior, studies with the IMA modeling of chemical evolution (Côté *et al.*, 2017; Hotokezaka *et al.*, 2018; Côté *et al.*, 2018, 2019a; Siegel, 2019) come to the conclusion that mergers would not be able to reproduce the galactic evolution for metallicities $[\text{Fe}/\text{H}] > -2$, including the decline of $[\text{Eu}/\text{Fe}]$ at $[\text{Fe}/\text{H}] = -1$. This would require either a different delay time distribution (Vigna-Gómez *et al.*, 2018; Beniamini and Piran, 2019; Simonetti *et al.*, 2019) or an additional source for the main, strong, r-process. Schönrich and Weinberg (2019) suggested another solution: star formation takes only place in cooled regions of the ISM, i.e. not all recently ejected matter can already be incorporated and stars contain lower metallicities $[\text{Fe}/\text{H}]$ than the overall ISM at the time of their birth. This shifts e.g. $[\text{Eu}/\text{Fe}]$ ratios to lower $[\text{Fe}/\text{H}]$ and has a similar effect as a steeper delay-time distribution.

In order to address the challenges of explaining the $[\text{r}/\text{Fe}]$ scatter at metallicities $[\text{Fe}/\text{H}] < -2$, inhomogeneous chemical evolution studies are needed and have been implemented (Argast *et al.*, 2004; van de Voort *et al.*, 2015; Shen *et al.*, 2015; Wehmeyer *et al.*, 2015; Hirai *et al.*, 2015; Mennekens and Vanbeveren, 2016; Komiya and Shigeyama, 2016; Hirai *et al.*, 2017; Wehmeyer *et al.*, 2019; Haynes and Kobayashi, 2019; van de Voort *et al.*, 2019). At these low metallicities, there is an important difference between the scenarios (e), (f) and (g): MHD supernova and collapsars result from the final phases of a single massive star, while in the merger scenario two supernova explosions are required before the merger happens after a delay. Scenarios (e) and (f) can act at earliest times in galactic evolution, while we have to examine which effect the delay time in scenario (g)

plays.

Therefore the question arises, whether in addition to the scatter of r-process elements like Eu compared to Fe, $[\text{Eu}/\text{Fe}]$, covering more than two orders of magnitude, see Figs. 7 and 38), especially also the early appearance of high $[\text{Eu}/\text{Fe}]$ values, can be consistent with a “delayed” process like compact binary mergers. The supernovae responsible for producing at least one neutron star produce also Fe, which can shift the appearance of a typical r-process element like Eu to higher metallicities $[\text{Fe}/\text{H}]$. This effect has been discussed in inhomogeneous galactic evolution models utilizing neutron star mergers, i.e. events with two prior supernovae and their Fe-ejecta (Argast *et al.*, 2004; Cescutti *et al.*, 2015; Wehmeyer *et al.*, 2015; Haynes and Kobayashi, 2019; van de Voort *et al.*, 2019). These authors come to the conclusion that neutron star mergers have problems to explain $[\text{Eu}/\text{Fe}]$ at lowest metallicities, while other/earlier inhomogeneous models came to the conclusion that they can do so (van de Voort *et al.*, 2015; Shen *et al.*, 2015; Hirai *et al.*, 2015; Ramirez-Ruiz *et al.*, 2015; Komiya and Shige-yama, 2016; Hirai *et al.*, 2017). The difference is related to resolution and mixing issues discussed in the previous subsection, but it should be noted that the high resolution run of van de Voort *et al.* (2015) as well as recent further investigations (van de Voort *et al.*, 2019, see Fig. 40) indicate the rise of $[\text{Eu}/\text{Fe}]$ to occur at too high metallicities. Whether and how much the use of NS-BH mergers, which explode in an environment polluted only with Fe by one prior supernova, improve this situation needs to be seen (Wehmeyer *et al.*, 2019, see Fig.41).

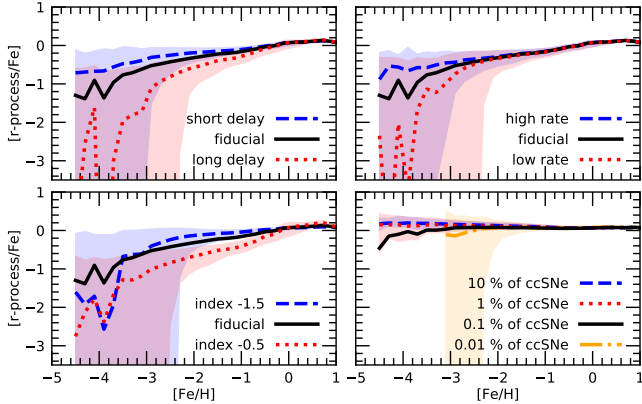


FIG. 40 Results from chemodynamical inhomogeneous evolution models of van de Voort *et al.* (2019), predicting median values (lines) and distributions of $[\text{r}/\text{Fe}]$ ratios in newly born stars of the Milky Way for three different neutron star merger rates, different indices of the coalescence delay time distributions t^{index} , and an additional admixture of r-process events occurring with rates proportional to CCSNe. The combination of additional r-process events proportional to the CCSN rate, being of strong importance at low metallicities early in the evolution of the Galaxy, and neutron star mergers permits an $[\text{r}/\text{Fe}]$ dependence on $[\text{Fe}/\text{H}]$ which does not decline towards low metallicities.

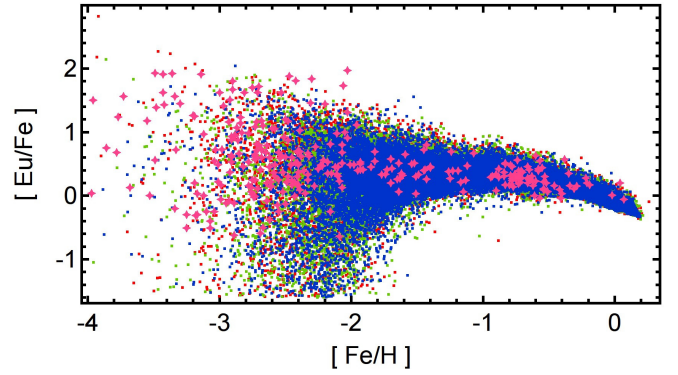


FIG. 41 Evolution of $[\text{Eu}/\text{Fe}]$ in a stochastic inhomogeneous galactic evolution model, including both neutron star and neutron star-black hole mergers as r-process sites, under the assumption that all NS-BH mergers eject r-process matter (for details see Wehmeyer *et al.*, 2019). Magenta crosses represent observations, whereas different choices for black hole formation are utilized at low metallicities: Red (green, blue) squares represent models where all stars $\geq 20 M_{\odot}$ ($\geq 25 M_{\odot}$, $\geq 30 M_{\odot}$) at metallicities $Z \leq 10^{-2} Z_{\odot}$ lead to failed SNe and black holes at the end of their life. The combination of these two r-process sources permits a good fit with observations also at low metallicities.

Thus, problems would remain to explain the strong r-process by NS-mergers alone. But the path to a binary merger is a complex one. The mass, ejecta, and explosion energy of the second supernova in a binary system have to be addressed for a full understanding (Müller *et al.*, 2018, 2019). This includes the fact that neutron star kicks from supernova explosions could move the neutron star binary far out of the reach of the initial supernova remnant which polluted the local ISM with Ni and Fe (e.g. Fryer and Kalogera, 1997; Kalogera and Fryer, 1999; Abbott *et al.*, 2017e; Safarzadeh *et al.*, 2019). If in such a way the merger event can be displaced from the original supernovae, Wehmeyer *et al.* (2018) finds that mergers could be made barely consistent with the $[\text{Eu}/\text{Fe}]$ observations, if such a displacement is taken into account and very short coalescence timescales of 10^6 yr are used. In addition, triple and multiple stellar systems can cause different delay time distributions for neutron star mergers (Bonetti *et al.*, 2018; Hamers and Thompson, 2019). And, as mentioned above, compact binary mergers include also neutron star-black hole mergers, which experience only the pollution by one prior supernova (Wehmeyer *et al.*, 2019).

A different issue is the formation of the Galaxy from small substructures like (ultra-faint) dwarf galaxies (UFDs), which, due to different gas densities, experience different star formation efficiencies and, due to small gravity, the loss of metals from explosive events (Simon, 2019), both shifting the occurrence of abundance features to lower metallicities. The baryonic mass of these UFDs, as small as $10^4 M_{\odot}$, is too small to be followed by the

global simulations discussed above, while local simulations have been performed (see e.g. [Emerick et al., 2018](#); [Corlies et al., 2018](#); [Tarumi et al., 2020](#)). The IMA, combined with outflow, can probably be utilized as a first order approximation locally in UFDs. Observations indicate that star formation continues only for about a few 10^8 yr, permitting still to observe features from type Ia supernovae contributions, leading to the $[\alpha/\text{Fe}]$ downturn at $[\text{Fe}/\text{H}] < -2$ ([Pakhomov et al., 2019](#)), which takes place in the Milky Way only at -1 . As strong r-process sites are rare events (by a factor of 100 to 1000 less frequent than both types of supernovae) only a few UFDs show noticeable r-process contributions, as observed in Reticulum II and Tucana III (e.g. [Ji et al., 2016](#); [Beniamini et al., 2016](#); [Ji and Frebel, 2018](#); [Marshall et al., 2019b](#)), while displaying underabundances in most cases ([Simon, 2019](#); [Ji et al., 2019b](#)). Only about 10% of UFDs experience a strong early r-process contribution ([Brauer et al., 2019](#)). An early simpler IMA approach by [Ishimaru et al. \(2015\)](#), recently extended by a stochastic inclusion of neutron star mergers, which are permitted to vary statistically with respect to coalescence time scales ([Ojima et al., 2018](#)), indicates a possible solution to the question whether neutron star mergers alone could be responsible for the appearance of r-process products at lowest metallicities. This relates to the question whether the apparent uniform r-process abundances observed in stars of UFDs can be consistent with NS merger scenarios ([Tsujiimoto and Shigeyama, 2014](#); [Komiya and Shigeyama, 2016](#); [Bonetti et al., 2019](#); [Tarumi et al., 2020](#)).

The discussion in this subsection, focusing on the question whether galactic chemical evolution studies can determine which of the three sites — (e) magneto-rotational jet supernovae, (f) collapsars/hypernovae, or (g) compact binary mergers — are consistent with or required from observations, came to a still somewhat open result whether neutron star mergers alone can provide the explanation for a strong r-process throughout and also in the early Galaxy. The behavior of $[\text{Eu}/\text{Fe}]$ around $[\text{Fe}/\text{H}] = -1$ puts challenges on their delay time distribution, the early rise of $[\text{Eu}/\text{Fe}]$ at lowest metallicities can be hardly achieved within global galactic evolution studies, not resolving scales of ultra-faint dwarf galaxies. These studies argue for a contribution of (e) and/or (f) at early times in galactic evolution. If UFDs are considered, there seems to be a possible option out of this conclusion. However, there are independent observational indications, combining results from the Milky Way and its dwarf galaxy satellites Sagittarius, Fornax, and Sculptor, that there exist two distinct r-process contributions from an early quick source and a delayed source ([Skúladóttir et al., 2019](#); [Skúladóttir and Salvadori, 2020](#)). Thus, the answer is still somewhat open, depending also on the question whether on average mergers alone can reproduce the lanthanide fraction X_{La} observed in low metallicity

stars ([Ji et al., 2019b](#)). It also needs to be shown whether the turbulent diffusion coefficients, deduced by [Beniamini and Hotokezaka \(2020\)](#) from occurrence frequencies and production yields of different r-process sites, in order to reproduce the abundance scatter at low metallicities, agrees with those from self-consistent simulations ([van de Voort et al., 2019](#)).

D. Long-lived Radioactivities: r-process cosmochronometers and actinide boost stars

A complete list of isotopes with half-lives in the range 10^7 – 10^{11} yr is given in Table II. They cover a time span from a lower limit in excess of the evolution time of massive stars up to (and beyond) the age of the Universe. Such nuclei can be utilized as “chronometers” for nucleosynthesis processes in galactic evolution and also serve as a measure for the age of the Galaxy (and thus as a lower limit for the age of the Universe, see the earlier discussion in II.D). The list is not long. Two of the nuclei require predictions for the production of the ground and isomeric states (^{92}Nb , ^{176}Lu). With the exception of ^{40}K , all of the remaining nuclei are heavier than the “Fe-group” and can only be made via neutron capture.

TABLE II Isotopes with half-lives in the range 10^7 – 10^{11} yr

Isotope	Half-Life	Isotope	Half-Life
^{40}K	1.3×10^9 yr	^{205}Pb	1.5×10^7 yr
^{87}Rb	4.8×10^{10} yr	^{232}Th	1.4×10^{10} yr
^{92}Nb	3.5×10^7 yr	^{235}U	7.0×10^8 yr
^{129}I	1.6×10^7 yr	^{236}U	2.3×10^7 yr
^{147}Sm	1.1×10^{11} yr	^{238}U	4.5×10^9 yr
^{176}Lu	3.7×10^{10} yr	^{244}Pu	8.0×10^7 yr
^{187}Re	4.4×10^{10} yr	^{247}Cm	1.6×10^7 yr

The nuclei with half-lives comparable to the age of the Galaxy/Universe, ^{232}Th and ^{238}U , as well as all other actinide isotopes, are products of a single nucleosynthesis process, the r-process. The possible astrophysical settings have been discussed in the previous sections. The question is how to predict reliable production ratios for these long-lived isotopes, if (a) not even the site is completely clear, and (b) even for a given site nuclear uncertainties enter.

Nevertheless, for many years such chronometers have been utilized to attempt predictions for the age of the Galaxy (see e.g. [Fowler and Hoyle, 1960](#); [Schramm and Wasserburg, 1970](#); [Cowan et al., 1991](#); [Panov et al., 2017](#)). This has been performed initially with simplified chemical evolution models via (i) the prediction of $^{232}\text{Th}/^{238}\text{U}$ and $^{235}\text{U}/^{238}\text{U}$ ratios in r-process calculations, (ii) applying them in galactic evolution models, which include as-

assumptions about the histories of star formation rates and r-process production, and finally (iii) comparing these ratios with meteoritic data, which provide the $^{232}\text{Th}/^{238}\text{U}$ and $^{235}\text{U}/^{238}\text{U}$ ratios at the formation of the solar system. An advantage (somewhat decreasing the nuclear uncertainties involved) is that ^{232}Th and $^{235,238}\text{U}$ are populated by α -decay chains, summing up the contributions of a number of nuclei, and therefore uncertainties in the predictions of the individual isotopes involved average out to some extent (Thielemann *et al.*, 1983; Cowan *et al.*, 1991; Goriely and Clerbaux, 1999).

Observations of elemental Th and U with respect to the r-process reference element Eu in individual old stars can also be used to estimate the age. However, in general this requires a chemical evolution model except for the case of low-metallicity stars. The metallicities of the halo stars for which neutron-capture element data have become available range from $-3 \lesssim [\text{Fe}/\text{H}] \lesssim -2$. Typical, still simple, galactic chemical evolution calculations suggest roughly the metallicity-age relation $[\text{Fe}/\text{H}] = -1$ at 10^9 yr, $[\text{Fe}/\text{H}] = -2$ at 10^8 yr, and $[\text{Fe}/\text{H}] = -3$ at 10^7 yr (if the IMA could be applied at such low metallicities, see, e.g. Tsujimoto *et al.*, 1997; Chiappini *et al.*, 2000). Even if these estimates are uncertain by factors of 2–3, very low metallicity stars most certainly were born when the Galaxy was only 10^7 – 10^8 yr old, a tiny fraction of its present age. Thus, the neutron-capture elements observed in very low metallicity stars were generated in only one or at most a few prior nucleosynthesis episodes (see also Beniamini and Hotokezaka, 2020). If several events contributed, the time interval between these events had to be very short in comparison to Th decay ages. Thus, it is justified to treat the sum as a single r-process abundance distribution which undergoes decay from the time of its incorporation into a (low metallicity) star until its detection in present observations.

Such considerations can also be employed for the ratio of Th and U to stable Pb, which has in addition to the s-process contribution (i) a direct r-process contribution to the $^{206,207,208}\text{Pb}$ isotopes, (ii) a contribution due to fast α - and β -decay chains from unstable nuclei produced in the r-process beyond Pb (decaying within less than 10^6 yr), and finally (iii) a contribution from the long-lived decay chains originating at ^{232}Th and $^{235,238}\text{U}$ (Roederer *et al.*, 2009; Frebel and Kratz, 2009).

The prediction of required isotopic/elemental production ratios, lacking (until recently) site-specific detailed information, has been based on parametrized, so-called site-independent fits, utilizing a superposition of neutron densities which reproduce all solar r-process abundances from $A = 130$ through the actinides (see e.g. Freiburghaus *et al.*, 1999a; Cowan *et al.*, 1999; Goriely and Arnould, 2001; Schatz *et al.*, 2002; Kratz *et al.*, 2004; Roederer *et al.*, 2009). Alternatively neutrino wind models were employed with a superposition of contributing entropy components (Freiburghaus *et al.*, 1999a; Farouqi

et al., 2010; Kratz *et al.*, 2014; Hill *et al.*, 2017). Goriely and Janka (2016) used steady-state neutrino-driven wind models with adiabatic expansion and the superposition of many contributing components.

Making use of such so-called site-independent predictions for standard r-process production ratios, combined with observed abundance ratios found in low-metallicity stars, gives an indication for the decay time of radioactive isotopes since the star was born, polluted by an original r-process pattern. Typical results for ages of most low-metallicity r-process enhanced stars are in the range of 12–14 Gyr (Cowan *et al.*, 1999; Schatz *et al.*, 2002; Kratz *et al.*, 2004; Roederer *et al.*, 2009; Hill *et al.*, 2017). This approach assumes that the production ratios of the site(s) responsible for these observations are consistent with those reproducing a solar r-process. It should be kept in mind that, independent of the uncertainties in abundance predictions discussed above, such age determinations are clearly also affected by observational uncertainties. Ludwig *et al.* (2010) provide a detailed analysis of the affects to be expected, which also apply for the discussion in the upcoming paragraphs.

Among the stars with observed Th and U, there exist a number of so-called actinide-boost stars with an enhanced ratio of Th/Eu and U/Eu in comparison to all other r-process enhanced stars (see e.g. Roederer *et al.*, 2009; Holmbeck *et al.*, 2018), observed especially at low metallicities around $[\text{Fe}/\text{H}] \approx -3$. When utilizing as initial abundance patterns the parametrized fits discussed above (reproducing solar r-abundances), the age estimates for those stars are unrealistically low or even negative (see right scale of Fig. 9 in section II, from Holmbeck *et al.*, 2018). Although it appears that most of the elemental abundances in actinide-boost stars, up to the third r-process peak, are close to a solar r-process pattern, one should investigate further possible correlations between the actinide boost and other abundance features. The question is whether these features point either to a different site than the dominant one responsible for the solar r-process abundances or to variations of conditions in the same type of events, dependent on still unknown aspects (Holmbeck *et al.*, 2019a,b).

The actinide to Eu ratio is related to the path of the r-process and the timing (a) when the actinides are reached via the r-process flow and (b) when fission plays a role during the further flow onto heavier nuclei. Due to this, the r-process results are dependent on the proton/nucleon ratio Y_e in the expanding matter, determining the neutron/seed ratio. Intuitively one could expect that the lowest (most neutron-rich) Y_e 's would lead to the highest actinide production. Holmbeck *et al.* (2019b) showed, with their nuclear physics input, that the ratio is highest for a Y_e in the range 0.1–0.15 (see their Figs. 16 and 17), with the highest values found around $Y_e = 0.125$. Higher Y_e -values (i.e. less neutron-rich conditions) lead to a smaller actinide production, because

of a less strong r-process. Lower Y_e -values (i.e. more or very neutron-rich conditions) lead also to smaller ratios. This is due to the fact that an initially higher actinide production is reduced later by fission cycling, which can be very effective in destroying the actinides. The details depend on mass models and related fission barriers.

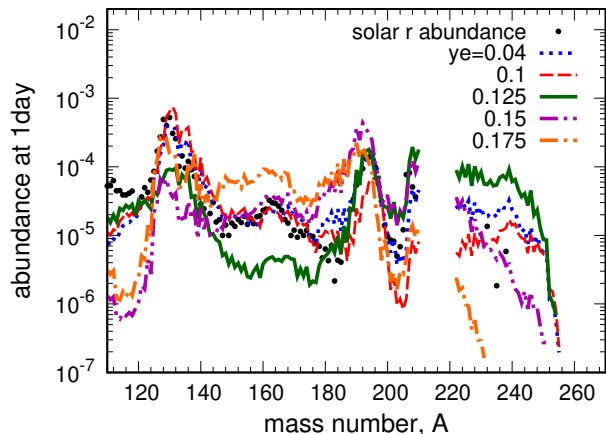


FIG. 42 From [Wu et al. \(2017\)](#): Utilizing the DZ mass model ([Duflo and Zuker, 1995](#)) and trajectories from [Barnes et al. \(2016\)](#) permits large variations in actinide production, even at low Y_e . The highest actinide production is found at $Y_e = 0.125$

[Wu et al. \(2017\)](#) presented a similar behavior, as indicated in Fig. 42, using trajectories adopted from [Barnes et al. \(2016\)](#), finding also an actinide boost for Y_e -conditions close to 0.125. [Eichler et al. \(2019\)](#) did an independent study, testing in detail the influence of nuclear physics uncertainties. They found slightly higher Y_e -values of 0.15 for the maximum actinide production, but similar conclusions, examining also the actinide decline for lower Y_e 's as a function of the number of resulting fission cycles. In all these cases the Th/U ratio, involving two actinide nuclei close in mass numbers, is not strongly affected by a variation in Y_e .

[Holmbeck et al. \(2019a\)](#) argue, that a variety of neutron star merger characteristics (possible due to e.g. different binary masses and/or mass ratios, affecting the total amount of dynamic ejecta - including tidal tails, neutrino wind, and black hole accretion disk outflows), can be responsible for varying outcomes, ranging from solar-type r-process patterns to actinide boosts. [Wu et al. \(2019\)](#) discuss how variations in the produced abundance patterns can affect kilonova lightcurves and spectra, with the aim to identify the exact pattern for individual observed events. [Ji et al. \(2019a\)](#) give hints that the observed merger GW170817 is not as lanthanide- and actinide-rich as required for the dominant solar r-process site.

Thus, the question remains, based on low-metallicity observations, why most events lead apparently to a solar r-process pattern and some others cause an actinide

boost (keep in mind also the discussion above on observational uncertainties [Ludwig et al., 2010](#)). And, it remains to be seen whether different sites are the reason for these two features or whether one site, i.e. neutron star mergers, can lead to this variety. Which Y_e -interval is resulting from specific events, stopping above 0.125, including 0.125, or also continuing to values below 0.125? What are the dominant conditions in MHD jet supernovae, what are the properties of accretion disk outflows in collapsars, what is the role of the individual components in compact binary mergers — dynamic ejecta (including prompt ejecta and tidal tails), neutrino winds, accretion disk outflows, and do all of these subcomponents exist if one of the compact objects is a black hole or the combined mass is sufficiently high, preventing the intermediate existence of a hypermassive neutron star?

Conclusions on this are still speculative, but variations among the different sites should be investigated further (see e.g. [Nishimura et al., 2017](#); [Wu et al., 2019](#); [Eichler et al., 2019](#); [Holmbeck et al., 2019a](#); [Siegel et al., 2019](#); [Siegel, 2019](#)). Improved predictions for all the most probable main r-process sites, discussed in the previous section (plus possibly exotic scenarios, [Fuller et al., 2017](#), but see also [Camelio et al., 2018](#)) can hopefully lead to a one-to-one connection between responsible production sites and observations (although still affected both by astrophysical site as well as nuclear physics uncertainties).

Independent of these considerations, concerning actinide boosts, it should be kept in mind that chemical evolution findings ([Wehmeyer et al., 2015](#); [Cescutti et al., 2015](#); [Côté et al., 2017, 2018](#); [Hotokezaka et al., 2018](#); [Côté et al., 2019a](#); [Haynes and Kobayashi, 2019](#); [van de Voort et al., 2019](#)) and observations ([Skúladóttir et al., 2019](#); [Skúladóttir and Salvadori, 2020](#)) seem to indicate that there exist two distinct r-process contributions from an early quick source and a delayed source.

In addition to the identification and possible explanation of the abundance pattern in actinide boost stars, related to long-lived unstable Th and U isotopes, shorter-lived radioactive isotopes have been addressed by [Lugaro et al. \(2018\)](#), [Vescovi et al. \(2018\)](#), and [Côté et al. \(2019b\)](#). Nuclei with half-lives of a few 10^6 to 10^7 yr permit observers to probe recent nucleosynthesis events in the vicinity of the presolar nebula. In the present context only nuclei of an r-process origin are of interest here. Of these [Côté et al. \(2019b\)](#) point out ^{129}I and ^{247}Cm with identical half-lives, and [Côté et al. \(2020\)](#) utilize them to measure the strength of the last r-process event affecting the pre-solar nebula, as indicated from meteoritic data. In this respect it is also of interest what composition even later occurring events contribute, affecting only the delivery of ^{244}Pu onto earth and the deposition in deep-sea sediments over the past few hundred million years (see section II.D). Very recent investigations by [Wallner et al. \(2019\)](#), possibly indicating that ^{60}Fe from the last CCSNe might have been accompanied by a (very) mi-

nor ^{244}Pu contribution, would possibly permit a frequent weak r-process, producing very small, but not negligible amounts of actinides.

IX. FINAL REMARKS AND CONCLUSIONS

In this review we have reported on recent developments and new data from nuclear and atomic physics experiments and constraints from astronomical observations. We also discussed their impact, combined with advances in astrophysical modelling, on our understanding of the astrophysical r-process. This includes the operation of the r-process, its potential astrophysical sites and its contribution to the chemical evolution of our Galaxy. Despite the tremendous progress achieved since the r-process was proposed by Burbidge *et al.* (1957) and by Cameron (1957), several open questions still remain. In these final remarks we specify these challenges, but also the future opportunities how to overcome them.

With respect to the NUCLEAR PHYSICS, which enters decisively in producing the abundance pattern of the r-process, major achievements have been accomplished. This is related to experimental progress in accessing unstable nuclei far from stability, combined with a growing theoretical understanding of their properties.

1. Novel detection technologies, employed at operational RIB facilities, have allowed to determine *nuclear masses* for nuclei far from stability with improved precision. This in turn served as stringent constraints to improve (empirical and microscopic) global mass models which in r-process simulations determine the location of the r-process path in the nuclear chart. Further improvements are required to remove uncertainties which have decisive consequences for the r-process mass flow across neutron-shell closures shaping the final r-process abundance distribution.
2. The measurement of β -decay *half-lives* for medium-mass neutron-rich nuclei at and near the r-process path at RIKEN has been a major recent achievement. The data are of crucial importance for the speed with which the r-process moves matter to heavier nuclei and (in combination with the location of the r-process path) for the height of peaks and the overall final abundance distribution. Progress has also been reached to measure β -delayed neutron emissions (important in the late phases during decay back to stability), in particular for nuclei close to the $N = 126$ shell closure. However, no β -decay data exist yet for $N = 126$ (or heavier) nuclei on the r-process path. Such measurements, which can be expected from the next-generation RIB facilities, will be of crucial relevance

to determine the amount of matter which is transported beyond the third r-process peak into the fission region.

3. *Fission* plays a crucial role in current r-process models, in particular related to high neutron density environments, as e.g. in neutron star mergers. Here fission terminates the flow to heavier nuclei beyond the actinides, causing fission-cycling. This returns matter to lighter nuclei and is also a source of neutrons which can shape the final abundance pattern. In these models fission yields contribute strongly to the second r-process peak, which needs confirmation in future work. Fission also affects the heaviest long-lived nuclei that are produced by the r-process. Heavy neutron-rich nuclei, in particular those at the $N = 184$ shell closure, are still experimentally out-of-reach. But experimental programs are envisioned to push the measurement of fission rates and yields to more neutron-rich nuclei than currently accessible. Such improvements are also required to address the question whether super-heavy elements can be produced by the r-process.
4. Simulations identify α -decays, especially the decay-chains originating from actinide nuclei, as important contributors to the kilonova light curve and to determine the r-process Pb abundance. Many of these decays are experimentally studied. It is an open question whether α -decays can compete with fission for heavy neutron-rich nuclei.
5. *Neutron captures* (and their inverse photodisintegration) affect the final abundance distribution during the r-process freeze-out period. (Fortunately for a large variety of conditions during the r-process build-up a chemical equilibrium between these two reactions can be maintained and the r-process path is determined solely by nuclear masses.) The nuclei involved can have very low neutron separation energies (with a low density of states) so that direct neutron captures might be favored over compound nucleus reactions. Direct measurements of neutron capture rates for r-process nuclei are experimentally out-of-reach. Advances have been made to develop surrogate techniques to constrain the rates indirectly or to reduce nuclear uncertainties entering statistical model capture rate evaluations. If the direct capture is dominated by individual resonances, the rate can be constrained by indirect determination of the resonance parameters.

In the investigation of all these aspects much progress has occurred, but major uncertainties are remaining, as experiments have touched nuclei in the r-process path only at a limited number of locations in the nuclear chart.

Besides these nuclear aspects, there exist also other challenges in MODELLING ASTROPHYSICAL SITES of the r-process:

1. Most environments expected to be sites of a strong r-process involve objects at high densities and temperatures, making it necessary to determine the *nuclear equation of state* at these extreme conditions. Constraints for the EoS have been obtained in relativistic heavy-ion collisions and by astronomical observations. Decisive progress is expected from upcoming nuclear experiments at heavy-ion facilities and by dedicated experiments probing the nuclear symmetry energy as well as from astronomical observations exploiting upgraded and novel detectors. Improved knowledge of the nuclear EoS is also important to answer the question whether in compact binary mergers a hypermassive neutron star exists temporarily or even remains as a final outcome.
2. The modelling of r-process sites requires multi-scale general relativistic, multidimensional radiation magneto-hydrodynamics simulations. Such calculations are computationally very demanding and involve approximations and numerical methods whose reliability need to be critically assessed.
3. Many of the discussed effects involve the modelling of *magnetic fields*, possibly as a major ingredient to predict jet ejection. A decisive aspect is whether and how magnetic fields can be enhanced during these events, where the magneto-rotational instability MRI plays a major role. High resolution magneto-hydrodynamics modeling is a field only at the brink of getting reliable results for the modelling of complete astrophysical sites.
4. As reactions mediated by the weak interaction are not in equilibrium, processes like electron/positron captures and *neutrino interactions with matter* have to be explicitly modelled. Neutrino-flavor transformations, especially via matter-neutrino resonances and fast pairwise flavor conversion, have been identified to play an essential role in compact binary mergers. Weak-interaction reactions are also crucial to determine the proton-to-nucleon ratio Y_e , which is a key ingredient for r-process nucleosynthesis. The adequate treatment of the neutrino processes requires multi-D transport simulations. Such studies for the complicated geometries involved in neutrino-flavor transformations are just in their infancy.
5. In addition to neutrino transport, general *radiation transport via photons* is important to predict the electromagnetic aftermath of explosions in order to make a connection to observational features

like lightcurves and spectra. Fundamental ingredients for these predictions are the total energy released by radioactive matter, its thermalization and the yet unknown atomic opacities of (especially multiply-ionized) heavy elements. Progress in this field will permit to test whether the lanthanide fraction X_{La} in observed events is consistent with solar r-process abundances

Based on the presently available input for nuclear properties and the present status with respect to modelling POSSIBLE R-PROCESS SITES, three major options for sites of a strong r-process have emerged. For one of these sites (NS mergers) observational evidence exists, while for the other two observational proofs of r-process ejecta are still missing.

1. Models of *compact binary mergers* indicate that they are prolific sites of r-process nucleosynthesis, with up to $10^{-2} M_{\odot}$ of r-process matter in the dynamic ejecta and a few times $10^{-2} M_{\odot}$ from accretion disk outflows. When including all components — dynamic ejecta, neutrino winds, and viscous/secular accretions disk outflows — they produce not only the heaviest r-process nuclei but also significant amounts of the standard solar r-process abundances for mass numbers with $A < 130$. The first observation of a neutron star merger (GW170817), accompanied by the AT 2017gfo macronova/kilonova thermal afterglow, makes this the first proven and confirmed production site of heavy r-process elements; variations, depending on the mass of the merged object, as well as neutron star — black hole mergers need further observational confirmation and theoretical modeling.
2. There exist observational indications of 10^{15} Gauss neutron stars (magnetars) which could be produced by a rare class of *magneto-rotational core-collapse supernovae*. Dependent on high initial magnetic field strengths and rotation rates before collapse, they might eject r-process matter in polar jets. However, better predictions of these initial parameters from stellar evolution are needed in order to understand whether fast ejection via jets takes place or whether a magneto-rotational instability (MRI) will only eventually cause an explosion, ejecting less neutronized matter. Investigating the role of the MRI during the collapse/explosion phase is impossible without high resolution simulations.
3. A very recent multi-D MHD simulation for *accretion disk outflows from collapsars*, i.e. objects which result from the final collapse of massive stars and end in the formation of a black hole, suggest that large amounts of r-process material ($> 0.1 M_{\odot}$) can be ejected. Further simulations are needed, in particular to understand the relation of collapsars to

hypernovae and long-duration GRBs and their potential for the galactic inventory of r-process material.

While the three above mentioned sites are candidates for a strong r-process, producing heavy elements up to the actinides, there exist further options to produce a so-called *weak or limited r-process*, probably also synthesizing elements up to Eu (and beyond?), but with a steeper decline as a function of nuclear mass number than found in the solar system r-abundance pattern; such possible sites include electron capture supernovae, regular core-collapse supernovae, and also quark deconfinement supernovae.

All of these models have to be confronted with and scrutinized by ASTRONOMICAL OBSERVATIONS. An interesting aspect is that one of the listed and confirmed sites is related to binary systems, while the others are resulting from the evolution of massive single stars. Observations supporting and constraining r-process sites exist in a number of ways:

1. The requirement to reproduce the total amount of r-process matter in the Galaxy, puts very stringent constraints on the occurrence and frequency of r-process events. For compact binary mergers as well as magneto-rotational jet supernovae this frequency should be between 1 event per 100 to 1000 regular supernovae. For mergers this would be consistent with population synthesis studies, while for collapsars should be less frequent by a factor of about 10.
2. The *radioactive r-process tracer* ^{244}Pu is found in *deep sea sediments*, however the observed amount rules out a quasi-continuous production of r-process elements as expected for sites with occurrence frequencies like supernovae and points to much rarer events. There exist indications from deep sea sediments that point to events where ^{60}Fe and ^{244}Pu are co-produced, however with relative amounts of ^{244}Pu strongly reduced in comparison to the solar value. Such events could be related to a weak r-process (see above).
3. *Observations indicate the presence of r-process elements in halo stars at lowest metallicities*, showing either a complete or only a partial (or incomplete) r-process abundance pattern, in the latter case possibly pointing to a weak r-process origin. These abundance detections act as proof for nucleosynthesis early in the history of the Galaxy and provide important clues about the nature of the earliest stars.
4. Observations of lowest metallicity stars in our Galaxy and (ultra-faint) dwarf galaxies show sub-

stantial variations in r-process elemental abundances, indicating a production site with a low event rate and consistent high amounts of r-process ejecta in order to explain solar abundances; this is also underlined by the *large scatter of Eu/Fe* (Eu being an r-process element and Fe stemming from core-collapse supernovae at these low metallicities) *seen in the earliest stars of the Galaxy*; this is explained by a not yet well mixed interstellar medium with respect to contributions of products from regular core-collapse supernovae and the rare r-process events.

5. Due to the availability of experimental atomic data and high resolution, precision observations, r-process abundance determinations have improved much over time; this permitted also to detect *the presence of long-lived radioactive nuclei like Th and U* in the same star, making even a *“dating” of old stars* possible; the observed variations in the actinide to intermediate mass r-process elements like Eu, leading to so-called *actinide-boost stars*, would even give clues about different r-process sites.

The above observations indicate a rare site for the strong r-process, a requirement which is matched by all three candidate sites. Moreover, the observations related to the overall evolution of heavy r-process elements in comparison to Fe, and especially its large scatter at low metallicities, require inhomogeneous GALACTIC EVOLUTION simulations, which can reproduce this behavior and might actually point to favored sites:

1. A major open question is: *can products of the neutron star merger r-process alone explain the observations of a large scatter of Eu/Fe and other r-process elements seen already at metallicities of $[\text{Fe}/\text{H}] \leq -3$?* As the supernovae which produce the neutron stars of a merger already lead to a substantial floor of Fe, they enhance $[\text{Fe}/\text{H}]$. Thus, the high $[\text{Eu}/\text{Fe}]$ due to the new ejecta would then be seen first at the metallicity $[\text{Fe}/\text{H}]$ inherited from the prior supernovae, if the merger ejecta are mixed with the same interstellar medium as the prior supernova ejecta. For a typical explosion energy of 10^{51} erg and typical densities of the interstellar medium, this mixing would occur via a Sedov-Taylor blast wave in a range of about $5 \times 10^4 M_{\odot}$. Although matter is ejected with different energies in neutron star mergers than in supernovae, recent investigations indicate that it would mix with a similar amount of interstellar medium. Stochastic inhomogeneous chemical evolution calculations, utilizing this effect alone, show the appearance of Eu only at about $[\text{Fe}/\text{H}] = -2$ for neutron star mergers. First investigations have been performed how this would be affected in the case of neutron

star-black hole mergers, as they would only lead to Fe-ejecta by one prior supernova.

2. Like other hydrodynamic calculations, *large-scale SPH simulations* can suffer from resolution problems, which overestimate the material mixing. This mixes Fe with larger amounts of interstellar medium and thus causes a decrease in the metallicity at which r-process nucleosynthesis sets in. On the other hand, these simulations can handle substantial turbulent mixing of interstellar medium matter in the early Galaxy. Some of these simulations seem to be able to reproduce the r-process behavior of low-metallicity observations with compact binary mergers, but the most recent ones also favor an additional site or source at lowest metallicities.
3. *Neutron star kicks*, resulting from a supernova explosion, could have the binary neutron star system move out of its supernova remnants (polluted with Fe and Ni), and the merger event could take place in galactic regions unpolluted by Fe from earlier supernovae. This could permit the ejection of r-process matter in environments with a lower $[\text{Fe}/\text{H}]$, also in the case of neutron star mergers. Preliminary simulations with stochastic inhomogeneous models (see above) are able to reproduce observations, if coalescence delay times are as short as 1 Myr.
4. Another option is that early on, in *galactic substructures of the size of dwarf galaxies*, different star formation rates can exist, combined with a loss of nucleosynthesis ejecta out of these galaxies due to smaller gravity. This can shift the behavior of the $[\text{Eu}/\text{Fe}]$ ratio as a function of metallicity $[\text{Fe}/\text{H}]$ to lower metallicities. When also considering a statistical distribution of (down to small) coalescence timescales in the individual substructures, the low-metallicity observations could possibly be matched, while the merging of these substructures within the early Galaxy at later times can be made consistent with the $[\text{Eu}/\text{Fe}]$ decline (similar to alpha elements) at $[\text{Fe}/\text{H}] = -1$. However, it should be noted that also in dwarf galaxies indications for two different sources, an early quick and a delayed r-process contribution exist.
5. In somewhat simpler galactic evolution models, employing the instantaneous mixing approximation (IMA) and *coalescence delay time distributions following a t^{-1} power law*, as expected from population synthesis studies and statistics of short duration gamma-ray bursts, apparently no model can reproduce the metallicity dependence of the r-process/Fe abundance ratios with neutron star

mergers alone. But further constraints of the delay time distribution, and considering hot and cold phases of the interstellar medium might help.

The discussion above underlines that it is still inconclusive whether binary compact mergers alone can explain low metallicity observations. Although mergers could be responsible for the dominant amount of r-process products in the solar system and present Galaxy, an additional component which acts at lowest metallicities may still be required. The detection of actinide boost stars, found in particular at metallicities as low as $[\text{Fe}/\text{H}] \approx -3$, could be a further argument for such an additional component.

This review of all aspects of the astrophysical r-process, from nuclear physics via stellar (explosive) modeling, astronomical observations, as well as galactic evolution, has shown that substantial progress has been made since the r-process was postulated in the 1950s by [Burbidge et al. \(1957\)](#) and [Cameron \(1957\)](#). But it also shows that, despite the very first observation of an r-process production site (GW170817) in 2017, confirming neutron star mergers as probably the most important site, many open questions remain and further progress on all fronts is required in a truly interdisciplinary effort, in order to answer them.

Existing and upcoming nuclear facilities world-wide (FAIR, FRIB, HIAF, RAON, RIKEN, SPIRAL) will allow to produce neutron-rich nuclei along the r-process path and to determine their properties, including, for the first time, nuclei of the third r-process peak. Relativistic heavy-ion collision experiments envisioned for FAIR, NICA and RHIC will generate and investigate nuclear matter at the temperatures and densities as they exist in neutron-star mergers (and core-collapse supernovae). These exciting experimental perspectives will constrain and guide advances in global nuclear models, and together they will decisively reduce the nuclear uncertainties currently hampering r-process studies.

Observational programs targeting abundances in low-metallicity stars, like RAVE, Gaia, and APOGEE will be incorporated in future surveys such as SDSS V, 4MOST, and WEAVE. This will provide highest quality information about the chemical structure of the galactic disc, the halo, and the bulge. Multi-messenger astronomy with present and future gravitational wave detectors like LIGO, VIRGO, KAGRA, and IndIGO is expected to detect up to 10 compact binary mergers per year, which can be followed up with observations of related gamma-ray bursts and the electromagnetic afterglow. This permits to analyse the outcome of many sources with different viewing angles and will help our further understanding of this site and possible variations, producing the heaviest elements in the Universe.

The upcoming experimental facilities and observational tools have to be supplemented by theory advances to lead us to a deeper and detailed understanding of the

origin of the heavy elements from Fe to U, produced by the r-process. These theory efforts have to include improved models for the nuclear equation of state and for neutron-rich nuclei far from stability, but also for stellar atmospheres, stellar evolution and explosions, and finally for the chemo-dynamical history of the Galaxy.

In summary, we are living in exciting times for unravelling the mysteries of r-process nucleosynthesis.

ACKNOWLEDGMENTS

We thank a very large number of colleagues and friends for helpful collaborations and discussions, but especially Al Cameron and Willy Fowler should be mentioned here who motivated many of us to explore the topic of this review. This research was supported in part by: NASA grant HST-GO-14232 (JJC), NSF grant AST1616040 (CS), NASA grant NNX16AE96G and NSF grant AST-1516182 (JEL), NSF grant Phys-0758100 and the Joint Institute for Nuclear Astrophysics through NSF Grant Phys-0822648 (AA and MW), NSF award PHY-1430152 (JINA Center for the Evolution of the Elements AA, JJC, and MW), the Extreme Matter Institute EMMI (KL and GMP), the Deutsche Forschungsgemeinschaft (DFG, German Research Foundation) – Project-ID 279384907 – SFB 1245 (GMP), the Swiss SNF, ERC Advanced Grant FISH 321263 and COST Actions NewCompstar MP1304 (FKT) and ChETEC CA16117 (FKT and GMP).

REFERENCES

- Abbott, B P, *et al.* (LIGO Scientific Collaboration and Virgo Collaboration) (2017a), “Estimating the Contribution of Dynamical Ejecta in the Kilonova Associated with GW170817,” *Astrophys. J. Lett.* **850**, L39.
- Abbott, B P, *et al.* (LIGO Scientific Collaboration and Virgo Collaboration, Fermi Gamma-ray Burst Monitor, INTEGRAL) (2017b), “Gravitational Waves and Gamma-Rays from a Binary Neutron Star Merger: GW170817 and GRB 170817A,” *Astrophys. J. Lett.* **848**, L13.
- Abbott, B P, *et al.* (LIGO Scientific Collaboration and Virgo Collaboration) (2017c), “Gw170817: Observation of gravitational waves from a binary neutron star inspiral,” *Phys. Rev. Lett.* **119**, 161101.
- Abbott, B P, *et al.* (2017d), “Multi-messenger Observations of a Binary Neutron Star Merger,” *Astrophys. J. Lett.* **848**, L12.
- Abbott, B P, *et al.* (LIGO Scientific Collaboration and Virgo Collaboration) (2017e), “On the Progenitor of Binary Neutron Star Merger GW170817,” *Astrophys. J. Lett.* **850**, L40.
- Abbott, B P, *et al.* (The LIGO Scientific Collaboration and the Virgo Collaboration) (2018), “Gw170817: Measurements of neutron star radii and equation of state,” *Phys. Rev. Lett.* **121**, 161101.
- Abbott, B P, *et al.* (LIGO Scientific Collaboration and Virgo Collaboration) (2019), “Properties of the binary neutron star merger gw170817,” *Phys. Rev. X* **9**, 011001.
- Abbott, B P, *et al.* (2020), “GW190425: Observation of a Compact Binary Coalescence with Total Mass $\sim 3.4M_{\odot}$,” arXiv e-prints [arXiv:2001.01761](https://arxiv.org/abs/2001.01761) [astro-ph.HE].
- Aboussir, Y, J. M. Pearson, A. K. Dutta, and F. Tondeur (1995), “Nuclear mass formula via an approximation to the Hartree-Fock method,” *At. Data Nucl. Data Tables* **61**, 127–176.
- Ackley, K, *et al.* (2020), “Observational constraints on the optical and near-infrared emission from the neutron star-black hole binary merger S190814bv,” arXiv e-prints [arXiv:2002.01950](https://arxiv.org/abs/2002.01950) [astro-ph.SR].
- Adrich, P, *et al.* (LAND-FRS Collaboration) (2005), “Evidence for Pygmy and Giant Dipole Resonances in ^{130}Sn and ^{132}Sn ,” *Phys. Rev. Lett.* **95**, 132501.
- Agramunt, J, *et al.* (2016), “Characterization of a neutron-beta counting system with beta-delayed neutron emitters,” *Nucl. Instruments Methods Phys. Res. Sect. A Accel. Spectrometers, Detect. Assoc. Equip.* **807**, 69–78.
- Akram, Waheed, Khalil Farouqi, Oliver Hallmann, and Karl-Ludwig Kratz (2020), “Nucleosynthesis of light trans-Fe isotopes in ccSNe: Implications from presolar SiC-X grains,” in *European Physical Journal Web of Conferences*, European Physical Journal Web of Conferences, Vol. 227, p. 01009.
- Alhassid, Y, G. F. Bertsch, S. Liu, and H. Nakada (2000), “Parity Dependence of Nuclear Level Densities,” *Phys. Rev. Lett.* **84**, 4313.
- Alhassid, Y, S. Liu, and H. Nakada (1999), “Particle-Number Reprojection in the Shell Model Monte Carlo Method: Application to Nuclear Level Densities,” *Phys. Rev. Lett.* **83**, 4265–4268.
- Alhassid, Y, S. Liu, and H. Nakada (2007), “Spin Projection in the Shell Model Monte Carlo Method and the Spin Distribution of Nuclear Level Densities,” *Phys. Rev. Lett.* **99**, 162504.
- Anderson, Matthew, Eric W. Hirschmann, Luis Lehner, Steven L. Liebling, Patrick M. Motl, David Neilsen, Carlos Palenzuela, and Joel E. Tohline (2008), “Magnetized Neutron-Star Mergers and Gravitational-Wave Signals,” *Phys. Rev. Lett.* **100**, 191101.
- Annala, Eemeli, Tyler Gorda, Alekski Kurkela, and Alekski Vuorinen (2018), “Gravitational-wave constraints on the neutron-star-matter equation of state,” *Phys. Rev. Lett.* **120**, 172703.
- Antoniadis, John, *et al.* (2013), “A Massive Pulsar in a Compact Relativistic Binary,” *Science* **340**, 1233232.
- Aoki, M, Y. Ishimaru, W. Aoki, and S. Wanajo (2017), “Diversity of Abundance Patterns of Light Neutron-capture Elements in Very-metal-poor Stars,” *Astrophys. J.* **837**, 8.
- Aoki, W, T. C. Beers, Y. S. Lee, S. Honda, H. Ito, M. Takada-Hidai, A. Frebel, T. Suda, M. Y. Fujimoto, D. Carollo, and T. Sivarani (2013), “High-resolution Spectroscopy of Extremely Metal-poor Stars from SDSS/SEGUE. I. Atmospheric Parameters and Chemical Compositions,” *Astron. J.* **145**, 13.
- Arcavi, I, G. Hosseinzadeh, D. A. Howell, C. McCully, D. Poznanski, D. Kasen, J. Barnes, M. Zaltzman, S. Vasylyev, D. Maoz, and S. Valenti (2017), “Optical emission from a kilonova following a gravitational-wave-detected neutron star merger,” *Nature* **551**, 64–66.
- Arcones, A, and H.-T. Janka (2011), “Nucleosynthesis-relevant conditions in neutrino-driven supernova outflows. II. The reverse shock in two-dimensional simulations,” *Astron. & Astrophys.* **526**, A160.

- Arcones, A, H.-T. Janka, and L. Scheck (2007), “Nucleosynthesis-relevant conditions in neutrino-driven supernova outflows. I. Spherically symmetric hydrodynamic simulations,” *Astron. & Astrophys.* **467**, 1227–1248.
- Arcones, A, and G. Martínez-Pinedo (2011), “Dynamical r -process studies within the neutrino-driven wind scenario and its sensitivity to the nuclear physics input,” *Phys. Rev. C* **83**, 045809.
- Arcones, A, G. Martínez-Pinedo, L. F. Roberts, and S. E. Woosley (2010), “Electron fraction constraints based on nuclear statistical equilibrium with beta equilibrium,” *Astron. & Astrophys.* **522**, A25.
- Arcones, A, and F. Montes (2011), “Production of Light-element Primary Process Nuclei in Neutrino-driven Winds,” *Astrophys. J.* **731**, 5.
- Arcones, A, and F.-K. Thielemann (2013), “Neutrino-driven wind simulations and nucleosynthesis of heavy elements,” *J. Phys. G: Nucl. Part. Phys.* **40**, 013201.
- Ardevol-Pulpillo, Ricard, H. Thomas Janka, Oliver Just, and Andreas Bauswein (2018), “Improved Leakage-Equilibration-Absorption Scheme (ILEAS) for Neutrino Physics in Compact Object Mergers,” arXiv e-prints [arXiv:1808.00006 \[astro-ph.HE\]](https://arxiv.org/abs/1808.00006).
- Argast, D, M. Samland, F.-K. Thielemann, and Y.-Z. Qian (2004), “Neutron star mergers versus core-collapse supernovae as dominant r -process sites in the early Galaxy,” *Astron. & Astrophys.* **416**, 997–1011.
- Arlandini, C, F. Käppeler, K. Wisshak, R. Gallino, M. Lugaro, M. Busso, and O. Straniero (1999), “Neutron Capture in Low-Mass Asymptotic Giant Branch Stars: Cross Sections and Abundance Signatures,” *Astrophys. J.* **525**, 886–900.
- Armbruster, P, M. Asghar, J. P. Bocquet, R. Decker, H. Ewald, J. Greif, E. Moll, B. Pfeiffer, H. Schrader, F. Schussler, G. Siegert, and H. Wollnik (1976), “The recoil separator Lohengrin: Performance and special features for experiments,” *Nucl. Instruments Methods* **139**, 213–222.
- Arnett, W D (1980), “Analytic solutions for light curves of supernovae of Type II,” *Astrophys. J.* **237**, 541–549.
- Arnett, W D (1982), “Type I supernovae. I - Analytic solutions for the early part of the light curve,” *Astrophys. J.* **253**, 785–797.
- Arnould, M, and S. Goriely (2003), “The p -process of stellar nucleosynthesis: astrophysics and nuclear physics status,” *Phys. Rep.* **384**, 1–84.
- Arnould, M, S. Goriely, and K. Takahashi (2007), “The r -process of stellar nucleosynthesis: Astrophysics and nuclear physics achievements and mysteries,” *Phys. Rep.* **450**, 97–213.
- Arzhanov, A (2017), *Microscopic nuclear mass model for r -process nucleosynthesis*, Ph.D. thesis (Technische Universität Darmstadt).
- Ascenzi, Stefano, Michael W. Coughlin, Tim Dietrich, Ryan J. Foley, Enrico Ramirez-Ruiz, Silvia Piranomonte, Brenna Mockler, Ariadna Murguía-Berthier, Chris L. Fryer, Nicole M. Lloyd-Ronning, and Stephan Rosswog (2019), “A luminosity distribution for kilonovae based on short gamma-ray burst afterglows,” *Mon. Not. Roy. Astron. Soc.* **486**, 672–690.
- Asplund, M, N. Grevesse, A. J. Sauval, and P. Scott (2009), “The Chemical Composition of the Sun,” *Annu. Rev. Astron. Astrophys.* **47**, 481–522.
- Atanasov, D, *et al.* (2015), “Precision Mass Measurements of Cd -131₁₂₉ and Their Impact on Stellar Nucleosynthesis via the Rapid Neutron Capture Process,” *Phys. Rev. Lett.* **115**, 232501.
- Audi, G, F.G. Kondev, M. Wang, B. Pfeiffer, X. Sun, J. Blachot, and M. MacCormick (2012), “The Nubase2012 evaluation of nuclear properties,” *Chinese Phys. C* **36**, 1157.
- Audi, G, A.H. Wapstra, and C. Thibault (2003), “The Ame2003 atomic mass evaluation: (II). Tables, graphs and references,” *Nucl. Phys. A* **729**, 337–676.
- Audouze, J, and B. M. Tinsley (1976), “Chemical evolution of galaxies,” *Annu. Rev. Astron. Astrophys.* **14**, 43–79.
- Avrigneanu, M, and V. Avrigneanu (2016), “On deuteron interactions within surrogate reactions and nuclear level density studies,” in *Journal of Physics Conference Series*, Vol. 724, p. 012003.
- Avrigneanu, V, and M. Avrigneanu (2015), “Consistent optical potential for incident and emitted low-energy α particles,” *Phys. Rev. C* **91**, 064611.
- Avrigneanu, V, M. Avrigneanu, and C. Mănăilescu (2014), “Further explorations of the α -particle optical model potential at low energies for the mass range A 45–209,” *Phys. Rev. C* **90**, 044612.
- Baade, W, and F. Zwicky (1934), “Remarks on Super-Novae and Cosmic Rays,” *Phys. Rev.* **46**, 76–77.
- Baiotti, Luca, and Luciano Rezzolla (2017), “Binary neutron star mergers: a review of Einstein’s richest laboratory,” *Rep. Prog. Phys.* **80**, 096901.
- Baldo, M, and G.F. Burgio (2016), “The nuclear symmetry energy,” *Prog. Part. Nucl. Phys.* **91**, 203–258.
- Banerjee, P, W. C. Haxton, and Y.-Z. Qian (2011), “Long, Cold, Early r Process? Neutrino-Induced Nucleosynthesis in He Shells Revisited,” *Phys. Rev. Lett.* **106**, 201104.
- Banerjee, P, Y.-Z. Qian, A. Heger, and W. Haxton (2016), “Neutrino-Induced Nucleosynthesis in Helium Shells of Early Core-Collapse Supernovae,” in *European Physical Journal Web of Conferences*, Vol. 109, p. 06001, [arXiv:1512.01523 \[astro-ph.SR\]](https://arxiv.org/abs/1512.01523).
- Barbieri, C, O. S. Salafia, M. Colpi, G. Ghirlanda, and A. Perego (2020), “The kilonova of GW190425-like events,” arXiv e-prints [arXiv:2002.09395 \[astro-ph.HE\]](https://arxiv.org/abs/2002.09395).
- Barbieri, C, O. S. Salafia, M. Colpi, G. Ghirlanda, A. Perego, and A. Colombo (2019), “Filling the Mass Gap: How Kilonova Observations Can Unveil the Nature of the Compact Object Merging with the Neutron Star,” *Astrophys. J. Lett.* **887**, L35.
- Barklem, P S, N. Christlieb, T. C. Beers, V. Hill, M. S. Bessell, J. Holmberg, B. Marsteller, S. Rossi, F.-J. Zickgraf, and D. Reimers (2005), “The Hamburg/ESO R -process enhanced star survey (HERES). II. Spectroscopic analysis of the survey sample,” *Astron. & Astrophys.* **439**, 129–151.
- Barnes, J, D. Kasen, M.-R. Wu, and G. Martínez-Pinedo (2016), “Radioactivity and Thermalization in the Ejecta of Compact Object Mergers and Their Impact on Kilonova Light Curves,” *Astrophys. J.* **829**, 110.
- Barnes, Jennifer, and Daniel Kasen (2013), “Effect of a High Opacity on the Light Curves of Radioactively Powered Transients from Compact Object Mergers,” *Astrophys. J.* **775**, 18.
- Bartos, I, P. Brady, and S. Márka (2013), “How gravitational-wave observations can shape the gamma-ray burst paradigm,” *Class. Quantum Gravity* **30**, 123001.
- Battistini, C, and T. Bensby (2016), “The origin and evolution of r - and s -process elements in the Milky Way stellar disk,” *Astron. & Astrophys.* **586**, A49.
- Bauge, E, J. P. Delaroche, and M. Girod (2001),

- “Lane-consistent, semimicroscopic nucleon-nucleus optical model,” *Phys. Rev. C* **63**, 024607.
- Baumgarte, T W, S. L. Shapiro, and M. Shibata (2000), “On the Maximum Mass of Differentially Rotating Neutron Stars,” *Astrophys. J. Lett.* **528**, L29–L32.
- Bauswein, A, T. W. Baumgarte, and H.-T. Janka (2013), “Prompt Merger Collapse and the Maximum Mass of Neutron Stars,” *Phys. Rev. Lett.* **111**, 131101.
- Bauswein, A, S. Goriely, and H.-T. Janka (2013), “Systematics of dynamical mass ejection, nucleosynthesis, and radioactively powered electromagnetic signals from neutron-star mergers,” *Astrophys. J.* **773**, 78.
- Bauswein, A, and H.-T. Janka (2012), “Measuring neutron-star properties via gravitational waves from neutron-star mergers,” *Phys. Rev. Lett.* **108**, 011101.
- Bauswein, A, and N. Stergioulas (2017), “Semi-analytic derivation of the threshold mass for prompt collapse in binary neutron-star mergers,” *Mon. Not. Roy. Astron. Soc.* **471**, 4956–4965.
- Bauswein, A, and N. Stergioulas (2019), “Spectral classification of gravitational-wave emission and equation of state constraints in binary neutron star mergers,” *J. Phys. G: Nucl. Part. Phys.* **46**, 113002.
- Bauswein, A, N. Stergioulas, and H.-T. Janka (2016), “Exploring properties of high-density matter through remnants of neutron-star mergers,” *Eur. Phys. J. A* **52**, 56.
- Bauswein, Andreas, Oliver Just, Hans-Thomas Janka, and Nikolaos Stergioulas (2017), “Neutron-star Radius Constraints from GW170817 and Future Detections,” *Astrophys. J. Lett.* **850**, L34.
- Beard, M, E. Uberseder, R. Crowter, and M. Wiescher (2014), “Comparison of statistical model calculations for stable isotope neutron capture,” *Phys. Rev. C* **90**, 034619.
- Beers, T C, and N. Christlieb (2005), “The Discovery and Analysis of Very Metal-Poor Stars in the Galaxy,” *Annu. Rev. Astron. Astrophys.* **43**, 531–580.
- Belczynski, K, M. Dominik, T. Bulik, R. O’Shaughnessy, C. Fryer, and D. E. Holz (2010), “The Effect of Metallicity on the Detection Prospects for Gravitational Waves,” *Astrophys. J. Lett.* **715**, L138–L141.
- Belczynski, K, R. O’Shaughnessy, V. Kalogera, F. Rasio, R. E. Taam, and T. Bulik (2008), “The Lowest-Mass Stellar Black Holes: Catastrophic Death of Neutron Stars in Gamma-Ray Bursts,” *Astrophys. J.* **680**, L129.
- Beloborodov, A M (2003), “Nuclear Composition of Gamma-Ray Burst Fireballs,” *Astrophys. J.* **588**, 931–944.
- Beloborodov, A M (2008), “Hyper-accreting black holes,” in *American Institute of Physics Conference Series*, Vol. 1054, edited by M. Axelsson, pp. 51–70, 0810.2690.
- Bengtsson, R, and W. M. Howard (1975), “Mass asymmetric fission and the termination of the astrophysical r-process,” *Phys. Lett. B* **55**, 281–285.
- Beniamini, Paz, and Kenta Hotokezaka (2020), “Turbulent mixing of r-process elements in the Milky Way,” arXiv e-prints [arXiv:2003.01129](https://arxiv.org/abs/2003.01129) [astro-ph.HE].
- Beniamini, Paz, Kenta Hotokezaka, and Tsvi Piran (2016), “r-process Production Sites as Inferred from Eu Abundances in Dwarf Galaxies,” *Astrophys. J.* **832**, 149.
- Beniamini, Paz, Kenta Hotokezaka, Alexander van der Horst, and Chryssa Kouveliotou (2019), “Formation rates and evolution histories of magnetars,” *Mon. Not. Roy. Astron. Soc.* **487**, 1426–1438.
- Beniamini, Paz, and Tsvi Piran (2019), “The Gravitational waves merger time distribution of binary neutron star systems,” *Mon. Not. Roy. Astron. Soc.* **487**, 4847–4854.
- Bensby, T, S. Feltzing, and M. S. Oey (2014), “Exploring the Milky Way stellar disk. A detailed elemental abundance study of 714 F and G dwarf stars in the solar neighbourhood,” *Astron. & Astrophys.* **562**, A71.
- Bersten, M C, and P. A. Mazzali (2017), “Light Curves of Type I Supernovae,” in *Handbook of Supernovae*, edited by A. W. Alsabti and P. Murdin (Springer International Publishing, Cham).
- Bethe, H A (1990), “Supernova mechanisms,” *Rev. Mod. Phys.* **62**, 801–866.
- Bisterzo, S, R. Gallino, F. Käppeler, M. Wiescher, G. Imbriani, O. Straniero, S. Cristallo, J. Görres, and R. J. deBoer (2015), “The branchings of the main s-process: their sensitivity to α -induced reactions on ^{13}C and ^{22}Ne and to the uncertainties of the nuclear network,” *Mon. Not. Roy. Astron. Soc.* **449**, 506–527.
- Bisterzo, S, C. Travaglio, M. Wiescher, F. Käppeler, and R. Gallino (2017), “Galactic Chemical Evolution: The Impact of the ^{13}C -pocket Structure on the s-process Distribution,” *Astrophys. J.* **835**, 97.
- Blake, J B, and D. N. Schramm (1976), “A Possible Alternative to the R-Process,” *Astrophys. J.* **209**, 846–849.
- Blaum, K, J. Dilling, and W. Nörtershäuser (2013), “Precision atomic physics techniques for nuclear physics with radioactive beams,” *Phys. Scr.* **152**, 014017.
- Blaum, Klaus (2006), “High-accuracy mass spectrometry with stored ions,” *Phys. Rep.* **425**, 1–78.
- Bohle, D, A. Richter, W. Steffen, A. E. L. Dieperink, N. Lo Iudice, F. Palumbo, and O. Scholten (1984), “New magnetic dipole excitation mode studied in the heavy deformed nucleus ^{156}Gd by inelastic electron scattering,” *Phys. Lett. B* **137**, 27–31.
- Bollig, R, H.-T. Janka, A. Lohs, G. Martínez-Pinedo, C. J. Horowitz, and T. Melson (2017), “Muon creation in supernova matter facilitates neutrino-driven explosions,” *Phys. Rev. Lett.* **119**, 242702.
- Bonetti, M, A. Perego, P. R. Capelo, M. Dotti, and M. C. Miller (2018), “r-Process Nucleosynthesis in the Early Universe Through Fast Mergers of Compact Binaries in Triple Systems,” *Publ. Astron. Soc. Austr.* **35**, e017.
- Bonetti, Matteo, Albino Perego, Massimo Dotti, and Gabriele Cescutti (2019), “Neutron star binary orbits in their host potential: effect on early r-process enrichment,” *Mon. Not. Roy. Astron. Soc.* **490**, 296–311.
- Borzov, I, and S. Goriely (2000), “Weak interaction rates of neutron-rich nuclei and the r-process nucleosynthesis,” *Phys. Rev. C* **62**, 035501.
- Borzov, I N (2003), “Gamow-teller and first-forbidden decays near the r-process paths at $n = 50, 82$, and 126 ,” *Phys. Rev. C* **67**, 025802.
- Borzov, I N, J. J. Cuenca-García, K. Langanke, G. Martínez-Pinedo, and F. Montes (2008), “Beta-decay of $z \geq 50$ nuclei near the $n=82$ closed neutron shell,” *Nucl. Phys. A* **814**, 159–173.
- Bovard, Luke, Dirk Martin, Federico Guercilena, Almudena Arcones, Luciano Rezzolla, and Oleg Korobkin (2017), “r-process nucleosynthesis from matter ejected in binary neutron star mergers,” *Phys. Rev. D* **96**, 124005.
- Boyd, R N, M. A. Famiano, B. S. Meyer, Y. Motizuki, T. Kajino, and I. U. Roederer (2012), “The r-process in Metal-poor Stars and Black Hole Formation,” *Astrophys. J.* **744**, L14.
- Brauer, Kaley, Alexander P. Ji, Anna Frebel, Gregory A.

- Dooley, Facundo A. Gómez, and Brian W. O’Shea (2019), “The Origin of r-process Enhanced Metal-poor Halo Stars In Now-destroyed Ultra-faint Dwarf Galaxies,” *Astrophys. J.* **871**, 247.
- Brault, J W (1976), “Rapid-scan high-resolution Fourier spectrometer for the visible.” *Journal of the Optical Society of America* (1917-1983) **66**, 1081.
- Bravo, E, and D. García-Senz (1999), “Coulomb corrections to the equation of state of nuclear statistical equilibrium matter: implications for SNIa nucleosynthesis and the accretion-induced collapse of white dwarfs,” *Mon. Not. Roy. Astron. Soc.* **307**, 984–992.
- Brege, Wyatt, Matthew D. Duez, Francois Foucart, M. Brett Deaton, Jesus Caro, Daniel A. Hemberger, Lawrence E. Kidder, Evan O’Connor, Harald P. Pfeiffer, and Mark A. Scheel (2018), “Black hole-neutron star mergers using a survey of finite-temperature equations of state,” *Phys. Rev. D* **98**, 063009.
- Brink, D M (1955), Ph.D. thesis (Oxford University).
- Brink, D M (1957), “Individual particle and collective aspects of the nuclear photoeffect,” *Nucl. Phys. A* **4**, 215–220.
- Brown, B A, and A. C. Larsen (2014), “Large Low-Energy M 1 Strength for ^{56}Fe within the Nuclear Shell Model,” *Phys. Rev. Lett.* **113**, 252502.
- Bruske, C, K. H. Burkard, W. Hüller, R. Kirchner, O. Klepper, and E. Roeckl (1981), “Status report on the GSI online mass separator facility,” *Nucl. Instruments Methods Phys. Res.* **186**, 61–69.
- Bugli, M, J. Guilet, M. Obergaulinger, P. Cerdá-Durán, and M. A. Aloy (2020), “The impact of non-dipolar magnetic fields in core-collapse supernovae,” *Mon. Not. Roy. Astron. Soc.* **492**, 58–71.
- Burbidge, E M, G. R. Burbidge, W. A. Fowler, and F. Hoyle (1957), “Synthesis of the Elements in Stars,” *Rev. Mod. Phys.* **29**, 547–650.
- Burbidge, G R, F. Hoyle, E. M. Burbidge, R. F. Christy, and W. A. Fowler (1956), “Californium-254 and Supernovae,” *Phys. Rev.* **103**, 1145–1149.
- Burris, D L, C. A. Pilachowski, T. E. Armandroff, C. Sneden, J. J. Cowan, and H. Roe (2000), “Neutron-Capture Elements in the Early Galaxy: Insights from a Large Sample of Metal-poor Giants,” *Astrophys. J.* **544**, 302–319.
- Burrows, A, D. Vartanyan, J. C. Dolence, M. A. Skinner, and D. Radice (2018), “Crucial Physical Dependencies of the Core-Collapse Supernova Mechanism,” *Space Sci. Rev.* **214**, 33.
- Burrows, Adam (2013), “Colloquium: Perspectives on core-collapse supernova theory,” *Rev. Mod. Phys.* **85**, 245–261.
- Burrows, Adam, David Radice, David Vartanyan, Hiroki Nagakura, M. Aaron Skinner, and Joshua C. Dolence (2020), “The overarching framework of core-collapse supernova explosions as revealed by 3D FORNAX simulations,” *Mon. Not. Roy. Astron. Soc.* **491**, 2715–2735.
- Busso, M, R. Gallino, and G. J. Wasserburg (1999), “Nucleosynthesis in Asymptotic Giant Branch Stars: Relevance for Galactic Enrichment and Solar System Formation,” *Annu. Rev. Astron. Astrophys.* **37**, 239–309.
- Caballero, O L, A. Arcones, I. N. Borzov, K. Langanke, and G. Martínez-Pinedo (2014), “Local and global effects of beta decays on r-process,” *ArXiv e-prints arXiv:1405.0210 [nucl-th]*.
- Caballero-Folch, R, *et al.* (2016), “First Measurement of Several β -Delayed Neutron Emitting Isotopes Beyond $N=126$,” *Phys. Rev. Lett.* **117**, 012501.
- Cabezón, Rubén M, Kuo-Chuan Pan, Matthias Liebendörfer, Takami Kuroda, Kevin Ebinger, Oliver Heinemann, Albino Perego, and Friedrich-Karl Thielemann (2018), “Core-collapse supernovae in the hall of mirrors. A three-dimensional code-comparison project,” *Astron. & Astrophys.* **619**, A118.
- Calvino, F, *et al.* (2014), *TDR BEta-deLayEd Neutron detector*, Tech. Rep. (FAIR).
- Camelio, Giovanni, Tim Dietrich, and Stephan Rosswog (2018), “Disc formation in the collapse of supramassive neutron stars,” *Mon. Not. Roy. Astron. Soc.* **480**, 5272–5285.
- Cameron, A G W (1957), *Stellar Evolution, Nuclear Astrophysics, and Nucleogenesis*, Report CRL-41 (Chalk River).
- Cameron, A G W (1959), “A Revised Table of Abundances of the Elements,” *Astrophys. J.* **129**, 676.
- Cameron, A G W (2003), “Some Nucleosynthesis Effects Associated with r-Process Jets,” *Astrophys. J.* **587**, 327–340.
- Cameron, A G W, J. J. Cowan, and J. W. Truran (1983), “The waiting point approximation in R-process calculations,” *Astrophys. Space Sci.* **91**, 235–243.
- Capano, Collin D, Ingo Tews, Stephanie M. Brown, Ben Margalit, Soumi De, Sumit Kumar, Duncan A. Brown, Badri Krishnan, and Sanjay Reddy (2020), “Stringent constraints on neutron-star radii from multimessenger observations and nuclear theory,” *Nature Astronomy* **10.1038/s41550-020-1014-6**.
- Caurier, E, K. Langanke, G. Martínez-Pinedo, and F. Nowacki (1999), “Shell model calculations of stellar weak interaction rates: I. gamow-teller distributions and spectra of nuclei in the mass range $a=45-65$,” *Nucl. Phys. A* **653**, 439–452.
- Caurier, E, G. Martínez-Pinedo, Frédéric Nowacki, A. Poves, and A. P. Zuker (2005), “The shell Model as unified view of nuclear structure,” *Rev. Mod. Phys.* **77**, 427–488.
- Cayrel, R, E. Depagne, M. Spite, V. Hill, F. Spite, P. François, B. Plez, T. Beers, F. Primas, J. Andersen, B. Barbuy, P. Bonifacio, P. Molaro, and B. Nordström (2004), “First stars V - Abundance patterns from C to Zn and supernova yields in the early Galaxy,” *Astron. & Astrophys.* **416**, 1117–1138.
- Cayrel, R, V. Hill, T. C. Beers, B. Barbuy, M. Spite, F. Spite, B. Plez, J. Andersen, P. Bonifacio, P. François, P. Molaro, B. Nordström, and F. Primas (2001), “Measurement of stellar age from uranium decay,” *Nature* **409**, 691–692.
- Cescutti, G, D. Romano, F. Matteucci, C. Chiappini, and R. Hirschi (2015), “The role of neutron star mergers in the chemical evolution of the Galactic halo,” *Astron. & Astrophys.* **577**, A139.
- Chawla, Sarvniyun, Matthew Anderson, Michael Besselman, Luis Lehner, Steven L. Liebling, Patrick M. Motl, and David Neilsen (2010), “Mergers of magnetized neutron stars with spinning black holes: Disruption, accretion, and fallback,” *Phys. Rev. Lett.* **105**, 111101.
- Chen, B, J. Dobaczewski, K.-L. Kratz, K. Langanke, B. Pfeiffer, F.-K. Thielemann, and P. Vogel (1995), “Influence of shell-quenching far from stability on the astrophysical r-process,” *Phys. Lett. B* **355**, 37–44.
- Chiappini, C, F. Matteucci, and P. Padoan (2000), “The Chemical Evolution of the Galaxy with Variable Initial Mass Functions,” *Astrophys. J.* **528**, 711–722.
- Chiappini, C, F. Matteucci, and D. Romano (2001), “Abundance Gradients and the Formation of the Milky Way,” *Astrophys. J.* **554**, 1044–1058.

- Chornock, R, *et al.* (2017), “The Electromagnetic Counterpart of the Binary Neutron Star Merger LIGO/Virgo GW170817. IV. Detection of Near-infrared Signatures of r-process Nucleosynthesis with Gemini-South,” *Astrophys. J. Lett.* **848**, L19.
- Christie, I M, A. Lalakos, A. Tchekhovskoy, R. Fernández, F. Foucart, E. Quataert, and D. Kasen (2019), “The role of magnetic field geometry in the evolution of neutron star merger accretion discs,” *Mon. Not. Roy. Astron. Soc.* **490**, 4811–4825.
- Ciolfi, Riccardo, Wolfgang Kastaun, Bruno Giacomazzo, Andrea Endrizzi, Daniel M. Siegel, and Rosalba Perna (2017), “General relativistic magnetohydrodynamic simulations of binary neutron star mergers forming a long-lived neutron star,” *Phys. Rev. D* **95**, 063016.
- Cizewski, J A, A. Ratkiewicz, J. E. Escher, A. Lepailleur, S. D. Pain, and G. Potel (2018), “Informing neutron capture nucleosynthesis on short-lived nuclei with (d,p) reactions,” in *European Physical Journal Web of Conferences*, Vol. 165, p. 01013.
- Clayton, D D (1968), *Principles of stellar evolution and nucleosynthesis* (New York: McGraw-Hill, 1968).
- Cohen, J G, N. Christlieb, A. McWilliam, S. Shtetman, I. Thompson, G. J. Wasserburg, I. Ivans, M. Dehn, T. Karlsson, and J. Melendez (2004), “Abundances In Very Metal-Poor Dwarf Stars,” *Astrophys. J.* **612**, 1107–1135.
- Cole, A L, T. S. Anderson, R. G. T. Zegers, Sam M. Austin, B. A. Brown, L. Valdez, S. Gupta, G. W. Hitt, and O. Fawwaz (2012), “Gamow-teller strengths and electron-capture rates for pf -shell nuclei of relevance for late stellar evolution,” *Phys. Rev. C* **86**, 015809.
- Corlies, Lauren, Kathryn V. Johnston, and John H. Wise (2018), “Exploring simulated early star formation in the context of the ultrafaint dwarf galaxies,” *Mon. Not. Roy. Astron. Soc.* **475**, 4868–4880.
- Côté, B, K. Belczynski, C. L. Fryer, C. Ritter, A. Paul, B. Wehmeyer, and B. W. O’Shea (2017), “Advanced LIGO Constraints on Neutron Star Mergers and r-process Sites,” *Astrophys. J.* **836**, 230.
- Côté, B, C. L. Fryer, K. Belczynski, O. Korobkin, M. Chruślińska, N. Vassh, M. R. Mumpower, J. Lippuner, T. M. Sprouse, R. Surman, and R. Wollaeger (2018), “The Origin of r-process Elements in the Milky Way,” *Astrophys. J.* **855**, 99.
- Côté, B, *et al.* (2020), private communication.
- Côté, Benoit, Marius Eichler, Almudena Arcones, Camilla J. Hansen, Paolo Simonetti, Anna Frebel, Chris L. Fryer, Marco Pignatari, Moritz Reichert, Krzysztof Belczynski, and Francesca Matteucci (2019a), “Neutron Star Mergers Might Not Be the Only Source of r-process Elements in the Milky Way,” *Astrophys. J.* **875**, 106.
- Côté, Benoit, Andrés Yagüe, Blanka Világos, and Maria Lugaro (2019b), “Stochastic Chemical Evolution of Radioactive Isotopes with a Monte Carlo Approach,” *Astrophys. J.* **887**, 213.
- Coughlin, Michael W, Tim Dietrich, Ben Margalit, and Brian D. Metzger (2019), “Multimessenger Bayesian parameter inference of a binary neutron star merger,” *Mon. Not. Roy. Astron. Soc.* **489**, L91–L96.
- Coulter, D A, R. J. Foley, C. D. Kilpatrick, M. R. Drout, A. L. Piro, B. J. Shappee, M. R. Siebert, J. D. Simon, N. Ulloa, D. Kasen, B. F. Madore, A. Murguia-Berthier, Y.-C. Pan, J. X. Prochaska, E. Ramirez-Ruiz, A. Rest, and C. Rojas-Bravo (2017), “Swope Supernova Survey 2017a (SSS17a), the optical counterpart to a gravitational wave source,” *Science* **358**, 1556–1558.
- Cowan, J J, A. G. W. Cameron, and J. W. Truran (1980), “Seed abundances for r-processing in the helium shells of supernovae,” *Astrophys. J.* **241**, 1090–1093.
- Cowan, J J, A. G. W. Cameron, and J. W. Truran (1983), “Explosive helium burning in supernovae - A source of r-process elements,” *Astrophys. J.* **265**, 429–442.
- Cowan, J J, A. G. W. Cameron, and J. W. Truran (1985), “R-process nucleosynthesis in dynamic helium-burning environments,” *Astrophys. J.* **294**, 656–662.
- Cowan, J J, B. Pfeiffer, K.-L. Kratz, F.-K. Thielemann, C. Sneden, S. Burles, D. Tytler, and T. C. Beers (1999), “R-Process Abundances and Chronometers in Metal-poor Stars,” *Astrophys. J.* **521**, 194–205.
- Cowan, J J, and W. K. Rose (1977), “Production of C-14 and neutrons in red giants,” *Astrophys. J.* **212**, 149–158.
- Cowan, J J, C. Sneden, T. C. Beers, J. E. Lawler, J. Simmerer, J. W. Truran, F. Primas, J. Collier, and S. Burles (2005), “Hubble Space Telescope Observations of Heavy Elements in Metal-Poor Galactic Halo Stars,” *Astrophys. J.* **627**, 238–250.
- Cowan, J J, C. Sneden, S. Burles, I. I. Ivans, T. C. Beers, J. W. Truran, J. E. Lawler, F. Primas, G. M. Fuller, B. Pfeiffer, and K.-L. Kratz (2002), “The Chemical Composition and Age of the Metal-poor Halo Star BD +17^{deg}3248,” *Astrophys. J.* **572**, 861–879.
- Cowan, J J, F.-K. Thielemann, and J. W. Truran (1991), “The r-process and nucleochronology,” *Phys. Rep.* **208**, 267–394.
- Cowperthwaite, P S, *et al.* (2017), “The Electromagnetic Counterpart of the Binary Neutron Star Merger LIGO/Virgo GW170817. II. UV, Optical, and Near-infrared Light Curves and Comparison to Kilonova Models,” *Astrophys. J. Lett.* **848**, L17.
- Crease, R P, and R. W. Seidel (2000), “Making Physics: A Biography of Brookhaven National Laboratory, 1946 1972,” *Physics Today* **53**, 55.
- Curtis, Sanjana, Kevin Ebinger, Carla Fröhlich, Matthias Hempel, Albino Perego, Matthias Liebendörfer, and Friedrich-Karl Thielemann (2019), “PUSHing Core-collapse Supernovae to Explosions in Spherical Symmetry. III. Nucleosynthesis Yields,” *Astrophys. J.* **870**, 2.
- Cyburt, R H, B. D. Fields, K. A. Olive, and T.-H. Yeh (2016), “Big bang nucleosynthesis: Present status,” *Rev. Mod. Phys.* **88**, 015004, 1505.01076.
- Davies, M B, W. Benz, T. Piran, and F. K. Thielemann (1994), “Merging neutron stars. 1. Initial results for coalescence of noncorotating systems,” *Astrophys. J.* **431**, 742–753.
- Davis, A M, and K. D. McKeegan (2014), “Short-Lived Radionuclides and Early Solar System Chronology,” in *Meteorites and Cosmochemical Processes*, edited by A. M. Davis, pp. 361–395.
- De, Soumi, Daniel Finstad, James M. Lattimer, Duncan A. Brown, Edo Berger, and Christopher M. Biwer (2018), “Tidal deformabilities and radii of neutron stars from the observation of gw170817,” *Phys. Rev. Lett.* **121**, 091102.
- De Donder, E, and D. Vanbeveren (2004), “The influence of neutron star mergers on the galactic chemical enrichment of r-process elements,” *New Astron.* **9**, 1–16.
- Demetriou, P, C. Grama, and S. Goriely (2002), “Improved global α -optical model potentials at low energies,” *Nucl. Phys. A* **707**, 253–276.
- Demetriou, P, C. Grama, and S. Goriely (2003), “Improved

- global α -optical model potential at low energies,” *Nucl. Phys. A* **718**, 510–512.
- Demorest, P B, T Pennucci, S M Ransom, M S E Roberts, and J W T Hessels (2010), “A two-solar-mass neutron star measured using Shapiro delay,” *Nature* **467**, 1081–1083.
- Den Hartog, E A, M. E. Wickliffe, and J. E. Lawler (2002), “Radiative Lifetimes of Eu I, II, and III and Transition Probabilities of Eu I,” *Astrophys. J. Suppl.* **141**, 255–265.
- Denissenkov, P A, F. Herwig, U. Battino, C. Ritter, M. Pig-natari, S. Jones, and B. Paxton (2017), “i-process Nucleosynthesis and Mass Retention Efficiency in He-shell Flash Evolution of Rapidly Accreting White Dwarfs,” *Astrophys. J.* **834**, L10.
- Desai, D, B. D. Metzger, and F. Foucart (2019), “Imprints of r-process heating on fall-back accretion: distinguishing black hole-neutron star from double neutron star mergers,” *Mon. Not. Roy. Astron. Soc.* **485**, 4404–4412.
- Dessart, L, C. D. Ott, A. Burrows, S. Rosswog, and E. Livne (2009), “Neutrino Signatures and the Neutrino-Driven Wind in Binary Neutron Star Mergers,” *Astrophys. J.* **690**, 1681–1705.
- Diehl, R, and F. X. Timmes (1998), “Gamma-ray line emission from radioactive isotopes in stars and galaxies,” *Publ. Astron. Soc. Pacific* **110**, 637–659.
- Dillmann, I, K.-L. Kratz, A. Wöhr, O. Arndt, B. A. Brown, P. Hoff, M. Hjorth-Jensen, U. Köster, A. N. Ostrowski, B. Pfeiffer, D. Seweryniak, J. Shergur, and W. B. Walters (2003), “N=82 Shell Quenching of the Classical r-Process “Waiting-Point” Nucleus ^{130}Cd ,” *Phys. Rev. Lett.* **91**, 162503.
- Drout, M R, *et al.* (2017), “Light curves of the neutron star merger GW170817/SSS17a: Implications for r-process nucleosynthesis,” *Science* **358**, 1570–1574.
- Duflo, J, and A. P. Zuker (1995), “Microscopic mass formulas,” *Phys. Rev. C* **52**, R23–R27.
- Duncan, R C, S. L. Shapiro, and I. Wasserman (1986), “Neutrino-driven winds from young, hot neutron stars,” *Astrophys. J.* **309**, 141–160.
- Duncan, R C, and C. Thompson (1992), “Formation of very strongly magnetized neutron stars - Implications for gamma-ray bursts,” *Astrophys. J. Lett.* **392**, L9–L13.
- Dunlop, R, *et al.* (2019), “ β decay and β -delayed neutron decay of the N = 82 nucleus $^{8249131}\text{In}$,” *Phys. Rev. C* **99**, 045805.
- Duquette, D W, S. Salih, and J. E. Lawler (1981), “Radiative lifetimes in MoI using a novel atomic beam source,” *Physics Letters A* **83**, 214–216.
- Ebinger, Kevin, Sanjana Curtis, Carla Fröhlich, Matthias Hempel, Albino Perego, Matthias Liebendörfer, and Friedrich-Karl Thielemann (2019), “PUSHing Core-collapse Supernovae to Explosions in Spherical Symmetry. II. Explodability and Remnant Properties,” *Astrophys. J.* **870**, 1.
- Ebinger, Kevin, Sanjana Curtis, Somdutta Ghosh, Carla Fröhlich, Matthias Hempel, Albino Perego, Matthias Liebendörfer, and Friedrich-Karl Thielemann (2020), “PUSHing Core-collapse Supernovae to Explosions in Spherical Symmetry. IV. Explodability, Remnant Properties, and Nucleosynthesis Yields of Low-metallicity Stars,” *Astrophys. J.* **888**, 91.
- Eichler, D, M. Livio, T. Piran, and D. N. Schramm (1989), “Nucleosynthesis, neutrino bursts and gamma-rays from coalescing neutron stars,” *Nature* **340**, 126–128.
- Eichler, M, A. Arcones, A. Kelic, O. Korobkin, K. Langanke, T. Marketin, G. Martínez-Pinedo, I. Panov, T. Rauscher, S. Rosswog, C. Winteler, N. T. Zinner, and F.-K. Thielemann (2015), “The role of fission in neutron star mergers and its impact on the r-process peaks,” *Astrophys. J.* **808**, 30.
- Eichler, M, K. Nakamura, T. Takiwaki, T. Kuroda, K. Kotake, M. Hempel, R. Cabezón, M. Liebendörfer, and F.-K. Thielemann (2018), “Nucleosynthesis in 2D core-collapse supernovae of 11.2 and 17.0 M_{\odot} progenitors: implications for Mo and Ru production,” *J. Phys. G: Nucl. Part. Phys.* **45**, 014001.
- Eichler, M, W. Sayar, A. Arcones, and T. Rauscher (2019), “Probing the Production of Actinides under Different r-process Conditions,” *Astrophys. J.* **879**, 47.
- Ejnisman, R, I. D. Goldman, K. S. Krane, P. Mohr, Y. Nakazawa, E. B. Norman, T. Rauscher, and J. Reel (1998), “Neutron capture cross section of ^{44}Ti ,” *Phys. Rev. C* **58**, 2531–2537.
- Eliseev, S, K. Blaum, M. Block, C. Droese, M. Goncharov, E. Minaya Ramirez, D. A. Nesterenko, Y. N. Novikov, and L. Schweikhard (2013), “Phase-Imaging Ion-Cyclotron-Resonance Measurements for Short-Lived Nuclides,” *Phys. Rev. Lett.* **110**, 082501.
- Emerick, Andrew, Greg L. Bryan, Mordecai-Mark Mac Low, Benoit Côté, Kathryn V. Johnston, and Brian W. O’Shea (2018), “Metal Mixing and Ejection in Dwarf Galaxies Are Dependent on Nucleosynthetic Source,” *Astrophys. J.* **869**, 94.
- Engel, J, M. Bender, J. Dobaczewski, W. Nazarewicz, and R. Surman (1999), “Beta decay of r-process waiting-point nuclei in a self-consistent approach,” *Phys. Rev. C* **60**, 014302.
- Epstein, Richard I, Stirling A. Colgate, and Wick C. Haxton (1988), “Neutrino-Induced r-Process Nucleosynthesis,” *Phys. Rev. Lett.* **61**, 2038–2041.
- Erler, J, K. Langanke, H. Loens, Gabriel Martínez-Pinedo, and P.-G. Reinhard (2012), “Fission properties for r-process nuclei,” *Phys. Rev. C* **85**, 025802.
- Ertl, T, H.-T. Janka, S. E. Woosley, T. Sukhbold, and M. Ugliano (2016), “A Two-parameter Criterion for Classifying the Explodability of Massive Stars by the Neutrino-driven Mechanism,” *Astrophys. J.* **818**, 124.
- Ertl, T, S. E. Woosley, Tuguldur Sukhbold, and H. T. Janka (2020), “The Explosion of Helium Stars Evolved with Mass Loss,” *Astrophys. J.* **890**, 51.
- Escher, J E, J. T. Burke, F. S. Dietrich, N. D. Sielzo, I. J. Thompson, and W. Younes (2012), “Compound-nuclear reaction cross sections from surrogate measurements,” *Rev. Mod. Phys.* **84**, 353–397.
- Escher, J E, and F. S. Dietrich (2006), “Determining (n,f) cross sections for actinide nuclei indirectly: Examination of the surrogate ratio method,” *Phys. Rev. C* **74**, 054601.
- Evans, P A, *et al.* (2017), “Swift and NuSTAR observations of GW170817: Detection of a blue kilonova,” *Science* **358**, 1565–1570.
- Faber, Joshua A, Thomas W. Baumgarte, Stuart L. Shapiro, Keisuke Taniguchi, and Frederic A. Rasio (2006), “Black Hole-Neutron Star Binary Merger Calculations: GRB Progenitors and the Stability of Mass Transfer,” in *Albert Einstein Century International Conference*, American Institute of Physics Conference Series, Vol. 861, edited by Jean-Michel Alimi and André Füzfa, pp. 622–629.
- Farouqi, K, K.-L. Kratz, B. Pfeiffer, T. Rauscher, F.-K. Thielemann, and J. W. Truran (2010), “Charged-particle

- and Neutron-capture Processes in the High-entropy Wind of Core-collapse Supernovae,” *Astrophys. J.* **712**, 1359–1377.
- Fattoyev, F J, J. Piekarewicz, and C. J. Horowitz (2018), “Neutron skins and neutron stars in the multimessenger era,” *Phys. Rev. Lett.* **120**, 172702.
- Fernández, R, D. Kasen, B. D. Metzger, and E. Quataert (2015), “Outflows from accretion discs formed in neutron star mergers: effect of black hole spin,” *Mon. Not. Roy. Astron. Soc.* **446**, 750–758.
- Fernández, R, and B. D. Metzger (2016), “Electromagnetic Signatures of Neutron Star Mergers in the Advanced LIGO Era,” *Annu. Rev. Nucl. Part. Sci.* **66**, 23–45.
- Fernandez, R, and Brian D. Metzger (2013), “Delayed outflows from black hole accretion tori following neutron star binary coalescence,” *Mon. Not. Roy. Astron. Soc.* **435**, 502–517, 1304.6720.
- Fernández, Rodrigo, Alexander Tchekhovskoy, Eliot Quataert, Francois Foucart, and Daniel Kasen (2019), “Long-term GRMHD simulations of neutron star merger accretion discs: implications for electromagnetic counterparts,” *Mon. Not. Roy. Astron. Soc.* **482**, 3373–3393.
- Fields, Brian, *et al.* (2019), “Near-Earth Supernova Explosions: Evidence, Implications, and Opportunities,” *Bull. Am. Astron. Soc.* **51**, 410.
- Fischer, T, I. Sagert, G. Pagliara, M. Hempel, J. Schaffner-Bielich, T. Rauscher, F.-K. Thielemann, R. Käppeli, G. Martínez-Pinedo, and M. Liebendörfer (2011), “Core-collapse supernova explosions triggered by a quark-hadron phase transition during the early post-bounce phase,” *Astrophys. J. Suppl.* **194**, 39.
- Fischer, T, S. C. Whitehouse, A. Mezzacappa, F.-K. Thielemann, and M. Liebendörfer (2010), “Protoneutron star evolution and the neutrino-driven wind in general relativistic neutrino radiation hydrodynamics simulations,” *Astron. & Astrophys.* **517**, A80.
- Fischer, Tobias, Niels-Uwe F. Bastian, Meng-Ru Wu, Petr Baklanov, Elena Sorokina, Sergei Blinnikov, Stefan Typel, Thomas Klähn, and David B. Blaschke (2018), “Quark deconfinement as a supernova explosion engine for massive blue supergiant stars,” *Nature Astronomy* **2**, 980–986.
- Fischer, Tobias, Gang Guo, Alan A. Dzhioev, Gabriel Martínez-Pinedo, Meng-Ru Wu, Andreas Lohs, and Yong-Zhong Qian (2020a), “Neutrino signal from proto-neutron star evolution: Effects of opacities from charged-current-neutrino interactions and inverse neutron decay,” *Phys. Rev. C* **101**, 025804.
- Fischer, Tobias, Meng-Ru Wu, Benjamin Wehmeyer, Niels-Uwe F. Bastian, Gabriel Martínez-Pinedo, and Friedrich-Karl Thielemann (2020b), “Core-collapse supernova explosions driven by the hadron-quark phase transition as rare r process site,” arXiv e-prints [arXiv:2003.00972](https://arxiv.org/abs/2003.00972) [astro-ph.HE].
- Fogelberg, B, H. Gausemel, K. A. Mezilev, P. Hoff, H. Mach, M. Sanchez-Vega, A. Lindroth, E. Ramström, J. Genevey, J. A. Pinston, and M. Rejmund (2004), “Decays of ^{131}In , ^{131}Sn , and the position of the $h_{11/2}$ neutron hole state,” *Phys. Rev. C* **70**, 034312.
- Foglizzo, T, R. Kaseroni, J. Guilet, F. Masset, M. González, B. K. Krueger, J. Novak, M. Oertel, J. Margueron, J. Faure, N. Martin, P. Blottiau, B. Peres, and G. Durand (2015), “The explosion mechanism of core-collapse supernovae: Progress in supernova theory and experiments,” *Publ. Astron. Soc. Austr.* **32**, e009.
- Foley, Ryan J, David A. Coulter, Charles D. Kilpatrick, Anthony L. Piro, Enrico Ramirez-Ruiz, and Josiah Schwab (2020), “Updated Parameter Estimates for GW190425 Using Astrophysical Arguments and Implications for the Electromagnetic Counterpart,” *Mon. Not. Roy. Astron. Soc.* [10.1093/mnras/staa725](https://arxiv.org/abs/2002.00956), [arXiv:2002.00956](https://arxiv.org/abs/2002.00956) [astro-ph.HE].
- Fontes, C J, C. L. Fryer, A. L. Hungerford, R. T. Wollaeger, and O. Korobkin (2020), “A line-binned treatment of opacities for the spectra and light curves from neutron star mergers,” *Mon. Not. Roy. Astron. Soc.* **493**, 4143–4171.
- Fontes, Christopher J, Chris L. Fryer, Aimee L. Hungerford, Ryan T. Wollaeger, Stephan Rosswog, and Edo Berger (2017), “A line-smearred treatment of opacities for the spectra and light curves from macronovae,” arXiv e-prints [arXiv:1702.02990](https://arxiv.org/abs/1702.02990) [astro-ph.HE].
- Fontes, CJ, C.L. Fryer, A.L. Hungerford, P. Hakel, J. Colgan, D.P. Kilcrease, and M.E. Sherrill (2015), “Relativistic opacities for astrophysical applications,” *High Energy Density Phys.* **16**, 53–59.
- Forssén, C, F. S. Dietrich, J. Escher, R. D. Hoffman, and K. Kelley (2007), “Determining neutron capture cross sections via the surrogate reaction technique,” *Phys. Rev. C* **75**, 055807.
- Foucart, F, M. B. Deaton, M. D. Duez, L. E. Kidder, I. Macdonald, C. D. Ott, H. P. Pfeiffer, M. A. Scheel, B. Szilagyi, and S. A. Teukolsky (2013), “Black-hole-neutron-star mergers at realistic mass ratios: Equation of state and spin orientation effects,” *Phys. Rev. D* **87**, 084006.
- Foucart, F, M. B. Deaton, M. D. Duez, E. O’Connor, C. D. Ott, R. Haas, L. E. Kidder, H. P. Pfeiffer, M. A. Scheel, and B. Szilagyi (2014), “Neutron star-black hole mergers with a nuclear equation of state and neutrino cooling: Dependence in the binary parameters,” *Phys. Rev. D* **90**, 024026.
- Foucart, F, M. D. Duez, L. E. Kidder, R. Nguyen, H. P. Pfeiffer, and M. A. Scheel (2018), “Evaluating radiation transport errors in merger simulations using a Monte Carlo algorithm,” *Phys. Rev. D* **98**, 063007.
- Foucart, F, E. O’Connor, L. Roberts, M. D. Duez, R. Haas, L. E. Kidder, C. D. Ott, H. P. Pfeiffer, M. A. Scheel, and B. Szilagyi (2015), “Post-merger evolution of a neutron star-black hole binary with neutrino transport,” *Phys. Rev. D* **91**, 124021.
- Foucart, Francois (2012), “Black-hole-neutron-star mergers: Disk mass predictions,” *Phys. Rev. D* **86**, 124007.
- Foucart, Francois, Evan O’Connor, Luke Roberts, Lawrence E. Kidder, Harald P. Pfeiffer, and Mark A. Scheel (2016), “Impact of an improved neutrino energy estimate on outflows in neutron star merger simulations,” *Phys. Rev. D* **94**, 123016.
- Fowler, W A, and F. Hoyle (1960), “Nuclear cosmochronology,” *Annals of Physics* **10**, 280–302.
- François, P, E. Depagne, V. Hill, M. Spite, F. Spite, B. Plez, T. C. Beers, J. Andersen, G. James, B. Barbuy, R. Cayrel, P. Bonifacio, P. Molaro, B. Nordström, and F. Primas (2007), “First stars. VIII. Enrichment of the neutron-capture elements in the early Galaxy,” *Astron. & Astrophys.* **476**, 935–950.
- Frebel, A, N. Christlieb, J. E. Norris, C. Thom, T. C. Beers, and J. Rhee (2007), “Discovery of HE 1523-0901, a Strongly r-Process-enhanced Metal-poor Star with Detected Uranium,” *Astrophys. J. Lett.* **660**, L117–L120.
- Frebel, A, and K.-L. Kratz (2009), “Stellar age dating with thorium, uranium and lead,” in *The Ages of Stars*, IAU Symposium, Vol. 258, edited by E. E. Mamajek, D. R.

- Soderblom, and R. F. G. Wyse, pp. 449–456.
- Frebel, A, and J. E. Norris (2015), “Near-Field Cosmology with Extremely Metal-Poor Stars,” *Annu. Rev. Astron. Astrophys.* **53**, 631–688.
- Freiburghaus, C, J.-F. Rembges, T. Rauscher, E. Kolbe, F.-K. Thielemann, K.-L. Kratz, B. Pfeiffer, and J. J. Cowan (1999a), “The Astrophysical r-Process: A Comparison of Calculations following Adiabatic Expansion with Classical Calculations Based on Neutron Densities and Temperatures,” *Astrophys. J.* **516**, 381–398.
- Freiburghaus, C, S. Rosswog, and F.-K. Thielemann (1999b), “R-Process in Neutron Star Mergers,” *Astrophys. J.* **525**, L121–L124.
- Frensel, M, M.-R. Wu, C. Volpe, and A. Perego (2017), “Neutrino flavor evolution in binary neutron star merger remnants,” *Phys. Rev. D* **95**, 023011.
- Friskhnecht, U, R. Hirschi, M. Pignatari, A. Maeder, G. Meynet, C. Chiappini, F.-K. Thielemann, T. Rauscher, C. Georgy, and S. Ekström (2016), “s-process production in rotating massive stars at solar and low metallicities,” *Mon. Not. Roy. Astron. Soc.* **456**, 1803–1825.
- Fröhlich, C, P. Hauser, M. Liebendörfer, G. Martínez-Pinedo, F.-K. Thielemann, E. Bravo, N. T. Zinner, W. R. Hix, K. Langanke, A. Mezzacappa, and K. Nomoto (2006a), “Composition of the Innermost Supernova Ejecta,” *Astrophys. J.* **637**, 415–426.
- Fröhlich, C, G. Martínez-Pinedo, M. Liebendörfer, F.-K. Thielemann, E. Bravo, W. R. Hix, K. Langanke, and N. T. Zinner (2006b), “Neutrino-induced nucleosynthesis of $A > 64$ nuclei: The νp -process,” *Phys. Rev. Lett.* **96**, 142502.
- Fryer, C, and V. Kalogera (1997), “Double Neutron Star Systems and Natal Neutron Star Kicks,” *Astrophys. J.* **489**, 244–253.
- Fryer, C L, K. Belczynski, E. Ramirez-Ruiz, S. Rosswog, G. Shen, and A. W. Steiner (2015), “The Fate of the Compact Remnant in Neutron Star Mergers,” *Astrophys. J.* **812**, 24.
- Fujibayashi, S, K. Kiuchi, N. Nishimura, Y. Sekiguchi, and M. Shibata (2018), “Mass Ejection from the Remnant of a Binary Neutron Star Merger: Viscous-radiation Hydrodynamics Study,” *Astrophys. J.* **860**, 64.
- Fujibayashi, S, Y. Sekiguchi, K. Kiuchi, and M. Shibata (2017), “Properties of Neutrino-driven Ejecta from the Remnant of a Binary Neutron Star Merger: Pure Radiation Hydrodynamics Case,” *Astrophys. J.* **846**, 114.
- Fujibayashi, Sho, Masaru Shibata, Shinya Wanajo, Kenta Kiuchi, Koutarou Kyutoku, and Yuichiro Sekiguchi (2020), “Mass ejection from disks surrounding a low-mass black hole: Viscous neutrino-radiation hydrodynamics simulation in full general relativity,” arXiv e-prints [arXiv:2001.04467](https://arxiv.org/abs/2001.04467) [[astro-ph.HE](https://arxiv.org/abs/2001.04467)].
- Fujimoto, S-i, M.-a. Hashimoto, K. Arai, and R. Matsuba (2004), “Nucleosynthesis inside an Accretion Disk and Disk Winds Related to Gamma-Ray Bursts,” *Astrophys. J.* **614**, 847–857.
- Fujimoto, S-i, M.-a. Hashimoto, O. Koike, K. Arai, and R. Matsuba (2003), “p-Process Nucleosynthesis inside Supernova-driven Supercritical Accretion Disks,” *Astrophys. J.* **585**, 418–428.
- Fujimoto, S-i, M.-a. Hashimoto, K. Kotake, and S. Yamada (2007), “Heavy-Element Nucleosynthesis in a Collapsar,” *Astrophys. J.* **656**, 382–392.
- Fujimoto, S-i, K. Kotake, S. Yamada, M.-a. Hashimoto, and K. Sato (2006), “Magnetohydrodynamic Simulations of a Rotating Massive Star Collapsing to a Black Hole,” *Astrophys. J.* **644**, 1040–1055.
- Fujimoto, S-i, N. Nishimura, and M.-a. Hashimoto (2008), “Nucleosynthesis in Magnetically Driven Jets from Collapsars,” *Astrophys. J.* **680**, 1350–1358.
- Fulbright, J P (2000), “Abundances and Kinematics of Field Halo and Disk Stars. I. Observational Data and Abundance Analysis,” *Astron. J.* **120**, 1841–1852.
- Fuller, G M, W. A. Fowler, and M. J. Newman (1980), “Stellar weak-interaction rates for sd-shell nuclei. i - nuclear matrix element systematics with application to al-26 and selected nuclei of importance to the supernova problem,” *Astrophys. J. Suppl.* **42**, 447–473.
- Fuller, George M, Alexander Kusenko, and Volodymyr Takhistov (2017), “Primordial Black Holes and r-Process Nucleosynthesis,” *Phys. Rev. Lett.* **119**, 061101.
- Galama, T J, *et al.* (1998), “An unusual supernova in the error box of the γ -ray burst of 25 April 1998,” *Nature* **395**, 670–672.
- Geissel, H, *et al.* (1992), “The GSI projectile fragment separator (FRS): a versatile magnetic system for relativistic heavy ions,” *Nucl. Instruments Methods Phys. Res. Sect. B Beam Interact. with Mater. Atoms* **70**, 286–297.
- Giacomazzo, B, L. Rezzolla, and L. Baiotti (2009), “Can magnetic fields be detected during the inspiral of binary neutron stars?” *Mon. Not. Roy. Astron. Soc.* **399**, L164–L168.
- Giacomazzo, B, J. Zrake, P. C. Duffell, A. I. MacFadyen, and R. Perna (2015), “Producing magnetar magnetic fields in the merger of binary neutron stars,” *Astrophys. J.* **809**, 39.
- Gilroy, K K, C. Sneden, C. A. Pilachowski, and J. J. Cowan (1988), “Abundances of neutron capture elements in Population II stars,” *Astrophys. J.* **327**, 298–320.
- Giuliani, S A, Z. Matheson, W. Nazarewicz, E. Olsen, P.-G. Reinhard, J. Sadhukhan, B. Schuetrumpf, N. Schunck, and P. Schwerdtfeger (2019), “Colloquium: Superheavy elements: Oganesson and beyond,” *Rev. Mod. Phys.* in press.
- Giuliani, Samuel A, Gabriel Martínez-Pinedo, and Luis M. Robledo (2018), “Fission properties of superheavy nuclei for r-process calculations,” *Phys. Rev. C* **97**, 034323.
- Giuliani, Samuel A, Gabriel Martínez-Pinedo, Meng-Ru Wu, and Luis M. Robledo (2019), “Fission and the r-process nucleosynthesis of translead nuclei,” arXiv e-prints [arXiv:1904.03733](https://arxiv.org/abs/1904.03733) [[nucl-th](https://arxiv.org/abs/1904.03733)].
- Giuliani, Samuel A, Luis M. Robledo, and R. Rodríguez-Guzmán (2014), “Dynamic versus static fission paths with realistic interactions,” *Phys. Rev. C* **90**, 054311.
- Giunti, C, M. Laveder, Y. F. Li, Q. Y. Liu, and H. W. Long (2012), “Update of short-baseline electron neutrino and antineutrino disappearance,” *Phys. Rev. D* **86**, 113014.
- Goldstein, D A, and D. Kasen (2018), “Evidence for Sub-Chandrasekhar Mass Type Ia Supernovae from an Extensive Survey of Radiative Transfer Models,” *Astrophys. J.* **852**, L33.
- Gómez-Hornillos, M B, *et al.* (2011), “First Measurements with the Beta deLayEd Neutron Detector (BELEN-20) at JYFLTRAP,” in *Journal of Physics Conference Series*, Vol. 312, p. 052008.
- Gompertz, B P, *et al.* (2018), “The Diversity of Kilonova Emission in Short Gamma-Ray Bursts,” *Astrophys. J.* **860**, 62.
- Goriely, S (1997), “Direct neutron captures and the r-process nucleosynthesis,” *Astron. & Astrophys.* **325**, 414–424.
- Goriely, S (1998), “Radiative neutron captures by neutron-

- rich nuclei and the r-process nucleosynthesis,” *Phys. Lett. B* **436**, 10–18.
- Goriely, S (1999), “Uncertainties in the solar system r-abundance distribution,” *Astron. & Astrophys.* **342**, 881–891.
- Goriely, S (2015), “The fundamental role of fission during r-process nucleosynthesis in neutron star mergers,” *Eur. Phys. J. A* **51**, 22.
- Goriely, S, and M. Arnould (2001), “Actinides: How well do we know their stellar production?” *Astron. & Astrophys.* **379**, 1113–1122.
- Goriely, S, A. Bauswein, and H.-T. Janka (2011), “r-process Nucleosynthesis in Dynamically Ejected Matter of Neutron Star Mergers,” *Astrophys. J.* **738**, L32.
- Goriely, S, A. Bauswein, H. T. Janka, J. L. Sida, J. F. Lemaître, S. Panebianco, N. Dubray, and S. Hilaire (2014), “The r-process nucleosynthesis during the decompression of neutron star crust material,” in *American Institute of Physics Conference Series*, Vol. 1594, edited by Sunchan Jeong, Nobuaki Imai, Hiroari Miyatake, and Toshitaka Kajino, pp. 357–364.
- Goriely, S, A. Bauswein, O. Just, E. Plumbi, and H.-T. Janka (2015), “Impact of weak interactions of free nucleons on the r-process in dynamical ejecta from neutron star mergers,” *Mon. Not. Roy. Astron. Soc.* **452**, 3894–3904.
- Goriely, S, N. Chamel, and J. M. Pearson (2010), “Further explorations of Skyrme-Hartree-Fock-Bogoliubov mass formulas. XII. Stiffness and stability of neutron-star matter,” *Phys. Rev. C* **82**, 035804.
- Goriely, S, N. Chamel, and J. M. Pearson (2016), “Further explorations of Skyrme-Hartree-Fock-Bogoliubov mass formulas. XVI. Inclusion of self-energy effects in pairing,” *Phys. Rev. C* **93**, 034337.
- Goriely, S, and B. Clerbaux (1999), “Uncertainties in the Th cosmochronometry,” *Astron. & Astrophys.* **346**, 798–804.
- Goriely, S, and J.-P. Delaroche (2007), “The isovector imaginary neutron potential: A key ingredient for the r-process nucleosynthesis,” *Phys. Lett. B* **653**, 178–183.
- Goriely, S, S. Hilaire, and M. Girod (2012), “Latest development of the combinatorial model of nuclear level densities,” in *Journal of Physics Conference Series*, Vol. 337, p. 012027.
- Goriely, S, S. Hilaire, and A. J. Koning (2008), “Improved microscopic nuclear level densities within the Hartree-Fock-Bogoliubov plus combinatorial method,” *Phys. Rev. C* **78**, 064307.
- Goriely, S, S. Hilaire, A. J. Koning, M. Sin, and R. Capote (2009), “Towards a prediction of fission cross sections on the basis of microscopic nuclear inputs,” *Phys. Rev. C* **79**, 024612.
- Goriely, S, S. Hilaire, S. Péru, and K. Sieja (2018), “Gogny-hfb+qrpa dipole strength function and its application to radiative nucleon capture cross section,” *Phys. Rev. C* **98**, 014327.
- Goriely, S, and H.-T. Janka (2016), “Solar r-process-constrained actinide production in neutrino-driven winds of supernovae,” *Mon. Not. Roy. Astron. Soc.* **459**, 4174–4182.
- Goriely, S, and E. Khan (2002), “Large-scale qrpa calculation of el-strength and its impact on the neutron capture cross section,” *Nucl. Phys. A* **706**, 217–232.
- Goriely, S, E. Khan, and M. Samyn (2004), “Microscopic HFB + QRPA predictions of dipole strength for astrophysics applications,” *Nucl. Phys. A* **739**, 331–352, [nucl-th/0306005](#).
- Goriely, S, and G. Martínez-Pinedo (2015), “The production of transuranium elements by the r-process nucleosynthesis,” *Nucl. Phys. A* **944**, 158–176.
- Goriely, S, J.-L. Sida, J.-F. Lemaître, S. Panebianco, N. Dubray, S. Hilaire, A. Bauswein, and H.-T. Janka (2013), “New fission fragment distributions and r-process origin of the rare-earth elements,” *Phys. Rev. Lett.* **111**, 242502.
- Görres, J, M. Wiescher, and F.-K. Thielemann (1995), *Phys. Rev. C* **51**, 392.
- Gottlieb, Ore, Ehud Nakar, and Tsvi Piran (2018), “The cocoon emission - an electromagnetic counterpart to gravitational waves from neutron star mergers,” *Mon. Not. Roy. Astron. Soc.* **473**, 576–584.
- Grawe, H, K. Langanke, and G. Martínez-Pinedo (2007), “Nuclear structure and astrophysics,” *Rep. Prog. Phys.* **70**, 1525–1582.
- Grebenev, S A, A. A. Lutovinov, S. S. Tsygankov, and C. Winkler (2012), “Hard-X-ray emission lines from the decay of ^{44}Ti in the remnant of supernova 1987A,” *Nature* **490**, 373–375.
- Greiner, J, *et al.* (2015), “A very luminous magnetar-powered supernova associated with an ultra-long γ -ray burst,” *Nature* **523**, 189–192.
- Grichener, Aldana, and Noam Soker (2019), “The Common Envelope Jet Supernova (CEJSN) r-process Scenario,” *Astrophys. J.* **878**, 24.
- Griffin, R, B. Gustafsson, T. Vieira, and R. Griffin (1982), “HD 115444 - A barium star of extreme Population II,” *Mon. Not. Roy. Astron. Soc.* **198**, 637–658.
- Grisoni, V, G. Cescutti, F. Matteucci, R. Forsberg, H. Jönsson, and N. Ryde (2020), “Modelling the chemical evolution of Zr, La, Ce, and Eu in the Galactic discs and bulge,” *Mon. Not. Roy. Astron. Soc.* **492**, 2828–2834.
- Grossjean, M K, and H. Feldmeier (1985), “Level density of a Fermi gas with pairing interactions,” *Nucl. Phys. A* **444**, 113–132.
- Grossman, D, O. Korobkin, S. Rosswog, and T. Piran (2014), “The long-term evolution of neutron star merger remnants - II. Radioactively powered transients,” *Mon. Not. Roy. Astron. Soc.* **439**, 757–770.
- Guerrero, C, C. Domingo-Pardo, F. Käppeler, J. Lerendegui-Marco, F. R. Palomo, J. M. Quesada, and R. Reifarh (2017), “Prospects for direct neutron capture measurements on s-process branching point isotopes,” *Eur. Phys. J. A* **53**, 87.
- Guilet, J, A. Bauswein, O. Just, and H.-T. Janka (2017), “Magnetorotational instability in neutron star mergers: impact of neutrinos,” *Mon. Not. Roy. Astron. Soc.* **471**, 1879–1887.
- Guttormsen, M, T. Ramsøy, and J. Rekestad (1987), “The first generation of γ -rays from hot nuclei,” *Nucl. Instruments Methods Phys. Res. Sect. A Accel. Spectrometers, Detect. Assoc. Equip.* **255**, 518–523.
- Guttormsen, M, *et al.* (2005), “Radiative strength functions in $^{93-98}\text{Mo}$,” *Phys. Rev. C* **71**, 044307.
- Haensel, P, A. Y. Potekhin, and D. G. Yakovlev (2007), *Neutron Stars 1: Equation of State and Structure*, Astrophysics and Space Science Library, Vol. 326 (Springer, New York).
- Halevi, G, and P. Mösta (2018), “r-Process Nucleosynthesis from Three-dimensional Jet-driven Core-Collapse Supernovae with Magnetic Misalignments,” *Mon. Not. Roy. Astron. Soc.* **477**, 2366–2375.
- Hamers, Adrian S, and Todd A. Thompson (2019), “Double

- Neutron Star Mergers from Hierarchical Triple-star Systems,” *Astrophys. J.* **883**, 23.
- Hannaford, P, and R. M. Lowe (1981), “Determination of atomic lifetimes using pulsed laser excitation of sputtered metal vapours,” *Journal of Physics B Atomic Molecular Physics* **14**, L5–L9.
- Hansen, C J, and F. Primas (2011), “The origin of palladium and silver,” *Astron. & Astrophys.* **525**, L5.
- Hansen, C J, F. Primas, H. Hartman, K. L. Kratz, S. Wanajo, B. Leibundgut, K. Farouqi, O. Hallmann, N. Christlieb, and H. Nilsson (2012), “Silver and palladium help unveil the nature of a second r-process,” *Astron. & Astrophys.* **545**, A31.
- Hansen, T T, *et al.* (DES Collaboration) (2017), “An r-process Enhanced Star in the Dwarf Galaxy Tucana III,” *Astrophys. J.* **838**, 44.
- Hansen, Terese T, Erika M. Holmbeck, Timothy C. Beers, Vinicius M. Placco, Ian U. Roederer, Anna Frebel, Charli M. Sakari, Joshua D. Simon, and Ian B. Thompson (2018), “The R-process Alliance: First Release from the Southern Search for R-process-enhanced Stars in the Galactic Halo,” *Astrophys. J.* **858**, 92.
- Harikae, Seiji, Tomoya Takiwaki, and Kei Kotake (2009), “Long-Term Evolution of Slowly Rotating Collapsar in Special Relativistic Magnetohydrodynamics,” *Astrophys. J.* **704**, 354–371.
- Hartmann, D, S. E. Woosley, and M. F. El Eid (1985), “Nucleosynthesis in neutron-rich supernova ejecta,” *Astrophys. J.* **297**, 837–845.
- Hatarik, R, *et al.* (2010), “Benchmarking a surrogate reaction for neutron capture,” *Phys. Rev. C* **81**, 011602.
- Hausmann, M, *et al.* (2000), “First isochronous mass spectrometry at the experimental storage ring ESR,” *Nucl. Instruments Methods Phys. Res. Sect. A Accel. Spectrometers, Detect. Assoc. Equip.* **446**, 569–580.
- Hausmann, M, *et al.* (2001), “Isochronous Mass Measurements of Hot Exotic Nuclei,” *Hyperfine Interactions* **132**, 289–295.
- Haxton, W C, K. Langanke, Y.-Z. Qian, and P. Vogel (1997), “Neutrino-induced nucleosynthesis and the site of the r process,” *Phys. Rev. Lett.* **78**, 2694–2697.
- Hayek, W, U. Wiesendahl, N. Christlieb, K. Eriksson, A. J. Korn, P. S. Barklem, V. Hill, T. C. Beers, K. Farouqi, B. Pfeiffer, and K.-L. Kratz (2009), “The Hamburg/ESO R-process enhanced star survey (HERES). IV. Detailed abundance analysis and age dating of the strongly r-process enhanced stars CS 29491-069 and HE 1219-0312,” *Astron. & Astrophys.* **504**, 511–524.
- Haynes, Christopher J, and Chiaki Kobayashi (2019), “Galactic simulations of r-process elemental abundances,” *Mon. Not. Roy. Astron. Soc.* **483**, 5123–5134.
- Hebel, K, J. D. Holt, J. Menéndez, and A. Schwenk (2015), “Nuclear Forces and Their Impact on Neutron-Rich Nuclei and Neutron-Rich Matter,” *Annu. Rev. Nucl. Part. Sci.* **65**, 457–484.
- Hebel, K, J. M. Lattimer, C. J. Pethick, and A. Schwenk (2013), “Equation of State and Neutron Star Properties Constrained by Nuclear Physics and Observation,” *Astrophys. J.* **773**, 11.
- Heger, A, C. L. Fryer, S. E. Woosley, N. Langer, and D. H. Hartmann (2003), “How Massive Single Stars End Their Life,” *Astrophys. J.* **591**, 288–300.
- Hewish, A, and S. E. Okoye (1965), “Evidence for an Unusual Source of High Radio Brightness Temperature in the Crab Nebula,” *Nature* **207**, 59–60.
- Hilaire, S, S. Goriely, M. Girod, A. J. Koning, R. Capote, and M. Sin (2010), “Combinatorial level densities for practical applications,” in *European Physical Journal Web of Conferences*, Vol. 2, p. 04005.
- Hill, V, N. Christlieb, T. C. Beers, P. S. Barklem, K. L. Kratz, B. Nordström, B. Pfeiffer, and K. Farouqi (2017), “The Hamburg/ESO R-process Enhanced Star survey (HERES). XI. The highly r-process-enhanced star CS 29497-004,” *Astron. & Astrophys.* **607**, A91.
- Hill, V, B. Plez, R. Cayrel, T. C. Beers, B. Nordström, J. Andersen, M. Spite, F. Spite, B. Barbuy, P. Bonifacio, E. Depagne, P. François, and F. Primas (2002), “First stars. I. The extreme r-element rich, iron-poor halo giant CS 31082-001. Implications for the r-process site(s) and radioactive cosmochronology,” *Astron. & Astrophys.* **387**, 560–579.
- Hill, V, Á. Skúladóttir, E. Tolstoy, K. A. Venn, M. D. Shetrone, P. Jablonka, F. Primas, G. Battaglia, T. J. L. de Boer, P. François, A. Helmi, A. Kaufer, B. Letarte, E. Starkenburg, and M. Spite (2019), “VLT/FLAMES high-resolution chemical abundances in Sculptor: a textbook dwarf spheroidal galaxy,” *Astron. & Astrophys.* **626**, A15.
- Hillebrandt, W (1978), “The rapid neutron-capture process and the synthesis of heavy and neutron-rich elements,” *Space Sci. Rev.* **21**, 639–702.
- Hillebrandt, W, T. Kodama, and K. Takahashi (1976), “R-process nucleosynthesis - A dynamical model,” *Astron. & Astrophys.* **52**, 63–68.
- Hillebrandt, W, M. Kromer, F. K. Röpkke, and A. J. Ruiter (2013), “Towards an understanding of Type Ia supernovae from a synthesis of theory and observations,” *Frontiers of Physics* **8**, 116–143.
- Hillebrandt, W, F. K. Thielemann, H. V. Klapdor, and T. Oda (1981), “The r-process during explosive helium burning in supernovae,” *Astron. & Astrophys.* **99**, 195–198.
- Hirai, Y, Y. Ishimaru, T. R. Saitoh, M. S. Fujii, J. Hidaka, and T. Kajino (2015), “Enrichment of r-process Elements in Dwarf Spheroidal Galaxies in Chemo-dynamical Evolution Model,” *Astrophys. J.* **814**, 41.
- Hirai, Y, Y. Ishimaru, T. R. Saitoh, M. S. Fujii, J. Hidaka, and T. Kajino (2017), “Early chemo-dynamical evolution of dwarf galaxies deduced from enrichment of r-process elements,” *Mon. Not. Roy. Astron. Soc.* **466**, 2474–2487.
- Hix, W R, E. J. Lentz, S. W. Bruenn, A. Mezzacappa, O. E. B. Messer, E. Endeve, J. M. Blondin, J. A. Harris, P. Maronetti, and K. N. Yakunin (2016), “The Multi-dimensional Character of Core-collapse Supernovae,” *Acta Phys. Pol. B* **47**, 645.
- Hix, W R, and B. S. Meyer (2006), “Thermonuclear kinetics in astrophysics,” *Nucl. Phys. A* **777**, 188–207.
- Hix, W R, and F.-K. Thielemann (1999), “Silicon burning. ii. quasi-equilibrium and explosive burning,” *Astrophys. J.* **511**, 862–875.
- Hix, W Raphael, Suzanne T. Parete-Koon, Christian Freiburghaus, and Friedrich-Karl Thielemann (2007), “The QSE-Reduced Nuclear Reaction Network for Silicon Burning,” *Astrophys. J.* **667**, 476–488.
- Hix, W Raphael, and Friedrich-Karl Thielemann (1999), “Computational methods for nucleosynthesis and nuclear energy generation,” *J. Comput. Appl. Math.* **109**, 321–351.
- Hoffman, R D, S. E. Woosley, and Y.-Z. Qian (1997), “Nucleosynthesis in Neutrino-driven Winds. II. Implications for Heavy Element Synthesis,” *Astrophys. J.* **482**, 951–962.

- Holmbeck, E M, T. C. Beers, I. U. Roederer, V. M. Placco, T. T. Hansen, C. M. Sakari, C. Sneden, C. Liu, Y. S. Lee, J. J. Cowan, and A. Frebel (2018), “The R-Process Alliance: 2MASS J09544277+5246414, the Most Actinide-enhanced R-II Star Known,” *Astrophys. J.* **859**, L24.
- Holmbeck, Erika M, Anna Frebel, G. C. McLaughlin, Matthew R. Mumpower, Trevor M. Sprouse, and Rebecca Surman (2019a), “Actinide-rich and Actinide-poor r-process-enhanced Metal-poor Stars Do Not Require Separate r-process Progenitors,” *Astrophys. J.* **881**, 5.
- Holmbeck, Erika M, Trevor M. Sprouse, Matthew R. Mumpower, Nicole Vassh, Rebecca Surman, Timothy C. Beers, and Toshihiko Kawano (2019b), “Actinide Production in the Neutron-rich Ejecta of a Neutron Star Merger,” *Astrophys. J.* **870**, 23.
- Honda, S, W. Aoki, Y. Ishimaru, and S. Wanajo (2007), “Neutron-Capture Elements in the Very Metal-poor Star HD 88609: Another Star with Excesses of Light Neutron-Capture Elements,” *Astrophys. J.* **666**, 1189–1197.
- Honda, S, W. Aoki, Y. Ishimaru, S. Wanajo, and S. G. Ryan (2006), “Neutron-Capture Elements in the Very Metal Poor Star HD 122563,” *Astrophys. J.* **643**, 1180–1189.
- Honda, S, W. Aoki, T. Kajino, H. Ando, T. C. Beers, H. Izumiura, K. Sadakane, and M. Takada-Hidai (2004), “Spectroscopic Studies of Extremely Metal-Poor Stars with the Subaru High Dispersion Spectrograph. II. The r-Process Elements, Including Thorium,” *Astrophys. J.* **607**, 474–498.
- Horowitz, C J (2002), “Weak magnetism for antineutrinos in supernovae,” *Phys. Rev. D* **65**, 043001.
- Horowitz, C J, G. Shen, Evan O’Connor, and Christian D. Ott (2012), “Charged-current neutrino interactions in core-collapse supernovae in a virial expansion,” *Phys. Rev. C* **86**, 065806.
- Horowitz, C J, *et al.* (2019), “r-process nucleosynthesis: connecting rare-isotope beam facilities with the cosmos,” *J. Phys. G: Nucl. Part. Phys.* **46**, 083001.
- Hosmer, P, *et al.* (2010), “Half-lives and branchings for β -delayed neutron emission for neutron-rich Co-Cu isotopes in the r-process,” *Phys. Rev. C* **82**, 025806.
- Hosmer, P T, *et al.* (2005), “Half-life of the doubly magic r-process nucleus ^{78}Ni ,” *Phys. Rev. Lett.* **94**, 112501.
- Hosseinzadeh, G, *et al.* (2019), “Follow-up of the Neutron Star Bearing Gravitational-wave Candidate Events S190425z and S190426c with MMT and SOAR,” *Astrophys. J. Lett.* **880**, L4.
- Hotokezaka, K, P. Beniamini, and T. Piran (2018), “Neutron star mergers as sites of r-process nucleosynthesis and short gamma-ray bursts,” *International Journal of Modern Physics D* **27**, 1842005.
- Hotokezaka, K, K. Kyutoku, and M. Shibata (2013), “Exploring tidal effects of coalescing binary neutron stars in numerical relativity,” *Phys. Rev. D* **87**, 044001.
- Hotokezaka, K, T. Piran, and M. Paul (2015), “Short-lived ^{244}Pu points to compact binary mergers as sites for heavy r-process nucleosynthesis,” *Nature Physics* **11**, 1042.
- Hotokezaka, K, S. Wanajo, M. Tanaka, A. Bamba, Y. Terada, and T. Piran (2016), “Radioactive decay products in neutron star merger ejecta: heating efficiency and γ -ray emission,” *Mon. Not. Roy. Astron. Soc.* **459**, 35–43.
- Hotokezaka, Kenta, Kenta Kiuchi, Koutarou Kyutoku, Takayuki Muranushi, Yu-ichiro Sekiguchi, Masaru Shibata, and Keisuke Taniguchi (2013a), “Remnant massive neutron stars of binary neutron star mergers: Evolution process and gravitational waveform,” *Phys. Rev. D* **88**, 044026.
- Hotokezaka, Kenta, Kenta Kiuchi, Koutarou Kyutoku, Hiro-tada Okawa, Yu-ichiro Sekiguchi, Masaru Shibata, and Keisuke Taniguchi (2013b), “Mass ejection from the merger of binary neutron stars,” *Phys. Rev. D* **87**, 024001.
- Hotokezaka, Kenta, Koutarou Kyutoku, Hiro-tada Okawa, Masaru Shibata, and Kenta Kiuchi (2011), “Binary neutron star mergers: Dependence on the nuclear equation of state,” *Phys. Rev. D* **83**, 124008.
- Hotokezaka, Kenta, and Ehud Nakar (2020), “Radioactive Heating Rate of r-process Elements and Macronova Light Curve,” *Astrophys. J.* **891**, 152.
- Hotokezaka, Kenta, Re’em Sari, and Tsvi Piran (2017), “Analytic heating rate of neutron star merger ejecta derived from Fermi’s theory of beta decay,” *Mon. Not. Roy. Astron. Soc.* **468**, 91–96.
- Howard, W M, W. D. Arnett, D. D. Clayton, and S. E. Woosley (1972), “Nucleosynthesis of Rare Nuclei from Seed Nuclei in Explosive Carbon Burning,” *Astrophys. J.* **175**, 201.
- Howard, W M, and P. Möller (1980), “Calculated Fission Barriers, Ground-State Masses, and Particle Separation Energies for Nuclei with $76 \leq Z \leq 100$ and $140 \leq N \leq 184$,” *At. Data Nucl. Data Tables* **25**, 219.
- Hüdepohl, L, B. Müller, H.-T. Janka, A. Marek, and G. G. Raffelt (2010), “Neutrino Signal of Electron-Capture Supernovae from Core Collapse to Cooling,” *Phys. Rev. Lett.* **104**, 251101.
- Hulse, R A, and J. H. Taylor (1975), “Discovery of a pulsar in a binary system,” *Astrophys. J.* **195**, L51–L53.
- Iliadis, C (2007), *Nuclear Physics of Stars* (Wiley-VCH Verlag, Weinheim, Germany).
- Ishii, Ayako, Toshikazu Shigeyama, and Masaomi Tanaka (2018), “Free Neutron Ejection from Shock Breakout in Binary Neutron Star Mergers,” *Astrophys. J.* **861**, 25.
- Ishimaru, Y, and S. Wanajo (1999), “Enrichment of the R-Process Element Europium in the Galactic Halo,” *Astrophys. J.* **511**, L33–L36.
- Ishimaru, Y, S. Wanajo, and N. Prantzos (2015), “Neutron Star Mergers as the Origin of r-process Elements in the Galactic Halo Based on the Sub-halo Clustering Scenario,” *Astrophys. J.* **804**, L35.
- Ivans, I I, J. Simmerer, C. Sneden, J. E. Lawler, J. J. Cowan, R. Gallino, and S. Bisterzo (2006), “Near-ultraviolet observations of hd 221170: New insights into the nature of r-process-rich stars,” *Astrophys. J.* **645**, 613–633.
- Iwamoto, K, *et al.* (1998), “A hypernova model for the supernova associated with the γ -ray burst of 25 April 1998,” *Nature* **395**, 672–674.
- Janiuk, A (2014), “Nucleosynthesis of elements in gamma-ray burst engines,” *Astron. & Astrophys.* **568**, A105.
- Janiuk, A (2019a), “Nucleosynthesis from dynamical outflows of long Gamma-Ray Burst Accretion Disks,” private communication.
- Janiuk, Agnieszka (2017), “Microphysics in the Gamma-Ray Burst Central Engine,” *Astrophys. J.* **837**, 39.
- Janiuk, Agnieszka (2019b), “The r-process Nucleosynthesis in the Outflows from Short GRB Accretion Disks,” *Astrophys. J.* **882**, 163.
- Janiuk, Agnieszka, and Kostas Sapountzis (2018), “Gamma Ray Bursts. Progenitors, accretion in the central engine, jet acceleration mechanisms,” arXiv e-prints [arXiv:1803.07873](https://arxiv.org/abs/1803.07873) [astro-ph.HE].
- Janiuk, Agnieszka, Petra Sukova, and Ishika Palit (2018), “Accretion in a Dynamical Spacetime and the Spinning

- Up of the Black Hole in the Gamma-Ray Burst Central Engine,” *Astrophys. J.* **868**, 68.
- Janka, H-T (2017a), “Neutrino-Driven Explosions,” in *Handbook of Supernovae*, edited by A. W. Alsabti and P. Murdin (Springer International Publishing, Cham).
- Janka, H-T (2017b), “Neutrino Emission from Supernovae,” in *Handbook of Supernovae*, edited by A. W. Alsabti and P. Murdin (Springer International Publishing, Cham).
- Janka, H-T, B. Müller, F. S. Kitaura, and R. Buras (2008), “Dynamics of shock propagation and nucleosynthesis conditions in O-Ne-Mg core supernovae,” *Astron. & Astrophys.* **485**, 199–208, 0712.4237.
- Janka, Hans-Thomas, Tobias Melson, and Alexander Summa (2016), “Physics of Core-Collapse Supernovae in Three Dimensions: A Sneak Preview,” *Annu. Rev. Nucl. Part. Sci.* **66**, 341–375.
- Jeukenne, J-P, A. Lejeune, and C. Mahaux (1977), “Optical-model potential in finite nuclei from Reid’s hard core interaction,” *Phys. Rev. C* **16**, 80–96.
- Ji, A P, A. Frebel, J. D. Simon, and A. Chiti (2016), “Complete Element Abundances of Nine Stars in the r-process Galaxy Reticulum II,” *Astrophys. J.* **830**, 93.
- Ji, Alexander P, Maria R. Drout, and Terese T. Hansen (2019a), “The Lanthanide Fraction Distribution in Metal-poor Stars: A Test of Neutron Star Mergers as the Dominant r-process Site,” *Astrophys. J.* **882**, 40.
- Ji, Alexander P, and Anna Frebel (2018), “From Actinides to Zinc: Using the Full Abundance Pattern of the Brightest Star in Reticulum II to Distinguish between Different r-process Sites,” *Astrophys. J.* **856**, 138.
- Ji, Alexander P, Joshua D. Simon, Anna Frebel, Kim A. Venn, and Terese T. Hansen (2019b), “Chemical Abundances in the Ultra-faint Dwarf Galaxies Grus I and Triangulum II: Neutron-capture Elements as a Defining Feature of the Faintest Dwarfs,” *Astrophys. J.* **870**, 83.
- Jin, Zhi-Ping, Stefano Covino, Neng-Hui Liao, Xiang Li, Paolo D’Avanzo, Yi-Zhong Fan, and Da-Ming Wei (2020), “A kilonova associated with GRB 070809,” *Nature Astronomy* **4**, 77–82.
- Jin, Zhi-Ping, Kenta Hotokezaka, Xiang Li, Masaomi Tanaka, Paolo D’Avanzo, Yi-Zhong Fan, Stefano Covino, Da-Ming Wei, and Tsvi Piran (2016), “The Macronova in GRB 050709 and the GRB-macronova connection,” *Nature Communications* **7**, 12898.
- Jin, Zhi-Ping, Xiang Li, Zach Cano, Stefano Covino, Yi-Zhong Fan, and Da-Ming Wei (2015), “The Light Curve of the Macronova Associated with the Long-Short Burst GRB 060614,” *Astrophys. J. Lett.* **811**, L22.
- Johnson, C W, S. E. Koonin, G. H. Lang, and W. E. Ormand (1992), “Monte Carlo methods for the nuclear shell model,” *Phys. Rev. Lett.* **69**, 3157–3160.
- Jones, K L, *et al.* (2010), “The magic nature of ^{132}Sn explored through the single-particle states of ^{133}Sn ,” *Nature* **465**, 454–457.
- Jones, S, R. Hirschi, and K. Nomoto (2014), “The Final Fate of Stars that Ignite Neon and Oxygen Off-center: Electron Capture or Iron Core-collapse Supernova?” *Astrophys. J.* **797**, 83.
- Jones, S, C. Ritter, F. Herwig, C. Fryer, M. Pignatari, M. G. Bertolli, and B. Paxton (2016a), “H ingestion into He-burning convection zones in super-AGB stellar models as a potential site for intermediate neutron-density nucleosynthesis,” *Mon. Not. Roy. Astron. Soc.* **455**, 3848–3863, 1510.07417 [astro-ph.SR].
- Jones, S, F. K. Röpke, R. Pakmor, I. R. Seitenzahl, S. T. Ohlmann, and P. V. F. Edelmann (2016b), “Do electron-capture supernovae make neutron stars?. First multidimensional hydrodynamic simulations of the oxygen deflagration,” *Astron. & Astrophys.* **593**, A72.
- Junghans, A R, M. de Jong, H.-G. Clerc, A. V. Ignatyuk, G. A. Kudyaev, and K.-H. Schmidt (1998), “Projectile-fragment yields as a probe for the collective enhancement in the nuclear level density,” *Nucl. Phys. A* **629**, 635–655.
- Juodagalvis, A, Karlheinz Langanke, W.R. Hix, Gabriel Martínez-Pinedo, and J.M. Sampaio (2010), “Improved estimate of electron capture rates on nuclei during stellar core collapse,” *Nucl. Phys. A* **848**, 454–478.
- Just, O, A. Bauswein, R. A. Pulpillo, S. Goriely, and H.-T. Janka (2015a), “Comprehensive nucleosynthesis analysis for ejecta of compact binary mergers,” *Mon. Not. Roy. Astron. Soc.* **448**, 541–567.
- Just, O, M. Obergaulinger, and H. T. Janka (2015b), “A new multidimensional, energy-dependent two-moment transport code for neutrino-hydrodynamics,” *Mon. Not. Roy. Astron. Soc.* **453**, 3386–3413.
- Just, O, M. Obergaulinger, H.-T. Janka, A. Bauswein, and N. Schwarz (2016), “Neutron-star Merger Ejecta as Obstacles to Neutrino-powered Jets of Gamma-Ray Bursts,” *Astrophys. J.* **816**, L30.
- Kajino, T, and G. J. Mathews (2017), “Impact of new data for neutron-rich heavy nuclei on theoretical models for r-process nucleosynthesis,” *Rep. Prog. Phys.* **80**, 084901.
- Kalogera, V, and C. L. Fryer (1999), “Formation of the observed double neutron star systems,” *Astronomical and Astrophysical Transactions* **18**, 515–520.
- Kaplan, J D, C. D. Ott, E. P. O’Connor, K. Kiuchi, L. Roberts, and M. Duez (2014), “The Influence of Thermal Pressure on Equilibrium Models of Hypermassive Neutron Star Merger Remnants,” *Astrophys. J.* **790**, 19.
- Käppeler, F (1999), “The Origin of the Heavy Elements: The s Process,” *Prog. Part. Nucl. Phys.* **43**, 419–483.
- Käppeler, F, R. Gallino, S. Bisterzo, and W. Aoki (2011), “The s process: Nuclear physics, stellar models, and observations,” *Rev. Mod. Phys.* **83**, 157–194.
- Karakas, A I, and J. C. Lattanzio (2014), “The Dawes Review 2: Nucleosynthesis and Stellar Yields of Low- and Intermediate-Mass Single Stars,” *Publ. Astron. Soc. Austr.* **31**, e030.
- Kasen, D, N. R. Badnell, and J. Barnes (2013), “Opacities and Spectra of the r-process Ejecta from Neutron Star Mergers,” *Astrophys. J.* **774**, 25.
- Kasen, D, and L. Bildsten (2010), “Supernova Light Curves Powered by Young Magnetars,” *Astrophys. J.* **717**, 245–249.
- Kasen, Daniel, and Jennifer Barnes (2019), “Radioactive Heating and Late Time Kilonova Light Curves,” *Astrophys. J.* **876**, 128.
- Kasen, Daniel, Brian Metzger, Jennifer Barnes, Eliot Quataert, and Enrico Ramirez-Ruiz (2017), “Origin of the heavy elements in binary neutron-star mergers from a gravitational-wave event,” *Nature* **551**, 80–84.
- Kasliwal, M M, *et al.* (2017), “Illuminating gravitational waves: A concordant picture of photons from a neutron star merger,” *Science* **358**, 1559–1565.
- Kasliwal, Mansi M, Daniel Kasen, Ryan M. Lau, Daniel A. Perley, Stephan Rosswog, Eran O. Ofek, Kenta Hotokezaka, Ranga-Ram Chary, Jesper Sollerman, Ariel Goobar, and David L. Kaplan (2019), “Spitzer Mid-Infrared

- Detections of Neutron Star Merger GW170817 Suggests Synthesis of the Heaviest Elements,” *Mon. Not. Roy. Astron. Soc.*, **L14**.
- Kaspi, V M, and A. M. Beloborodov (2017), “Magnetars,” *Annu. Rev. Astron. Astrophys.* **55**, 261–301.
- Kastaun, W, R. Ciolfi, and B. Giacomazzo (2016), “Structure of stable binary neutron star merger remnants: A case study,” *Phys. Rev. D* **94**, 044060.
- Kawaguchi, Kyohei, Koutarou Kyutoku, Masaru Shibata, and Masaomi Tanaka (2016), “Models of Kilonova/Macronova Emission from Black Hole-Neutron Star Mergers,” *Astrophys. J.* **825**, 52.
- Kawaguchi, Kyohei, Masaru Shibata, and Masaomi Tanaka (2018), “Radiative Transfer Simulation for the Optical and Near-infrared Electromagnetic Counterparts to GW170817,” *Astrophys. J.* **865**, L21.
- Kawaguchi, Kyohei, Masaru Shibata, and Masaomi Tanaka (2020), “Diversity of Kilonova Light Curves,” *Astrophys. J.* **889**, 171.
- Kelic, A, M. V. Ricciardi, and K.-H. Schmidt (2008), “New Insight Into the Fission Process from Experiments with Relativistic Heavy-Ion Beams,” in *Dynamical Aspects of Nuclear Fission*, edited by J. Kliman, M. G. Itkis, and Š. Gmuca, pp. 203–215.
- Kelic, Aleksandra, M. Valentina Ricciardi, and Karl-Heinz Schmidt (2009), “ABLA07 - towards a complete description of the decay channels of a nuclear system from spontaneous fission to multifragmentation,” arXiv e-prints arXiv:0906.4193 [nucl-th].
- Kirby, E N, J. G. Cohen, P. Guhathakurta, L. Cheng, J. S. Bullock, and A. Gallazzi (2013), “The Universal Stellar Mass-Stellar Metallicity Relation for Dwarf Galaxies,” *Astrophys. J.* **779**, 102.
- Kirsebom, O S, *et al.* (2019a), “Discovery of an Exceptionally Strong β -Decay Transition of ^{20}F and Implications for the Fate of Intermediate-Mass Stars,” *Phys. Rev. Lett.* **123**, 262701.
- Kirsebom, O S, *et al.* (2019b), “Measurement of the $2^+ \rightarrow 0^+$ ground-state transition in the β decay of ^{20}F ,” *Phys. Rev. C* **100**, 065805.
- Kirson, M W (2008), “Mutual influence of terms in a semi-empirical mass formula,” *Nucl. Phys. A* **798**, 29–60.
- Kiss, G G, P. Mohr, Z. Fülöp, D. Galaviz, G. Gyürky, Z. Elekes, E. Somorjai, A. Kretschmer, K. Sonnabend, A. Zilges, and M. Avrigneanu (2009), “High precision $Y89(\alpha,\alpha)Y89$ scattering at low energies,” *Phys. Rev. C* **80**, 045807.
- Kitaura, F S, H.-T. Janka, and W. Hillebrandt (2006), “Explosions of O-Ne-Mg cores, the Crab supernova, and subluminal type II-P supernovae,” *Astron. & Astrophys.* **450**, 345–350.
- Kiuchi, K, P. Cerdá-Durán, K. Kyutoku, Y. Sekiguchi, and M. Shibata (2015), “Efficient magnetic-field amplification due to the Kelvin-Helmholtz instability in binary neutron star mergers,” *Phys. Rev. D* **92**, 124034.
- Kiuchi, Kenta, Koutarou Kyutoku, and Masaru Shibata (2012), “Three-dimensional evolution of differentially rotating magnetized neutron stars,” *Phys. Rev. D* **86**, 064008.
- Kiuchi, Kenta, Yuichiro Sekiguchi, Masaru Shibata, and Keisuke Taniguchi (2009), “Long-term general relativistic simulation of binary neutron stars collapsing to a black hole,” *Phys. Rev. D* **80**, 064037.
- Kizivat, L-T, G. Martínez-Pinedo, K. Langanke, R. Surman, and G. C. McLaughlin (2010), “ γ -ray bursts black hole accretion disks as a site for the νp process,” *Phys. Rev. C* **81**, 025802.
- Klapdor, H V, T. Oda, J. Metzinger, W. Hillebrandt, and F. K. Thielemann (1981), “The beta strength function and the astrophysical site of the r-process,” *Zeitschrift für Phys. A Hadron. Nucl.* **299**, 213–229.
- Knie, K, G. Korschinek, T. Faestermann, E. A. Dorfi, G. Rugel, and A. Wallner (2004), “ ^{60}Fe Anomaly in a Deep-Sea Manganese Crust and Implications for a Nearby Supernova Source,” *Phys. Rev. Lett.* **93**, 171103.
- Knöbel, R, *et al.* (2016), “First direct mass measurements of stored neutron-rich $^{129,130,131}\text{Cd}$ isotopes with FRS-ESR,” *Phys. Lett. B* **754**, 288–293.
- Kobayashi, C (2016), “Inhomogeneous chemical enrichment in the Galactic Halo,” in *The General Assembly of Galaxy Halos: Structure, Origin and Evolution*, IAU Symposium, Vol. 317, edited by A. Bragaglia, M. Arnaboldi, M. Rejkuba, and D. Romano, pp. 57–63.
- Kobayashi, C, H. Umeda, K. Nomoto, N. Tominaga, and T. Ohkubo (2006), “Galactic Chemical Evolution: Carbon through Zinc,” *Astrophys. J.* **653**, 1145–1171.
- Kodama, Takeshi, and Kohji Takahashi (1975), “R-process nucleosynthesis and nuclei far from the region of beta-stability,” *Nucl. Phys. A* **239**, 489–510.
- Kolbe, E, K. Langanke, G. Martínez-Pinedo, and P. Vogel (2003), “Neutrino nucleus reactions and nuclear structure,” *J. Phys. G: Nucl. Part. Phys.* **29**, 2569–2596.
- Komiya, Yutaka, and Toshikazu Shigeyama (2016), “Contribution of Neutron Star Mergers to the r-Process Chemical Evolution in the Hierarchical Galaxy Formation,” *Astrophys. J.* **830**, 76.
- Koning, A J, and J. P. Delaroche (2003), “Local and global nucleon optical models from 1 keV to 200 MeV,” *Nucl. Phys. A* **713**, 231–310.
- Koning, A J, S. Hilaire, and S. Goriely (2008), “Global and local level density models,” *Nucl. Phys. A* **810**, 13–76.
- Koonin, S E, D. J. Dean, and K. Langanke (1997), “Shell model Monte Carlo methods,” *Phys. Rep.* **278**, 1–77, nucl-th/9602006.
- Korobkin, O, S. Rosswog, A. Arcones, and C. Winteler (2012), “On the astrophysical robustness of the neutron star merger r-process,” *Mon. Not. Roy. Astron. Soc.* **426**, 1940–1949.
- Korobkin, Oleg, Aimee M. Hungerford, Christopher L. Fryer, Matthew R. Mumpower, G. Wendell Misch, Trevor M. Sprouse, Jonas Lippuner, Rebecca Surman, Aaron J. Couture, Peter F. Bloser, Farzane Shirazi, Wesley P. Even, W. Thomas Vestrand, and Richard S. Miller (2020), “Gamma Rays from Kilonova: A Potential Probe of r-process Nucleosynthesis,” *Astrophys. J.* **889**, 168.
- Kotake, K, K. Sumiyoshi, S. Yamada, T. Takiwaki, T. Kuroda, Y. Suwa, and H. Nagakura (2012), “Core-collapse supernovae as supercomputing science: A status report toward six-dimensional simulations with exact Boltzmann neutrino transport in full general relativity,” *Prog. Theor. Exp. Phys.* **2012**, 01A301.
- Koura, H, T. Tachibana, M. Uno, and M. Yamada (2005), “Nuclidic Mass Formula on a Spherical Basis with an Improved Even-Odd Term,” *Prog. Theor. Phys.* **113**, 305–325.
- Kozub, R L, *et al.* (2012), “Neutron Single Particle Structure in ^{131}Sn and Direct Neutron Capture Cross Sections,” *Phys. Rev. Lett.* **109**, 172501.
- Kramer, M (2009), “Pulsars & Magnetars,” in *Cosmic Magnetic Fields: From Planets, to Stars and Galaxies*, IAU

- Symposium, Vol. 259, edited by K. G. Strassmeier, A. G. Kosovichev, and J. E. Beckman, pp. 485–492.
- Kratz, K., J. Bitouzet, F. Thielemann, P. Moeller, and B. Pfeiffer (1993), “Isotopic r-process abundances and nuclear structure far from stability - implications for the r-process mechanism,” *Astrophys. J.* **403**, 216–238.
- Kratz, K-L (1984), “ β -strength function phenomena of exotic nuclei: A critical examination of the significance of nuclear model predictions,” *Nucl. Phys. A* **417**, 447–476.
- Kratz, K-L (2001), “Measurements of r-process nuclei,” *Nucl. Phys. A* **688**, 308–317.
- Kratz, K-L, K. Farouqi, and P. Möller (2014), “A High-entropy-wind r-process Study Based on Nuclear-structure Quantities from the New Finite-range Droplet Model Frdm(2012),” *Astrophys. J.* **792**, 6.
- Kratz, K-L, H. Gabelmann, W. Hillebrandt, B. Pfeiffer, K. Schlosser, and F.-K. Thielemann (1986), “The beta-decay half-life of cd-130(48)82 and its importance for astrophysical r-process scenarios,” *Z. Phys. A* **325**, 489–490.
- Kratz, K L, and G. Herrmann (1973), “Systematics of neutron emission probabilities from delayed neutron precursors,” *Zeitschrift für Phys.* **263**, 435–442.
- Kratz, K-L, P. Möller, B. Pfeiffer, and W. B. Walters (2000), in *Capture Gamma-Rays and Related Studies*, Vol. 529, edited by S. Wender (AIP Conf. Proc.) p. 295.
- Kratz, K-L, B. Pfeiffer, J. J. Cowan, and C. Sneden (2004), “r-process chronometers,” *New Astron. Rev.* **48**, 105–108.
- Kratz, K-L, W. Rudolph, H. Ohm, H. Franz, M. Zendel, G. Herrmann, S. G. Prussin, F. M. Nuh, A. A. Shihab-Eldin, D. R. Slaughter, W. Halverson, and H. V. Klapdor (1979), “Investigation of beta strength functions by neutron and gamma-ray spectroscopy . (I). The decay of ^{87}Br , ^{137}I , ^{85}As and ^{135}Sb ,” *Nucl. Phys. A* **317**, 335–362.
- Kratz, K-L, A. Schröder, H. Ohm, M. Zendel, H. Gabelmann, W. Ziegert, P. Peuser, G. Jung, B. Pfeiffer, K. D. Wünsch, H. Wollnik, C. Ristori, and J. Crançon (1982), “Beta-delayed neutron emission from $^{93100}\text{Rb}$ to excited states in the residual Sr isotopes,” *Zeitschrift für Phys. A Hadron. Nucl.* **306**, 239–257.
- Kratz, K-L, F.-K. Thielemann, W. Hillebrandt, P. Möller, V. Harms, A. Wöhr, and J. W. Truran (1988), “Constraints on r-process conditions from beta-decay properties far off stability and r-abundances,” *J. Phys. G: Nucl. Part. Phys.* **14**, S331.
- Kratz, K-L, W. Ziegert, W. Hillebrandt, and F.-K. Thielemann (1983), “Determination of stellar neutron-capture rates for radioactive nuclei with the aid of beta-delayed neutron emission,” *Astron. & Astrophys.* **125**, 381–387.
- Kratz, Karl-Ludwig, Bernd Pfeiffer, Friedrich-Karl Thielemann, and William B. Walters (2000), “Nuclear structure studies at ISOLDE and their impact on the astrophysical r-process,” *Hyperfine Interactions* **129**, 185–221.
- Kugler, E, D. Fiander, B. Johnson, H. Haas, A. Przewloka, H. L. Ravn, D. J. Simon, K. Zimmer, and Isolde Collaboration (1992), “The new CERN-ISOLDE on-line mass-separator facility at the PS-Booster,” *Nucl. Instruments Methods Phys. Res. Sect. B Beam Interact. with Mater. Atoms* **70**, 41–49.
- Kulkarni, S R (2005), “Modeling Supernova-like Explosions Associated with Gamma-ray Bursts with Short Durations,” arXiv e-prints [arXiv:astro-ph/0510256](https://arxiv.org/abs/astro-ph/0510256) [astro-ph].
- Kurcewicz, J, *et al.* (2012), “Discovery and cross-section measurement of neutron-rich isotopes in the element range from neodymium to platinum with the FRS,” *Phys. Lett. B* **717**, 371–375.
- Kuroda, T, K. Kotake, T. Takiwaki, and F.-K. Thielemann (2018), “A full general relativistic neutrino radiation-hydrodynamics simulation of a collapsing very massive star and the formation of a black hole,” *Mon. Not. Roy. Astron. Soc.* **477**, L80–L84.
- Kyutoku, K, K. Ioka, H. Okawa, M. Shibata, and K. Taniguchi (2015), “Dynamical mass ejection from black hole-neutron star binaries,” *Phys. Rev. D* **92**, 044028.
- Kyutoku, K, K. Ioka, and M. Shibata (2013), “Anisotropic mass ejection from black hole-neutron star binaries: Diversity of electromagnetic counterparts,” *Phys. Rev. D* **88**, 041503.
- Kyutoku, K, K. Kiuchi, Y. Sekiguchi, M. Shibata, and K. Taniguchi (2018), “Neutrino transport in black hole-neutron star binaries: Neutrino emission and dynamical mass ejection,” *Phys. Rev. D* **97**, 023009.
- Kyutoku, Koutarou, Sho Fujibayashi, Kota Hayashi, Kyohei Kawaguchi, Kenta Kiuchi, Masaru Shibata, and Masaomi Tanaka (2020), “On the Possibility of GW190425 Being a Black Hole-Neutron Star Binary Merger,” *Astrophys. J. Lett.* **890**, L4.
- Landau, L D (1932), “On the theory of star,” *Phys. Z. Sowjet Union* **1**, 285–288.
- Langanke, K (1998), “Shell model Monte Carlo level densities for nuclei with $A \leq 50$,” *Phys. Lett. B* **438**, 235–241.
- Langanke, K (2006), “Shell model Monte Carlo studies of pairing correlations and level densities in medium-mass nuclei,” *Nucl. Phys. A* **778**, 233–246.
- Langanke, K, and E. Kolbe (2001), “Neutrino-induced charged-current reaction rates for r-process nuclei,” *At. Data Nucl. Data Tables* **79**, 293–315.
- Langanke, K, and E. Kolbe (2002), “Neutrino-induced neutral-current reaction rates for r-process nuclei,” *At. Data Nucl. Data Tables* **82**, 191–209.
- Langanke, K, and G. Martínez-Pinedo (2000), “Shell-model calculations of stellar weak interaction rates: Ii. weak rates for nuclei in the mass range $a=45-65$ in supernovae environment,” *Nucl. Phys. A* **673**, 481–508.
- Langanke, K, and G. Martínez-Pinedo (2001), “Rate Tables for the Weak Processes of pf-SHELL Nuclei in Stellar Environments,” *At. Data Nucl. Data Tables* **79**, 1–46.
- Langanke, K, and G. Martínez-Pinedo (2003), “Nuclear weak-interaction processes in stars,” *Rev. Mod. Phys.* **75**, 819–862.
- Larsen, A C, R. Chankova, M. Guttormsen, F. Ingebretsen, S. Messelt, J. Rekestad, S. Siem, N. U. H. Syed, S. W. Ødegård, T. Lönnroth, A. Schiller, and A. Voinov (2006), “Microcanonical entropies and radiative strength functions of $^{50,51}\text{V}$,” *Phys. Rev. C* **73**, 064301.
- Larsen, A C, and S. Goriely (2010), “Impact of a low-energy enhancement in the γ -ray strength function on the neutron-capture cross section,” *Phys. Rev. C* **82**, 014318.
- Larsen, A C, M. Guttormsen, R. Chankova, F. Ingebretsen, T. Lönnroth, S. Messelt, J. Rekestad, A. Schiller, S. Siem, N. U. H. Syed, and A. Voinov (2007), “Nuclear level densities and γ -ray strength functions in Sc44,45,” *Phys. Rev. C* **76**, 044303.
- Larsen, A C, A. Spyrou, S. N. Liddick, and M. Guttormsen (2019), “Novel techniques for constraining neutron-capture rates relevant for r-process heavy-element nucleosynthesis,” *Prog. Part. Nucl. Phys.* **107**, 69–108.
- Larsen, A C, *et al.* (2015), “Upbend and M1 Scissors Mode in Neutron-rich Nuclei – Consequences for r-process

- (n, γ) Reaction Rates,” *Acta Physica Polonica B* **46**, 509.
- Larson, N, S. N. Liddick, M. Bennett, A. Bowe, A. Chemev, C. Prokop, A. Simon, A. Spyrou, S. Suchyta, S. J. Quinn, S. L. Tabor, P. L. Tai, V. Tripathi, and J. M. VonMoss (2013), “High efficiency beta-decay spectroscopy using a planar germanium double-sided strip detector,” *Nucl. Instruments Methods Phys. Res. Sect. A Accel. Spectrometers, Detect. Assoc. Equip.* **727**, 59–64.
- Lattimer, J M (2012), “The Nuclear Equation of State and Neutron Star Masses,” *Annu. Rev. Nucl. Part. Sci.* **62**, 485–515.
- Lattimer, J M, and D. N. Schramm (1974), “Black-hole-neutron-star collisions,” *Astrophys. J.* **192**, L145–L147.
- Lattimer, J M, and D. N. Schramm (1976), “The tidal disruption of neutron stars by black holes in close binaries,” *Astrophys. J.* **210**, 549–567.
- Lattimer, James M (2019), “The Properties of a Black Hole-Neutron Star Merger Candidate,” arXiv e-prints arXiv:1908.03622 [astro-ph.HE].
- Lawler, J E, E. A. Den Hartog, C. Sneden, and J. J. Cowan (2006), “Improved Laboratory Transition Probabilities for Sm II and Application to the Samarium Abundances of the Sun and Three r-Process-rich, Metal-poor Stars,” *Astrophys. J. Suppl.* **162**, 227–260.
- Lawler, J E, E. A. Hartog, C. Sneden, and J. J. Cowan (2008), “Comparison of Sm II transition probabilities,” *Canadian Journal of Physics* **86**, 1033–1038.
- Lawler, J E, C. Sneden, J. J. Cowan, I. I. Ivans, and E. A. Den Hartog (2009), “Improved Laboratory Transition Probabilities for Ce II, Application to the Cerium Abundances of the Sun and Five r-Process-Rich, Metal-Poor Stars, and Rare Earth Lab Data Summary,” *Astrophys. J. Suppl.* **182**, 51–79.
- Lee, William H, and Enrico Ramirez-Ruiz (2007), “The progenitors of short gamma-ray bursts,” *New J. Phys.* **9**, 17–17.
- Lehner, L, S. L. Liebling, C. Palenzuela, O. L. Caballero, E. O’Connor, M. Anderson, and D. Neilsen (2016), “Unequal mass binary neutron star mergers and multimessenger signals,” *Class. Quantum Gravity* **33**, 184002.
- Leist, B, W. Ziegert, M. Wiescher, K.-L. Kratz, and F.-K. Thielemann (1985), “Neutron capture cross sections for neutron-rich isotopes,” *Zeitschrift für Phys. A Hadron. Nucl.* **322**, 531–532.
- Lhersonneau, G, H. Gabelmann, B. Pfeiffer, and K.-L. Kratz (1995a), “Structure of the highly deformed nucleus¹⁰¹Sr₆₃ and evidence for identical K=3/2 bands,” *Zeitschrift für Phys. A Hadron. Nucl.* **352**, 293–301.
- Lhersonneau, G, B. Pfeiffer, M. Huhta, A. Wöhr, I. Klöckl, K. L. Kratz, and J. Äystö (1995b), “First evidence for the 2⁺ level in the very neutron-rich nucleus¹⁰²Sr,” *Zeitschrift für Phys. A Hadron. Nucl.* **351**, 357–358.
- Li, Hai-Ning, Wako Aoki, Satoshi Honda, Gang Zhao, Norbert Christlieb, and Takuma Suda (2015), “Discovery of a strongly r-process enhanced extremely metal-poor star LAMOST J110901.22+075441.8,” *Res. Astron. Astrophys.* **15**, 1264.
- Li, L-X, and B. Paczyński (1998), “Transient Events from Neutron Star Mergers,” *Astrophys. J.* **507**, L59–L62.
- Li, Li-Xin (2019), “Line Expansion Opacity in Relativistically Expanding Media,” *Astrophys. J.* **887**, 60.
- Liddick, S N, *et al.* (2016), “Experimental Neutron Capture Rate Constraint Far from Stability,” *Phys. Rev. Lett.* **116**, 242502.
- Liebrandt, M, M. Rampp, H.-T. Janka, and A. Mezzacappa (2005), “Supernova Simulations with Boltzmann Neutrino Transport: A Comparison of Methods,” *Astrophys. J.* **620**, 840–860.
- Liebrandt, M, S. C. Whitehouse, and T. Fischer (2009), “The Isotropic Diffusion Source Approximation for Supernova Neutrino Transport,” *Astrophys. J.* **698**, 1174–1190.
- Limongi, M, and A. Chieffi (2018), “Presupernova Evolution and Explosive Nucleosynthesis of Rotating Massive Stars in the Metallicity Range $-3 \leq [\text{Fe}/\text{H}] \leq 0$,” *Astrophys. J. Suppl.* **237**, 13.
- Lippuner, J, R. Fernández, L. F. Roberts, F. Foucart, D. Kasen, B. D. Metzger, and C. D. Ott (2017), “Signatures of hypermassive neutron star lifetimes on r-process nucleosynthesis in the disc ejecta from neutron star mergers,” *Mon. Not. Roy. Astron. Soc.* **472**, 904–918.
- Lippuner, J, and L. F. Roberts (2017), “SkyNet: A Modular Nuclear Reaction Network Library,” *Astrophys. J. Suppl.* **233**, 18.
- Lippuner, Jonas, and Luke F. Roberts (2015), “r-process Lanthanide Production and Heating Rates in Kilonovae,” *Astrophys. J.* **815**, 82.
- Litvinov, Y A, *et al.* (2004), “Precision experiments with time-resolved Schottky mass spectrometry,” *Nucl. Phys. A* **734**, 473–476.
- Litvinova, E, and N. Belov (2013), “Low-energy limit of the radiative dipole strength in nuclei,” *Phys. Rev. C* **88**, 031302.
- Litvinova, E, H.P. Loens, K. Langanke, G. Martínez-Pinedo, T. Rauscher, P. Ring, F.-K. Thielemann, and V. Tselyaev (2009), “Low-lying dipole response in the relativistic quasiparticle time blocking approximation and its influence on neutron capture cross sections,” *Nucl. Phys. A* **823**, 26–37.
- Liu, Min, Ning Wang, Yangge Deng, and Xizhen Wu (2011), “Further improvements on a global nuclear mass model,” *Phys. Rev. C* **84**, 014333.
- Liu, Yuk Tung, Stuart L. Shapiro, Zachariah B. Etienne, and Keisuke Taniguchi (2008), “General relativistic simulations of magnetized binary neutron star mergers,” *Phys. Rev. D* **78**, 024012.
- Livio, M, and P. Mazzali (2018), “On the progenitors of Type Ia supernovae,” *Phys. Rep.* **736**, 1–23.
- Lodders, K, H. Palme, and H.-P. Gail (2009), “Abundances of the Elements in the Solar System,” *Landolt Börnstein*, **44**.
- Loens, H P, K. Langanke, G. Martínez-Pinedo, and K. Sieja (2012), “M1 strength functions from large-scale shell-model calculations and their effect on astrophysical neutron capture cross-sections,” *Eur. Phys. J. A* **48**, 34.
- Loens, HP, K. Langanke, G. Martínez-Pinedo, T. Rauscher, and F.-K. Thielemann (2008), “Complete inclusion of parity-dependent level densities in the statistical description of astrophysical reaction rates,” *Phys. Lett. B* **666**, 395–399.
- Lorusso, G, *et al.* (2015), “ β -Decay Half-Lives of 110 Neutron-Rich Nuclei across the N=82 Shell Gap: Implications for the Mechanism and Universality of the Astrophysical r-Process,” *Phys. Rev. Lett.* **114**, 192501.
- Ludwig, H G, E. Caffau, M. Steffen, P. Bonifacio, and L. Sbordone (2010), “Accuracy of spectroscopy-based radioactive dating of stars,” *Astron. & Astrophys.* **509**, A84.
- Ludwig, P, *et al.* (2016), “Time-resolved 2-million-year-old supernova activity discovered in Earth’s microfossil record,”

- Proceedings of the National Academy of Science **113**, 9232–9237.
- Lugaro, M, U. Ott, and Á. Kereszturi (2018), “Radioactive nuclei from cosmochemistry to habitability,” *Prog. Part. Nucl. Phys.* **102**, 1–47.
- MacFadyen, A I, and S. E. Woosley (1999), “Collapsars: Gamma-Ray Bursts and Explosions in “Failed Supernovae”,” *Astrophys. J.* **524**, 262–289.
- MacFadyen, A I, S. E. Woosley, and A. Heger (2001), “Supernovae, Jets, and Collapsars,” *Astrophys. J.* **550**, 410–425.
- Macias, Phillip, and Enrico Ramirez-Ruiz (2019), “Constraining Collapsar r-process Models through Stellar Abundances,” *Astrophys. J. Lett.* **877**, L24.
- Malkus, A, J. P. Kneller, G. C. McLaughlin, and R. Surman (2012), “Neutrino oscillations above black hole accretion disks: Disks with electron-flavor emission,” *Phys. Rev. D* **86**, 085015.
- Malkus, A, G. C. McLaughlin, and R. Surman (2016), “Symmetric and standard matter neutrino resonances above merging compact objects,” *Phys. Rev. D* **93**, 045021.
- Mamdouh, A, J.M. Pearson, M. Rayet, and F. Tondeur (2001), “Fission barriers of neutron-rich and superheavy nuclei calculated with the etfsi method,” *Nucl. Phys. A* **679**, 337–358.
- Manning, B, *et al.* (2019), “Informing direct neutron capture on tin isotopes near the N =82 shell closure,” *Phys. Rev. C* **99**, 041302.
- Maoz, D, F. Mannucci, and G. Nelemans (2014), “Observational Clues to the Progenitors of Type Ia Supernovae,” *Annu. Rev. Astron. Astrophys.* **52**, 107–170.
- Margalit, Ben, and Brian Metzger (2017), “Constraining the Maximum Mass of Neutron Stars From Multi-Messenger Observations of GW170817,” *Astrophys. J. Lett.* **850**, L19.
- Margalit, Ben, and Brian D. Metzger (2019), “The Multimessenger Matrix: The Future of Neutron Star Merger Constraints on the Nuclear Equation of State,” *Astrophys. J. Lett.* **880**, L15.
- Marketin, T, L. Huther, and G. Martínez-Pinedo (2016a), “Large-scale evaluation of β -decay rates of r-process nuclei with the inclusion of first-forbidden transitions,” *Phys. Rev. C* **93**, 025805.
- Marketin, T, L. Huther, J. Petković, N. Paar, and G. Martínez-Pinedo (2016b), “Beta decay rates of neutron-rich nuclei,” in *American Institute of Physics Conference Series*, Vol. 1743, p. 040006.
- Marketin, T, D. Vretenar, and P. Ring (2007), “Calculation of beta-decay rates in a relativistic model with momentum-dependent self-energies,” *Phys. Rev. C* **75**, 024304.
- Marshall, J L, *et al.* (DES Collaboration) (2019a), “Chemical Abundance Analysis of Tucana III, the Second r-process Enhanced Ultra-faint Dwarf Galaxy,” *Astrophys. J.* **882**, 177.
- Marshall, J L, *et al.* (2019b), “Chemical Abundance Analysis of Tucana III, the Second r-process Enhanced Ultra-faint Dwarf Galaxy,” *Astrophys. J.* **882**, 177.
- Martin, D, A. Arcones, W. Nazarewicz, and E. Olsen (2016), “Impact of nuclear mass uncertainties on the r process,” *Phys. Rev. Lett.* **116**, 121101.
- Martin, D, A. Perego, A. Arcones, F.-K. Thielemann, O. Korobkin, and S. Rosswog (2015), “Neutrino-driven Winds in the Aftermath of a Neutron Star Merger: Nucleosynthesis and Electromagnetic Transients,” *Astrophys. J.* **813**, 2.
- Martin, D, A. Perego, W. Kastaun, and A. Arcones (2018), “The role of weak interactions in dynamic ejecta from binary neutron star mergers,” *Class. Quantum Gravity* **35**, 034001.
- Martin, W C, R. Zalubas, and L. Hagan (1971), *Atomic Energy Levels - The Rare Earth Elements, Nat. Ref. Data Ser. 60* (National Bureau of Standards, Washington: US GPO).
- Martínez-Pinedo, G, T Fischer, and L Huther (2014), “Supernova neutrinos and nucleosynthesis,” *J. Phys. G: Nucl. Part. Phys.* **41**, 044008.
- Martínez-Pinedo, G, T. Fischer, A. Lohs, and L. Huther (2012), “Charged-current weak interaction processes in hot and dense matter and its impact on the spectra of neutrinos emitted from protoneutron star cooling,” *Phys. Rev. Lett.* **109**, 251104.
- Martínez-Pinedo, G, Y. H. Lam, K. Langanke, R. G. T. Zegers, and C. Sullivan (2014), “Astrophysical weak-interaction rates for selected $A = 20$ and $A = 24$ nuclei,” *Phys. Rev. C* **89**, 045806.
- Martínez-Pinedo, G, D. Mocerlj, N.T. Zinner, A. Kelić, K. Langanke, I. Panov, B. Pfeiffer, T. Rauscher, K.-H. Schmidt, and F.-K. Thielemann (2007), “The role of fission in the r-process,” *Prog. Part. Nucl. Phys.* **59**, 199–205.
- Martínez-Pinedo, Gabriel, Tobias Fischer, Karlheinz Langanke, Andreas Lohs, Andre Sieverding, and Meng-Ru Wu (2017), “Neutrinos and Their Impact on Core-Collapse Supernova Nucleosynthesis,” in *Handbook of Supernovae*, edited by A. W. Alsabti and P. Murdin (Springer International Publishing, Cham).
- Mashonkina, L, N. Christlieb, and K. Eriksson (2014), “The Hamburg/ESO R-process Enhanced Star survey (HERES). X. HE 2252-4225, one more r-process enhanced and actinide-boost halo star,” *Astron. & Astrophys.* **569**, A43.
- Mathews, G J, A. Mengoni, F.-K. Thielemann, and W. A. Fowler (1983), “Neutron capture rates in the r-process - The role of direct radiative capture,” *Astrophys. J.* **270**, 740–745.
- Matteucci, F, and C. Chiappini (2001), “The evolution of the oxygen abundance in the Galaxy,” *New Astron. Rev.* **45**, 567–570.
- Matteucci, F, and L. Greggio (1986), “Relative roles of type I and II supernovae in the chemical enrichment of the interstellar gas,” *Astron. & Astrophys.* **154**, 279–287.
- Matteucci, F, D. Romano, A. Arcones, O. Korobkin, and S. Rosswog (2014), “Europium production: neutron star mergers versus core-collapse supernovae,” *Mon. Not. Roy. Astron. Soc.* **438**, 2177–2185.
- Matteucci, Francesca (2012), *Chemical Evolution of Galaxies*, Astronomy and Astrophysics Library (Springer-Verlag, Berlin Heidelberg).
- McConnell, J R, and W. L. Talbert (1975), “The Tristan online isotope separator facility,” *Nuclear Instruments and Methods* **128**, 227–243.
- McFadden, L, and G. R. Satchler (1966), “Optical-model analysis of the scattering of 24.7 MeV alpha particles,” *Nucl. Phys. A* **84**, 177–200.
- McKinney, J C, A. Tchekhovskoy, and R. D. Blandford (2013), “Alignment of Magnetized Accretion Disks and Relativistic Jets with Spinning Black Holes,” *Science* **339**, 49.
- McLaughlin, G C, J. M. Fetter, A. B. Balantekin, and G. M. Fuller (1999), “Active-sterile neutrino transformation solution for r-process nucleosynthesis,” *Phys. Rev. C* **59**, 2873–2887.
- McLaughlin, G C, and R. Surman (2005), “Prospects for obtaining an r process from Gamma Ray Burst Disk Winds,” *Nucl. Phys. A* **758**, 189–196.

- Meisel, Z, and S. George (2013), “Time-of-flight mass spectrometry of very exotic systems,” *Int. J. Mass Spectrom.* **349-350**, 145–150.
- Mendoza-Temis, Joel Jesús (2017), *Nuclear masses and their impact in r-process nucleosynthesis*, Ph.D. thesis (Technische Universität Darmstadt).
- Mendoza-Temis, Joel Jesús, Meng-Ru Wu, Karlheinz Langanke, Gabriel Martínez-Pinedo, Andreas Bauswein, and Hans-Thomas Janka (2015), “Nuclear robustness of the r process in neutron-star mergers,” *Phys. Rev. C* **92**, 055805.
- Mennekens, N, and D. Vanbeveren (2014), “Massive double compact object mergers: gravitational wave sources and r -process element production sites,” *Astron. & Astrophys.* **564**, A134.
- Mennekens, N, and D. Vanbeveren (2016), “The delay time distribution of massive double compact star mergers,” *Astron. & Astrophys.* **589**, A64.
- Mention, G, M. Fechner, Th. Lasserre, Th.A. Mueller, D. Lhuillier, *et al.* (2011), “The Reactor Antineutrino Anomaly,” *Phys. Rev. D* **83**, 073006.
- Merrill, P W (1952), “Spectroscopic Observations of Stars of Class,” *Astrophys. J.* **116**, 21.
- Metzger, B D (2017a), “Kilonovae,” *Living Reviews in Relativity* **20**, 3.
- Metzger, B D (2017b), “Welcome to the Multi-Messenger Era! Lessons from a Neutron Star Merger and the Landscape Ahead,” ArXiv e-prints [arXiv:1710.05931](https://arxiv.org/abs/1710.05931) [astro-ph.HE].
- Metzger, B D, A. Arcones, E. Quataert, and G. Martínez-Pinedo (2010a), “The effects of r -process heating on fallback accretion in compact object mergers,” *Mon. Not. Roy. Astron. Soc.* **402**, 2771–2777.
- Metzger, B D, A. Bauswein, S. Goriely, and D. Kasen (2015), “Neutron-powered precursors of kilonovae,” *Mon. Not. Roy. Astron. Soc.* **446**, 1115–1120.
- Metzger, B D, and E. Berger (2012), “What is the Most Promising Electromagnetic Counterpart of a Neutron Star Binary Merger?” *Astrophys. J.* **746**, 48.
- Metzger, B D, and R. Fernández (2014), “Red or blue? A potential kilonova imprint of the delay until black hole formation following a neutron star merger,” *Mon. Not. Roy. Astron. Soc.* **441**, 3444–3453.
- Metzger, B D, G. Martínez-Pinedo, S. Darbha, E. Quataert, A. Arcones, D. Kasen, R. Thomas, P. Nugent, I. V. Panov, and N. T. Zinner (2010b), “Electromagnetic counterparts of compact object mergers powered by the radioactive decay of r -process nuclei,” *Mon. Not. Roy. Astron. Soc.* **406**, 2650–2662.
- Metzger, B D, A. L. Piro, and E. Quataert (2009), “Neutron-rich freeze-out in viscously spreading accretion discs formed from compact object mergers,” *Mon. Not. Roy. Astron. Soc.* **396**, 304–314.
- Metzger, B D, T. A. Thompson, and E. Quataert (2008), “On the Conditions for Neutron-rich Gamma-Ray Burst Outflows,” *Astrophys. J.* **676**, 1130–1150.
- Metzger, B D, T. A. Thompson, and E. Quataert (2018), “A Magnetar Origin for the Kilonova Ejecta in GW170817,” *Astrophys. J.* **856**, 101.
- Meyer, B S (1993), “Entropy and nucleosynthesis,” *Phys. Rep.* **227**, 257–267.
- Meyer, B S, G. J. Mathews, W. M. Howard, S. E. Woosley, and R. D. Hoffman (1992), “ R -process nucleosynthesis in the high-entropy supernova bubble,” *Astrophys. J.* **399**, 656–664.
- Meyer, B S, G. C. McLaughlin, and G. M. Fuller (1998), “Neutrino capture and r -process nucleosynthesis,” *Phys. Rev. C* **58**, 3696–3710.
- Meyer, B S, and D. N. Schramm (1988), “Nucleosynthesis from the Decompression of Initially Cold Neutron Star Matter,” in *Origin and Distribution of the Elements*, edited by G. J. Mathews, p. 610.
- Minchev, I, C. Chiappini, and M. Martig (2014), “Chemodynamical evolution of the Milky Way disk. II. Variations with Galactic radius and height above the disk plane,” *Astron. & Astrophys.* **572**, A92.
- Mirizzi, A (2015), “Breaking the symmetries in self-induced flavor conversions of neutrino beams from a ring,” *Phys. Rev. D* **92**, 105020.
- Mirizzi, A, G. Mangano, and N. Saviano (2015), “Self-induced flavor instabilities of a dense neutrino stream in a two-dimensional model,” *Phys. Rev. D* **92**, 021702.
- Mirizzi, A, I. Tamborra, H.-T. Janka, N. Saviano, K. Scholberg, R. Bollig, L. Hüdepohl, and S. Chakraborty (2016), “Supernova neutrinos: production, oscillations and detection,” *Nuovo Cimento Rivista Serie* **39**, 1–112.
- Mishenina, T, M. Pignatari, T. Gorbaneva, S. Bisterzo, C. Travaglio, F. K. Thielemann, and C. Soubiran (2019a), “Enrichment of the Galactic disc with neutron capture elements: Sr,” *Mon. Not. Roy. Astron. Soc.* **484**, 3846–3864.
- Mishenina, T, M. Pignatari, T. Gorbaneva, C. Travaglio, B. Côté, F. K. Thielemann, and C. Soubiran (2019b), “Enrichment of the Galactic disc with neutron-capture elements: Mo and Ru,” *Mon. Not. Roy. Astron. Soc.* **489**, 1697–1708.
- Mocelj, D, T. Rauscher, G. Martínez-Pinedo, K. Langanke, L. Paceaescu, A. Faessler, F.-K. Thielemann, and Y. Alhassid (2007), “Large-scale prediction of the parity distribution in the nuclear level density and application to astrophysical reaction rates,” *Phys. Rev. C* **75**, 045805.
- Mohr, P, G. Gyürky, and Z. Fülöp (2017), “Statistical model analysis of α -induced reaction cross sections of ^{64}Zn at low energies,” *Phys. Rev. C* **95**, 015807.
- Mohr, P, G. G. Kiss, Z. Fülöp, D. Galaviz, G. Gyürky, and E. Somorjai (2013), “Elastic alpha scattering experiments and the alpha-nucleus optical potential at low energies,” *At. Data Nucl. Data Tables* **99**, 651–679.
- Möller, P, W. D. Myers, H. Sagawa, and S. Yoshida (2012a), “New Finite-Range Droplet Mass Model and Equation-of-State Parameters,” *Phys. Rev. Lett.* **108**, 052501.
- Möller, P, J. R. Nix, and K.-L. Kratz (1997), “Nuclear Properties for Astrophysical and Radioactive-Ion Beam Applications,” *At. Data Nucl. Data Tables* **66**, 131–343.
- Möller, P, J. R. Nix, W. D. Myers, and W. J. Swiatecki (1995), “Nuclear Ground-State Masses and Deformations,” *At. Data Nucl. Data Tables* **59**, 185.
- Möller, P, B. Pfeiffer, and K.-L. Kratz (2003), “New calculations of gross beta-decay properties for astrophysical applications: Speeding-up the classical r process,” *Phys. Rev. C* **67**, 055802.
- Möller, P, A. J. Sierk, R. Bengtsson, H. Sagawa, and T. Ichikawa (2012b), “Nuclear shape isomers,” *At. Data Nucl. Data Tables* **98**, 149–300.
- Möller, P, A. J. Sierk, T. Ichikawa, A. Iwamoto, and M. Mumpower (2015), “Fission barriers at the end of the chart of the nuclides,” *Phys. Rev. C* **91**, 024310.
- Möller, P, A. J. Sierk, T. Ichikawa, and H. Sagawa (2016), “Nuclear ground-state masses and deformations: FRDM(2012),” *At. Data Nucl. Data Tables* **109**, 1–204.
- Montes, F, *et al.* (2006), “ β -decay half-lives and β -delayed

- neutron emission probabilities for neutron rich nuclei close to the $N=82$ -process path,” *Phys. Rev. C* **73**, 035801.
- Montes, G, E. Ramirez-Ruiz, J. Naiman, S. Shen, and W. H. Lee (2016), “Transport and Mixing of r-process Elements in Neutron Star Binary Merger Blast Waves,” *Astrophys. J.* **830**, 12.
- Mooley, K P, *et al.* (2018), “A mildly relativistic wide-angle outflow in the neutron-star merger event GW170817,” *Nature* **554**, 207–210.
- Moore, C E (1971), *Atomic Energy Levels, Nat. Ref. Data Ser. 60* (National Bureau of Standards, Washington: US GPO).
- Moriya, Takashi J, Nozomu Tominaga, Norbert Langer, Ken’ichi Nomoto, Sergei I. Blinnikov, and Elena I. Sorokina (2014), “Electron-capture supernovae exploding within their progenitor wind,” *Astron. & Astrophys.* **569**, A57.
- Most, Elias R, Lukas R. Weih, Luciano Rezzolla, and Jürgen Schaffner-Bielich (2018), “New constraints on radii and tidal deformabilities of neutron stars from gw170817,” *Phys. Rev. Lett.* **120**, 261103.
- Mösta, P, C. D. Ott, D. Radice, L. F. Roberts, E. Schnetter, and R. Haas (2015), “A large-scale dynamo and magnetoturbulence in rapidly rotating core-collapse supernovae,” *Nature* **528**, 376–379.
- Mösta, P, S. Richers, C. D. Ott, R. Haas, A. L. Piro, K. Boydston, E. Abdikamalov, C. Reisswig, and E. Schnetter (2014), “Magnetorotational core-collapse supernovae in three dimensions,” *Astrophys. J.* **785**, L29.
- Mösta, P, L. F. Roberts, G. Halevi, C. D. Ott, J. Lipuner, R. Haas, and E. Schnetter (2018), “r-process Nucleosynthesis from Three-dimensional Magnetorotational Core-collapse Supernovae,” *Astrophys. J.* **864**, 171.
- Mueller, E (1986), “Nuclear-reaction networks and stellar evolution codes - The coupling of composition changes and energy release in explosive nuclear burning,” *Astron. & Astrophys.* **162**, 103–108.
- Müller, B (2016), “The Status of Multi-Dimensional Core-Collapse Supernova Models,” *Publ. Astron. Soc. Austr.* **33**, e048.
- Müller, B, D. W. Gay, A. Heger, T. M. Tauris, and S. A. Sim (2018), “Multidimensional simulations of ultrastripped supernovae to shock breakout,” *Mon. Not. Roy. Astron. Soc.* **479**, 3675–3689.
- Müller, Bernhard, Thomas M. Tauris, Alexander Heger, Projwal Banerjee, Yong-Zhong Qian, Jade Powell, Conrad Chan, Daniel W. Gay, and Norbert Langer (2019), “Three-dimensional simulations of neutrino-driven core-collapse supernovae from low-mass single and binary star progenitors,” *Mon. Not. Roy. Astron. Soc.* **484**, 3307–3324.
- Mumpower, M R, P. Jaffke, M. Verriere, and J. Randrup (2019), “Primary fission fragment mass yields across the chart of nuclides,” arXiv e-prints [arXiv:1911.06344](https://arxiv.org/abs/1911.06344) [nucl-th].
- Mumpower, M R, T. Kawano, T. M. Sprouse, N. Vassh, E. M. Holmbeck, R. Surman, and P. Möller (2018), “ β -delayed Fission in r-process Nucleosynthesis,” *Astrophys. J.* **869**, 14.
- Mumpower, M R, T. Kawano, J. L. Ullmann, M. Kr̕tička, and T. M. Sprouse (2017a), “Estimation of M1 scissors mode strength for deformed nuclei in the medium- to heavy-mass region by statistical Hauser-Feshbach model calculations,” *Phys. Rev. C* **96**, 024612.
- Mumpower, M R, G. C. McLaughlin, R. Surman, and A. W. Steiner (2017b), “Reverse engineering nuclear properties from rare earth abundances in the r process,” *J. Phys. G: Nucl. Part. Phys.* **44**, 034003.
- Mumpower, M R, R. Surman, D.-L. Fang, M. Beard, P. Möller, T. Kawano, and A. Aprahamian (2015), “Impact of individual nuclear masses on r-process abundances,” *Phys. Rev. C* **92**, 035807.
- Mumpower, M R, R. Surman, G. C. McLaughlin, and A. Aprahamian (2016), “The impact of individual nuclear properties on r-process nucleosynthesis,” *Prog. Part. Nucl. Phys.* **86**, 86–126.
- Munson, J M, *et al.* (2018), “Recoil-ion detection efficiency for complex β decays studied using the Beta-decay Paul Trap,” *Nuclear Instruments and Methods in Physics Research A* **898**, 60–66.
- Münzel, J, H. Wollnik, B. Pfeiffer, and G. Jung (1981), “A high-temperature ion source for the on-line separator OS-TIS,” *Nucl. Instruments Methods Phys. Res.* **186**, 343–347.
- Mustafa, M G, M. Blann, A. V. Ignatyuk, and S. M. Grimes (1992), “Nuclear level densities at high excitations,” *Phys. Rev. C* **45**, 1078–1083.
- Mustonen, M T, and J. Engel (2016), “Global description of β^- decay in even-even nuclei with the axially-deformed Skyrme finite-amplitude method,” *Phys. Rev. C* **93**, 014304.
- Myers, W D, and W. J. Świątecki (1999), “Thomas-Fermi fission barriers,” *Phys. Rev. C* **60**, 014606.
- Nadyozhin, D K, and I. V. Panov (2007), “Weak r-process component as a result of the neutrino interaction with the helium shell of a supernova,” *Astronomy Letters* **33**, 385–389.
- Nagataki, S (2011), “Grb-Sn Connection: Central Engine of Long GRBs and Explosive Nucleosynthesis,” *International Journal of Modern Physics D* **20**, 1975–1978.
- Nagataki, S, R. Takahashi, A. Mizuta, and T. Takiwaki (2007), “Numerical Study of Gamma-Ray Burst Jet Formation in Collapsars,” *Astrophys. J.* **659**, 512–529.
- Nakada, H, and Y. Alhassid (1997), “Total and Parity-Projected Level Densities of Iron-Region Nuclei in the Auxiliary Fields Monte Carlo Shell Model,” *Phys. Rev. Lett.* **79**, 2939–2942.
- Nakamura, K, T. Kajino, G. J. Mathews, S. Sato, and S. Harikae (2015), “r-process nucleosynthesis in the MHD+neutrino-heated collapsar jet,” *Astron. & Astrophys.* **582**, A34.
- Nakamura, T, H. Umeda, K. Iwamoto, K. Nomoto, M.-a. Hashimoto, W. R. Hix, and F.-K. Thielemann (2001), “Explosive Nucleosynthesis in Hypernovae,” *Astrophys. J.* **555**, 880–899.
- Nakar, Ehud (2007), “Short-hard gamma-ray bursts,” *Phys. Rep.* **442**, 166–236.
- National Research Council, (2003), *Connecting Quarks with the Cosmos: Eleven Science Questions for the New Century* (The National Academies Press, Washington, DC).
- Neufcourt, Léo, Yuchen Cao, Witold Nazarewicz, and Frederi Viens (2018), “Bayesian approach to model-based extrapolation of nuclear observables,” *Phys. Rev. C* **98**, 034318.
- Nicholl, M, J. Guillochon, and E. Berger (2017a), “The Magnetar Model for Type I Superluminous Supernovae. I. Bayesian Analysis of the Full Multicolor Light-curve Sample with MOSFIT,” *Astrophys. J.* **850**, 55.
- Nicholl, M, *et al.* (2017b), “The Electromagnetic Counterpart of the Binary Neutron Star Merger LIGO/Virgo GW170817. III. Optical and UV Spectra of a Blue Kilonova from Fast Polar Ejecta,” *Astrophys. J. Lett.* **848**, L18.

- Nishimura, N, T. Rauscher, R. Hirschi, A. S. J. Murphy, G. Cescutti, and C. Travaglio (2018), “Uncertainties in the production of p nuclides in thermonuclear supernovae determined by Monte Carlo variations,” *Mon. Not. Roy. Astron. Soc.* **474**, 3133–3139.
- Nishimura, N, H. Sawai, T. Takiwaki, S. Yamada, and F.-K. Thielemann (2017), “The Intermediate r-process in Core-collapse Supernovae Driven by the Magneto-rotational Instability,” *Astrophys. J.* **836**, L21.
- Nishimura, N, T. Takiwaki, and F.-K. Thielemann (2015), “The r-process Nucleosynthesis in the Various Jet-like Explosions of Magnetorotational Core-collapse Supernovae,” *Astrophys. J.* **810**, 109.
- Nishimura, S, K. Kotake, M.-a. Hashimoto, S. Yamada, N. Nishimura, S. Fujimoto, and K. Sato (2006), “r-Process Nucleosynthesis in Magnetohydrodynamic Jet Explosions of Core-Collapse Supernovae,” *Astrophys. J.* **642**, 410–419.
- Nolden, F, P. Hülsmann, Y. A. Litvinov, P. Moritz, C. Peschke, P. Petri, M. S. Sanjari, M. Steck, H. Weick, J. X. Wu, Y. D. Zang, S. H. Zhang, and T. C. Zhao (2011), “A fast and sensitive resonant Schottky pick-up for heavy ion storage rings,” *Nucl. Instruments Methods Phys. Res. Sect. A Accel. Spectrometers, Detect. Assoc. Equip.* **659**, 69–77.
- Nomoto, K (2017), “Nucleosynthesis in Hypernovae Associated with Gamma-Ray Bursts,” in *Handbook of Supernovae*, edited by A. W. Alsabti and P. Murdin (Springer International Publishing) p. 1931.
- Nomoto, K, C. Kobayashi, and N. Tominaga (2013), “Nucleosynthesis in Stars and the Chemical Enrichment of Galaxies,” *Annu. Rev. Astron. Astrophys.* **51**, 457–509.
- Nomoto, K, F.-K. Thielemann, and S. Miyaji (1985), “The triple alpha reaction at low temperatures in accreting white dwarfs and neutron stars,” *Astron. & Astrophys.* **149**, 239–245.
- Nomoto, K, N. Tominaga, H. Umeda, C. Kobayashi, and K. Maeda (2006), “Nucleosynthesis yields of core-collapse supernovae and hypernovae, and galactic chemical evolution,” *Nucl. Phys. A* **777**, 424–458.
- Nomoto, Ken’ichi, and Shing-Chi Leung (2017a), “Electron Capture Supernovae from Super Asymptotic Giant Branch Stars,” in *Handbook of Supernovae*, edited by A. W. Alsabti and P. Murdin (Springer International Publishing, Cham).
- Nomoto, Ken’ichi, and Shing-Chi Leung (2017b), “Thermonuclear Explosions of Chandrasekhar Mass White Dwarfs,” in *Handbook of Supernovae*, edited by Athem W. Alsabti and Paul Murdin (Springer International Publishing, Cham).
- Nomoto, Ken’ichi, Masaomi Tanaka, Nozomu Tominaga, and Keiichi Maeda (2010), “Hypernovae, gamma-ray bursts, and first stars,” *New Astron. Rev.* **54**, 191–200.
- Nunokawa, H, J. T. Peltoniemi, A. Rossi, and J. W. F. Valle (1997), “Supernova bounds on resonant active-sterile neutrino conversions,” *Phys. Rev. D* **56**, 1704–1713.
- Obergaulinger, M, and M. Á. Aloy (2020), “Magneto-rotational core collapse of possible GRB progenitors - I. Explosion mechanisms,” *Mon. Not. Roy. Astron. Soc.* **492**, 4613–4634.
- Obergaulinger, M, M. A. Aloy, and E. Müller (2010), “Local simulations of the magnetized Kelvin-Helmholtz instability in neutron-star mergers,” *Astron. & Astrophys.* **515**, A30.
- Obergaulinger, M, O. Just, and M. A. Aloy (2018), “Core collapse with magnetic fields and rotation,” *J. Phys. G: Nucl. Part. Phys.* **45**, 084001.
- Oechslin, R, H.-T. Janka, and A. Marek (2007), “Relativistic neutron star merger simulations with non-zero temperature equations of state. I. Variation of binary parameters and equation of state,” *Astron. & Astrophys.* **467**, 395–409.
- Oechslin, R, S. Rosswog, and F.-K. Thielemann (2002), “Conformally flat smoothed particle hydrodynamics application to neutron star mergers,” *Phys. Rev. D* **65**, 103005.
- Oechslin, R, K. Uryū, G. Poghosyan, and F. K. Thielemann (2004), “The influence of quark matter at high densities on binary neutron star mergers,” *Mon. Not. Roy. Astron. Soc.* **349**, 1469–1480.
- Oertel, M, M. Hempel, T. Klähn, and S. Typel (2017), “Equations of state for supernovae and compact stars,” *Rev. Mod. Phys.* **89**, 015007.
- Ojima, T, Y. Ishimaru, S. Wanajo, N. Prantzos, and P. François (2018), “Stochastic Chemical Evolution of Galactic Subhalos and the Origin of r-process Elements,” *Astrophys. J.* **865**, 87.
- Ono, M, M. Hashimoto, S. Fujimoto, K. Kotake, and S. Yamada (2012), “Explosive Nucleosynthesis in Magnetohydrodynamical Jets from Collapsars. II — Heavy-Element Nucleosynthesis of s, p, r-Processes,” *Prog. Theor. Phys.* **128**, 741–765.
- Orford, R, *et al.* (2018), “Precision mass measurements of neutron-rich neodymium and samarium isotopes and their role in understanding rare-earth peak formation,” *Phys. Rev. Lett.* **120**, 262702.
- Ormand, W E (1997), “Estimating the nuclear level density with the Monte Carlo shell model,” *Phys. Rev. C* **56**, R1678–R1682.
- Otsuki, K, A. Burrows, G. Martinez-Pinedo, S. Typel, K. Langanke, and M. Matos (2010), “r-process in Type II supernovae and the role of direct capture,” in *American Institute of Physics Conference Series*, Vol. 1238, edited by H. Susa, M. Arnould, S. Gales, T. Motobayashi, C. Scheidenberger, and H. Utsunomiya, pp. 240–242.
- Otsuki, K, H. Tagoshi, T. Kajino, and S. Wanajo (2000), “General relativistic effects on neutrino-driven winds from young, hot neutron stars and r-process nucleosynthesis,” *Astrophys. J.* **533**, 424–439.
- Özel, Feryal, and Paulo Freire (2016), “Masses, radii, and the equation of state of neutron stars,” *Annu. Rev. Astron. Astrophys.* **54**, 401–440.
- Özen, C, Y. Alhassid, and H. Nakada (2015), “Nuclear state densities of odd-mass heavy nuclei in the shell model Monte Carlo approach,” *Phys. Rev. C* **91**, 034329.
- Pagel, B E J (2009), *Nucleosynthesis and Chemical Evolution of Galaxies*, by Bernard E. J. Pagel, Cambridge, UK: Cambridge University Press, 2009.
- Pain, S D, J. A. Cizewski, R. Hatarik, K. L. Jones, J. S. Thomas, D. W. Bardayan, J. C. Blackmon, C. D. Nesaraja, M. S. Smith, R. L. Kozub, and M. S. Johnson (2007), “Development of a high solid-angle silicon detector array for measurement of transfer reactions in inverse kinematics,” *Nucl. Instruments Methods Phys. Res. Sect. B Beam Interact. with Mater. Atoms* **261**, 1122–1125.
- Pakhomov, Yu V, L. I. Mashonkina, T. M. Sitnova, and P. Jablonka (2019), “Contribution of Type Ia Supernovae to the Chemical Enrichment of the Ultra-Faint Dwarf Galaxy Boötes I,” *Astronomy Letters* **45**, 259–275.
- Palenzuela, Carlos, Steven L. Liebling, David Neilsen, Luis Lehner, O. L. Caballero, Evan O’Connor, and Matthew Anderson (2015), “Effects of the microphysical equation of state in the mergers of magnetized neutron stars with neutrino cooling,” *Phys. Rev. D* **92**, 044045.

- Pan, K-C, M. Liebendörfer, S. M. Couch, and F.-K. Thielemann (2018), “Equation of State Dependent Dynamics and Multi-messenger Signals from Stellar-mass Black Hole Formation,” *Astrophys. J.* **857**, 13.
- Pan, Kuo-Chuan, Carlos Mattes, Evan P. O’Connor, Sean M. Couch, Albino Perego, and Almudena Arcones (2019), “The impact of different neutrino transport methods on multidimensional core-collapse supernova simulations,” *J. Phys. G: Nucl. Part. Phys.* **46**, 014001.
- Panov, I V, E. Kolbe, B. Pfeiffer, T. Rauscher, K.-L. Kratz, and F.-K. Thielemann (2005), “Calculations of fission rates for r-process nucleosynthesis,” *Nucl. Phys. A* **747**, 633–654.
- Panov, I V, I. Y. Korneev, Y. S. Lutostansky, and F.-K. Thielemann (2013), “Probabilities of delayed processes for nuclei involved in the r-process,” *Phys. Atom. Nuclei* **76**, 88–101.
- Panov, I V, I. Y. Korneev, T. Rauscher, G. Martínez-Pinedo, A. Kelić-Heil, N. T. Zinner, and F.-K. Thielemann (2010), “Neutron-induced astrophysical reaction rates for translead nuclei,” *Astron. & Astrophys.* **513**, A61.
- Panov, I V, I. Y. Korneev, and F.-K. Thielemann (2008), “The r-Process in the region of transuranium elements and the contribution of fission products to the nucleosynthesis of nuclei with $A \leq 130$,” *Astronomy Letters* **34**, 189–197.
- Panov, I V, Y. S. Lutostansky, M. Eichler, and F.-K. Thielemann (2017), “Determination of the Galaxy age by the method of uranium-thorium-plutonium isotopic ratios,” *Phys. Atom. Nuclei* **80**, 657–665.
- Panov, I V, Y. S. Lutostansky, and F.-K. Thielemann (2016), “Beta-decay half-lives for the r-process nuclei,” *Nucl. Phys. A* **947**, 1–11.
- Panov, I V, and F.-K. Thielemann (2004), “Fission and the r-Process: Competition between Neutron-Induced and Beta-Delayed Fission,” *Astronomy Letters* **30**, 647–655.
- Papenfort, L Jens, Roman Gold, and Luciano Rezzolla (2018), “Dynamical ejecta and nucleosynthetic yields from eccentric binary neutron-star mergers,” *Phys. Rev. D* **98**, 104028.
- Pardo, Richard C, Guy Savard, and Robert V. F. Janssens (2016), “ATLAS with CARIBU: A Laboratory Portrait,” *Nuclear Physics News* **26**, 5–11.
- Patat, F, A. Piemonte, C. Lidman, T. Augusteijn, O. R. Hainaut, H. Boehnhardt, B. Leibundgut, and J. Brewer (1998), “Supernova 1998bw in ESO 184-G82,” *IAU Circ.* **7017**, 2.
- Perego, A, D. Radice, and S. Bernuzzi (2017a), “AT 2017gfo: An Anisotropic and Three-component Kilonova Counterpart of GW170817,” *Astrophys. J.* **850**, L37.
- Perego, A, S. Rosswog, R. M. Cabezón, O. Korobkin, R. Käppeli, A. Arcones, and M. Liebendörfer (2014), “Neutrino-driven winds from neutron star merger remnants,” *Mon. Not. Roy. Astron. Soc.* **443**, 3134–3156.
- Perego, A, H. Yasin, and A. Arcones (2017b), “Neutrino pair annihilation above merger remnants: implications of a long-lived massive neutron star,” *J. Phys. G: Nucl. Part. Phys.* **44**, 084007.
- Perego, Albino, Sebastiano Bernuzzi, and David Radice (2019), “Thermodynamics conditions of matter in neutron star mergers,” *Eur. Phys. J. A* **55**, 124.
- Pereira, J, *et al.* (2009), “ β -decay half-lives and β -delayed neutron emission probabilities of nuclei in the region $A \lesssim 110$, relevant for the r process,” *Phys. Rev. C* **79**, 035806.
- Pereira, J, *et al.* (2010), “The neutron long counter NERO for studies of β -delayed neutron emission in the r-process,” *Nucl. Instruments Methods Phys. Res. Sect. A Accel. Spectrometers, Detect. Assoc. Equip.* **618**, 275–283.
- Petermann, I, K. Langanke, G. Martínez-Pinedo, I. V. Panov, P.-G. Reinhard, and F.-K. Thielemann (2012), “Have superheavy elements been produced in nature?” *Eur. Phys. J. A* **48**, 122.
- Pfeiffer, B, K. L. Kratz, and F. K. Thielemann (1997), “Analysis of the solar-system r-process abundance pattern with the new ETFSI-Q mass formula,” *Zeitschrift für Phys. A Hadron. Nucl.* **357**, 235–238.
- Pfeiffer, B, K.-L. Kratz, F.-K. Thielemann, and W. B. Walters (2001), “Nuclear structure studies for the astrophysical r-process,” *Nucl. Phys. A* **693**, 282–324.
- Pian, E, *et al.* (2017), “Spectroscopic identification of r-process nucleosynthesis in a double neutron-star merger,” *Nature* **551**, 67–70.
- Pinto, P A, and R. G. Eastman (2000a), “The Physics of Type IA Supernova Light Curves. I. Analytic Results and Time Dependence,” *Astrophys. J.* **530**, 744–756.
- Pinto, P A, and R. G. Eastman (2000b), “The Physics of Type IA Supernova Light Curves. II. Opacity and Diffusion,” *Astrophys. J.* **530**, 757–776.
- Piran, T (2004), “The physics of gamma-ray bursts,” *Rev. Mod. Phys.* **76**, 1143–1210.
- Piran, T, E. Nakar, and S. Rosswog (2013), “The electromagnetic signals of compact binary mergers,” *Mon. Not. Roy. Astron. Soc.* **430**, 2121–2136.
- Pitrou, C, A. Coc, J.-P. Uzan, and E. Vangioni (2018), “Precision big bang nucleosynthesis with improved Helium-4 predictions,” *Phys. Rep.* **754**, 1–66.
- Placco, V M, E. M. Holmbeck, A. Frebel, T. C. Beers, R. A. Surman, A. P. Ji, R. Ezzeddine, S. D. Points, C. C. Kaleida, T. T. Hansen, C. M. Sakari, and A. R. Casey (2017), “RAVE J203843.2-002333: The First Highly R-process-enhanced Star Identified in the RAVE Survey,” *Astrophys. J.* **844**, 18.
- Pllumbi, Else, Irene Tamborra, Shinya Wanajo, Hans-Thomas Janka, and Lorenz Hudepohl (2015), “Impact of Neutrino Flavor Oscillations on the Neutrino-driven Wind Nucleosynthesis of an Electron-capture Supernova,” *Astrophys. J.* **808**, 188.
- Potel, G, F. M. Nunes, and I. J. Thompson (2015), “Establishing a theory for deuteron-induced surrogate reactions,” *Phys. Rev. C* **92**, 034611.
- Prantzos, N (2012), “Production and evolution of Li, Be, and B isotopes in the Galaxy,” *Astron. & Astrophys.* **542**, A67.
- Price, D J, and S. Rosswog (2006), “Producing Ultrastrong Magnetic Fields in Neutron Star Mergers,” *Science* **312**, 719–722.
- Pruet, J, R. D. Hoffman, S. E. Woosley, H.-T. Janka, and R. Buras (2006), “Nucleosynthesis in Early Supernova Winds II: The Role of Neutrinos,” *Astrophys. J.* **644**, 1028–1039.
- Pruet, J, T. A. Thompson, and R. D. Hoffman (2004), “Nucleosynthesis in Outflows from the Inner Regions of Collapsars,” *Astrophys. J.* **606**, 1006–1018.
- Pruet, J, S. E. Woosley, and R. D. Hoffman (2003), “Nucleosynthesis in Gamma-Ray Burst Accretion Disks,” *Astrophys. J.* **586**, 1254–1261.
- Qian, Y Z, W. C. Haxton, K. Langanke, and P. Vogel (1997), “Neutrino-induced neutron spallation and supernova r-process nucleosynthesis,” *Phys. Rev. C* **55**, 1532–1544.
- Qian, Y-Z, P. Vogel, and G. J. Wasserburg (1998), “Supernovae as the Site of the r-Process: Implications for Gamma-

- Ray Astronomy,” *Astrophys. J.* **506**, 868–873.
- Qian, Y-Z, P. Vogel, and G. J. Wasserburg (1999), “Probing r-Process Production of Nuclei Beyond ^{209}Bi with Gamma Rays,” *Astrophys. J.* **524**, 213–219.
- Qian, Y-Z, and G. J. Wasserburg (2007), “Where, oh where has the r-process gone?” *Phys. Rep.* **442**, 237–268.
- Qian, Y-Z, and S. E. Woosley (1996), “Nucleosynthesis in Neutrino-driven Winds. I. The Physical Conditions,” *Astrophys. J.* **471**, 331–351.
- Qian, Yong-Zhong (2014), “Diverse, massive-star-associated sources for elements heavier than Fe and the roles of neutrinos,” *J. Phys. G: Nucl. Part. Phys.* **41**, 044002.
- Quinn, M, *et al.* (2012), “ β decay of nuclei around ^{90}Se : Search for signatures of a $N=56$ subshell closure relevant to the r process,” *Phys. Rev. C* **85**, 035807.
- Radice, D, F. Galeazzi, J. Lippuner, L. F. Roberts, C. D. Ott, and L. Rezzolla (2016), “Dynamical mass ejection from binary neutron star mergers,” *Mon. Not. Roy. Astron. Soc.* **460**, 3255–3271.
- Radice, D, A. Perego, K. Hotokezaka, S. Bernuzzi, S. A. Fromm, and L. F. Roberts (2018a), “Viscous-dynamical Ejecta from Binary Neutron Star Mergers,” *Astrophys. J. Lett.* **869**, L35.
- Radice, D, A. Perego, K. Hotokezaka, S. A. Fromm, S. Bernuzzi, and L. F. Roberts (2018b), “Binary Neutron Star Mergers: Mass Ejection, Electromagnetic Counterparts, and Nucleosynthesis,” *Astrophys. J.* **869**, 130.
- Radice, David, Sebastiano Bernuzzi, and Albino Perego (2020), “The Dynamics of Binary Neutron Star Mergers and of GW170817,” arXiv e-prints [arXiv:2002.03863](https://arxiv.org/abs/2002.03863) [[astro-ph.HE](https://arxiv.org/abs/2002.03863)].
- Radon, T, *et al.* (2000), “Schottky mass measurements of stored and cooled neutron-deficient projectile fragments in the element range of $57 \leq Z \leq 84$,” *Nucl. Phys. A* **677**, 75–99.
- Radziūte, Laima, Gediminas Gaigalas, Daiji Kato, Pavel Rynkun, and Masaomi Tanaka (2020), “Extended calculations of energy levels and transition rates for singly ionized lanthanide elements I: Pr - Gd,” arXiv e-prints [arXiv:2002.08075](https://arxiv.org/abs/2002.08075) [[physics.atom-ph](https://arxiv.org/abs/2002.08075)].
- Raman, S, B. Fogelberg, J. A. Harvey, R. L. Macklin, P. H. Stelson, A. Schröder, and K.-L. Kratz (1983), “Overlapping beta decay and resonance neutron spectroscopy of levels in ^{87}Kr ,” *Phys. Rev. C* **28**, 602–622.
- Ramirez-Ruiz, E, M. Trenti, M. MacLeod, L. F. Roberts, W. H. Lee, and M. I. Saladino-Rosas (2015), “Compact Stellar Binary Assembly in the First Nuclear Star Clusters and r-process Synthesis in the Early Universe,” *Astrophys. J.* **802**, L22.
- Rauscher, T (2011), “The Path to Improved Reaction Rates for Astrophysics,” *Int. J. Mod. Phys. E* **20**, 1071–1169.
- Rauscher, T (2013), “Suppression of excited-state contributions to stellar reaction rates,” *Phys. Rev. C* **88**, 035803.
- Rauscher, T, R. Bieber, H. Oberhummer, K. L. Kratz, J. Dobaczewski, P. Möller, and M. M. Sharma (1998), “Dependence of direct neutron capture on nuclear-structure models,” *Phys. Rev. C* **57**, 2031–2039.
- Rauscher, T, N. Dauphas, I. Dillmann, C. Fröhlich, Z. Fülöp, and G. Gyürky (2013), “Constraining the astrophysical origin of the p-nuclei through nuclear physics and meteoritic data,” *Rep. Prog. Phys.* **76**, 066201.
- Rauscher, T, and F.-K. Thielemann (2000), “Astrophysical Reaction Rates From Statistical Model Calculations,” *At. Data Nucl. Data Tables* **75**, 1–351.
- Rauscher, T, and F.-K. Thielemann (2001), “Tables of Nuclear Cross Sections and Reaction Rates: AN Addendum to the Paper “ASTROPHYSICAL Reaction Rates from Statistical Model Calculations” (),” *At. Data Nucl. Data Tables* **79**, 47–64, [nucl-th/0104003](https://arxiv.org/abs/nucl-th/0104003).
- Rauscher, T, F.-K. Thielemann, and K.-L. Kratz (1997), “Nuclear level density and the determination of thermonuclear rates for astrophysics,” *Phys. Rev. C* **56**, 1613–1625.
- Rauscher, Thomas (2008), “Astrophysical relevance of γ transition energies,” *Phys. Rev. C* **78**, 032801.
- Ravn, H L, S. Sundell, and L. Westgaard (1975), “Target Techniques for the isolate on-line isotope separator,” *Nuclear Instruments and Methods* **123**, 131–144.
- Recchi, S, F. Calura, and P. Kroupa (2009), “The chemical evolution of galaxies within the IGIMF theory: the $[\alpha/\text{Fe}]$ ratios and downsizing,” *Astron. & Astrophys.* **499**, 711–722, [0903.2395](https://arxiv.org/abs/0903.2395).
- Recchi, S, F. Matteucci, and A. D’Ercole (2001), “Dynamical and chemical evolution of gas-rich dwarf galaxies,” *Mon. Not. Roy. Astron. Soc.* **322**, 800–820.
- Reddy, B E, D. L. Lambert, and C. Allende Prieto (2006), “Elemental abundance survey of the Galactic thick disc,” *Mon. Not. Roy. Astron. Soc.* **367**, 1329–1366.
- Reddy, B E, J. Tomkin, D. L. Lambert, and C. Allende Prieto (2003), “The chemical compositions of Galactic disc F and G dwarfs,” *Mon. Not. Roy. Astron. Soc.* **340**, 304–340.
- Rehse, S J, R. Li, T. J. Scholl, A. Sharikova, R. Chate-lain, R. A. Holt, and S. D. Rosner (2006), “Fast-ion-beam laser-induced-fluorescence measurements of spontaneous-emission branching ratios and oscillator strengths in SmII,” *Canadian Journal of Physics* **84**, 723–771.
- Reichert, M, M. Obergaulinger, and A. Arcones (2019), “r-process in magneto-rotational supernova explosions,” in preparation.
- Reifarth, R, K. Göbel, T. Heftrich, M. Weigand, B. Jurado, F. Käppeler, and Y. A. Litvinov (2017), “Spallation-based neutron target for direct studies of neutron-induced reactions in inverse kinematics,” *Phys. Rev. Accel. Beams* **20**, 044701.
- Reifarth, R, C. Lederer, and F. Käppeler (2014), “Neutron reactions in astrophysics,” *J. Phys. G: Nucl. Part. Phys.* **41**, 053101.
- Reifarth, R, and Y. A. Litvinov (2014), “Measurements of neutron-induced reactions in inverse kinematics,” *Phys. Rev. Accel. Beams* **17**, 014701.
- Reiter, M P, *et al.* (2020), “Mass measurements of neutron-rich gallium isotopes refine production of nuclei of the first r-process abundance peak in neutron-star merger calculations,” *Phys. Rev. C* **101**, 025803.
- Rembges, F, C. Freiburghaus, T. Rauscher, F.-K. Thielemann, H. Schatz, and M. Wiescher (1997), “An Approximation for the rp-Process,” *Astrophys. J.* **484**, 412–423.
- Renaud, M, J. Vink, A. Decourchelle, F. Lebrun, P. R. den Hartog, R. Terrier, C. Couvreur, J. Knödseder, P. Martin, N. Prantzos, A. M. Bykov, and H. Bloemen (2006), “The Signature of ^{44}Ti in Cassiopeia A Revealed by IBIS/ISGRI on INTEGRAL,” *Astrophys. J. Lett.* **647**, L41–L44.
- Rezzolla, Luciano, Elias R. Most, and Lukas R. Weih (2018), “Using Gravitational-wave Observations and Quasi-universal Relations to Constrain the Maximum Mass of Neutron Stars,” *Astrophys. J.* **852**, L25.
- Richers, S, H. Nagakura, C. D. Ott, J. Dolence, K. Sumiyoshi, and S. Yamada (2017), “A Detailed Comparison of Multidimensional Boltzmann Neutrino Transport Methods in

- Core-collapse Supernovae,” *Astrophys. J.* **847**, 133.
- Ripley, J L, B. D. Metzger, A. Arcones, and G. Martínez-Pinedo (2014), “X-ray decay lines from heavy nuclei in supernova remnants as a probe of the r-process origin and the birth periods of magnetars,” *Mon. Not. Roy. Astron. Soc.* **438**, 3243–3254.
- Roberts, L F (2012), “A New Code for Proto-neutron Star Evolution,” *Astrophys. J.* **755**, 126.
- Roberts, L F, J. Lippuner, M. D. Duez, J. A. Faber, F. Foucart, J. C. Lombardi, Jr., S. Ning, C. D. Ott, and M. Ponce (2017), “The influence of neutrinos on r-process nucleosynthesis in the ejecta of black hole-neutron star mergers,” *Mon. Not. Roy. Astron. Soc.* **464**, 3907–3919.
- Roberts, L F, S. Reddy, and G. Shen (2012), “Medium modification of the charged-current neutrino opacity and its implications,” *Phys. Rev. C* **86**, 065803.
- Roberts, L F, G. Shen, V. Cirigliano, J. A. Pons, S. Reddy, and S. E. Woosley (2012), “Proton-neutron star cooling with convection: The effect of the symmetry energy,” *Phys. Rev. Lett.* **108**, 061103.
- Roberts, L F, S. E. Woosley, and R. D. Hoffman (2010), “Integrated Nucleosynthesis in Neutrino-driven Winds,” *Astrophys. J.* **722**, 954–967.
- Roberts, Luke F, Dan Kasen, William H. Lee, and Enrico Ramirez-Ruiz (2011), “Electromagnetic Transients Powered by Nuclear Decay in the Tidal Tails of Coalescing Compact Binaries,” *Astrophys. J.* **736**, L21.
- Roberts, Luke F, and Sanjay Reddy (2017), “Charged current neutrino interactions in hot and dense matter,” *Phys. Rev. C* **95**, 045807.
- Rodríguez, Tomás R, Alexander Arzhanov, and Gabriel Martínez-Pinedo (2015), “Toward global beyond-mean-field calculations of nuclear masses and low-energy spectra,” *Phys. Rev. C* **91**, 044315.
- Roederer, I U (2013), “Are There Any Stars Lacking Neutron-capture Elements? Evidence from Strontium and Barium,” *Astron. J.* **145**, 26.
- Roederer, I U (2017), “The Origin of the Heaviest Metals in Most Ultra-faint Dwarf Galaxies,” *Astrophys. J.* **835**, 23.
- Roederer, I U, J. J. Cowan, A. I. Karakas, K.-L. Kratz, M. Lugaro, J. Simmerer, K. Farouqi, and C. Sneden (2010a), “The Ubiquity of the Rapid Neutron-capture Process,” *Astrophys. J.* **724**, 975–993.
- Roederer, I U, A. I. Karakas, M. Pignatari, and F. Herwig (2016), “The Diverse Origins of Neutron-capture Elements in the Metal-poor Star HD 94028: Possible Detection of Products of i-Process Nucleosynthesis,” *Astrophys. J.* **821**, 37.
- Roederer, I U, K.-L. Kratz, A. Frebel, N. Christlieb, B. Pfeiffer, J. J. Cowan, and C. Sneden (2009), “The End of Nucleosynthesis: Production of Lead and Thorium in the Early Galaxy,” *Astrophys. J.* **698**, 1963–1980.
- Roederer, I U, and J. E. Lawler (2012), “Detection of Elements at All Three r-process Peaks in the Metal-poor Star HD 160617,” *Astrophys. J.* **750**, 76.
- Roederer, I U, J. E. Lawler, J. J. Cowan, T. C. Beers, A. Frebel, I. I. Ivans, H. Schatz, J. S. Sobeck, and C. Sneden (2012), “Detection of the Second r-process Peak Element Tellurium in Metal-poor Stars,” *Astrophys. J. Suppl.* **747**, L8.
- Roederer, I U, H. Schatz, J. E. Lawler, T. C. Beers, J. J. Cowan, A. Frebel, I. I. Ivans, C. Sneden, and J. S. Sobeck (2014a), “New Detections of Arsenic, Selenium, and Other Heavy Elements in Two Metal-poor Stars,” *Astrophys. J.* **791**, 32.
- Roederer, I U, C. Sneden, J. E. Lawler, and J. J. Cowan (2010b), “New Abundance Determinations of Cadmium, Lutetium, and Osmium in the r-process Enriched Star BD +17 3248,” *Astrophys. J.* **714**, L123–L127.
- Roederer, Ian U, Kohei Hattori, and Monica Valluri (2018), “Kinematics of Highly r-process-enhanced Field Stars: Evidence for an Accretion Origin and Detection of Several Groups from Disrupted Satellites,” *Astron. J.* **156**, 179.
- Roederer, Ian U, George W. Preston, Ian B. Thompson, Stephen A. Shtetman, Christopher Sneden, Gregory S. Burley, and Daniel D. Kelson (2014b), “A Search for Stars of Very Low Metal Abundance. VI. Detailed Abundances of 313 Metal-poor Stars,” *Astron. J.* **147**, 136.
- Rolfs, CE, and W.S. Rodney (1988), *Cauldrons in the Cosmos: Nuclear Astrophysics* (University of Chicago Press, Chicago).
- Rosswog, S (2005), “Mergers of Neutron Star-Black Hole Binaries with Small Mass Ratios: Nucleosynthesis, Gamma-Ray Bursts, and Electromagnetic Transients,” *Astrophys. J.* **634**, 1202–1213.
- Rosswog, S (2007), “Fallback accretion in the aftermath of a compact binary merger,” *Mon. Not. Roy. Astron. Soc.* **376**, L48–L51.
- Rosswog, S, M. B. Davies, F.-K. Thielemann, and T. Piran (2000), “Merging neutron stars: asymmetric systems,” *Astron. & Astrophys.* **360**, 171–184.
- Rosswog, S, U. Feindt, O. Korobkin, M.-R. Wu, J. Sollerman, A. Goobar, and G. Martínez-Pinedo (2017), “Detectability of compact binary merger macronovae,” *Class. Quantum Gravity* **34**, 104001.
- Rosswog, S, O. Korobkin, A. Arcones, F.-K. Thielemann, and T. Piran (2014), “The long-term evolution of neutron star merger remnants - I. The impact of r-process nucleosynthesis,” *Mon. Not. Roy. Astron. Soc.* **439**, 744–756.
- Rosswog, S, M. Liebendörfer, F.-K. Thielemann, M. B. Davies, W. Benz, and T. Piran (1999), “Mass ejection in neutron star mergers,” *Astron. & Astrophys.* **341**, 499–526.
- Rosswog, S, J. Sollerman, U. Feindt, A. Goobar, O. Korobkin, R. Wollaeger, C. Fremling, and M. M. Kasliwal (2018), “The first direct double neutron star merger detection: Implications for cosmic nucleosynthesis,” *Astron. & Astrophys.* **615**, A132.
- Rosswog, Stephan (2015), “The multi-messenger picture of compact binary mergers,” *Int. J. Mod. Phys. D* **24**, 1530012.
- Rrapaj, Ermal, J. W. Holt, Alexander Bartl, Sanjay Reddy, and A. Schwenk (2015), “Charged-current reactions in the supernova neutrino-sphere,” *Phys. Rev. C* **91**, 035806.
- Ruffert, M, and H.-T. Janka (2001), “Coalescing neutron stars - A step towards physical models. III. Improved numerics and different neutron star masses and spins,” *Astron. & Astrophys.* **380**, 544–577.
- Ruffert, M, H.-T. Janka, and G. Schaefer (1996), “Coalescing neutron stars - a step towards physical models. I. Hydrodynamic evolution and gravitational-wave emission.” *Astron. & Astrophys.* **311**, 532–566.
- Ruffert, M, H.-T. Janka, K. Takahashi, and G. Schaefer (1997), “Coalescing neutron stars - a step towards physical models. ii. neutrino emission, neutron tori, and gamma-ray bursts.” *Astron. & Astrophys.* **319**, 122–153.
- Ruiz, Milton, Stuart L. Shapiro, and Antonios Tsokaros (2018), “Gw170817, general relativistic magnetohydrodynamic simulations, and the neutron star maximum mass,”

- Phys. Rev. D* **97**, 021501.
- Sadhukhan, J, W. Nazarewicz, and N. Schunck (2016), “Microscopic modeling of mass and charge distributions in the spontaneous fission of ^{240}Pu ,” *Phys. Rev. C* **93**, 011304.
- Sadhukhan, Jhilm, Samuel A. Giuliani, Zachary Matheson, and Witold Nazarewicz (2020), “Efficient method for estimation of fission fragment yields of r-process nuclei,” arXiv e-prints [arXiv:2001.08616 \[nucl-th\]](https://arxiv.org/abs/2001.08616).
- Sadhukhan, Jhilm, K. Mazurek, A. Baran, J. Dobaczewski, W. Nazarewicz, and J. A. Sheikh (2013), “Spontaneous fission lifetimes from the minimization of self-consistent collective action,” *Phys. Rev. C* **88**, 064314.
- Safarzadeh, Mohammadtaher, Enrico Ramirez-Ruiz, Jeff. J. Andrews, Phillip Macias, Tassos Fragos, and Evan Scannapieco (2019), “r-process Enrichment of the Ultra-faint Dwarf Galaxies by Fast-merging Double-neutron Stars,” *Astrophys. J.* **872**, 105.
- Sagert, I, T. Fischer, M. Hempel, G. Pagliara, J. Schaffner-Bielich, A. Mezzacappa, F.-K. Thielemann, and M. Liebendörfer (2009), “Signals of the QCD Phase Transition in Core-Collapse Supernovae,” *Phys. Rev. Lett.* **102**, 081101.
- Sakari, Charli M, *et al.* (2018), “The R-Process Alliance: First Release from the Northern Search for r-process-enhanced Metal-poor Stars in the Galactic Halo,” *Astrophys. J.* **868**, 110.
- Salih, S, and J. E. Lawler (1983), “Pulsed ion source for laser spectroscopy: Application to Nb ii p,” *Phys. Rev. A* **28**, 3653–3655.
- Sato, K (1974), “Formation of Elements in Neutron Rich Ejected Matter of Supernovae. II —Dynamical r-Process Stage—,” *Progress of Theoretical Physics* **51**, 726–744.
- Schäfer, F P, W. Schmidt, and J. Volze (1966), “Organic Dye Solution Laser,” *Appl. Phys. Lett.* **9**, 306–309.
- Schatz, H, R. Toenjes, B. Pfeiffer, T. C. Beers, J. J. Cowan, V. Hill, and K.-L. Kratz (2002), “Thorium and Uranium Chronometers Applied to CS 31082-001,” *Astrophys. J.* **579**, 626–638.
- Schiller, A, L. Bergholt, M. Guttormsen, E. Melby, J. Rektstad, and S. Siem (2000), “Extraction of level density and γ strength function from primary γ spectra,” *Nucl. Instruments Methods Phys. Res. Sect. A Accel. Spectrometers, Detect. Assoc. Equip.* **447**, 498–511.
- Schmidt, K-H H, B. Jurado, C. Amouroux, and C. Schmitt (2016), “General Description of Fission Observables: GEF Model Code,” *Nucl. Data Sheets* **131**, 107–221.
- Schmidt, Karl-Heinz, and Beatriz Jurado (2018), “Review on the progress in nuclear fission—experimental methods and theoretical descriptions,” *Rep. Prog. Phys.* **81**, 106301.
- Schmitt, C, K.-H. Schmidt, and B. Jurado (2018), “Benchmark of the GEF code for fission-fragment yields over an enlarged range in fissioning nucleus mass, excitation energy, and angular momentum,” *Phys. Rev. C* **98**, 044605.
- Schönrich, Ralph A, and David H. Weinberg (2019), “The chemical evolution of r-process elements from neutron star mergers: the role of a 2-phase interstellar medium,” *Mon. Not. Roy. Astron. Soc.* **487**, 580–594.
- Schramm, D N (1973), “Explosive r-PROCESS Nucleosynthesis,” *Astrophys. J.* **185**, 293–302.
- Schramm, D N, and G. J. Wasserburg (1970), “Nucleochronologies and the Mean Age of the Elements,” *Astrophys. J.* **162**, 57.
- Schwengner, R, S. Frauendorf, and B. A. Brown (2017), “Low-Energy Magnetic Dipole Radiation in Open-Shell Nuclei,” *Phys. Rev. Lett.* **118**, 092502.
- Schwengner, R, S. Frauendorf, and A. C. Larsen (2013), “Low-Energy Enhancement of Magnetic Dipole Radiation,” *Phys. Rev. Lett.* **111**, 232504.
- Seeger, P A, W. A. Fowler, and D. D. Clayton (1965), “Nucleosynthesis of Heavy Elements by Neutron Capture,” *Astrophys. J. Suppl.* **11**, 121–166.
- Seitenzahl, I R, P. Ghavamian, J. M. Laming, and F. P. A. Vogt (2019), “Optical Tomography of Chemical Elements Synthesized in Type Ia Supernovae,” *prl* **123**, 041101.
- Seitenzahl, I R, F. X. Timmes, and G. Magkotsios (2014), “The Light Curve of SN 1987A Revisited: Constraining Production Masses of Radioactive Nuclides,” *Astrophys. J.* **792**, 10.
- Seitenzahl, IR, and D.M. Townsley (2017), “Nucleosynthesis in Thermonuclear Supernovae,” in *Handbook of Supernovae*, edited by A. W. Alsabti and P. Murdin (Springer International Publishing, Cham).
- Sekiguchi, Y, K. Kiuchi, K. Kyutoku, and M. Shibata (2015), “Dynamical mass ejection from binary neutron star mergers: Radiation-hydrodynamics study in general relativity,” *Phys. Rev. D* **91**, 064059.
- Sekiguchi, Y, K. Kiuchi, K. Kyutoku, M. Shibata, and K. Taniguchi (2016), “Dynamical mass ejection from the merger of asymmetric binary neutron stars: Radiation-hydrodynamics study in general relativity,” *Phys. Rev. D* **93**, 124046.
- Sekiguchi, Y, and M. Shibata (2011), “Formation of Black Hole and Accretion Disk in a Massive High-entropy Stellar Core Collapse,” *Astrophys. J.* **737**, 6.
- Sekiguchi, Yuichiro, Kenta Kiuchi, Koutarou Kyutoku, and Masaru Shibata (2011), “Gravitational waves and neutrino emission from the merger of binary neutron stars,” *Phys. Rev. Lett.* **107**, 051102.
- Shafer, T, J. Engel, C. Fröhlich, G. C. McLaughlin, M. Mumpower, and R. Surman (2016), “ β decay of deformed r-process nuclei near $a = 80$ and $a = 160$, including odd- a and odd-odd nuclei, with the skyrme finite-amplitude method,” *Phys. Rev. C* **94**, 055802.
- Shen, S, R. J. Cooke, E. Ramirez-Ruiz, P. Madau, L. Mayer, and J. Guedes (2015), “The History of R-Process Enrichment in the Milky Way,” *Astrophys. J.* **807**, 115.
- Shetrone, M, K. A. Venn, E. Tolstoy, F. Primas, V. Hill, and A. Kaufer (2003), “VLT/UVES Abundances in Four Nearby Dwarf Spheroidal Galaxies. I. Nucleosynthesis and Abundance Ratios,” *Astron. J.* **125**, 684–706.
- Shetrone, M D, M. Bolte, and P. B. Stetson (1998), “Keck HIRES Abundances in the Dwarf Spheroidal Galaxy Draco,” *Astron. J.* **115**, 1888–1893.
- Shibagaki, S, T. Kajino, G. J. Mathews, S. Chiba, S. Nishimura, and G. Lorusso (2016), “Relative Contributions of the Weak, Main, and Fission-recycling r-process,” *Astrophys. J.* **816**, 79.
- Shibata, M, and K. Taniguchi (2011), “Coalescence of Black Hole-Neutron Star Binaries,” *Living Reviews in Relativity* **14**, 6.
- Shibata, Masaru (2018), “Mass ejection from neutron star mergers,” Talk at the EMMI Rapid Reaction Task Force: The physics of neutron star mergers at GSI/FAIR.
- Shibata, Masaru, Sho Fujibayashi, Kenta Hotokezaka, Kenta Kiuchi, Koutarou Kyutoku, Yuichiro Sekiguchi, and Masaomi Tanaka (2017), “Modeling GW170817 based on numerical relativity and its implications,” *Phys. Rev. D* **96**, 123012.

- Shibata, Masaru, and Kenta Hotokezaka (2019), “Merger and Mass Ejection of Neutron Star Binaries,” *Annu. Rev. Nucl. Part. Sci.* **69**, 41–64.
- Shibata, Masaru, and Keisuke Taniguchi (2006), “Merger of binary neutron stars to a black hole: Disk mass, short gamma-ray bursts, and quasinormal mode ringing,” *Phys. Rev. D* **73**, 064027.
- Shibata, Masaru, Keisuke Taniguchi, and Kōji Uryū (2005), “Merger of binary neutron stars with realistic equations of state in full general relativity,” *Phys. Rev. D* **71**, 084021.
- Shibata, Masaru, and Kōji Uryū (2000), “Simulation of merging binary neutron stars in full general relativity: $\Gamma = 2$ case,” *Phys. Rev. D* **61**, 064001.
- Shibata, Masaru, and Kōji Uryū (2006), “Merger of black hole-neutron star binaries: Nonspinning black hole case,” *Phys. Rev. D* **74**, 121503.
- Siegel, D M, and B. D. Metzger (2018), “Three-dimensional GRMHD Simulations of Neutrino-cooled Accretion Disks from Neutron Star Mergers,” *Astrophys. J.* **858**, 52.
- Siegel, Daniel M (2019), “GW170817 –the first observed neutron star merger and its kilonova: Implications for the astrophysical site of the r-process,” *Eur. Phys. J. A* **55**, 203.
- Siegel, Daniel M, Jennifer Barnes, and Brian D. Metzger (2019), “Collapsars as a major source of r-process elements,” *Nature* **569**, 241–244.
- Siegel, Daniel M, Riccardo Ciolfi, and Luciano Rezzolla (2014), “Magnetically Driven Winds from Differentially Rotating Neutron Stars and X-Ray Afterglows of Short Gamma-Ray Bursts,” *Astrophys. J. Lett.* **785**, L6.
- Siegel, Daniel M, and Brian D. Metzger (2017), “Three-Dimensional General-Relativistic Magnetohydrodynamic Simulations of Remnant Accretion Disks from Neutron Star Mergers: Outflows and r -Process Nucleosynthesis,” *Phys. Rev. Lett.* **119**, 231102.
- Siegl, K, *et al.* (2018), “Recoil ions from the β decay of ^{134}Sb confined in a Paul trap,” *Phys. Rev. C* **97** (3), 035504.
- Sieja, K (2017), “Electric and Magnetic Dipole Strength at Low Energy,” *Phys. Rev. Lett.* **119**, 052502.
- Sieja, K (2018), “Shell-model study of the $M1$ dipole strength at low energy in the $A > 100$ nuclei,” *Phys. Rev. C* **98**, 064312.
- Sieverding, A, K. Langanke, G. Martínez-Pinedo, R. Bollig, H. T. Janka, and A. Heger (2019), “The ν -process with Fully Time-dependent Supernova Neutrino Emission Spectra,” *Astrophys. J.* **876**, 151.
- Simmerer, J, C. Sneden, J. J. Cowan, J. Collier, V. M. Woolf, and J. E. Lawler (2004), “The Rise of the s-Process in the Galaxy,” *Astrophys. J.* **617**, 1091–1114.
- Simon, Joshua D (2019), “The Faintest Dwarf Galaxies,” *Annu. Rev. Astron. Astrophys.* **57**, 375–415.
- Simonetti, Paolo, Francesca Matteucci, Laura Greggio, and Gabriele Cescutti (2019), “A new delay time distribution for merging neutron stars tested against Galactic and cosmic data,” *Mon. Not. Roy. Astron. Soc.* **486**, 2896–2909.
- Siqueira Mello, C, M. Spite, B. Barbuy, F. Spite, E. Caffau, V. Hill, S. Wanajo, F. Primas, B. Plez, R. Cayrel, J. Andersen, B. Nordström, C. Sneden, T. C. Beers, P. Bonifacio, P. François, and P. Molaro (2013), “First stars. XVI. HST/STIS abundances of heavy elements in the uranium-rich metal-poor star CS 31082-001,” *Astron. & Astrophys.* **550**, A122.
- Skúladóttir, Á, C. J. Hansen, S. Salvadori, and A. Choplin (2019), “Neutron-capture elements in dwarf galaxies. I. Chemical clocks and the short timescale of the r-process,” *Astron. & Astrophys.* **631**, A171.
- Skúladóttir, Á, and S. Salvadori (2020), “Evidence for $\gtrsim 4$ Gyr timescales of neutron star mergers from Galactic archaeology,” *Astron. & Astrophys.* **634**, L2.
- Smartt, S J, *et al.* (2017), “A kilonova as the electromagnetic counterpart to a gravitational-wave source,” *Nature* **551**, 75–79.
- Sneden, C, J. J. Cowan, and R. Gallino (2008), “Neutron-Capture Elements in the Early Galaxy,” *Annu. Rev. Astron. Astrophys.* **46**, 241–288.
- Sneden, C, J. J. Cowan, J. E. Lawler, I. I. Ivans, S. Burles, T. C. Beers, F. Primas, V. Hill, J. W. Truran, G. M. Fuller, B. Pfeiffer, and K.-L. Kratz (2003), “The Extremely Metal-poor, Neutron Capture-rich Star CS 22892-052: A Comprehensive Abundance Analysis,” *Astrophys. J.* **591**, 936–953.
- Sneden, C, J. E. Lawler, J. J. Cowan, I. I. Ivans, and E. A. Den Hartog (2009), “New Rare Earth Element Abundance Distributions for the Sun and Five r-Process-Rich Very Metal-Poor Stars,” *Astrophys. J. Suppl.* **182**, 80–96.
- Sneden, C, A. McWilliam, G. W. Preston, J. J. Cowan, D. L. Burris, and B. J. Armosky (1996), “The Ultra-Metal-poor, Neutron-Capture-rich Giant Star CS 22892-052,” *Astrophys. J.* **467**, 819.
- Sneden, C, and M. Parthasarathy (1983), “The r- and s-process nuclei in the early history of the galaxy - HD 122563,” *Astrophys. J.* **267**, 757–778.
- Sneden, C, G. W. Preston, A. McWilliam, and L. Searle (1994), “Ultrametal-poor halo stars: The remarkable spectrum of CS 22892-052,” *Astrophys. J. Lett.* **431**, L27–L30.
- Sneden, Christopher, and John J. Cowan (2003), “Genesis of the Heaviest Elements in the Milky Way Galaxy,” *Science* **299**, 70–75.
- Soares-Santos, M, *et al.* (2017), “The Electromagnetic Counterpart of the Binary Neutron Star Merger LIGO/Virgo GW170817. I. Discovery of the Optical Counterpart Using the Dark Energy Camera,” *Astrophys. J. Lett.* **848**, L16.
- Söderström, P-A, *et al.* (2013), “Installation and commissioning of EURICA - Euroball-RIKEN Cluster Array,” *Nucl. Instruments Methods Phys. Res. Sect. B Beam Interact. with Mater. Atoms* **317**, 649–652.
- Sørensen, M, H. Svensmark, and U. Gråe Jørgensen (2017), “Near-Earth supernova activity during the past 35 Myr,” ArXiv e-prints [arXiv:1708.08248](https://arxiv.org/abs/1708.08248) [astro-ph.SR].
- Sorokin, P P, and J. R. Lankard (1966), “Stimulated Emission Observed from an Organic Dye Chloro-Aluminum Phthalocyanine,” *IBM Res. Develop.* **10**, 187.
- Spitoni, E, F. Matteucci, S. Recchi, G. Cescutti, and A. Pipino (2009), “Effects of galactic fountains and delayed mixing in the chemical evolution of the Milky Way,” *Astron. & Astrophys.* **504**, 87–96.
- Spyrou, A, *et al.* (2014), “Novel technique for Constraining r-Process (n, γ) Reaction Rates,” *Phys. Rev. Lett.* **113**, 232502.
- Spyrou, A, *et al.* (2017), “Neutron-capture rates for explosive nucleosynthesis: the case of $^{68}\text{Ni}(n, \gamma)^{69}\text{Ni}$,” *J. Phys. G: Nucl. Part. Phys.* **44**, 044002.
- Steinberg, E P, and B. D. Wilkins (1978), “Implications of fission mass distributions for the astrophysical r-process,” *Astrophys. J.* **223**, 1000–1014.
- Suda, Takuma, Yutaka Katsuta, Shimako Yamada, Tamon Suwa, Chikako Ishizuka, Yutaka Komiya, Kazuo Sorai, Masayuki Aikawa, and Masayuki Y. Fujimoto (2008), “Stellar Abundances for the Galactic Archeology (SAGA) Database — Compilation of the Characteristics of Known

- Extremely Metal-Poor Stars,” *Publ. Astron. Soc. Japan* **60**, 1159.
- Sukhbold, T, T. Ertl, S. E. Woosley, J. M. Brown, and H.-T. Janka (2016), “Core-collapse Supernovae from 9 to 120 Solar Masses Based on Neutrino-powered Explosions,” *Astrophys. J.* **821**, 38.
- Sumiyoshi, K, M. Terasawa, G. J. Mathews, T. Kajino, S. Yamada, and H. Suzuki (2001), “r-Process in Prompt Supernova Explosions Revisited,” *Astrophys. J.* **562**, 880–886.
- Sun, B, *et al.* (2008), “Nuclear structure studies of short-lived neutron-rich nuclei with the novel large-scale isochronous mass spectrometry at the FRS-ESR facility,” *Nucl. Phys. A* **812**, 1–12.
- Sun, B-H, and J. Meng (2008), “NUCLEAR PHYSICS: Challenge on the Astrophysical R-Process Calculation with Nuclear Mass Models,” *Chinese Phys. Lett.* **25**, 2429–2431.
- Surman, R, O. L. Caballero, G. C. McLaughlin, O. Just, and H.-T. Janka (2014), “Production of ^{56}Ni in black hole-neutron star merger accretion disc outflows,” *J. Phys. G: Nucl. Part. Phys.* **41**, 044006.
- Surman, R, J. Engel, J. R. Bennett, and B. S. Meyer (1997), “Source of the rare-earth element peak in r-process nucleosynthesis,” *Phys. Rev. Lett.* **79**, 1809–1812.
- Surman, R, G. C. McLaughlin, and W. R. Hix (2006), “Nucleosynthesis in the Outflow from Gamma-Ray Burst Accretion Disks,” *Astrophys. J.* **643**, 1057–1064.
- Surman, R, G. C. McLaughlin, M. Ruffert, H.-T. Janka, and W. R. Hix (2008), “r-Process Nucleosynthesis in Hot Accretion Disk Flows from Black Hole-Neutron Star Mergers,” *Astrophys. J.* **679**, L117.
- Suzuki, T, and T. Kajino (2013), “Element synthesis in the supernova environment and neutrino oscillations,” *J. Phys. G: Nucl. Part. Phys.* **40**, 083101.
- Suzuki, Toshio, Takashi Yoshida, Toshitaka Kajino, and Takaharu Otsuka (2012), “ β decays of isotones with neutron magic number of $n=126$ and r-process nucleosynthesis,” *Phys. Rev. C* **85**, 015802.
- Svanberg, S, J. Larsson, A. Persson, and C.-G. Wahlström (1994), “Lund high-power laser facility - systems and first results,” *Phys. Scr.* **49**, 187–197.
- Symbalisty, E, and D. N. Schramm (1982), “Neutron star collisions and the r-process,” *Astrophys. J.* **22**, 143–145.
- Symbalisty, E M D, D. N. Schramm, and J. R. Wilson (1985), “An expanding vortex site for the r-process in rotating stellar collapse,” *Astrophys. J.* **291**, L11–L14.
- Szücs, T, P. Mohr, Gy. Gyürky, Z. Halász, R. Huszánk, G. G. Kiss, T. N. Szegedi, Zs. Török, and Zs. Fülöp (2020), “Activation measurement of α -induced cross sections for ^{197}Au : analysis in the statistical model and beyond,” in *Journal of Physics: Conference Series* (IOP Publishing) to be published.
- Tachibana, T, M. Yamada, and Y. Yoshida (1990), “Improvement of the Gross Theory of β -Decay. II: One-Particle Strength Function,” *Prog. Theor. Phys.* **84**, 641–657.
- Takahashi, K, J. Wittit, and H.-Th. Janka (1994), “Nucleosynthesis in neutrino-driven winds from protoneutron stars II. The r-process,” *Astron. & Astrophys.* **286**, 857–869.
- Takiwaki, T, and K. Kotake (2011), “Gravitational Wave Signatures of Magnetohydrodynamically Driven Core-collapse Supernova Explosions,” *Astrophys. J.* **743**, 30.
- Takiwaki, T, K. Kotake, and K. Sato (2009), “Special Relativistic Simulations of Magnetically Dominated Jets in Collapsing Massive Stars,” *Astrophys. J.* **691**, 1360–1379.
- Talbert, W L, F. K. Wohn, J. C. Hill, A. R. Landin, M. A. Cullison, and R. L. Gill (1979), “Tristan II: Extension of the Tristan facility to the study of non-gaseous activities,” *Nuclear Instruments and Methods* **161**, 431–437.
- Tamborra, Irene, Bernhard Müller, Lorenz Hüdepohl, Hans-Thomas Janka, and Georg Raffelt (2012), “High-resolution supernova neutrino spectra represented by a simple fit,” *Phys. Rev. D* **86**, 125031.
- Tanaka, M (2016), “Kilonova/Macronova Emission from Compact Binary Mergers,” *Adv. Astron.* **2016**, 634197.
- Tanaka, M, D. Kato, G. Gaigalas, P. Rynkun, L. Radziūtė, S. Wanajo, Y. Sekiguchi, N. Nakamura, H. Tanuma, I. Murakami, and H. A. Sakaue (2018), “Properties of Kilonovae from Dynamical and Post-merger Ejecta of Neutron Star Mergers,” *Astrophys. J.* **852**, 109.
- Tanaka, M, *et al.* (2017), “Kilonova from post-merger ejecta as an optical and near-infrared counterpart of gw170817,” *Publ. Astron. Soc. Japan* **69**, 102.
- Tanaka, Masaomi, and Kenta Hotokezaka (2013), “Radiative Transfer Simulations of Neutron Star Merger Ejecta,” *Astrophys. J.* **775**, 113.
- Tanaka, Masaomi, Daiji Kato, Gediminas Gaigalas, and Kyohei Kawaguchi (2019), “Systematic Opacity Calculations for Kilonovae,” arXiv e-prints [arXiv:1906.08914](https://arxiv.org/abs/1906.08914) [[astro-ph.HE](https://arxiv.org/archive/hep)].
- Tang, T L, *et al.* (2020), “First exploration of neutron shell structure below lead and beyond $n = 126$,” *Phys. Rev. Lett.* **124**, 062502.
- Tanvir, N R, A. J. Levan, A. S. Fruchter, J. Hjorth, R. A. Hounsell, K. Wiersema, and R. L. Tunnicliffe (2013), “A ‘kilonova’ associated with the short-duration γ -ray burst GRB 130603B,” *Nature* **500**, 547–549.
- Tanvir, N R, *et al.* (2017), “The Emergence of a Lanthanide-rich Kilonova Following the Merger of Two Neutron Stars,” *Astrophys. J. Lett.* **848**, L27.
- Tarumi, Yuta, Naoki Yoshida, and Shigeki Inoue (2020), “r-process enrichment in ultrafaint dwarf galaxies,” *Mon. Not. Roy. Astron. Soc.* **10.1093/mnras/staa720**.
- Tauris, T M, M. Kramer, P. C. C. Freire, N. Wex, H.-T. Janka, N. Langer, P. Podsiadlowski, E. Bozzo, S. Chaty, M. U. Kruckow, E. P. J. van den Heuvel, J. Antoniadis, R. P. Breton, and D. J. Champion (2017), “Formation of Double Neutron Star Systems,” *Astrophys. J.* **846**, 170.
- Terasawa, M, K. Langanke, T. Kajino, G. J. Mathews, and E. Kolbe (2004), “Neutrino Effects before, during, and after the Freezeout of the r-Process,” *Astrophys. J.* **608**, 470–479.
- Terasawa, M, K. Sumiyoshi, T. Kajino, G. J. Mathews, and I. Tanihata (2001), “New nuclear reaction flow during r-process nucleosynthesis in supernovae: Critical role of light, neutron-rich nuclei,” *Astrophys. J.* **562**, 470–479.
- Tews, I, J. Margueron, and S. Reddy (2018), “Critical examination of constraints on the equation of state of dense matter obtained from gw170817,” *Phys. Rev. C* **98**, 045804.
- Tews, I, J. Margueron, and S. Reddy (2019), “Confronting gravitational-wave observations with modern nuclear physics constraints,” *Eur. Phys. J. A* **55**, 97.
- Thielemann, F-K, M. Arnould, and W. Hillebrandt (1979), “Meteoritic anomalies and explosive neutron processing of helium-burning shells,” *Astron. & Astrophys.* **74**, 175–185.
- Thielemann, F-K, A. G. W. Cameron, and J. J. Cowan (1989), “Fission in the Astrophysical r-Process,” in *50 Years with Nuclear Fission*, edited by J. Behrens and A.D. Carlson, p. 592.
- Thielemann, F-K, M. Eichler, I. V. Panov, M. Pignatari, and

- B. Wehmeyer (2017a), “Making the Heaviest Elements in a Rare Class of Supernovae,” in *Handbook of Supernovae*, edited by A. W. Alsabti and P. Murdin (Springer International Publishing, Cham).
- Thielemann, F-K, M. Eichler, I. V. Panov, and B. Wehmeyer (2017b), “Neutron Star Mergers and Nucleosynthesis of Heavy Elements,” *Annu. Rev. Nucl. Part. Sci.* **67**, 253–274.
- Thielemann, F-K, A. Heger, R. Hirschi, M. Liebendörfer, and R. Diehl (2018), “Massive Stars and Their Supernovae,” in *Astrophysics with Radioactive Isotopes, Berlin Springer Verlag*, Vol. 453, edited by R. Diehl, D. H. Hartmann, and N. Prantzos, pp. 173–286.
- Thielemann, F-K, R. Hirschi, M. Liebendörfer, and R. Diehl (2011), “Massive Stars and Their Supernovae,” in *Lecture Notes in Physics, Berlin Springer Verlag*, Vol. 812, edited by R. Diehl, D. H. Hartmann, and N. Prantzos, pp. 153–232.
- Thielemann, F-K, J. Metzinger, and H. V. Klapdor (1983), “Beta-delayed fission and neutron emission: Consequences for the astrophysical r-process and the age of the galaxy,” *Zeitschrift für Phys. A Hadron. Nucl.* **309**, 301–317.
- Thielemann, F-K, *et al.* (2011), “What are the astrophysical sites for the r-process and the production of heavy elements?” *Prog. Part. Nucl. Phys.* **66**, 346–353.
- Thielemann, Friedrich-Karl, Karl-Ludwig Kratz, Bernd Pfeiffer, Thomas Rauscher, Laura van Wormer, and Michael C. Wiescher (1994), “Astrophysics and nuclei far from stability,” *Nucl. Phys. A* **570**, 329–343.
- Thielemann, Friedrich-Karl, and James W. Truran (1986), “General implementation of screening effects in thermonuclear reaction rates,” in *Advances in Nuclear Astrophysics*, edited by Elisabeth Vangioni-Flam, Jean Audouze, Michel Casse, Jean-Pierre Chieze, and J. Tran Thanh Van, pp. 541–551.
- Thompson, T A, A. Burrows, and B. S. Meyer (2001), “The Physics of Proto-Neutron Star Winds: Implications for r-Process Nucleosynthesis,” *Astrophys. J.* **562**, 887–908.
- Timmes, F X (1999), “Integration of Nuclear Reaction Networks for Stellar Hydrodynamics,” *Astrophys. J. Suppl.* **124**, 241–263.
- Timmes, F X, S. E. Woosley, and T. A. Weaver (1995), “Galactic Chemical Evolution: Hydrogen through Zinc,” *Astrophys. J. Suppl.* **98**, 617.
- Tinsley, B M (1980), “Evolution of the Stars and Gas in Galaxies,” *fcp* **5**, 287–388.
- Tornyi, T G, M. Guttormsen, T. K. Eriksen, A. Görge, F. Giacoppo, T. W. Hagen, A. Krasznahorkay, A. C. Larsen, T. Renstrøm, S. J. Rose, S. Siem, and G. M. Tveten (2014), “Level density and γ -ray strength function in the odd-odd Np238 nucleus,” *Phys. Rev. C* **89**, 044323.
- Travaglio, C, D. Galli, R. Gallino, M. Busso, F. Ferrini, and O. Straniero (1999), “Galactic Chemical Evolution of Heavy Elements: From Barium to Europium,” *Astrophys. J.* **521**, 691–702.
- Travaglio, C, R. Gallino, E. Arnone, J. Cowan, F. Jordan, and C. Sneden (2004), “Galactic Evolution of Sr, Y, and Zr: A Multiplicity of Nucleosynthetic Processes,” *Astrophys. J.* **601**, 864–884.
- Travaglio, C, T. Rauscher, A. Heger, M. Pignatari, and C. West (2018), “Role of Core-collapse Supernovae in Explaining Solar System Abundances of p Nuclides,” *Astrophys. J.* **854**, 18, 1801.01929 [astro-ph.SR].
- Truran, J W, J. J. Cowan, and A. G. W. Cameron (1978), “The helium-driven r-process in supernovae,” *Astrophys. J.* **222**, L63–L67.
- Tsujimoto, T, and T. Shigeyama (2014), “Enrichment history of r-process elements shaped by a merger of neutron star pairs,” *Astron. & Astrophys.* **565**, L5.
- Tsujimoto, T, Y. Yoshii, K. Nomoto, F. Matteucci, F.-K. Thielemann, and M. Hashimoto (1997), “A New Approach to Determine the Initial Mass Function in the Solar Neighborhood,” *Astrophys. J.* **483**, 228–234.
- Ural, U, G. Cescutti, A. Koch, J. Kleyna, S. Feltzing, and M. I. Wilkinson (2015), “An inefficient dwarf: chemical abundances and the evolution of the Ursa Minor dwarf spheroidal galaxy,” *Mon. Not. Roy. Astron. Soc.* **449**, 761–770.
- van de Voort, F, E. Quataert, P. F. Hopkins, D. Kereš, and C.-A. Faucher-Giguère (2015), “Galactic r-process enrichment by neutron star mergers in cosmological simulations of a Milky Way-mass galaxy,” *Mon. Not. Roy. Astron. Soc.* **447**, 140–148.
- van de Voort, Freeke, Rüdiger Pakmor, Robert J. J. Grand, Volker Springel, Facundo A. Gómez, and Federico Marinacci (2019), “Neutron star mergers and rare core-collapse supernovae as sources of r-process enrichment in simulated galaxies,” arXiv e-prints [arXiv:1907.01557](https://arxiv.org/abs/1907.01557) [astro-ph.GA].
- Vangioni, E, S. Goriely, F. Daigne, P. François, and K. Belczynski (2016), “Cosmic neutron-star merger rate and gravitational waves constrained by the r-process nucleosynthesis,” *Mon. Not. Roy. Astron. Soc.* **455**, 17–34.
- Vassh, N, R. Vogt, R. Surman, J. Randrup, T. M. Sprouse, M. R. Mumpower, P. Jaffke, D. Shaw, E. M. Holmbeck, Y. Zhu, and G. C. McLaughlin (2019a), “Using excitation-energy dependent fission yields to identify key fissioning nuclei in r-process nucleosynthesis,” *J. Phys. G: Nucl. Part. Phys.* **46**, 065202.
- Vassh, Nicole, Matthew R. Mumpower, Gail C. McLaughlin, Trevor M. Sprouse, and Rebecca Surman (2019b), “Coproduction of light and heavy r-process elements via fission deposition,” arXiv e-prints [arXiv:1911.07766](https://arxiv.org/abs/1911.07766) [astro-ph.HE].
- Venn, K A, E. Tolstoy, A. Kaufer, E. D. Skillman, S. M. Clarkson, S. J. Smartt, D. J. Lennon, and R. P. Kudritzki (2003), “The Chemical Composition of Two Supergiants in the Dwarf Irregular Galaxy WLM,” *Astron. J.* **126**, 1326–1345.
- Vescovi, D, *et al.* (2018), “On the Origin of Early Solar System Radioactivities: Problems with the Asymptotic Giant Branch and Massive Star Scenarios,” *Astrophys. J.* **863** (2), 115, [arXiv:1807.01058](https://arxiv.org/abs/1807.01058) [astro-ph.SR].
- Vigna-Gómez, Alejandro, Coenraad J. Neijssel, Simon Stevenson, Jim W. Barrett, Krzysztof Belczynski, Stephen Justham, Selma E. de Mink, Bernhard Müller, Philipp Podsiadlowski, Mathieu Renzo, Dorottya Szécsi, and Ilya Mandel (2018), “On the formation history of Galactic double neutron stars,” *Mon. Not. Roy. Astron. Soc.* **481**, 4009–4029.
- Vilen, M, J. M. Kelly, A. Kankainen, M. Brodeur, A. Aprahamian, L. Canete, T. Eronen, A. Jokinen, T. Kuta, I. D. Moore, M. R. Mumpower, D. A. Nesterenko, H. Penttilä, I. Pohjalainen, W. S. Porter, S. Rinta-Antila, R. Surman, A. Voss, and J. Äystö (2018), “Precision Mass Measurements on Neutron-Rich Rare-Earth Isotopes at JYFLTRAP: Reduced Neutron Pairing and Implications for r-Process Calculations,” *Phys. Rev. Lett.* **120**, 262701.
- Villar, V A, P. S. Cowperthwaite, E. Berger, P. K. Blanchard, S. Gomez, K. D. Alexander, R. Margutti, R. Chornock,

- T. Eftekhari, G. G. Fazio, J. Guillochon, J. L. Hora, M. Nicholl, and P. K. G. Williams (2018), “Spitzer Space Telescope Infrared Observations of the Binary Neutron Star Merger GW170817,” *Astrophys. J. Lett.* **862**, L11.
- Villar, V A, J. Guillochon, E. Berger, B. D. Metzger, P. S. Cowperthwaite, M. Nicholl, K. D. Alexander, P. K. Blanchard, R. Chornock, T. Eftekhari, W. Fong, R. Margutti, and P. K. G. Williams (2017), “The Combined Ultraviolet, Optical, and Near-infrared Light Curves of the Kilonova Associated with the Binary Neutron Star Merger GW170817: Unified Data Set, Analytic Models, and Physical Implications,” *Astrophys. J. Lett.* **851**, L21.
- Vink, J, J. M. Laming, J. S. Kaastra, J. A. M. Bleeker, H. Bloemen, and U. Oberlack (2001), “Detection of the 67.9 and 78.4 keV Lines Associated with the Radioactive Decay of ^{44}Ti in Cassiopeia A,” *Astrophys. J. Lett.* **560**, L79–L82.
- Vink, Jacco (2008), “Supernova remnants with magnetars: Clues to magnetar formation,” *Advances in Space Research* **41**, 503–511.
- Vlasenko, Alexey, and G. C. McLaughlin (2018), “Matter-neutrino resonance in a multiangle neutrino bulb model,” *Phys. Rev. D* **97**, 083011.
- Wallner, A, T. Faestermann, J. Feige, C. Feldstein, K. Knie, G. Korschinek, W. Kutschera, A. Ofan, M. Paul, F. Quinto, G. Rugel, and P. Steier (2015), “Abundance of live ^{244}Pu in deep-sea reservoirs on Earth points to rarity of actinide nucleosynthesis,” *Nature Communications* **6**, 5956.
- Wallner, A, J. Feige, N. Kinoshita, M. Paul, L. K. Fifield, R. Golser, M. Honda, U. Linnemann, H. Matsuzaki, S. Merchel, G. Rugel, S. G. Tims, P. Steier, T. Yamagata, and S. R. Winkler (2016), “Recent near-Earth supernovae probed by global deposition of interstellar radioactive ^{60}Fe ,” *Nature* **532**, 69–72.
- Wallner, A, *et al.* (2019), private communication.
- Wanajo, S (2007), “Cold r-Process in Neutrino-driven Winds,” *Astrophys. J.* **666**, L77–L80.
- Wanajo, S, and Y. Ishimaru (2006), “r-process Calculations and Galactic Chemical Evolution,” *Nucl. Phys. A* **777**, 676–699.
- Wanajo, S, and H.-T. Janka (2012), “The r-process in the Neutrino-driven Wind from a Black-hole Torus,” *Astrophys. J.* **746**, 180.
- Wanajo, S, H.-T. Janka, and B. Müller (2013), “Electron-capture Supernovae as Sources of ^{60}Fe ,” *Astrophys. J.* **774**, L6.
- Wanajo, S, T. Kajino, G. J. Mathews, and K. Otsuki (2001), “The r-Process in Neutrino-driven Winds from Nascent, “Compact” Neutron Stars of Core-Collapse Supernovae,” *Astrophys. J.* **554**, 578–586.
- Wanajo, S, B. Müller, H.-T. Janka, and A. Heger (2018), “Nucleosynthesis in the Innermost Ejecta of Neutrino-driven Supernova Explosions in Two Dimensions,” *Astrophys. J.* **852**, 40.
- Wanajo, S, K. Nomoto, H.-T. Janka, F. S. Kitaura, and B. Müller (2009), “Nucleosynthesis in Electron Capture Supernovae of Asymptotic Giant Branch Stars,” *Astrophys. J.* **695**, 208–220.
- Wanajo, S, Y. Sekiguchi, N. Nishimura, K. Kiuchi, K. Kyutoku, and M. Shibata (2014), “Production of All the r-process Nuclides in the Dynamical Ejecta of Neutron Star Mergers,” *Astrophys. J.* **789**, L39.
- Wanajo, Shinya (2006), “The rp-Process in Neutrino-driven Winds,” *Astrophys. J.* **647**, 1323–1340.
- Wanajo, Shinya (2018), “Physical Conditions for the r-process. I. Radioactive Energy Sources of Kilonovae,” *Astrophys. J.* **868**, 65.
- Wanajo, Shinya, Hans-Thomas Janka, and Bernhard Müller (2011), “Electron-capture supernovae as the origin of elements beyond iron,” *Astrophys. J.* **726**, L15.
- Wanderman, D, and T. Piran (2015), “The rate, luminosity function and time delay of non-Collapsar short GRBs,” *Mon. Not. Roy. Astron. Soc.* **448**, 3026–3037.
- Wang, M, G. Audi, A.H. Wapstra, F.G. Kondev, M. MacCormick, X. Xu, and B. Pfeiffer (2012), “The Ame2012 atomic mass evaluation: (II) Tables, graphs and references,” *Chinese Phys. C* **36**, 1603–2014.
- Wang, Ning, Min Liu, and Xizhen Wu (2010), “Modification of nuclear mass formula by considering isospin effects,” *Phys. Rev. C* **81**, 044322.
- Watson, Darach, Camilla J. Hansen, Jonatan Selsing, Andreas Koch, Daniele B. Malesani, Anja C. Andersen, Johan P. U. Fynbo, Almudena Arcones, Andreas Bauswein, Stefano Covino, Aniello Grado, Kasper E. Heintz, Leslie Hunt, Chryssa Kouveliotou, Giorgos Leloudas, Andrew J. Levan, Paolo Mazzali, and Elena Pian (2019), “Identification of strontium in the merger of two neutron stars,” *Nature* **574**, 497–500.
- Waxman, E, E. O. Ofek, D. Kushmir, and A. Gal-Yam (2018), “Constraints on the ejecta of the GW170817 neutron star merger from its electromagnetic emission,” *Mon. Not. Roy. Astron. Soc.* **481**, 3423–3441.
- Waxman, Eli, Eran O. Ofek, and Doron Kushnir (2019), “Late-time Kilonova Light Curves and Implications to GW170817,” *Astrophys. J.* **878**, 93.
- Way, K, and E. P. Wigner (1948), “The Rate of Decay of Fission Products,” *Phys. Rev.* **73**, 1318–1330.
- Wehmeyer, B, C. Fröhlich, B. Côté, M. Pignatari, and F. K. Thielemann (2019), “Using failed supernovae to constrain the Galactic r-process element production,” *Mon. Not. Roy. Astron. Soc.* **487**, 1745–1753.
- Wehmeyer, B, M. Pignatari, and F.-K. Thielemann (2015), “Galactic evolution of rapid neutron capture process abundances: the inhomogeneous approach,” *Mon. Not. Roy. Astron. Soc.* **452**, 1970–1981.
- Wehmeyer, B, *et al.* (2018), private communication.
- Weisberg, J M, and Y. Huang (2016), “Relativistic Measurements from Timing the Binary Pulsar PSR B1913+16,” *Astrophys. J.* **829**, 55.
- Westin, J, C. Sneden, B. Gustafsson, and J. J. Cowan (2000), “The r-Process-enriched Low-Metallicity Giant HD 115444,” *Astrophys. J.* **530**, 783–799.
- Whaling, W, M. T. Carle, and M. L. Pitt (1993), “Argon branching ratios for spectrometer response calibration.” *J. Quant Spec. Rad. Trans.* **50**, 7–18.
- Wheeler, J C, J. J. Cowan, and W. Hillebrandt (1998), “The r-Process in Collapsing O/Ne/Mg Cores,” *Astrophys. J.* **493**, L101–L104.
- Wheeler, J C, C. Sneden, and J. W. Truran, Jr. (1989), “Abundance ratios as a function of metallicity,” *Annu. Rev. Astron. Astrophys.* **27**, 279–349.
- Winteler, C, R. Käppeli, A. Perego, A. Arcones, N. Vasset, N. Nishimura, M. Liebendörfer, and F.-K. Thielemann (2012), “Magnetorotationally Driven Supernovae as the Origin of Early Galaxy r-process Elements?” *Astrophys. J.* **750**, L22.
- Wisshak, K, F. Voss, C. Arlandini, F. Käppeler, and L. Kazakov (2000), “Stellar neutron capture cross sections of the

- Yb isotopes,” *Phys. Rev. C* **61**, 065801.
- Witti, J, H.-Th. Janka, and K. Takahashi (1994), “Nucleosynthesis in neutrino-driven winds from protoneutron stars I. The α -process,” *Astron. & Astrophys.* **286**, 841–856.
- Wojczuk, K, and A. Janiuk (2018), “Nucleosynthesis in black hole accretion flows feeding short GRBs,” in *XXXVIII Polish Astronomical Society Meeting*, Vol. 7, edited by A. Różańska, pp. 337–340.
- Woosley, S E, Ronald G. Eastman, and Brian P. Schmidt (1999), “Gamma-Ray Bursts and Type IC Supernova SN 1998BW,” *Astrophys. J.* **516**, 788–796.
- Woosley, S E, D. H. Hartmann, R. D. Hoffman, and W. C. Haxton (1990), “The ν -process,” *Astrophys. J.* **356**, 272–301.
- Woosley, S E, and A. Heger (2007), “Nucleosynthesis and remnants in massive stars of solar metallicity,” *Phys. Rep.* **442**, 269–283.
- Woosley, S E, A. Heger, and T. A. Weaver (2002), “The evolution and explosion of massive stars,” *Rev. Mod. Phys.* **74**, 1015–1071.
- Woosley, S E, and R. D. Hoffman (1992), “The α -process and the r -process,” *Astrophys. J.* **395**, 202–239.
- Woosley, S E, J. R. Wilson, G. J. Mathews, R. D. Hoffman, and B. S. Meyer (1994), “The r -process and neutrino-heated supernova ejecta,” *Astrophys. J.* **433**, 229–246.
- Wu, J, *et al.* (2017), “94 β -decay half-lives of neutron-rich ^{55}Cs to ^{67}Ho : Experimental feedback and evaluation of the r -process rare-earth peak formation,” *Phys. Rev. Lett.* **118**, 072701.
- Wu, M-R, R. Fernández, G. Martínez-Pinedo, and B. D. Metzger (2016), “Production of the entire range of r -process nuclides by black hole accretion disc outflows from neutron star mergers,” *Mon. Not. Roy. Astron. Soc.* **463**, 2323–2334.
- Wu, M-R, T. Fischer, L. Huther, G. Martínez-Pinedo, and Y.-Z. Qian (2014), “Impact of active-sterile neutrino mixing on supernova explosion and nucleosynthesis,” *Phys. Rev. D* **89**, 061303(R).
- Wu, M-R, *et al.* (2017), unpublished.
- Wu, Meng-Ru, Projwal Banerjee, Brian D. Metzger, Gabriel Martínez-Pinedo, Tsuguo Aramaki, Eric Burns, Charles J. Hailey, Jennifer Barnes, and Georgia Karagiorgi (2019), “Finding the Remnants of the Milky Way’s Last Neutron Star Mergers,” *Astrophys. J.* **880**, 23.
- Wu, Meng-Ru, J. Barnes, G. Martínez-Pinedo, and B. D. Metzger (2019), “Fingerprints of heavy-element nucleosynthesis in the late-time lightcurves of kilonovae,” *Phys. Rev. Lett.* **122**, 062701.
- Wu, Meng-Ru, Yong-Zhong Qian, Gabriel Martínez-Pinedo, Tobias Fischer, and Lutz Huther (2015), “Effects of neutrino oscillations on nucleosynthesis and neutrino signals for an 18 M_{\odot} supernova model,” *Phys. Rev. D* **91**, 065016.
- Wu, Meng-Ru, and Irene Tamborra (2017), “Fast neutrino conversions: Ubiquitous in compact binary merger remnants,” *Phys. Rev. D* **95**, 103007.
- Wu, Meng-Ru, Irene Tamborra, Oliver Just, and Hans-Thomas Janka (2017), “Imprints of neutrino-pair flavor conversions on nucleosynthesis in ejecta from neutron-star merger remnants,” *Phys. Rev. D* **96**, 123015.
- Wu, Yiyang, and Andrew MacFadyen (2018), “Constraining the Outflow Structure of the Binary Neutron Star Merger Event GW170817/GRB170817A with a Markov Chain Monte Carlo Analysis,” *Astrophys. J.* **869**, 55.
- Wünsch, K-D (1978), “An on-line mass-separator for thermally ionisable fission products: OSTIS,” *Nuclear Instruments and Methods* **155**, 347–351.
- Xu, Y, and S. Goriely (2012), “Systematic study of direct neutron capture,” *Phys. Rev. C* **86**, 045801.
- Xu, Y, S. Goriely, A. J. Koning, and S. Hilaire (2014), “Systematic study of neutron capture including the compound, pre-equilibrium, and direct mechanisms,” *Phys. Rev. C* **90**, 024604.
- Yakovlev, D G, L. R. Gasques, A. V. Afanasjev, M. Beard, and M. Wiescher (2006), “Fusion reactions in multicomponent dense matter,” *Phys. Rev. C* **74**, 035803.
- Yan, X L, K. Blaum, Y. A. Litvinov, X. L. Tu, H. S. Xu, Y. H. Zhang, and X. H. Zhou (ESR and CSRe Collaborations on In-Ring Mass Measurements) (2016), “Recent results on mass measurements of exotic nuclides in storage rings,” in *Journal of Physics Conference Series*, Vol. 665, p. 012053.
- Yang, Bin, Zhi-Ping Jin, Xiang Li, Stefano Covino, Xian-Zhong Zheng, Kenta Hotokezaka, Yi-Zhong Fan, Tsvi Piran, and Da-Ming Wei (2015), “A possible macronova in the late afterglow of the long-short burst GRB 060614,” *Nature Communications* **6**, 7323.
- Yee, R M, *et al.* (2013), “ β -Delayed Neutron Spectroscopy Using Trapped Radioactive Ions,” *Phys. Rev. Lett.* **110**, 092501.
- Yeh, T-R, D. D. Clark, G. Scharff-Goldhaber, R. E. Chrien, L.-J. Yuan, M. Shmid, R. L. Gill, A. E. Evans, H. Dautet, and J. Lee (1983), “High resolution measurements of delayed neutron emission spectra from fission products,” in *Nuclear Data for Science and Technology*, edited by K. H. Böckhoff (Springer Netherlands, Dordrecht) pp. 261–264.
- Yong, D, J. E. Norris, G. S. Da Costa, L. M. Stanford, A. I. Karakas, L. J. Shingles, R. Hirschi, and M. Pignatari (2017), “A Chemical Signature from Fast-rotating Low-metallicity Massive Stars: ROA 276 in ω Centauri,” *Astrophys. J.* **837**, 176.
- Zampieri, L (2017), “Light Curves of Type II Supernovae,” in *Handbook of Supernovae*, edited by A. W. Alsabti and P. Murdin (Springer International Publishing, Cham).
- Zhang, C L, B. Schuetrumpf, and W. Nazarewicz (2016), “Nucleon localization and fragment formation in nuclear fission,” *Phys. Rev. C* **94**, 064323.
- Zhi, Q, E. Caurier, J. J. Cuenca-García, K. Langanke, G. Martínez-Pinedo, and K. Sieja (2013), “Shell-model half-lives including first-forbidden contributions for r -process waiting-point nuclei,” *Phys. Rev. C* **87**, 025803.
- Zhou, Ping, Jacco Vink, Samar Safi-Harb, and Marco Miceli (2019), “Spatially resolved X-ray study of supernova remnants that host magnetars: Implication of their fossil field origin,” *Astron. & Astrophys.* **629**, A51.
- Zhu, Jin-Ping, Yuan-Pei Yang, Liang-Duan Liu, Yan Huang, Bing Zhang, Zhuo Li, Yun-Wei Yu, and He Gao (2020), “Kilonova Emission From Black Hole-Neutron Star Mergers. I. Viewing-Angle-Dependent Lightcurves,” arXiv e-prints [arXiv:2003.06733](https://arxiv.org/abs/2003.06733) [astro-ph.HE].
- Zhu, Y, *et al.* (2018), “Californium-254 and Kilonova Light Curves,” *Astrophys. J.* **863**, L23.
- Zhu, Y L, A. Perego, and G. C. McLaughlin (2016), “Matter-neutrino resonance transitions above a neutron star merger remnant,” *Phys. Rev. D* **94**, 105006.
- Zrake, J, and A. I. MacFadyen (2013), “Magnetic Energy Production by Turbulence in Binary Neutron Star Mergers,” *Astrophys. J.* **769**, L29.